Doctoral Thesis:
Neuronal structural plasticity of the rodent telencephalon: Role of PSA-NCAM and modulation by the antidepressant Fluoxetine

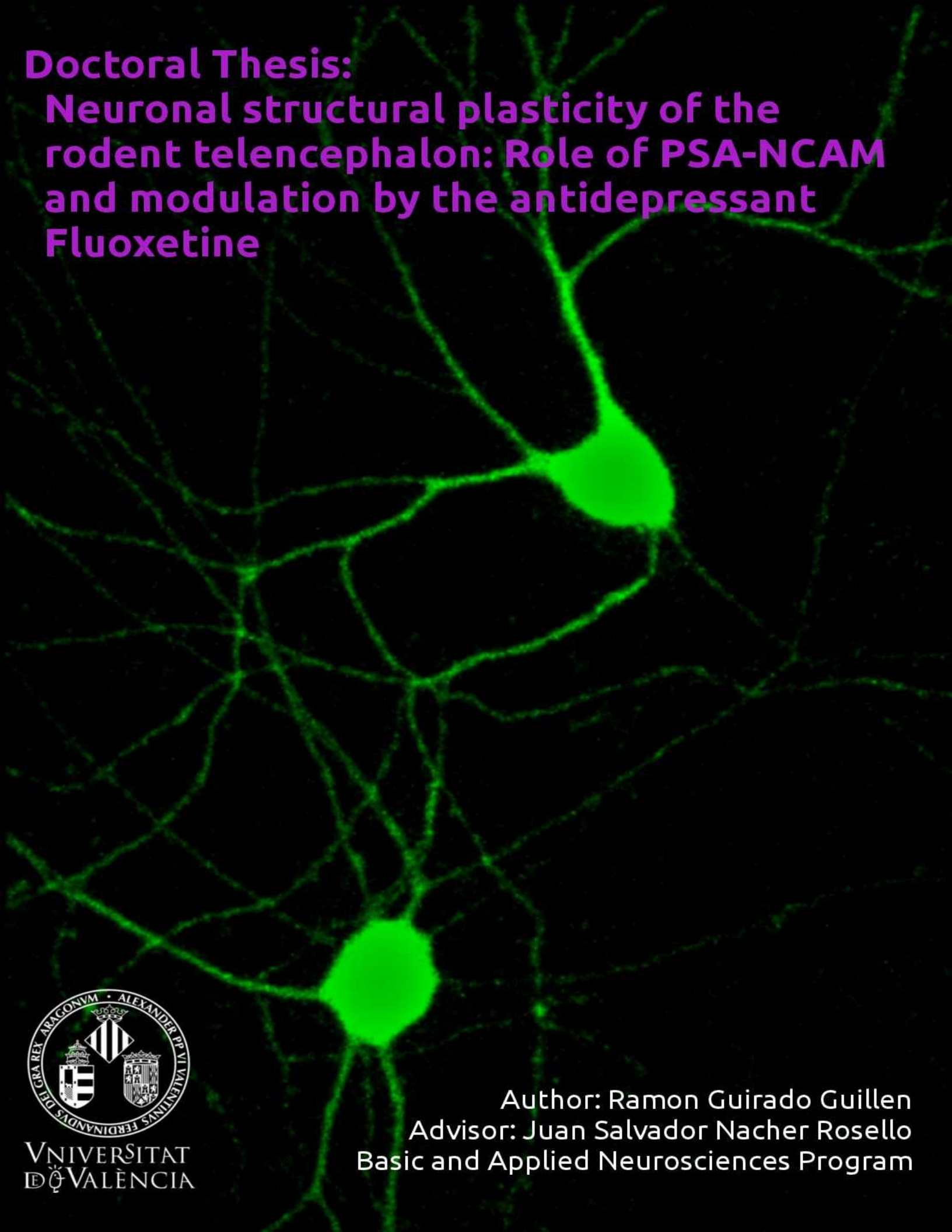

VNIVERSITAT DE VALÈNCIA

Author: Ramon Guirado Guillen
Advisor: Juan Salvador Nacher Rosello
Basic and Applied Neurosciences Program

Para la realización de esta tesis, el autor ha sido beneficiario de una ayuda predoctoral del Programa Nacional de Formación de Personal Investigador, concedida por el Ministerio de Educación y Ciencia (BES-2007-15757) según la resolución del 2 de enero de 2007, de la Secretaría de Estado de Universidades e Investigación.

To my young padawan learners

«Of course it is happening inside your head, Harry, but why on earth should that mean that it is not real?»

Albus Dumbledore

«El cielo es azul, just don't go tell anyone»

Conor Oberst

Acknowledgements/Agradecimientos

Mucha gente ha resultado clave a lo largo de mi vida, gracias a los cuales estoy aquí en este momento, pero en primer lugar quiero dar las gracias a mi director, Juan, por haberme dado la oportunidad de hacer la tesis en su laboratorio, poniendo a mi disposición todo lo que ha sido necesario, pero sobretodo por el tiempo y esfuerzo que ha dedicado a que las cosas saliesen adelante y a ofrecer una perspectiva optimista en todo momento, el sera para siempre mi padre científico. A Emilio gracias también porque me ha formado como investigador y me ha enseñado a ser mas crítico. A Carlos y Jose Miguel, muchas gracias por vuestros consejos y vuestra ayuda, disponible a tiempo completo, en especial a Jose Miguel por haberme enseñado microscopía electrónica y tantas otras cosas, como por ejemplo, a ser mas preciso (mas bien menos torpe). También quiero dar las gracias al resto de profesores del departamento que de uno u otro modo me han ayudado a lo largo de estos años, especialmente a Carlos López, Xavi, Chonchi, Quique e Isabel y personal administrativo como Pilar, Santi, Maricarmen o Sabina.

I would also like to thank the help from Curtis Rueden and specially Melissa Linkert, without your help I wouldn't have finished the thesis on time. I'm also grateful for all the work of Conor Oberst, you've been really inspiring and a good man to hear at difficult times.

Por supuesto también doy las gracias a mis compañeros de laboratorio, con quien mas he compartido las alegrías y las penas, y de quienes recordare multitud de momentos que me hacen feliz: el viaje a Washington, con Marian y Esther, el de Florencia con Javi, todo el tiempo compartido trabajando (y echándonos unas risas) para Carmen Sandi con Clara, los viajes al norte con Sandra o estar en una playa de piedras cortantes con Samuel. Las comidas en el ambit donde siempre suena la canción preferida de Teresa o de Laura, los mensajes de a las 9 en mi casa, las primas de Teresa (especialmente Alba), la canción de los lobos en el coche, comer pizza en el suelo de la calle o cualquier cosa en el palacio de oro, los viajes en verano con David o Ulisses, ya sea al Maestrazgo, a algún pantano de Teruel o a Nueva Zelanda, ir a jugar con el arco, o con Marta en Sheffield o en el bioparc, donde un pobre hipopótamo daba vueltas en círculos...

Gracias también por los buenos momentos durante las comidas, las discusiones de política y el trolling con Vicente y Sami, así como con Pau, y toda la gente del máster que hace tiempo que ya no vemos, como Oscar, Adri, Guillem, Maria y todos los demás!

En el laboratorio también me he beneficiado de vuestra ayuda y por eso quiero también agradecéroslo, como a Esther y Marian que me enseñaron todas las técnicas básicas del día a día y especialmente a Laura, porque todo hubiese sido mucho peor sin su constante apoyo, ya fuese para el animalario, para los cultivos, para autoclavar, para cualquier cosa siempre he contado contigo y siempre he recibido una sincera ayuda. También a Marta y Ulisses por haberme ayudado en todo y ser tanto unos buenos compañeros como unos íntimos amigos.

To all the people of Dominique's lab in Geneva, specially Olivier, for being such a good friend, for all the fridays drinking nice beers at the pink elephant with John, for all the jokes with Southpark and so many things! to Aline for being so open-minded and friendly, for teaching me all the molecular

stuff and her tricks with the cultures, to Bernadette for encouraging me any time I felt down and supporting my wine-research-ideas :) but also to Sylvain, Lorena, Mathias and Dominique, for all the time shared. I'll keep such good memories from my time there!

También estoy agradecido a toda la gente que me ha apoyado estos años fuera del laboratorio, como a Elena, por su profunda amistad, y por lo fácil que era convivir con ella, y todas las innumerables experiencias que hemos compartido juntos, como pintar cuadros los domingos con material de los chinos, tiempo que también compartía con Nico. Sin duda doy también las gracias a Nico y Toni por todas las ideas de ciencia que se nos han ocurrido juntos, tantos experimentos quedan por hacer... a Amparo por aguantarme todo este tiempo y haberme escuchado siempre con todas mis frustraciones ayudándome a soportar la dura realidad...

Gracias a la pandilla de la universidad, por vuestro apoyo y animo, Judit, Blanca, Carmen, Isa, Javi y tambien Mar y Neus, por haber contado siempre conmigo. También a mis amigos de Teruel, que tan importantes han sido en mi forma de ser desde la infancia, como Jaime y Fran, pero especialmente a Mateo por haberme enseñado tanto, haber estado siempre conmigo (aunque sea desde el ciberespacio) y ayudarme a resolver cualquier problema, fuese cual fuese. También a Rueda y a Moskhy por estar siempre ahí, por las cenas en los caprichos, por las reflexiones sobre la felicidad y tantas otras cosas! Pero también a Moya, Cote, Polo, Sergio, Miki y todos los demás! Como no, también para Amanda, y nuestras reflexiones sobre el amor, el odio y la naturaleza humana...

Finalmente quiero dar las gracias a mi familia, a mi hermano por confiar más en mi que yo mismo, y sobretodo a mis padres por la educación que me han dado, el apoyo incondicional y su sacrificio para darme la libertad de elegir que hacer con mi vida, respetando mis decisiones en todo momento por difíciles que fuesen. También a mi tía, que sin duda ha sido como una segunda madre, por su cariño, apoyo y motivación para convertirme en mejor persona.

Abbreviation List

5HT	5-hydroxytryptamine or Serotonin
BLA	Basolateral amygdala
BrdU	5-bromo-2'-deoxyuridine
BSA	Bovine serum albumin
CAM	Cell Adhesion Molecule
CAMKII	Ca2+/calmodulin-dependent protein kinases II
CCK	Cholecystokinin
CeA	Central amygdala
Cg1	Dorsal cingulate cortex
Cg2	Ventral cingulate cortex
CNS	Central nervous system
CR	Calretinin
DAB	3,3'-Diaminobenzidine
DCX	Doublecortin
DIV	Days *in vitro*
eGFP	Enhanced green fluorescent protein
EndoN	Endo-N-acetylneuraminidase
FGF	Fibroblast growth factor
Flx	Fluoxetine
GABA	γ-Aminobutyric acid
GAD	Glutamic acid decarboxylase
GFP	Green fluorescent protein
GIN	GFP-expressing inhibitory neurons
GPI	Glycosylphosphatidylinositol
HPA	Hypothalamic–pituitary–adrenal
IL	Infralimbic cortex
IP	Intraperitoneal
LA	Lateral amygdala
LMol	Lacunosum Moleculare
LTD	Long Term Depression
LTP	Long Term Potentiation
MAPK	Mitogen-activated protein kinase
MeA	Medial amygdala
Mol	Molecular layer
mPFC	Medial prefrontal cortex
NCAM	Neural cell adhesion molecule
NCAMff+	Floxed NCAM

NDS	Normal Donkey Serum
NGF	Nerve growth factor
NMDA	N-Methyl-D-aspartic acid
NPY	Neuropeptide Y
Or	Oriens stratum
PB	Phosphate Buffer
PBS	Phosphate buffered saline
PrL	Prelimibic cortex
PSA	Polysialic acid
PSA-NCAM	Polysialylated form of the neural cell adhesion molecule
PTK	Protein tyrosine kinase
PV	Parvalbumin
Rad	Radiatum stratum
RMS	Rostral migratory stream
SEM	Standard error of the mean
SGZ	Subgranular zone
SOM	Somatostatin
SSRI	Selective serotonin reuptake inhibitor
SVZ	Subventricular zone
SYN	Synaptophysin
Trk	Tyrosine receptor kinase
TUC-4	TOAD64/Ulip/CRMP-4
VGAT	Vesicular GABA transporter
VGluT1	Vesicular glutamate transporter type 1
VIP	Vasoactive intestinal peptide

Contents

List of Figures

Part I. Introduction

> "Once development was ended, the fonts of growth and regeneration of the axons and dendrites dried up irrevocably. In adult center, the nerve paths are something fixed and immutable: everything may die, nothing may be regenerated. It is for the science of the future to change, if possible, this harsh decree."

This statement by Ramon y Cajal (Ramon Y Cajal, 1913) led to the scientific community to think of the brain as a static structure. However, Ramon y Cajal also suggested other possibilities:

> "To explain the acquisition of new skills in adults ... it is necessary to admit ... the establishment of other new pathways, by means of branching and progressive growth of the terminal dendritic and axonal arborizations."

While the idea of neuroplasticity underlying learning was ignored, the concept of a fixed brain prevailed until the first ideas of a plastic nervous system appeared in the 70's, (Cummins et al., 1973; Diamond et al., 1971; Greenough, 1976).

Now we know that the remodeling of neural connectivity allows the brain to adapt to new situations, to learn and to cope with different intrinsic or extrinsic factors. These changes are required for the correct establishment of functional connections by cell migration, axon guidance and synaptogenesis during embryogenesis and early postnatal life (Hensch, 2004; De Graaf-Peters and Hadders-Algra, 2006). However, neural plasticity is not restricted to development, but also happens during the adult life, although to a much lesser extent. The adult brain retains the ability to undergo experience-dependent synaptic reorganization (De Magalhães and Sandberg, 2005), which is the basis for learning and memory (Sutton and Schuman, 2006). Moreover, this plasticity is crucial to cope with aversive experiences (McEwen and Gianaros, 2011) and to recover from brain damage or disease (Fox, 2009; Sabel, 2008).

In this regard, there are certain cerebral regions that have been demonstrated as extremely plastic, in which we have decided to focus our research. In particular, the medial prefrontal cortex (mPFC), the hippocampus and the amygdala undergo structural remodeling after many different experimental paradigms, specially in chronic stress (McEwen, 1999) and with antidepressant drugs (Castrén and Rantamäki, 2010; Nestler, 1998). Moreover, in these regions our laboratory and others have demonstrated the presence of the polysialylated form of the neural cell adhesion molecule (PSA-NCAM), a molecule involved in the modulation of different forms of structural plasticity (Bonfanti, 2006). Since various studies have also described the presence of structural remodeling in different neocortical regions, specialy those involved in sensory processing, we have also included in our analysis the somatosensory cortex. Finally, we have also included the study of the paleocortex, a region in which immature neurons expressing PSA-NCAM have been described (Pekcec et al., 2006; Shapiro et al., 2007).

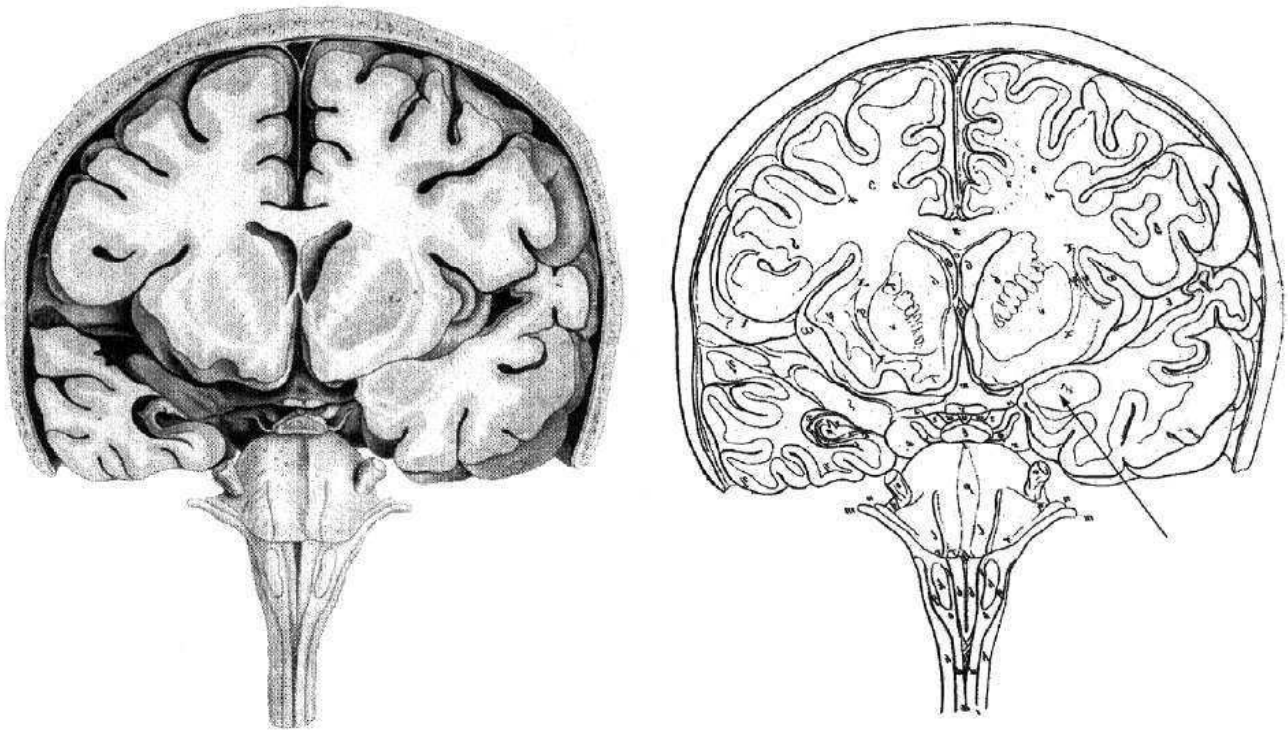

Fig. 1.1: Burdach's drawings of the human amygdala

1 Regions studied

1.1 The amygdala

Early in the 19th century, Burdach discovered a structure with an almond-shaped morphology, the amygdala (Fig. 1.1), which structure and function has been largely discussed all over these years. Meynert analyzed microscopically tissue sections and began an anatomical description of this region; then started the controversy about how to classify the amgydala . In fact, recent results suggest that the amygdala refers to an arbitrary set of cell groups (Swanson and Petrovich, 1998). However, based on immunohistological data, we can distinguish two different regions: The striatal amygdala, composed by the central and medial nuclei, with a high density of glutamate decarboxylase (GAD) expressing cells, resulting in a main γ-Aminobutyric acid (GABA) output. On the other hand, the rest of the amygdala, with a main presence of glutamatergic elements, represents the cortical amygdala. This region is divided into the chemosensory amygdala (composing the vomeronasal cortex and part of the olfactory cortex), the associative basal complex (formed by the basomedial, basolateral and lateral amygdala), and the extended amygdala (e.g. bed nucleus of the stria terminalis) (Gutiérrez-Castellanos et al., 2010; Swanson and Petrovich, 1998). Lesions in the amygdala of human patients lead to a behavioural disorder called Kluver-Bucy syndrome, characterized by changes in emotional behaviour, such as the complete loss of fear. This, together with different studies conducted in experimental animals, lead to the idea that the amygdala was an important part of the emotional circuits (Mair et al., 1979). Studies on rats have shown that damage to the amygdala affects the

acquisition and expression of fear conditioning (LaBar and LeDoux, 1996). Different experiments have demonstrated that the basolateral and basomedial divisions are involved in the acquisition of contextual conditioning, while the lateral nuclei is involved in auditory conditioning. These regions process the information and project to the central nuclei of the amygdala, which is involved in the interface with the motor system (freezing response) and other forms of expression of conditioned fear, such as blood pressure control (LeDoux, 2000). The last of the amygdaloid nuclei analyzed in this thesis is the medial amygdala, which represents an integrative area of vomeronasal and olfactive information, and therefore it is involved in the reproductive behavior elicited in response to the action of sexual pheromones (Wysocki et al., 1991; Halpern and Martínez-Marcos, 2003).

1.2 The hippocampus

The hippocampus is a structure formed by three layers: molecular, pyramidal and polymorphic. It has been classically divided in two interlocking regions: the Ammon's horn and the dentate gyrus. The dentate gyrus is formed by a layer of granular cells, which extend their dendrites to the external layer of this region, the molecular layer. In this stratum begins the so-called trisynaptic loop, where granule cells recieve the projection of entorhinal afferents that carry information about the external world. Beneath these granule cells is the hilus, where we can find a population of excitatory neurons denominated mossy cells. The axons of these mossy cells mainly innervate the dendrites of the granule cells in addition to some of their axons, which constitute the mossy fibers. These mossy fibers project to the CA3 subfield of the pyramidal layer, where they form giant *en passant* boutons, or mossy terminals, on the proximal dendrites of pyramidal cells. This connection represents the second stage of the trisynaptic loop. These pyramidal cells extend their apical dendrites in the strata radiatum and lacunosum moleculare, where they receive projections from the entorhinal cortex. The basal dendrites of the CA3 pyramidal neurons are extended in the stratum oriens, as well as their axons, which arborize profusely within CA3 and project densely to the CA1 subfield, a route originally described by Schaeffer (Schaeffer, 1892). These axons generate collaterals which reach both the stratum radiatum and, to a lesser extent, the stratum oriens, representing the third and final stage of the trisynaptic loop (Freund and Buzsáki, 1996).

The hippocampus is a region that has been related to memory formation during the last 50 years, initially due to the information obtained from the clinical cases of HM and RB. HM received surgery in an attempt to cure his epileptic seizures. The bilateral medial temporal lobe resection removed the amygdala, uncus, hippocampal gyrus and anterior two-thirds of the hippocampus and HM developed anterograde amnesia of declarative memories (those available to consciousness). His past memories were intact, but he could not remember any posterior events to the surgery. In the case of RB, after an ischemic episode during cardiac surgery, an anterograde amnesia was apparent, he was also unable to remember anything since the ischemic episode. But in his case, the lesion was restricted to the CA1 region of the whole hippocampus, demonstrating the role of this region in memory function. Posterior experiments of hippocampal lesions in rats demonstrated that the

hippocampus is also necessary for the establishment of new spatial memories (Eichenbaum, 2000).

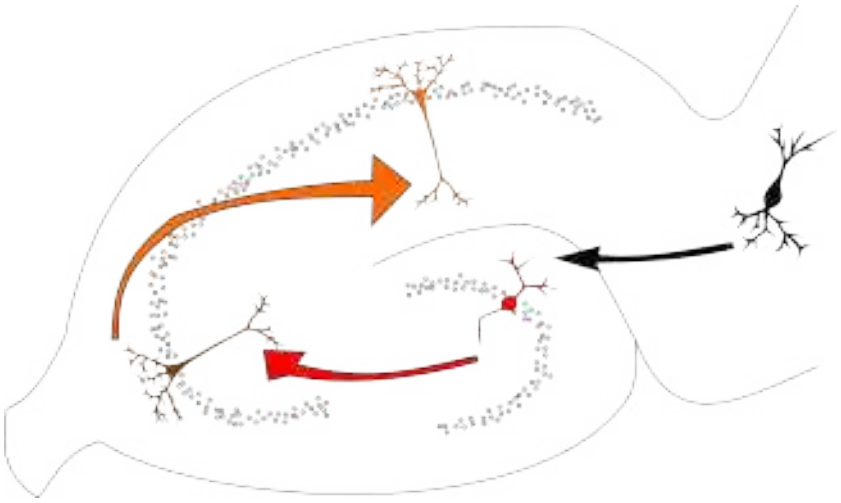

Fig. 1.2: Trisynaptic loop of the hippocampus

1.3 The medial prefrontal cortex

The mPFC can be divided into three areas with distinct anatomical and functional features: (1) the rostral portion of the anterior cingulate cortex, which in turn is divided into a dorsal (Cg1) and a ventral (Cg2) area; (2) the infralimbic cortex (IL) and, (3) the prelimbic cortex (PrL) (Uylings and Van Eden, 1990; Paxinos and Watson, 2007; Seamans et al., 2008).

The architectural order of cells and fibers in the rodent mPFC basically conforms to the structural plan prevailing throughout the neocortical regions in mammals, but lacking the internal granule cell layer (layer IV) (Gabbott et al., 1997; Fuster, 2008). Therefore, the rodent mPFC is organized in five layers that run parallel to the cortical surface and are numbered from the outer surface of the cortex (pia mater) to the white matter as follows (Kandel et al., 2000; Paxinos and Watson, 2007; Fuster, 2008):

- Layer I (molecular or plexiform layer) is an acellular layer occupied by the dendrites of the cells located deeper in the cortex and axons that travel through this layer or form connections in there.

- Layer II (external granule cell layer) is comprised mainly of small spherical cells called granule cells. Some small pyramidal cells are also present in this layer and connect with other cortical areas from the same hemisphere.

- Layer III (external pyramidal cell layer) contains a variety of cell types, many of which are pyramidally shaped and connect either with the contra-lateral hemisphere or with other cortical areas from the same hemisphere. In cortices organized in five layers, layer III receives most of the projections coming from the thalamus.

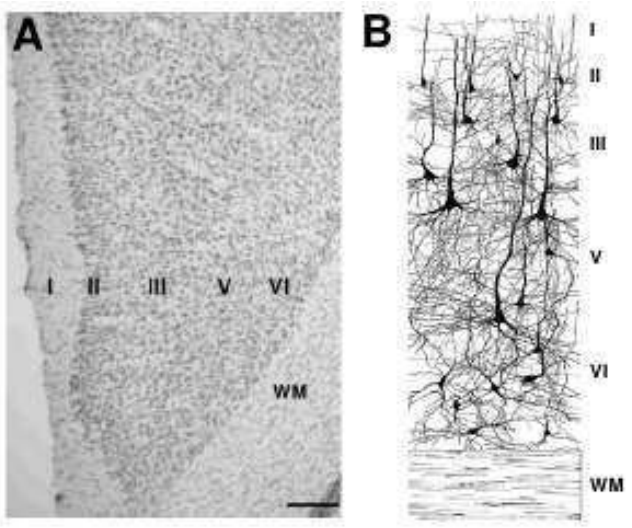

Fig. 1.3: Layers of the mPFC

- Layer V (internal pyramidal cell layer) contains mainly pyramidal neurons that are typically larger and more densely packed than those in layer III. Many of these neurons have been shown to project to the basal ganglia, the thalamus, many nuclei of the brainstem and midbrain, and to the spinal cord (Lambe et al., 2000).

- Layer VI (polymorphic or multiform layer) is a fairly heterogeneous layer of neurons. It blends into the white matter that forms the deep limit of the cortex and carries axons to the thalamus and to/from other areas of the cortex (DeFelipe and Farinas, 1992; Groenewegen et al., 1997).

Although each layer of the cerebral cortex is defined primarily by the presence or absence of neuronal cell bodies, each layer also contains additional elements. Thus, layers I-III contain the apical dendrites of neurons that have their cell bodies in layers V and VI, while layers V and VI contain the basal dendrites of neurons with cell bodies in layer II. The profile of inputs to a particular cortical neuron depends more on the distribution of its dendrites than on the location of its cell body (Kandel et al., 2000).

On cytoarchitectonic grounds, these regions are considered equivalent to the human/primate Brodmann's areas 24, 25 and 32 respectively. However, although the rodent PFC is not as differentiated as it is in primates, and the appearance of new specializations later in the evolution is likely, dorsolateral-like features (Brodmann's areas 46 and 9), including both anatomical and functional ones, are also present in rodents. In general, it appears that the rodent PrL region is involved in attentional and response selection functions, as well as visual working memory, whereas the more dorsal regions (Cg) are involved in the generation of rules associated with temporal ordering and motor sequencing of behavior. The IL region plays a special role in autonomic control, and especially in the modulation of fear-related behaviors (Uylings and Van Eden, 1990; Paxinos and Watson, 2007; Seamans et al., 2008).

1.4 The somatosensory cortex

The somatosensory cortex is divided in six layers similar to those described for the medial prefrontal cortex, but with a proper internal granular cell layer (or layer IV) that represents an exclusive feature of the rodent somatosensory cortex. This layer is anatomically organized in cylindrical structures denominated barrels, which receive the input from the rodent whiskers through the hypothalamus. Every whisker projects selectively to one barrel, representing therefore, a good model to study experience-dependent structural plasticity. In fact, it has been shown that whisker trimming induces the remodeling of the barrel structure to adapt to the new number of whiskers. This neocortical region is involved in the sensory representation of the different parts of the body. In fact, it contains a somatotopic map of the contralateral body surface and codifies information for the location (Penfield and Rasmussen, 1950) and orientation of stimuli (Mountcastle et al., 1967). In this line, lesions of this region in humans have been shown to produce symptoms such as agraphesthesia (disorder of cutaneous kinesthesia), astereognosia (inability to indentify an object by touch), loss of vibration, proprioception and fine touch.

1.5 The paleocortex

The paleocortex is a wide region of the brain defined by its structure organized in three to six layers, where the projections of the olfactory information terminate. In this regard, it is important to remember that the olfactory system represents the most important source of information from the outside world for rodents. Two different regions of the paleocortex were studied in this thesis: the entorhinal and the piriform cortices. The entorhinal cortex is strongly connected to the hippocampus, through axonal fibers that perforate the subiculum, therefore it has always been suspected that the function of both regions must be somehow related. Now the entorhinal cortex is considered an association area where inputs from different regions converge, before entering the hippocampus. Consequently, this region provides sensory information to the hippocampus for the development of learning and memory, and, in fact, lesions of this region are associated with failure in sensory integration and spatial learning impairments (Davis et al., 2001). The entorhinal cortex can be divided in two regions according to their projections to the dentate gyrus of the hippocampus: the lateral and the medial subdivisions. These anatomical divisions are related to different functions: the medial part receives spatial information, while the lateral part receives olfactory and somatosensory information. The entorhinal cortex is organized in six layers, similar to the neocortex, but the piriform cortex displays only three layers. However, in general terms, the cellular morphology, physiology and local circuitry are similar to the six-layered neocortex (Haberly and Price, 1978). The piriform cortex is characterized by the direct input that it receives from the olfactory bulb (Löscher and Ebert, 1996). The main recipients of this input are the pyramidal cells in the piriform cortex layer II. However, in addition to pyramidal cells in layer II, recent reports have described a distinct population of cells expressing immature neuronal markers, such as doublecortin (DCX) and TOAD/Ulip/CRMP-4 (TUC-4) in both entorhinal and piriform cortices (Nacher et al., 2000, 2002a).The involvement of

this region in olfactory processing has been shown by specific lesions, characterized by impairments in odour perception and odour memory (Dade et al., 2002).

2 Major cell types

From the first studies of Ramon y Cajal, Camillo Golgi and their successors, two major groups of cells were identified in the brain: neurons, specialized cells for electrical signaling over long distances, and glia, cells specialized in the support and nourishment of neurons. Nevertheless, recent studies have demonstrated that glial cells have a more complicated role, from synapse scaling to brain repair (Ben Achour and Pascual, 2010).

Neurons are identified by their morphology, they have an extensive dendritic arbour, which receives the main synaptic input from other neurons. On the other hand, the axon represents the neuronal output. There are two major types of neurons: interneurons, or local circuit neurons defined by a short axon, and the use of the inhibitory neurotransmitter GABA. This cell type represents a 20-30% of the total number of neurons in the cortex (Kawaguchi and Kubota, 1997). The rest of the neurons correspond to the principal/projection type, which display long axons that extend to distant targets and which mainly use the excitatory neurotransmitter glutamate. While excitatory neurons are relatively homogeneous regarding their features, interneurons constitute a heterogeneous population with diverse morphological, electrophysiological, neurochemical and synaptic characteristics. Consequently, multiple subpopulations of interneurons can be defined attending to these features, individually or in combination (Ascoli et al., 2008). A conservative classification describes four types of interneurons: (I) fast-spiking chandelier and basket interneurons, expressing parvalbumin (PV), (II) burst-spiking somatostatin-containing interneurons, (III), rapidly-adapting interneurons, which usually have a bipolar or double-bouquet morphology and express calretinin (CR) or vasointestinal peptide (VIP) and (IV) rapidly-adapting interneurons with multipolar morphology expressing reelin and neuropeptide Y (NPY) (Gelman and Marín, 2010).

Both excitatory and inhibitory neurons are present and constitute the main cell types in all the regions studied in this thesis. Nevertheless, there are characteristic differences in each region: while in the mPFC, the somatosensory cortex and the paleocortex the excitatory neurons are almost exclusively pyramidal neurons, in the hippocampus we have to include also the granule cells of the dentate gyrus. In the amygdala, the excitatory neurons are denominated class I cells, although they are also known as pyramidal-like neurons. Unlike the pyramidal neurons of the hippocampus and the neocortex, these pyramidal-like neurons neither show a clear orientation nor a stratification. Moreover, within this class I group there are also smaller cells, more similar to the spiny stellate cells of the cortex. Regarding the inhibitory neurons, we can find the four groups described above in all the regions studied in this thesis, although their specific function in each region is not completely understood. However, it has to be noted that this classification in four groups is too reductionist and does not represent the great diversity of interneurons present in the adult brain.

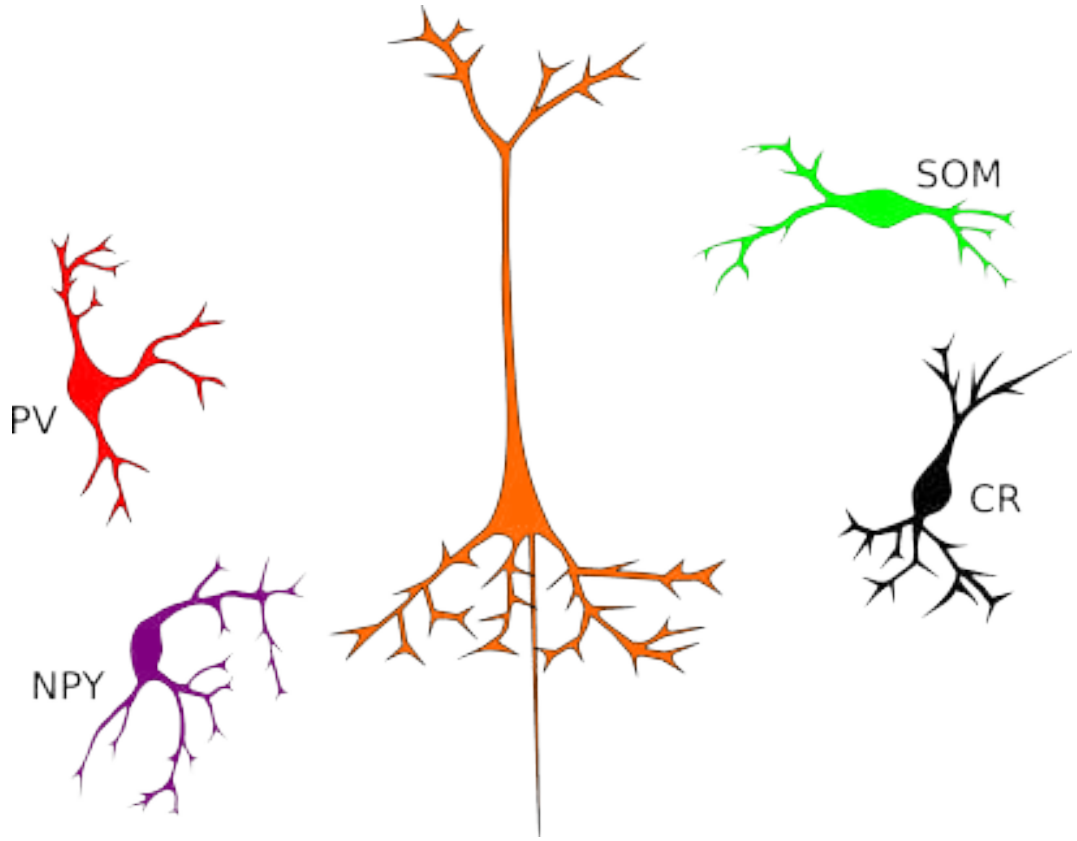

Fig. 2.1: Major cell types; interneuronal diversity

3 Neuronal plasticity

The term neuronal plasticity refers to the reorganization of the nervous system at different levels, from molecular to structural changes (Xerri, 2008).

3.1 Molecular plasticity

There is evidence of complex molecular mechanisms and signaling cascades involved in the modulation of neuronal plasticity. Many of these processes are largely dependent on protein dynamics in synapses, such as neurotransmitter receptor dynamics at excitatory and inhibitory synapses or the relationship between the exchange of these receptors and scaffolding proteins (Renner et al., 2008). For example, GABA and glycine receptors are clustered by gephyrin (Fritschy and Harvey, 2008), a scaffolding protein important for the appropriate activity-dependent diffusion of GABA receptors (Mukherjee et al., 2011). Some of these molecular changes underlie the structural remodeling of neurites and synapses and, consequently, they should involve regulation of the expression of neuronal cytoskeletal proteins and proteins implicated in cell to cell and cell to extracellular matrix adhesion. The remodeling of protein filaments in the neuronal cytoskeleton is highly regulated by conserved signaling pathways, which are known to accompany different changes in the structure of synapses, axons, dendrites and spines. In the synapse, the cytoskeleton is likely to control dynamic synaptic functions and might induce morphological changes. In fact, microtubule-associated proteins have

been implicated in synapse assembly and disassembly (Roos et al., 2000; Eaton et al., 2002). Different signaling pathways are also likely to regulate the actin cytoskeleton at the synapse (Meyer and Feldman, 2002). Actin remodeling in the postsynaptic compartment can also be initiated by a number of signaling molecules, such as the EphB2 receptor tyrosine kinase, via the small Rho GTPases, Rac1 and Cdc42. Other signaling molecules associated with the Rho GTPase pathway and with actin-binding proteins are also important for maintaining spine integrity (Dillon and Goda, 2005). In addition, adhesion molecules bind to a cytoplasmic network of scaffolding proteins, regulators of the actin cytoskeleton, and signal transduction pathways that control the structural and functional organization of synapses (Yamada and Nelson, 2007). Moreover, cell adhesion molecules (CAMs), such as N-cadherin, influence synaptic structure via indirect interactions with the actin cytoskeleton (Dillon and Goda, 2005). The neural cell adhesion molecule (NCAM) also interacts with cytoskeletal proteins. The NCAM 140 and 180 isoforms, are normally associated with α- and β-tubulin, as well as α-actinin 1. In contrast, β-actin, tropomyosin, microtubule-associated protein MAP1A, and rhoA-binding kinase-α preferentially bind to NCAM 180 (Büttner et al., 2003). Neural cell adhesion molecules can also activate *per se* transmembrane-signalling reactions and thereby contribute to the initiation of cellular responses directed to the regulation of synaptogenesis and synaptic plasticity. L1 and NCAM, activate intracellular signaling pathways in the growth cone, mediated by two different members of the src family of nonreceptor protein tyrosine kinases (PTKs), pp60 (c-src) and p59 (fyn5,6), and this activation induces neurite outgrowth (Maness et al., 1996). NCAM is also known to stimulate neurite outgrowth by the activation of both the Ras-mitogen-activated protein kinase (MAPK) pathway and the fibroblast growth factor (FGF) receptor-PLCg-PKC pathway (Kolkova et al., 2000). NCAM also has marked influence on both the structure of dendritic spines and their post synaptic densities (Stewart et al., 2010).

3.2 Structural plasticity

The term neuronal structural plasticity refers to all types of changes, which modify the shape and structure of the central nervous system (CNS). These morphological changes can be organized in different levels: (a) adult neurogenesis (proliferation of neuronal precursors, neuronal migration and incorporation to functional neuronal circuits) (b) neuritic remodeling (axonal and dendritic outgrowth/retraction) and (c) synapse turnover (synaptogenesis and synaptic removal); (McEwen and Gianaros, 2011).

3.2.1 Adult neurogenesis

Adult neurogenesis involves recruitment of new neurons to functional circuits (Aimone et al., 2006). The continuous production and incorporation of new neurons to the adult central nervous system occurs mainly in two restricted regions: The subventricular zone of the lateral ventricle (SVZ) (Alvarez-Buylla et al., 2000), which produces granule and periglomerular neurons which, through the rostral migratory stream, migrate and become integrated into the olfactory bulb, and the subgranular

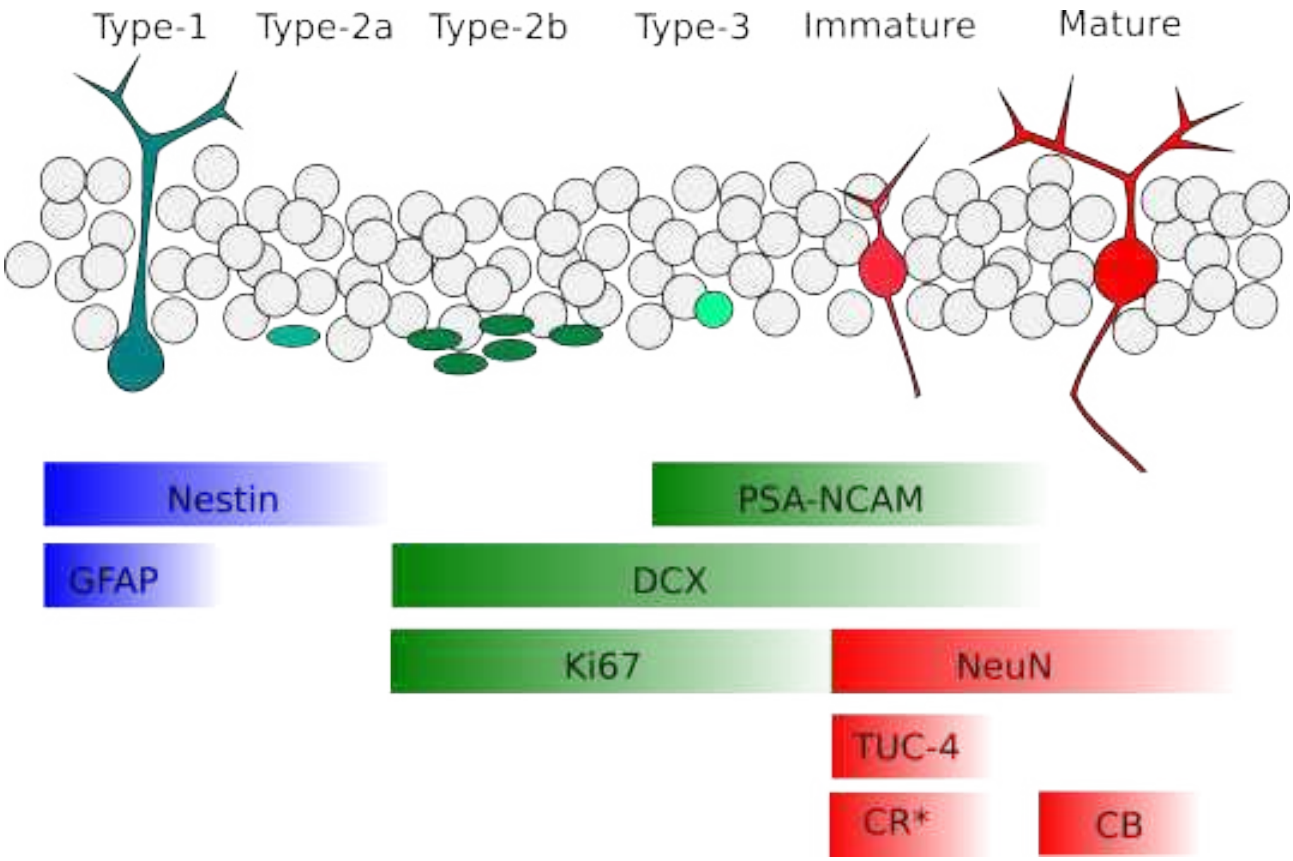

Fig. 3.1: Markers of neurogenesis in the SGZ of adult rodents
Asterisk indicates that calretinin is only expressed as an immature neuronal marker in the SGZ of mice and not in the SGZ of rats.

zone of dentate gyrus (SGZ) in the hippocampus (Gage et al., 1998), which produces granule neurons that incorporate to the granule cell layer. Several investigators also have reported evidence for adult neurogenesis in other areas of cerebral cortex, such as the neocortex or the piriform cortex. Different techniques have been used to identify neurogenesis in these areas, where it is likely to occur at a relatively low rate when compared with the SVZ and SGZ. The use of 3H-thymidine autoradiography or bromodeoxyuridine (BrdU) labeling and antibodies that detect immature neuronal markers and the subsequent analysis of labeled cells by electron and confocal microscopy, found double-labeled cells in the adult neocortex of several mammalian species, including hamsters, rats and macaques (Kaplan, 1981; Huang et al., 1998; Gould et al., 1999b, 2001; Dayer et al., 2005). However, several studies have been unable to replicate these findings (Rakic, 1985; Ehninger and Kempermann, 2003; Kodama et al., 2004; Kornack and Rakic, 2001; Bhardwaj et al., 2006). Moreover, other techniques as retroviral and 14C labeling, have also failed to find positive evidence for cortical neurogenesis in adults (Gould, 2007).

3.2.2 Neurite remodeling

Dendrites represent the location where neurons receive their main synaptic input. The geometry of the dendritic arbour influences the input that a neuron receives by modeling competitive interactions

of the innervating axons (Hume and Purves, 1981). Some dendrites display protrusions denominated dendritic spines, small morphological specializations considered to receive excitatory synaptic input. Studies *in vivo* have shown that there is a baseline turnover of spines, which is increased after sensory deprivation (Trachtenberg et al., 2002; Keck et al., 2008). In addition, changes in spine morphology and head size have been related to long-term potentiation (LTP; (De Roo et al., 2008b)). Plasticity associated with cognitive functions, aversive experiences or brain repair involves dynamic remodeling of dendritic and axonal arbors, including branch formation/elimination, as well as collateral branching and spine remodeling (Wong et al., 2000; Diana et al., 2007; Cline and Haas, 2008; Williams and Atkinson, 2008).

3.2.3 Synapse turnover

Synaptic plasticity is a concept that describes changes in the efficacy of synaptic transmission, including also the structural reorganization of synapses. Neurons communicate through synapses, and this communication generates action potentials near the cell body, which sub-sequentially propagate down the axon, opening Ca^{2+} channels that induce the release of vesicles containing neurotransmitters. Synapses are regulated by short (from tens of milliseconds to several minutes) and long term mechanisms that can lead to a decrease or an increase in synaptic strength. There are several forms of short term plasticty: 1) Synaptic facilitation, which consist in a rapid increase of synaptic strength when two action potentials concur a few milliseconds apart and which lasts tens of millisecons. This facilitation is due to the slow return of calcium to the basal levels. 2) Synaptic depression, which involves a decrease in the amount of neurotrasmitter released. 3) Synaptic potentiation and augmentation, which increase the amount of neurotransmitter released, but at different time scales. Finally, 4) an slower time course of the potentiation can lead to a post-tetanic potentiation (Zucker and Regehr, 2002).

The long-term mechanisms have received more attention during the last years. These mechanisms include a long-lasting increase (long-term potentiation; LTP) or a decrease (long-term depression; LTD) of the synaptic strength. They involve the transmission of a signal, by p42 MAPK, which can be transported to the nucleus and phosphorylate nuclear targets, inducing the transcription of specific genes (Pittenger and Duman, 2008). These changes in the strength of the synaptic transmission have been related to memory formation. The inhibition of LTP in the hippocampus through a local infusion of AP5 (a N-methyl-D-aspartate (NMDA) receptor antagonist) produced a profound impaired learning in the Morris water maze (Morris, 1984). Other molecules, such as the protein kinase PKM zeta and the NMDA receptor subunit NR1, have also been related to the blockade of LTP and spatial memory formation (Shimizu, 2000). These experiments led to the formulation of the "synaptic plasticity and memory hypothesis" by Morris and colleagues:

"Activity-dependent synaptic plasticity is induced at appropriate synapses during memory formation, and is both necessary and sufficient for the information storage underlying the type of memory mediated by the brain area in which that plasticity is observed."

4 Molecular mechanisms involved in triggering structural plasticity

4.1 Neurotrophins

Trophic factors are molecules that promote growth and survival of cells (Purves et al., 2008). There are several families of trophic factors, according to which receptor they activate: Neurotrophins, Epidermal Growth Factor, FGF, Bone Morphogenetic Proteins, Insulin-like Growth Factor, neurotransmitters and neuropeptides, cytokines and non-peptidic hormones (Sizonenko et al., 2007). In the CNS, the most relevant trophic factors are the neurotrophins, which mainly act through the tropomycin receptor kinase (Trk) receptors. The "neurotrophic hypothesis" states that the correct supply and availability of neurotrophins directs the formation of an appropriate number of connections, which will determine neuronal survival (Purves et al., 2008). Rita Levi-Montalcini and Viktor Hamburger discovered in the early 1950s the first molecule that supported the assumptions of the neurotrophic hypothesis: the nerve growth factor (NGF). They proved that the addition of this molecule to the medium of a ganglion organotypic culture, promoted both the neuronal survival and neurite outgrowth (Levi-Montalcini and Cohen, 1956). In addition to NGF, there are three other neurotrophins: neurotrophin-3, neurotrophin-4/5 and brain-derived neurotrophic factor (BDNF). Neurotrophins are polypeptides that homodimerize and have a mature and an immature form, each mediating different signaling cascades (Russo et al., 2009), which are involved in axon guidance (Baier and Bonhoeffer, 1992), clustering of postsynaptic ion channels (Elmariah et al., 2004), the correct maintenance and proliferation of dendritic spines (Danzer et al., 2008; Chakravarthy et al., 2006) or LTP (Fan et al., 2005). Therefore, it is accepted that neurotrophic dysfunction may underlie degenerative diseases such as Parkinson's disease, amyotrophic lateral sclerosis, Alzheimer's disease or Huntington's disease. (Arancio and Chao, 2007).

4.2 Cell adhesion molecules

Neuronal structural plasticity is largely dependent on cell adhesion molecules. CAMs are proteins located on the cell surface, which are involved in stabilizing and modulating cellular interactions with other cells and with the extracellular matrix. They are critical for the assembly of CNS architecture during developmental stages and are critical for the proper function of the mature nervous system. There are four important families of adhesion proteins according to their functional and structural resemblance. These families of CAMs are: (a) The immunoglobulin superfamily, which includes NCAM and L1; (b) Integrins; (c) Cadherins; and (d) Selectins (Walsh and Doherty, 1997; Murase and Schuman, 1999; Chothia and Jones, 1997). Among CAMs, NCAM is the most studied protein regarding cellular recognition processes and it is expressed on the surface of most neurons (Hoffman et al., 1982; Friedlander et al., 1986). NCAM is a surface glycoprotein (Gascon et al., 2007; Maness and Schachner, 2007; Katidou et al., 2008), which presents three major isoforms, generated by alternative splicing, denominated NCAM 120, NCAM 140 and NCAM 180, based on their molecular weights (Gegelashvili et al., 1990; Olsen et al., 1993; Kramer et al., 1997). All three isoforms share

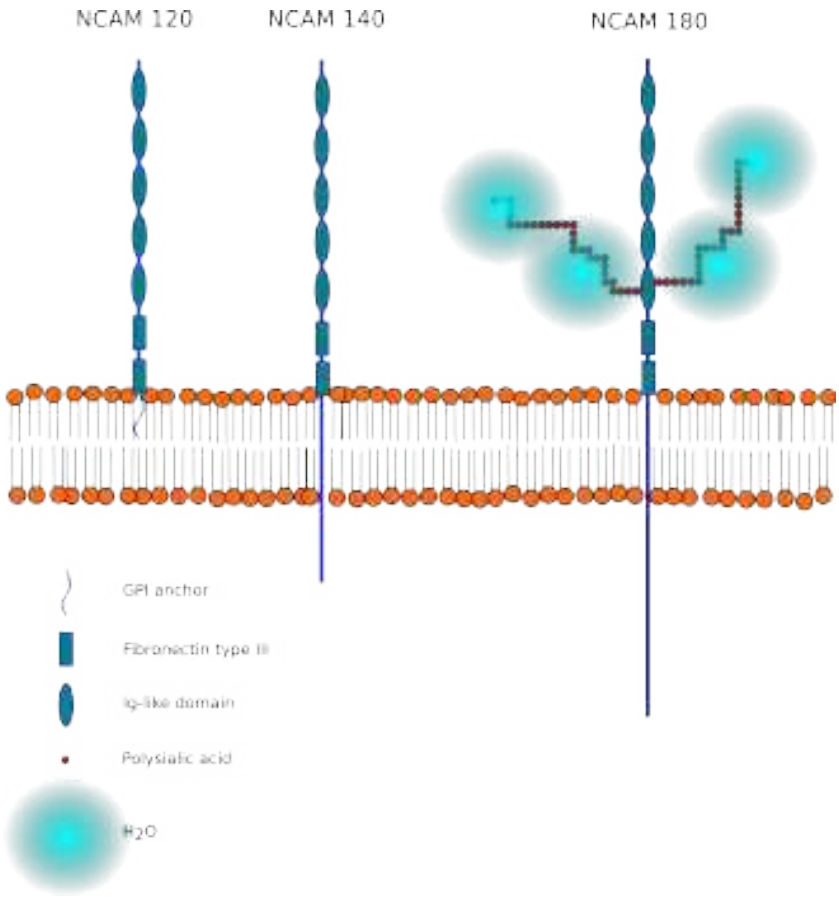

Fig. 4.1: NCAM isoforms

identical extracellular structures, consisting on five immunoglobulin-like domains and two fibronectin-type III repeats. The extracellular domain is a globular structure composed by around 70-110 amino acids. Both NCAM 140 and NCAM 180 isoforms contain a transmembrane and an intracellular domain, but the NCAM 120 isoform lacks those domains and it is anchored to the cell membrane via a glycosylphosphatidylinositol (GPI) linkage. Consequently, only NCAM 140 and NCAM 180 isoforms are detectable in synaptosomal membranes (Persohn et al., 1989; Rougon et al., 1990). NCAM 180 has a long cytoplasmic domain, it is predominantly expressed on mature neurons and it is particularly abundant at sites of cell contact and postsynaptic densities (Persohn et al., 1989); NCAM 140 has a shorter cytoplasmic domain and it is particularly expressed on developing neurons, mediating growth cone guidance and neurite outgrowth responses, although it can also be found in mature neurons, both in pre- and postsynaptic densities (Persohn et al., 1989; Doherty et al., 1992). While NCAM 140 is expressed both by neurons and glia (Williams et al., 1985), NCAM 120 is predominantly expressed by glial cells (Bhat and Silberberg, 1986; Walmod et al., 2004). NCAM molecules interact with like molecules (homophilic interaction) and non-like molecules (heterophilic interaction) on neighboring cells or on the extracellular matrix to regulate their position and dynamic interactions with other cells by diverse signal transduction pathways (Walmod et al., 2004). The functional properties of NCAM are strongly influenced by the addition of long chains of a complex sugar, the polysialic acid (Rutishauser, 1996; Bonfanti, 2006; Gascon et al., 2007).

4.3 The polysialylated form of NCAM (PSA-NCAM)

The NCAM protein core is subjected to several post-translational modifications, such as phosphorylations, addition of the carbohydrate epitopes L2 or HNK-1, sulfation, glypiation and glycosylation (Rougon et al., 1990; Walmod et al., 2004). One of the most important glycosilation events is the addition of PSA. This unique and highly regulated post-translational modification of NCAM is critical during brain development, neural regeneration and plastic processes, including learning and memory (Bork et al., 2007; Hildebrandt et al., 2007). In mammals, this molecule is a linear homopolymer of α-2,8-linked N-acetylneuraminic acid, which chains can extend to lengths ranging from 50 to 150 units (Kiss and Rougon, 1997; Livingston et al., 1988). PSA is attached exclusively to NCAM at the fifth immunoglobulin-like domain (Hoffman et al., 1982; Acheson et al., 1991). The degree of NCAM polysialylation is tightly regulated: PSA-NCAM levels are high during brain development but there is a progressive reduction until adulthood (Rutishauser, 1996; Bonfanti, 2006; Gascon et al., 2007). The synthesis of PSA in the Golgi compartment is catalyzed by two resident polysialyltransferases, ST8SiaII (also known as STX) and ST8SiaIV (also known as PST). Both enzymes are strongly expressed during prenatal development and this expression is dramatically downregulated after the perinatal period. During adulthood, the expression of ST8SiaII and ST8SiaIV is

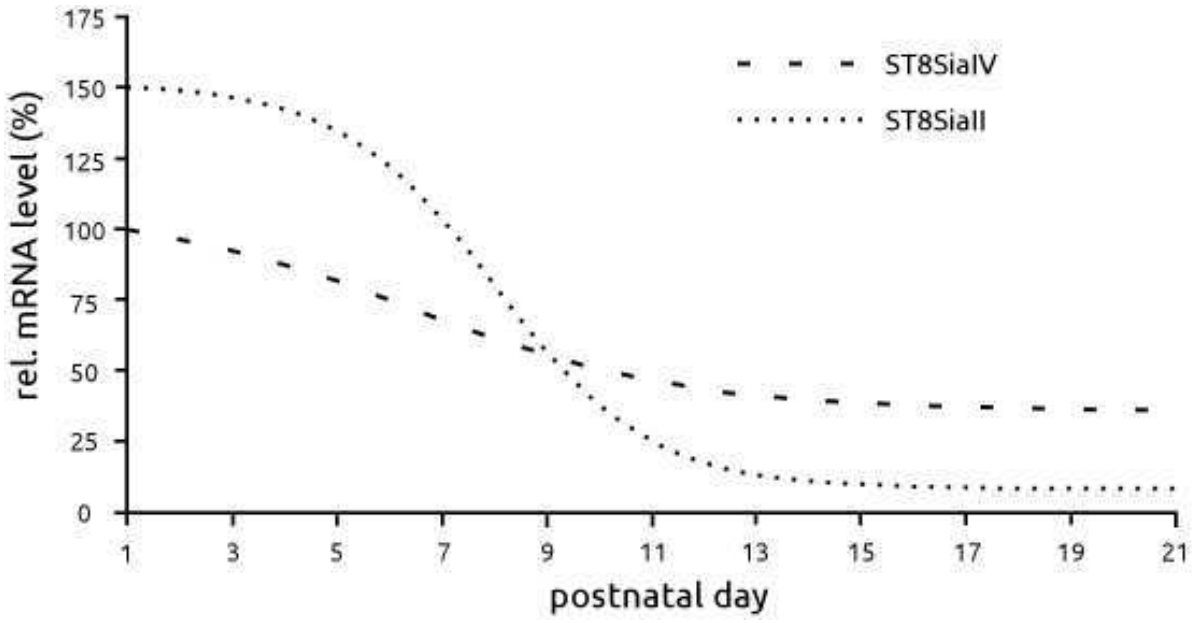

Fig. 4.2: Expression of the two polysialyltranferases during development

low, but the later is more abundant than the former (Nakayama and Fukuda, 1996; Kojima et al., 1996; Hildebrandt et al., 1998). PSA has been found also on other proteins: the α-subunit of the rat brain voltage-sensitive sodium channel (Zuber et al., 1992), SynCAM (Galuska et al., 2010), podocalyxin (Vitureira et al., 2010) and the polysialyltransferases ST8SiaII and ST8SiaIV, which are autopolysialylated *in vivo* (Close et al., 2000). However, NCAM is the principal carrier of PSA in the nervous system (Rutishauser, 1996, 2008). Carboxyl groups give their peculiar biochemical characteristics and negative charge to PSA, attracting water and ionic molecules. This large hy-

drated volume inhibits cell-cell apposition (steric impediment), which prevents both the homotypic and the heterotypic binding of NCAM (Yang et al., 1992). Therefore, the post-translational addition of PSA on NCAM increases the range and magnitude of intermembrane repulsion by increasing the nonspecific repulsive force between cells (Johnson et al., 2005). These anti-adhesive properties of PSA-NCAM are particularly evident during neuronal migration. This molecule is expressed by neural precursors migrating from the SVZ to the olfactory bulb by a mechanism in which the cells move forward in a stream by using each other as a substrate and PSA-NCAM enhances the cycles of adhesion and de-adhesion (Rousselot et al., 1995; Petridis et al., 2004). PSA-NCAM expression also participates in the axophilic migration of luteinizing hormone releasing neurons to the forebrain (Yoshida et al., 1999). Moreover, PSA-NCAM plays a permissive role in axon guidance, reducing the fasciculative interactions between axons and allowing them to respond more effectively to a variety of extrinsic signals and to reach their target, both in the peripheral and in the central nervous systems (Rutishauser and Landmesser, 1996; Kiss and Rougon, 1997; Brusés and Rutishauser, 2001; Rutishauser, 2008).

Multiple lines of evidence implicate NCAM in synaptic functions and suggest a role for PSA-NCAM in synaptic strength modulation (Dalva et al., 2007; Dityatev et al., 2008). One possibility is suggested by the finding that enzymatic removal of PSA (by Endo-N-acetylneuraminidase; EndoN) or its blockade with antibodies, prevents LTP, LTP-associated formation of perforated synapses and LTD in the CA1 region of the hippocampus (Becker et al., 1996; Muller et al., 1996; Dityatev et al., 2004). Hippocampus-dependent spatial learning protocols increase the expression levels of PSA-NCAM (Venero et al., 2006) and mice deficient in one of the two polysialyltransferases ST8SiaII or ST8SiaIV show normal basal synaptic transmission but defects in LTP and LTD in CA1 (Eckhardt et al., 2000; Angata et al., 2004). Functionally, PSA weakens homophilic and heterophilic NCAM interactions (Rutishauser, 1996, 2008), indicating that PSA-NCAM might mediate a downregulation of adhesion, which is a prerequisite for the structural changes underlying plasticity. In this model, PSA linkage would act as a switch between structural stability and plasticity.

On the other hand, it has been shown that the removal of PSA induces neuronal differentiation (Seidenfaden et al., 2003; Petridis et al., 2004) and increases BDNF binding capacity (Burgess and Aubert, 2006). These results led to the enunciation of the "shielding" hypothesis for the action of PSA: The addition of PSA to NCAM may cover membrane receptors, such as TrkB or p75, limiting their action on the portion of plasma membrane where PSA is expressed. Since BDNF increases dendritic spine density (Tyler and Pozzo-Miller, 2003) and its diffusion in the nervous parenchyma is very restricted (Horch and Katz, 2002), it is possible that PSA-NCAM expression may regulate some features of structural plasticity by limiting the binding of BDNF and other neurotrophins to their receptors.

PSA-NCAM might also indirectly regulate synaptic plasticity through interactions with other synaptic proteins. Currently, NCAM and PSA-NCAM have been shown to interact with a large number of molecules or signalling pathways that regulate aspects of LTP including AMPA receptors (Vaithianathan et al., 2004), NMDA receptors (Hoffman et al., 1998), brain-derived neurotrophic

factor (BDNF)-tyrosine receptor kinase B (TrkB) signaling (Muller et al., 2000b), the spectrin-based scaffold (Wechsler and Teichberg, 1998; Sytnyk et al., 2002, 2006), the FGF receptor (Cambon et al., 2004) and the non-receptor tyrosine kinase Fyn (Beggs et al., 1997). Unfortunately, in most of these cases, a direct link between the interactions and LTP has not been demonstrated. The exception is BDNF-TrkB signalling, where defects in LTP caused by enzymatic PSA removal are rescued by exogenous treatment with BDNF, indicating that PSA-dependent defects in LTP are due to an impaired BDNF signaling (Muller et al., 2000a). Nevertheless, the numerous interactions between NCAM and LTP-influencing pathways show that NCAM is a multifunctional protein capable of influencing synaptic plasticity at multiple levels (Dalva et al., 2007). PSA expression is also important in the development and function of the immune system. For instance, human NK cells modulate NCAM expression and its degree of polysialylation according to their activation state (Drake et al., 2008, 2009). PSA and NCAM have also a prominent role in oncology. These two molecules have been found in different human cancers, including small-cell lung carcinomas and multiple myeloma (Miyahara et al., 2001; Suzuki et al., 2005). As commented before, although PSA-NCAM levels are very high during the embryonic and early postnatal development of the mammalian brain, the expression of this molecule during adulthood remains relatively high in brain regions that display a high degree of neuronal plasticity, including the mPFC, the hippocampus or the amygdala (Bonfanti, 2006; Varea et al., 2005, 2007b, 2009; Nacher et al., 2002c). PSA-NCAM expressing cells in these regions mainly show a multipolar morphology, although their density is not homogeneous. In the mPFC there is a higher density of PSA-NCAM expressing cells in deep layers than in superficial layers (Varea et al., 2005) and there is a higher PSA-NCAM expression in the neuropil of the IL and the PrL than in the cingulate cortex. In the hippocampus there is a higher density of PSA-NCAM expressing cells in the ventral hippocampus (Nacher et al., 2002b) and a more intense neuropil expresion in the stratum lucidum or lacunosum moleculare than in other hippocampal layers. A higher neuropil expression of PSA-NCAM can also be found in the medial division of the amygdala when compared with the rest of amygdaloid nuclei (Nacher et al., 2002c). The expression of PSA-NCAM has been studied in other regions as well, such as the hypothalamus, where it is expressed by neurons and glia (Theodosis et al., 1991) or the suprachiasmatic nucleus, where it fluctuates rhythmically (Glass et al., 2003). It is also present in a subpopulation of primary sensory neurons (Quartu et al., 2008) and in the adult spinal cord gray matter (Seki and Arai, 1993b). PSA-NCAM is also expressed in certain regions of sub-ependymal tissue and at the surface of CNS ventricular cavities, on both sides of the ependymal wall (Aaron and Chesselet, 1989; Bonfanti et al., 1992; Szele et al., 1994). This molecule is also expressed in the adult optic nerve and the retina by astrocytes and Muller cells, as well as in the neuropil of specific retinal layers (Sawaguchi et al., 1999).

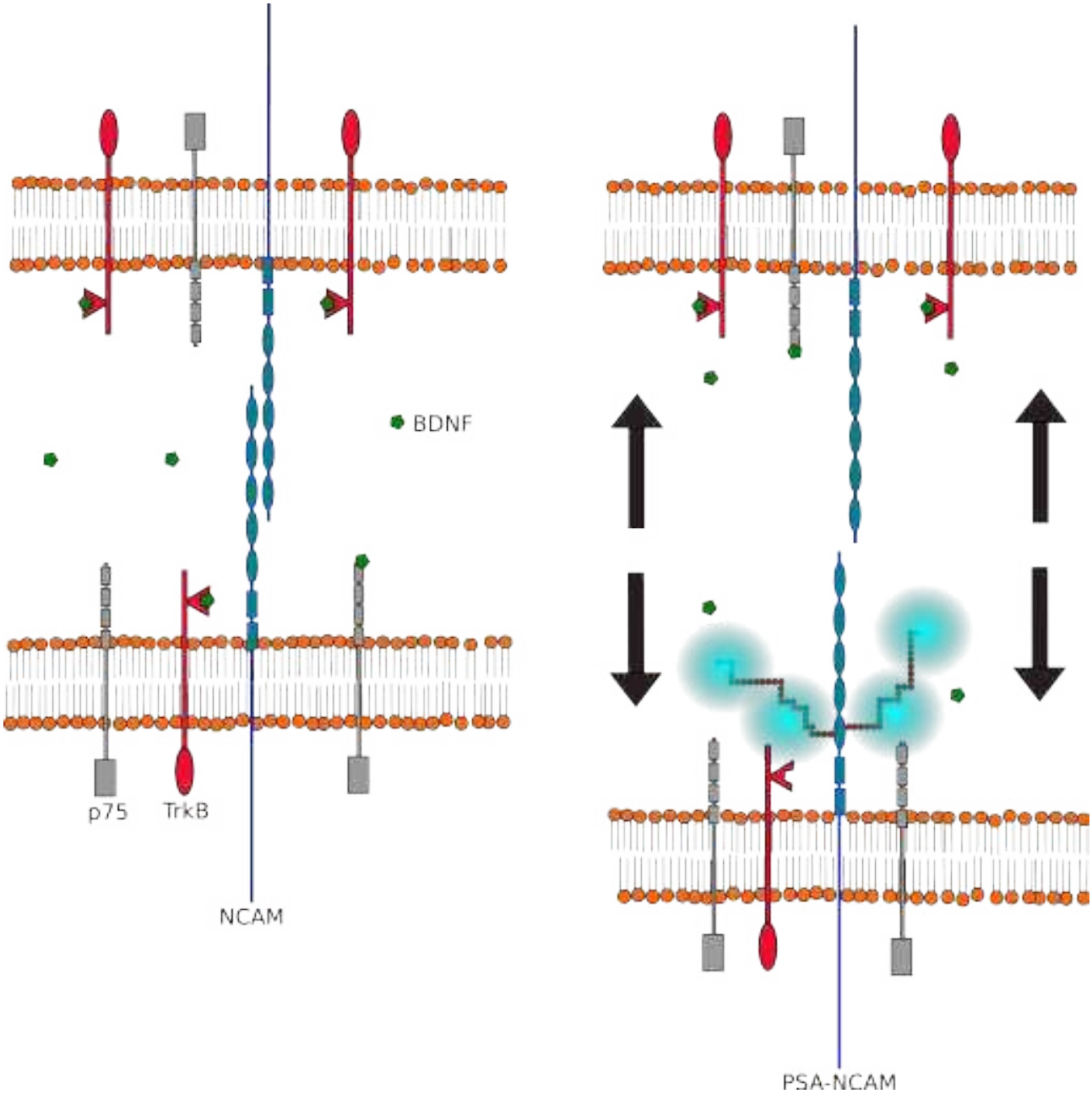

Fig. 4.3: PSA-NCAM functional hypothesis

5 Modulation of structural neuronal plasticity

5.1 Modulation of adult neurogenesis

Several intrinsic and extrinsic factors modulate the production of new neurons in the adult CNS and they are particularly well characterized in the hippocampus. Increases in the survival of newborn neurons in the SGZ have been found in rodents exposed to an enriched environment (Kempermann et al., 1997). Physical exercise, such as running, also promotes SGZ neurogenesis by increasing cell proliferation and the survival of the new granule neurons (Van Praag et al., 1999). Certain hippocampus-dependent learning tasks also increase the survival of new granule neurons that have been generated just before the training (Gould et al., 1999a; Leuner et al., 2003). Consequently, it has been proposed that integration of new neurons into functional circuits might be involved in learning and memory processes (Aimone et al., 2006). Pharmacological blockade of NMDA receptors also increases neurogenesis in the adult and aging SGZ (Cameron et al., 1995; Nacher et al., 2003). Besides, various neurotransmitters including dopamine, serotonin, acetylcholine, glutamate, neuropeptides and gaseous signaling molecules, have been implicated in regulating adult neurogenesis (Kempermann, 2002). Glutamate may influence neural progenitor cells either directly, as in cultured human neural progenitor cells, which respond to glutamate by increasing their neurogenic potential; or indirectly, by stimulating the production of neurotrophic factors and other signaling molecules in neurons, like BDNF, which increases in the hippocampus in response to exercise and cognitive stimulation and may mediate the increased survival of newly-generated neurons (Mattson, 2008). Recent studies have revealed GABA as a key signal within the neurogenic niche, which regulates the development of neural progenitor cells (Ge et al., 2007).

Elevated glucocorticoid levels and chronic stress also lead to decreases in cell proliferation in the SGZ (Duman et al., 2001). These effects on neurogenesis are not restricted to adrenal hormones, other hormones, such as estrogen and prolactin, also regulate adult neurogenesis (Ming and Song, 2005). Finally, all major classes of antidepressants stimulate neurogenesis in the dentate gyrus of adult rodents, as well as in non-human primates (Perera et al., 2008). Serotonin (5HT) modulation through chronic antidepressant treatment, increases neurogenesis in both the SGZ and the SVZ (Nasrallah et al., 2010; Couillard-Despres et al., 2009), and this increase appears to be required at least for part of the behavioral improvement observed in the treated animals (Santarelli et al., 2003). However, other studies are in disagreement with these findings and have found that antidepressants do not produce an increase in neurogenesis in the SGZ (Marlatt et al., 2010; Navailles et al., 2008). It has to be noted that most of the experiments are performed using young-adult rodents, usually 2-3 months old. Consequently, there is controversy on whether antidepressants, and specifically 5HT reuptake inhibitors, exhibit the same efficacy within different age groups. This is particularly interesting because aging reduces adult neurogenesis in the SGZ (Kuhn et al., 1996) and SVZ (Enwere et al., 2004; Jin et al., 2003). However, antidepressant treatments are not able to avoid this age-dependent decrease of neurogenesis, at least in the SGZ (Couillard-Despres et al., 2009; Cowen et al., 2008). The decrease of neurogenesis during aging may occur in response to chronically

elevated levels of glucocorticoids (Cameron and Gould, 1994). In fact, reducing corticosteroid levels in aged rats can restore the rate of cell proliferation in the SGZ (Cameron and McKay, 1999).

5.2 Modulation of structural remodeling

The structural remodeling of neurons is a basic mechanism of neural plasticity that allows the brain to cope with a changing environment (McEwen, 2000a). This morphological remodeling can occur at different levels, involving changes in the length of the dendritic branches, the complexity of the dendritic arbor, the density of dendritic spines or their morphology (Fu and Zuo, 2011). During the last 20 years, it has been shown that excitatory neurons experience structural plasticity when animals are subjected to a variety of experimental conditions. Animals raised in environmental enriched conditions have an increased dendritic branching in the visual cortex (Markham and Greenough, 2004). Different learning paradigms also influence neurite remodeling: Passive avoidance response increases spine number in the mid-molecular layer of the dorsal dentate gyrus at different post-training times (O'Malley et al., 1998, 2000) and trace eye blink conditioning, an associative learning task, also increases the density of dendritic spines on the pyramidal cells in hippocampal CA1 region (Leuner et al., 2003). Fear conditioning, another learning paradigm, increases dendritic spine density in the lateral amygdala (Radley et al., 2006a). Moreover, there is a strong correlation between long-term potentiation (LTP) and morphological changes in dendritic spines. Several studies have shown the possible association between this structural remodeling with LTP (Muller et al., 2000b; Yuste and Bonhoeffer, 2001). Abundant experiments have demonstrated that chronic stress affects dendritic branching: it induces dendritic atrophy in various hippocampal regions, like retraction and simplification of dendrites of pyramidal neurons in the CA3 region (McEwen, 1999, 2000b). Interestingly, the effects of chronic stress on neurite structure can be reverted or blocked by antidepressant treatment. Daily treatment with tianeptine, an atypical antidepressant (a selective serotonin reuptake enhancer), prior to stress sessions, prevented the structural effects of chronic stress in hippocampal CA3 pyramidal dendrites (Watanabe et al., 1992). The effects of chronic stress and antidepressants on neuronal structural remodeling will be further discussed later. Estrogens play also an important role in dendritic and spine remodeling within the CNS. Ovariectomy decreases the density of dendritic spines in the CA1 region of the hippocampus, but not in CA3, and this effect can be reversed by estradiol replacement (Wallace et al., 2006). Furthermore, an increment of spine and synapse density occurs within the natural late proestrous (Moult and Harvey, 2008), when estrogen levels are high. In the rodent mPFC, ovariectomy decreases spine densities in pyramidal neurons (Wallace et al., 2006). Long-term cyclic treatment with estradiol in ovariectomized rhesus monkeys, does not affect total dendritic length and branching in the mPFC, but increases apical and basal dendritic spine density (Hao et al., 2006). The structure of amygdaloid neurons is also a target for sexual steroids: In the posterodorsal medial amygdala, dendritic spine density increases following estradiol injections and this effect is potentiated by progesterone (De Castilhos et al., 2008). Age also influences dendritic and spine structure: Aging induces a reduction in spine density in the

mPFC (Markham and Juraska, 2002; Markham et al., 2002, 2005). By contrast, although aged rodents display significantly more dendritic material in basolateral amygdala, aging does not appear to influence spine density in this region (Rubinow et al., 2009).

5.3 Modulation of synaptic plasticity

Changes in synapse number and morphology are frequently associated with learning. Raising animals in an enriched environment or training them on a motor skill-learning task results in increases in the number of synapses in the visual cortex and in various hippocampal areas, including the dentate gyrus and CA3 (Markham and Greenough, 2004; Bruel-Jungerman et al., 2007). Stereological electron microscopy studies of the hippocampal dentate gyrus have shown that training rats to find a hidden platform in a Morris water maze induces a significant but transient increase in axo-spinous synapse density and in the ratio of synapse per neuron (Eyre et al., 2003). There is also strong evidence pointing at different hormones as major players in synaptic remodeling. Chronic stress and glucocorticoids strongly influence synaptic plasticity (McEwen, 2005). Other steroid hormones, such as the estrogens, also influence synaptic plasticity by increasing the density of axospinous synapses in the hippocampal stratum radiatum of CA1, both after estradiol treatment and during proestrus, when estradiol levels are naturally increased (Woolley and Mcewen, 1992). Aging also has a notorious influence in synaptic plasticity, especially in the hippocampus, where a decrease in the number of synaptic contacts in the mid-molecular layer of dentate gyrus has been found in aged animals (Rosenzweig and Barnes, 2003). Similarly, the numerical density of excitatory and inhibitory synapses is reduced in the neuropil of the primate prefrontal cortex during aging (Peters et al., 2008).

6 Structural plasticity of interneurons

As we have commented before, neuronal structural plasticity is known to have a major role in learning and memory, in the response to aversive experiences and in process of brain damage and repair (McEwen and Gianaros, 2011). However, the study of how these structural changes occur has been focused mainly on the major cell type in the brain, the excitatory neurons. Little attention has been paid to interneurons, despite the importance of these cells in the control of the activity of principal neurons (Buzsáki et al., 2007). It is known that a certain level of structural plasticity in inhibitory circuits must be involved in many psychiatric and neurological disorders (Kalus et al., 2002). In fact, it has been proposed that the aetiology of these disorders, from epilepsy to schizophrenia, may be based on a disruption of the excitatory/inhibitory balance and, therefore, the study of the structural changes of the inhibitory system is relevant to the understanding of these disorders (Nestler et al., 2002).

In this line, most of the studies on interneuronal structural plasticity have been focused on different neurological and neuropsychiatric disorders. A model of post-traumatic epilepsy called

"undercut" causes changes in the structure of interneurons, such as shrinkage of dendrites, decrease in axonal length and in the percentage of axonal boutons, as well as loss of inhibitory synapses on pyramidal neurons (Prince et al., 2009). In schizophrenic patients, changes in the structure of different groups of parvalbumin interneurons have been reported. Namely, decreases in soma size and the dendritic arbour, including reduced number of primary dendrites and a global reduction of the dendritic length (Kalus et al., 2002). A recent study from our laboratory has shown that mice subjected to chronic restrain stress experiment a decrease of interneuronal dendritic arborization in the amygdala (Gilabert-Juan et al., 2011). Other studies have reported decreases of interneuron density of different cerebral regions in different psychiatric disorders, as well as reductions in certain interneuronal subpopulations, like those expressing calbindin (Chance et al., 2005; Benes and Berretta, 2001). These changes in the cell number can be due to different factors, such as increased cell death, decreased neurogenesis or decreased expression of their molecular markers. Moreover, the possibility that some of these interneurons may be able to change the calcium binding proteins or neuropeptides that they express should also be contemplated.

In addition, recent work *in vivo* has shown that structural remodeling of interneurons also occurs in the adult brain, without the intervention of an external perturbation (apart from the unavoidable anesthesia). Using multiphoton microscopy in mice with cranial windows located on the visual or somatosensory cortices, it has been demonstrated that a wide range of different subpopulations of interneurons show structural changes, such as elongation/retraction of dendritic branch tips, whose dynamic is increased after sensory deprivation (Lee et al., 2008; Chen et al., 2011a).

Although dendritic spines once were thought to be a distinctive feature of principal neurons, some subpopulations of interneurons, such as those expressing somatostatin display dendritic spines (Kawaguchi et al., 2006). Unfortunately, studies focused on interneuronal dendritic spines are still scarce and we do not have abundant information on whether their synaptic inputs are similar to those found contacting the spines of excitatory neurons. Only a recent study has described that a subpopulation of interneurons in the visual cortex expressing VIP display dendritic spines, which receive mainly a glutamatergic input, and that their density and turnover rate are dynamic (Keck et al., 2011).

7 Implication of neuronal structural plasticity in depression and antidepressant treatment

Since the 1960s, major depression diagnoses is based on a subjective and variable set of symptoms such as depressed mood, irritability, feeling of hopelessness or decreased interest in pleasurable stimuli. These symptoms have to be reported for more than 2 weeks and they should disrupt normal social or occupational function (American-Psychiatric-Association, 2000). Around a 40-50% of the risk for depression is genetic (Fava and Kendler, 2000), however, non-genetic factors such as stress or emotional trauma have been implicated in the aetiology of this disorder (Akiskal et al., 2000; Nemeroff, 2007). Therefore, animal models of depression rely on stress response or on the action

of antidepressants (Nestler et al., 2002). One of the most studied animal models of depression is chronic stress (Willner, 1997). Consequently, the study of this aversive experience is highly relevant to understand human depressive illness. The stress response consists in the activation of the autonomic nervous system and the hypothalamo-pituitary-adrenal (HPA) axis, which usually allows body homeostatic maintenance. Glucocorticoid secretion is accomplished by HPA axis activation and has an important role in controlling the correct stress response.

Structural remodeling has been repeatedly found both in depression and after antidepressant treatments. Decreases in the volume of certain regions, such as in the hippocampus, the medial prefrontal cortex or the amygdala have been observed in both depressed human patients (Phillips et al., 2003) and chronically stressed animal models (Uno et al., 1994; Isgor et al., 2004; McEwen, 2008). This reduction of hippocampal volume is probably the reflection of changes in the structure and connectivity of hippocampal neurons. In fact, chronic stress also induces contrasting patterns of dendritic and spine remodeling in the hippocampus, mPFC and the amygdala of adult rats: Chronic stress induces dendritic atrophy in various hippocampal regions, including retraction and simplification of dendrites of pyramidal neurons in the CA3 region, CA1 pyramidal cells and granule cells (McEwen, 1999; Sousa et al., 2000). Chronic stress also induces dendritic atrophy in the mPFC (Radley et al., 2004; Cook and Wellman, 2003) and a reduction in spine density on proximal basal dendrites of pyramidal neurons in the rat prelimbic cortex (Perez-Cruz et al., 2009). On the contrary, it promotes dendritic growth in some regions of the amygdala (Vyas et al., 2002) and spinogenesis in the basolateral amygdaloid nucleus (Mitra et al., 2005). These results show the complexity of stress biology, which is regulated by multiple mediators and multiple systems, mediators that include the excitatory amino acids, acting via NMDA receptors. The modulation of SGZ neurogenesis and the neuritic remodeling induced by stress may be dependent on NMDA receptor activation, in fact, adrenal steroids and NMDA receptor activation regulate neurogenesis through a common pathway and NMDA receptor blockade prevents stress-induced dendritic remodeling (McEwen, 1999). The structural effects caused by chronic stress are lasting, but they are reversible if the stressful experience ends. However they may become irreversible if the stress persists for a very prolonged time. The alterations in dentate gyrus neurogenesis and hippocampal CA3 dendritic atrophy are normalized after 1 month of recovery (Sousa et al., 2000). Similarly, the dendritic atrophy in the mPFC is reversible after 3 weeks of recovery period (Radley et al., 2005a). On the contrary, there is a persistent dendritic hypertrophy effect in the basolateral amygdala, even after 21 days of recovery (Vyas et al., 2004). Structural changes induced by stress in experimental animals are reverted by antidepressant treatment. This reversion does not only occur on neurogenesis, as we have commented before, but also on the morphological remodeling. In this line, antidepressant treatment produces an increase of dendritic spine density of CA1 and CA3 pyramidal neurons in the hippocampus (Magariños et al., 1999; Hajszan et al., 2005).

The mode of action of most antidepressant drugs is based on the monoamine hypothesis of depression, which posits that this disorder is caused by altered monoamine function in the brain. Antidepressants increase monoamine transmission acutely, either by inhibiting neuronal reuptake or

by inhibiting degradation. However, the relationship between depression and monoamine concentrations is more complex than previously thought. Although rapidly, the effects of antidepressants on monoamine metabolism therapeutic usually need weeks to take place (Nestler, 1998). Few years ago, a new hypothesis for depression was suggested, the "neuroplastic" hypothesis, which posits that in the aetiology of depression alterations in the structure of neurons are involved. In this line, antidepressants would revert these structural changes, promoting structural plasticity (Castrén, 2005) (Fig. 7.1). In fact, recent studies have demonstrated that NCAM and its polysialylated form mediate the effects observed after chronic stress or antidepressant treatments (Sandi and Loscertales, 1999; Sandi et al., 2003).

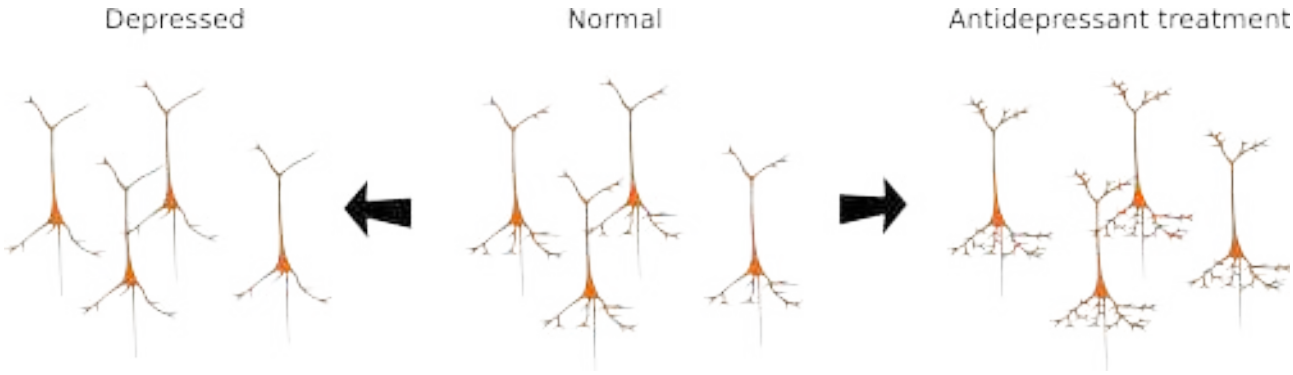

Fig. 7.1: Neuroplastic hypothesis of depression

The lack of information regarding the plastic structure of interneurons, and specially their implication in psychiatric disorders, prompted us to study the role of PSA-NCAM a plastic molecule intensely expressed in a subpopulation of interneurons in the adult brain, in different aspects of neuronal structural plasticity. If the neuroplastic hypothesis of depression is correct, the understanding of the remodeling of the structure of interneurons will be crucial to design new drugs to palliate this and other psychiatric disorders.

Part II. Objectives

The main objectives of this thesis are to study the influence of PSA-NCAM expression on neuronal structural plasticity and to evaluate the effects of the antidepressant fluoxetine on the expression of PSA-NCAM and other features of neuronal structural plasticity in the rodent brain. From these two main objectives, we derive the subsequent specific objectives:

1. To map the distribution and to analyze the neurochemical phenotype, structure and ultrastructure of PSA-NCAM expressing interneurons, comparing them with other interneurons.

2. To study the basal plasticity of inhibitory networks analyzing the expression of gephyrin, a protein specific of inhibitory synapses.

3. To study the ultrastructure of PSA-NCAM expressing cells in the paleocortex layer II.

4. To evaluate the divergent impact of the polysialyltransferases St8SiaII and St8SiaIV on the polysialylation of NCAM.

5. To analyze the effects of PSA depletion from NCAM using the enzyme Endo-N-acetylneuraminidase (EndoN) on the dendritic spine density of interneurons *in vivo* and on the turnover of these spines *in vitro*.

6. To analyze the effects of the antidepressant fluoxetine on different parameters of neuronal structural plasticity in the somatosensory cortex of young-adult rats, on different cerebral regions of middle-aged rats and on the hippocampus and the medial prefrontal cortex of young-adult transgenic mice displaying fluorescent interneurons.

Part III. MATERIAL & METHODS

8 Animals

8.1 Rats

Twelve male Sprague-Dawley rats (3 months-old, Harlan Interfauna Iberica) were used to study the effect of the selective serotonin reuptake inhibitor (SSRI) fluoxetine in the somatosensory cortex. Sixty male Wistar rats were used as follows: 14 to analyze the effects of fluoxetine on the middle-aged (8 months-old) brain, 6 (3 months-old) for electron microscopy analysis and 40 pups of postnatal day 10 (P10) for the preparation of hippocampal organotypic cultures.

8.2 Genetically modified mice

Sixty-eight GIN (GFP-expressing inhibitory neurons, Tg(GadGFP)45704Swn) (Oliva et al., 2000) male (3 months-old) mice were used in this thesis as follows: 12 received a chronic fluoxetine treatment, 6 were used to study the neurochemical phenotype of PSA-NCAM expressing neurons and 6 to study the dendritic arbour and spine density of these cells. Twenty-four mice were used to study the effects of Endo-N-acetylneuraminidase (EndoN) injected intracerebrally. In addition, 20 pups (P7) of this mice strain were used to prepare hippocampal organotypic cultures.

Four NCAMff+ (CaMKII) and four wild-type littermates (NCAMff-) males (3 month-old) were used to study whether PSA-NCAM expression was present in principal neurons. These mice were generated by a Cre-loxP recombination system to generate a mutant, in which the NCAM gene is ablated under the control of the CaMKII promoter (Bukalo et al., 2004). Since CamKII is expressed in the somata of excitatory neurons throughout the rodent brain, these animals did not express NCAM (and therefore neither PSA-NCAM) in excitatory neurons.

Five NCAM (−/−) mice and 5 wild-type littermates (NCAM+/+) on a C57BL/6J background (males, 3 months old) (Cremer et al., 1994) were used to study whether PSA expression in interneurons was associated to NCAM or to other putative polysialylated proteins. These animals were processed for double PSA-NCAM/GAD67 immunofluorescence as described below.

Five ST8SiaII knockout mice and five wild-type littermates were obtained through backcrossing with C57BL/6J mice for six generations (Angata et al., 2004), and the heterozygous mice were interbred. Similarly, five ST8SiaIV knockout mice and five wild-type littermates were generated (Eckhardt et al., 2000). These 20 males (5 knockout and 5 wild-type for each gene) were used to analyze the impact of these enzymes on the polysialylation of the adult rodent brain.

8.3 Housing conditions and bioethics

Rats and mice were housed in groups of 3 or 4 in our animal facility, maintained in a temperature and humidity controlled environment of light cycles, with ad libitum access to food and water. All animal

experimentation was conducted in accordance with the Directives 86/609/EEC and 2010/63/EU of the European Communities Council of November 24th 1986 and September 22nd 2010, respectively, on the protection of animals used for scientific purposes and was approved by the Committee on Bioethics of the Universitat de València. Every effort was made to minimize the number of animals used and their suffering.

9 *In vivo* treatments

9.1 Fluoxetine

Rat males were injected daily at 10 am intraperitoneally (IP) with a dose of 10 mg/Kg of fluoxetine hydrochloride (Ascent Scientific) in saline solution (0.9% NaCl) or only with saline, during 14 days. Animals were weighted every day. The day after the last IP injection they were transcardially perfused. The male mice receiving fluoxetine treatment were treated similarly, but with a dose of 20 mg/Kg.

9.2 EndoN

Twenty-four GIN mice were separated in 4 experimental groups (n=6). Under deep anaesthesia (5 mg/g xylazine and 0.5 ml/kg intraperitoneally), they were placed in a stereotaxic instrument (David Kopf Instruments) and received a stereotaxic intracerebral injection (using a Flexifil tapertip syringe; World Precision Instruments) of Endo-N-acetylneuraminidase (EndoN; 369 U/μl in glycerol; AbCys) or the vehicle solution (1μl; saline and glycerol 1:1) in the primary somatosensory cortex (Bregma -1.7 mm, Lateral $\pm$ 1.5 mm, Deep – 0.6 mm; (Paxinos and Franklin, 2001)). The needle was left in position for 1 minute and then 1 μl of the enzyme EndoN was injected over a one minute period into one hemisphere. After the injection was completed, the needle was left in place for 2 minutes to reduce reflux of the solution into the track of the injection needle and then withdrawn. The EndoN is a phage enzyme that specifically cleaves α-2,8-linked N-acetylneuraminic acid polymers with minimum chain length of 8. One group injected with EndoN and other injected with vehicle were perfused transcardially 2 days after the injection, while the other two groups were perfused after 7 days.

10 Histological procedures

10.1 Perfusion and microtomy techniques

Rats and mice were transcardially perfused under deep chloral hydrate anaesthesia, first for 1 minute with NaCl 0.9% and then with 4% paraformaldehyde in PB. In rats, the paraformaldehyde solution was delivered for 30 minutes with a flux of 10 ml/min and in mice it was delivered for 15 minutes with a flux of 4 ml/min. Thirty minutes after the perfusion, brains were extracted from the skull

and their hemispheres separated. Brain hemispheres destined to Golgi impregnation were washed in cold PB 0.1 M (4 ºC) for one day and then cut in 5 mm-thick coronal blocks, which were then impregnated following the Golgi method as described below. Brain hemispheres destined to study neuronal morphology were stored in PB 0.1 M (4 ºC) with sodium azide 0.05 % until cut with a vibratome (Leica VT 1000E, Leica) into 150 μm thick coronal sections. The rest of the brains were cryoprotected with 30% sucrose in cold PB 0.1 M (4 ºC) for 48 hours and then cut in 50 μm thick coronal sections using a freezing-sliding microtome (Leica SM2000R, Leica). Slices were collected in 10 (for rats) or 6 subseries (for mice) and stored at -20 ºC in a cryoprotective solution until used (30% glycerol, 30% ethylene glycol in PB 0.1 M). Rats processed for electron microscopy were perfused transcardially under deep chloral hydrate anesthesia, first with saline for 1 minute, followed by 450 ml solution of: (1) paraformaldehyde 2% in a lysine-phosphate buffer, pH 7 for PSA-NCAM immunohistochemistry, this is prepared 1:1 from a solution of PB 0.1 M pH 7.4 and a solution 0.2 M of lysine adjusted to pH 7.4 using a solution of Na_2HPO_4 0.1 M. The buffer was mixed with a concentrated solution of paraformaldehyde 3:1 and 0.214 g of sodium peryodate were added for each 100 ml just before use. (2) For TUC-4 immunohistochemistry, animals were perfused with acrolein 3.8% and paraformaldehyde 2% in PB 0.1 M. Brains were then extracted and sliced with a vibratome at 50 μm as described above.

10.2 Inclusion and ultramicrotomy

All the sections processed for electron microscopy were stained with uranyl acetate 1% in ethanol 70% for 1 hour at 20 °C, dehydrated through increasing graded ethanol series and propylene oxide and flat-embedded in Durcupan (Fluka, Sigma-Aldrich). After analysis of this material under the light microscope, selected PSA-NCAM expressing interneurons were re-embedded in Durcupan and 60 nm-thick ultrathin sections were cut with an ultramicrotome (Leica, EM-UC6). Ultrathin sections were serially collected on formvar-coated single-slot copper grids and stained using lead citrate. Selected cells were observed and partially reconstructed from serial sections under a JEOL JEM-1010 electron microscope.

10.3 Golgi method

Coronal blocks were processed using the Golgi-Colonnier method (Colonnier, 1964) with some modifications. In brief, blocks were post-fixed with 3% potassium dichromate and 5% glutaraldehyde for 7 days at 4 ºC and then impregnated with 0.75% silver nitrate solution for 48 hours. Blocks were then cut into 150 μm-thick coronal sections with a vibratome, dehydrated with ascending alcohols and mounted with epoxy resin between two coverslips. To avoid any bias in the analysis, the slides were coded and the code was not broken until the analysis was completed.

11 Hippocampal organotypic slice cultures

P7 transgenic GIN mice pups were decapitated and their brains were removed from the skull under sterile conditions. Brains were placed into Petri dishes filled with cold (4 ºC) dissecting medium (1.2% Tris buffer, 1% Penicilin/streptomicin, 97.8% MEM). The hippocampus was extracted following the methodology described by Stoppini et al. (1991) and cut into 300 μm thick slices using a McIlwain tissue chopper. The slices were placed on a small membrane confetti (Millipore), which was on the top of the membrane inserts (Millipore) on 1 ml of culture medium (50% MEM, 25% Horse serum and 25% HBSS, 1% penicilin/streptomicin, 0.6% Tris buffer). Three slices were cultured in the same insert and six inserts were placed together in six-well plates. Cultures were stored in a humid atmosphere at 33 ºC in 5% CO_2 for 11-19 days (HERAcell 150i, Thermo Scientific) and culture medium was changed 3 times per week. Rat pups were treated using the same methodology, but using P10 animals instead of P7.

12 *In vitro* treatments

12.1 EndoN

After 12 days *in vitro* (DIV 12), 2 U/ml of the enzyme EndoN were added to the culture medium containing slices from the treated group, whereas slices from control group received the same amount of vehicle solution (glycerol) in their culture medium. The morphology of eGFP expressing interneurons, was studied 24 hours before the addition of EndoN (DIV 11), just prior to the addition of EndoN and 24 hours after the addition of EndoN. Immediately afterwards (DIV 13), the slices were fixed with 4% paraformaldehyde in PB during 1 hour.

12.2 Biolistic transfection

In the rat hippocampal cultures, to analyze the dynamic and distribution of gephyrin, the slices were cotransfected with pcDNA-DsRed2 and pcDNA-GEPH-EGFP plasmids, using a biolistic method (Helios Gene Gun, Bio-Rad) 3 days before the first observation. In brief, this method requires the use of cartridges loaded with gold bullets covered with the plasmid DNA and shot with a pressure gun. The number of cells suitable for the analysis (pyramidal neurons from the CA1 region) varied between 0 to 5 per slice culture; fluorescence usually started to be expressed after 24-48 hours and remained stable for all the time of analysis.

13 Immunohistochemistry

All the antibodies employed in this doctoral thesis, their dilutions and incubation conditions can be found in Table 1. For each experiment, all the studied sections passed through all procedures simultaneously to minimize any difference from immunohistochemical staining itself. To avoid any

bias, all slides were coded prior to the analysis and the codes were not broken until the experiment was finished.

13.1 Light microscopy

Tissue was processed "free-floating" for immunohistochemistry using the avidin-biotin-peroxidase (ABC) method as follows. Fifty μm-thick sections were first treated for 1 minute with an antigen unmasking solution (0.01 M citrate buffer, pH 6) at 100ºC. After cooling down sections to room temperature, they were incubated with 3% H_2O_2 in phosphate buffered saline (PBS) for 10 minutes to block endogenous peroxidase activity. After this, sections were treated for 1 hour with 10% normal donkey serum (NDS; Jackson ImmunoResearch Laboratories) in PBS with 0.2% Triton-X100 (Sigma-Aldrich) and then they were incubated with the appropriate primary antibody (table 1) in PBS with 0.2% Triton-X100 and 5% NDS. Next, sections were incubated for 1 hour with the right biotinylated secondary antibody (table 1) diluted in PBS with 0.2% Triton-X-100 and 5% NDS, followed by a 30 minutes incubation with an avidin-biotin-peroxidase complex diluted in PBS (ABC; Vector Laboratories). Color development was achieved by incubating with 3,3'- diaminobenzidine tetrahydrochloride (DAB; Sigma-Aldrich) and 0.033% H_2O_2 for 4 minutes. Finally, sections were mounted on slides, dried for one day at room temperature, dehydrated with ascending alcohols and rinsed in xylene. After this, sections were coverslipped using Eukitt mounting medium.

13.2 Confocal microscopy

In general, tissue was processed "free-floating" for immunohistochemistry as described above, but omitting the endogenous peroxidase block. Sections were incubated with a cocktail of two, three or four primary antibodies and then with the appropriate fluorescent secondary antibodies (table 1). Finally, sections were mounted on slides and coverslipped using DakoCytomation fluorescent mounting medium (Dako North America Inc). When it was necessary to use two primary antibodies generated in the same species in the same immunohistochemistry, subclass specific secondary antibodies were used.

13.3 Electron microscopy

13.3.1 Immunogold labelling

The tissue was processed "free-floating" and, in addition to the incubations with serum, primary and secondary antibodies; the slices were previously cryoprotected during 30 minutes (25% sucrose, 10% glycerol in 0.01 M phosphate buffer) and then procesed for freeze-thawing using liquid nitrogen. Sections were then washed in 0.1 M phosphate buffer, pH 7.4 (PB) and sequentially incubated in: (1) blocking solution, containing 2% BSA and 0.1% gelatin in PB for 45 min; (2) monoclonal anti-PSA-NCAM antibody for 48 hours at 4ºC (1:700); (3) biotinylated donkey anti-mouse IgM secondary antibody for 1 hour (1:200, Jackson Immunoresearch); (4) goat anti-biotin antibody conjugated

Primary antibodies					
Anti-	Host	Isotype	Dilution	Incubation	Company
5HT1A	Rabbit	IgG	1:100	24 hours, 25ºC	Santa Cruz Biotechnology
5HT2A	Mouse	IgG	1:1000	24 hours, 25ºC	BD Pharmanigen
5HT2C	Mouse	IgG	1:1000	24 hours, 25ºC	BD Pharmanigen
5HT3	Rabbit	IgG	1:250	24 hours, 25ºC	Calbiochem
c-fos	Rabbit	IgG	1:2000	24 hours, 25ºC	Santa Cruz Biotechnology
CAMKII	Mouse	IgG1	1:500	48 hours, 4ºC	Abcam
CB	Rabbit	IgG	1:2000	24 hours, 25ºC	Swant
CCK	Mouse	IgG	1:1000	24 hours, 25ºC	Cure
CR	Rabbit	IgG	1:2000	24 hours, 25ºC	Swant
DCX	Goat	IgG	1:250	24 hours, 25ºC	Santa Cruz Biotechnology
GAD6	Mouse	IgG2a	1:500	24 hours, 25ºC	DSHB
GAD67	Mouse	IgG2a	1:500	24 hours, 25ºC	Millipore
GFP	Chicken	IgY	1:1000	24 hours, 25ºC	Millipore
Ki67	Rabbit	IgG	1:2000	24 hours, 25ºC	Novocastra
NeuN	Mouse	IgG1	1:100	24 hours, 25ºC	Millipore
PSA-NCAM	Mouse	IgM	1:700	48 hours, 4ºC	Abcys
PV	Guinea pig	IgG	1:2000	24 hours, 25ºC	Synaptic Systems
SOM	Rabbit	IgG	1:200	24 hours, 25ºC	Provided by Dr. Gorcs
SYN	Rabbit	IgG	1:1000	24 hours, 25ºC	Millipore
TUC-4	Rabbit	IgG	1:1000	24 hours, 25ºC	Millipore
VGAT	Rabbit	IgG	1:1000	24 hours, 25ºC	Synaptic Systems
VGluT1	Guiena pig	IgG	1:2000	24 hours, 25ºC	Millipore
VIP	Rabbit	IgG	1:1000	24 hours, 25ºC	Provided by Dr. Gorcs
Secondary Antibodies					
Anti-	Host	Label	Dilution	Incuabtion	Company
Biotin	Goat	0.8 nm gold particles	1:500	2 hours, 25ºC	Amersham Biosciences
Chicken IgY	Donkey	Dylight 488	1:400	1 hour, 25ºC	Jackson ImmunoResearch
Goat IgG	Donkey	Biotin	1:400	1 hour, 25ºC	Jackson ImmunoResearch
Guiena pig IgG	Donkey	Biotin	1:400	1 hour, 25ºC	Jackson ImmunoResearch
Guinea pig IgG	Donkey	Cy5	1:400	1 hour, 25ºC	Jackson ImmunoResearch
Mouse IgM	Donkey	Biotin	1:400	1 hour, 25ºC	Jackson ImmunoResearch
Mouse IgM	Goat	Alexa Fluor 555	1:400	1 hour, 25ºC	Invitrogen
Mouse IgM	Donkey	Alexa Fluor 488	1:400	1 hour, 25ºC	Invitrogen
Mouse IgG	Goat	Alexa Fluor 555	1:400	1 hour, 25ºC	Invitrogen
Mouse IgG	Goat	Alexa Fluor 647	1:400	1 hour, 25ºC	Invitrogen
Mouse IgG	Donkey	Biotin	1:400	1 hour, 25ºC	Jackson ImmunoResearch
Rabbit IgG	Donkey	Biotin	1:400	2 hours, 25ºC	Jackson ImmunoResearch
Rabbit IgG	Donkey	Alexa Fluor 555	1:400	1 hour, 25ºC	Invitrogen
Rabbit IgG	Donkey	Alexa Fluor 488	1:400	1 hour, 25ºC	Invitrogen
Rabbit IgG	Donkey	Alexa Fluor 647	1:400	1 hour, 25ºC	Invitrogen
Rat IgG	Donkey	Alexa Fluor 488	1:400	1 hour, 25ºC	Invitrogen
Rat IgG	Goat	Alexa Fluor 647	1:400	1 hour, 25ºC	Invitrogen

Tab. 2: List of Primary and Secondary antibodies used

Abbreviations: 5HT1A, 5HT2A, 5HT2C, 5HT3, serotonin receptors type 1A, 2A, 2C and 3; CaMKII, α subunit of the Ca^{2+} /calmodulin dependent protein kinase II; CB, calbindin; CCK, cholecystokinine; CR , calretinin; DCX, doublecortin; GAD6, both 65 and 67 kDa isoforms of the glutamate decarboxilase enzyme; GAD67, 67 kDa isoform of the glutamate decarboxilase enzyme; GFP, green fluorescent protein; PSA-NCAM, polysialylated form of de neural cell adhesion molecule; PV, parvalbumin; SOM, somatostatin; SYN, synaptophysin; TUC-4, Turned on After Division/Ulip/CRMP-4; VGAT, vesicular γ-aminobutyric acid (GABA) transporter; VGLUT1, vesicular glutamate transporter 1; VIP, vasoactive intestinal peptide

with 0,8 nm gold particles for 2 hours (1:500, Amersham Biosciences); (5) 2% glutaraldehyde in PB for 10 min to fix the gold particles. After each step, sections were rinsed (3×10 minutes) in PB. In order to improve the microscopic analysis of the staining, gold particles were enlarged using silver enhancer Aurion R-Gent SE-LM (Electron Microscopy Sciences) for 15 minutes at 20 °C. The enhancement was stopped in 0.03 M sodium thiosulphate in an enhancement conditioning solution (Aurion) for 10 min. Afterwards, the sections were washed in PBS and then treated with 1% osmium tetroxide in PB for 60 min at 20 °C. Then the tissue was procesed for inclusion and ultramicrotomy as described above.

13.3.2 Diaminobenzidine immunohistochemistry

The sections destined for electron microscopy were cryoprotected as described above and then underwent freeze–thawing three times with liquid nitrogen to enhance antibody penetration. Then, sections were washed in PB and the endogenous peroxidase activity was blocked as described above. Subsequently, non-specific binding sites were blocked with NDS 10% in PB with glycine 0.2% and lysine 0.2%. After washing, sections were processed using primary antibodies against PSA or TUC-4, as described for conventional immunohistochemistry. Immunolabeling was intensified by treating the sections with 1% osmium tetroxide (EMS) in PB for 60 min, protected from light. After each step, sections were carefully rinsed in PB. Finally, sections were processed for inclusion and ultramicrotomy as described above. For animals perfused with acrolein, the procedure was similar but in addition, sections were incubated with sodium borohydride 1% (in H_2O for 10 minutes) and with Tris buffer (0.5 N, pH 7.2 for 30 minutes) to block and quench free aldehydes, respectively.

14 Analysis of results

14.1 Body weight

In rats and mice from the chronic fluoxetine treatment experiments, body weight was measured daily and the differences at the beginning and the end of the experiment were calculated and analyzed by unpaired Student's t-test.

14.2 Volumetric analysis

The volumes of the mPFC, the hippocampus and the lateral and basolateral regions of the amygdala were estimated using Volumest, an ImageJ plugin for volume estimation using an stereological method (Roberts et al., 2000). For this analysis we used the tissue processed for PSA-NCAM immunohistochemistry and developed with DAB.

14.3 Neuropil quantification

14.3.1 Analysis of gray levels

From each immunostaining analyzed, three sections per animal were selected within the different regions studied: the rat primary somatosensory cortex (Bregma -2.8 mm to -3.1 mm, (Paxinos and Watson, 2007) and the mouse cingulate cortex (Bregma +1.1 mm to +0.5 mm, (Paxinos and Franklin, 2001)). Sections were examined with an Olympus CX41 microscope under bright-field illumination, homogeneously lighted and digitalized using a CCD camera. Photographs to the different areas and layers were taken at 20X magnification. Means were determined for each experimental group and data were subjected to Student's t-test or ANOVA.

14.3.2 Analysis of single confocal planes of puncta

We analyzed the density of puncta expressing different markers in focal planes of different regions of the rat and mouse brain after the chronic treatment with the antidepressant fluoxetine. In the rat brain, we analyzed layer V of the mPFC. In this layer reside the pyramidal neurons that provide the main output projection of this region, which project extensively to the striatum (Berendse et al., 1992; Jones et al., 1977; Lévesque and Parent, 1998). We analyzed two different regions of the mPFC: the prelimbic cortex (PrL) in sections corresponding to Bregma +2.20 mm and the dorsal cingulate cortex (Cg2) (Bregma +1 mm). In the amygdala, five nuclei were analyzed (Bregma -3.30 mm): basomedial, lateral, medial, central and basolateral. Different regions and strata of the hippocampus were also analyzed (Bregma -4.30 mm): the stratum lucidum, the molecular layer of the dentate gyrus, the stratum lacunosum-moleculare, radiatum and oriens of CA1 and the stratum lucidum of CA3. Confocal z-stacks covering the whole depth of the sections were taken with 1 μm step size and only subsets of confocal planes with the optimal penetration level for each antibody were selected. On these planes, small regions of the neuropil (505 μm^2) were selected for analysis, in order to avoid blood vessels and cell somata. Images were processed using ImageJ software as follows: the background was subtracted with rolling value of 50, converted to 8-bit deep images and binarized using a determined threshold value. This value depended on the marker and the area analyzed and was kept the same for all images with the same marker and area. Then, the images were processed with a blur filter to reduce noise and separate closely apposed puncta. Finally, the number of the resulting dots per region was counted, as well as the colocalization between PSA-NCAM and the different pre-synaptic markers. Means were determined for each animal group and the data were subjected to two-way ANOVAs with repeated measures, followed by Bonferroni post hoc tests. The methodology used with the GIN mice was similar, but the analysis was performed using sections with the correspondent values of Bregma for the mouse hippocampus (Bregma -2.18 mm).

14.4 Estimation of the total number of cells

The number of DCX, PSA-NCAM and Ki67 expressing cells in the SGZ of the dentate gyrus was estimated as described before (Nacher et al., 2002b). Briefly, sections were selected by a 1:10 fractionator sampling covering the whole rostral to caudal extension of the dentate gyrus and on each section all labeled cells within the region of interest were counted. Cell somata were identified and counted with a 40x objective using an Olympus CX41 microscope. The volume of the different areas analyzed was determined for each animal using the Cavalieri's method. Student's t-test was performed for statistical analysis. In the SVZ, a single section between Bregma -0.26 and +1 mm, was analyzed for DCX, PSA-NCAM and Ki67 immunohistochemistry. The number of immunoreactive cells was estimated following a modification of the method described by Hansson et al. (2010). Ki67 expressing nuclei were counted using automatic counting software as described above for immunoreactive puncta, analyzing an area of 100 μm^2 and then expressed as the number of immunoreactive positive cells per mm^2. Densities of DCX and PSA-NCAM expressing cells were too high for a correct individual cell count. Therefore, we performed densitometry of small areas within the SVZ using also 40x magnification.

14.5 Analysis of neurochemical phenotype

Sections double or triple labeled for PSA-NCAM and different markers were observed under a confocal microscope (Leica TCS-SPE) using a 63X oil objective. PSA-NCAM expressing cells were first identified using conventional fluorescence microscopy and then z-series of optical sections (1 μm apart) covering all its three-dimensional extension were obtained using sequential scanning mode. These stacks were processed with ImageJ software. In each immunostaining, fifty PSA-NCAM immunoreactive neurons per animal from the region studied were randomly selected to determine the co-expression of PSA-NCAM and each marker. Percentages of colocalization were determined for each animal and means $\pm$ S.E.M. were calculated.

14.6 Quantification of dendritic spine density in pyramidal cells

Dendritic spine density was analyzed following a previously described methodology (Magariños and McEwen, 1995) in rat tissue processed with the Golgi-Colonnier method. Spine quantification was carried out in each animal in six pyramidal neurons from layers III, IV and V, which were randomly selected inside the somatosensory primary cortex (S1) area. A total of 48 neurons were analyzed. In order to be suitable for dendritic spine analysis, neurons should follow these features: (i) they must display complete Golgi impregnation of the principal apical dendrite, (ii) the cell type must be identifiable and (iii) the minimum length of the apical dendrite must be 200 μm from the soma. Each neuron was traced using a 100X oil objective in a light microscope with a camera lucida drawing tube attachment (Nikon, Japan) and spines were quantified in four successive segments of 50 μm distances up to a total length of 200 μm. Overall spine density values or densities per segment

were expressed as number of spines/μm length. For each experimental group, mean $\pm$ S.E.M. was determined and the resulting values analyzed by one-way ANOVA with the number of neurons as the "n".

14.7 Quantification of dendritic arborization and spine density in interneurons

Dendritic arborization and spine density were studied using confocal microscopy (Leica TCS SPE). Z-series of optical sections (0.4 μm apart) covering the dendritic tree of selected interneurons (6 GFP+/PSA+ and/or 6 GFP+/PSA- per mouse). In order to be analyzed, GFP-expressing cells had to fulfill the following features: (1) the cell must not show any truncated dendrites, (2) the dendritic arbor of the cell must show at least a process with a length greater than 120 μm and (3) the soma must be located at least 30 μm deep from the surface of the tissue. The stacks obtained were then processed using ImageJ software (NIH) in order to render 3D reconstructions, in which the exact distance of the branching and terminal points of the dendrites of a given interneuron were analyzed. The degree of dendritic arborization was analyzed using a procedure for deriving the Sholl profile (Gutierrez and Davies, 2007). The Sholl analysis consists on the measure of the number of intersections of the dendrites with circles of increasing radius centered in the soma.

To study the spine density of interneurons we selected individual dendrites from hippocampal GFP-expressing neurons. Stacks of confocal images were obtained with the 63x objective and an additional 3.5 digital zoom. The spines were counted in three dendritic fragments (60 μm each) expanding to 180 μm from the soma.

14.8 Quantification of dendritic spine turnover in cultured interneurons

For *in vitro* analysis in hippocampal organotypic cultures, short imaging sessions (10-15 minutes) were carried out with a 40x water immersion objective. Using an additional 10x zoom to analyze dendritic segments of about 35 μm in length and located between 100 and 150 μm from the soma (Z step size of 0.5 μm). Laser intensity was kept at the minimum observable, and acquisition conditions maintained mostly unchanged over the different days of observation. Control experiments showed that this procedure does not produce any deleterious effect on cell viability by absence of cell death or dendritic beadings.

14.9 Ultrastructural analysis

The density of synaptic contacts on the plasma membrane was studied analyzing profiles of interneuron somata from selected regions of the ventral hippocampus and the deep layers of mPFC, where PSA-NCAM expressing interneurons were specially abundant. Both DAB- and gold-stained material was used in this study. The interneurons were identified by their profound invagination of the nucleus and an electron-dense cytoplasm with high density of mitochondria, endoplasmic

reticulum, and Golgi apparatus. Nine interneurons expressing PSA in the plasma membrane and 9 lacking expression of this molecule were analyzed in each region. Thirty profiles of pyramidal neuron somata of the mPFC cortex were also studied under the electron microscope in order to analyze PSA-NCAM expression in their perisomatic region.

Part IV. Results I: Analysis of PSA-NCAM expressing cells: distribution, phenotype, structure and ultrastructure

15 Distribution of PSA-NCAM expressing cells throughout the adult rodent telencephalon.

In the adult rodent dorsal telencephalon we can distinguish three subpopulations of cells expressing the polysialylated form of the neural cell adhesion molecule (PSA-NCAM): (1) immature cells that have been recently generated, such as those in the subgranular zone (SGZ) of the hippocampus or the subventricular zone (SVZ) and the rostral migratory stream (RMS), (2) immature cells that have not been recently generated, such as those in the paleocortex layer II and (3) interneurons dispersed throughout the neocortex, paleocortex, archicortex and the amygdala (Fig. 15.1). This thesis will be focused mainly on the immature PSA-NCAM expressing cells of the paleocortex layer II and the cortical interneurons expressing PSA-NCAM. The distribution of PSA-NCAM expressing cells in the telencephalon was similar in rats and mice. PSA-NCAM expressing cells with a multipolar morphology, were found widely dispersed in every region and layer of the neocortex, although they were more abundant in deep layers. These cells also populated the deep layers of paleocortex (piriform cortex layer III and entorhinal cortex layers III to VI) but were extremely rare in layers II or I. In the paleocortex layer II, most of the cells expressing PSA resembled those previously described as neurogliaform neurons or semilunar-pyramidal transitional neurons, with a small soma and with irregular trajectories and in clusters of 2 to 5 cells (Haberly, 1983). The distribution of PSA-NCAM expressing cells in the amygdala and of PSA-NCAM expressing non-granule neurons in the hippocampus was similar to that described previously in the rat (Nacher et al., 2002c,b). PSA-NCAM expression was detected in the neuropil of neocortical, paleocortical, archicortical and extracortical regions, as described before (Nacher et al., 2002a; Varea et al., 2005, 2007c; Nacher et al., 2002c; Seki and Arai, 1993a). In some cases, particularly in neocortical layers III and V, some PSA-NCAM expressing puncta were found delineating the profiles of the soma and the juxtasomatic portion of the principal apical dendrite of pyramidal neurons (Castillo-Gómez et al., 2011).

Since the ultrastructural details of the PSA-NCAM expressing cells in the subgranular zone of the hippocampus have already been studied (Seki and Arai, 1991b; Seki, 2002b), only the ultrastructure of PSA-NCAM cells resembling interneurons and those located in the paleocortex layer II will be analyzed in this thesis.

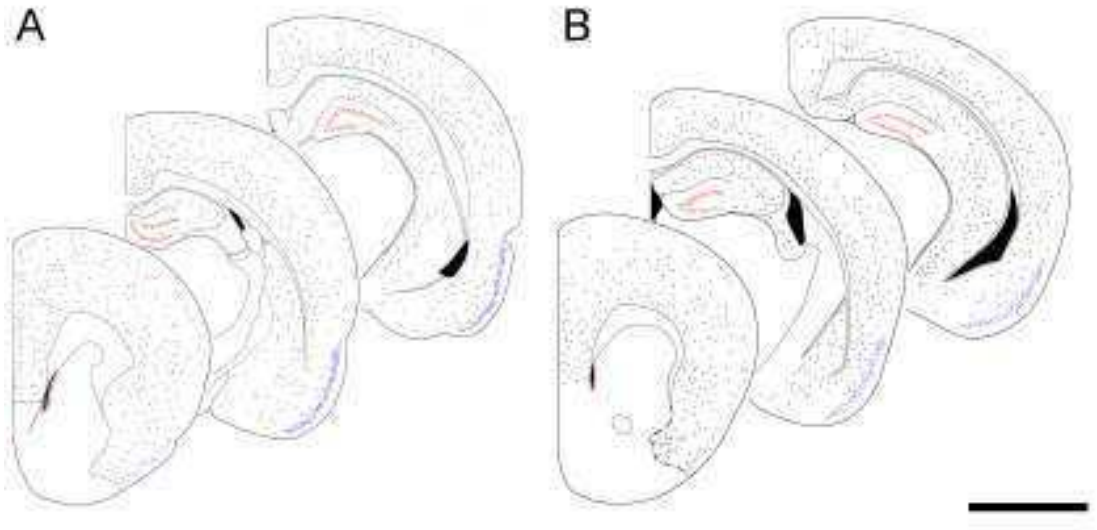

Fig. 15.1: Distribution of PSA-NCAM expressing cells

Distribution of PSA-NCAM expressing cells in the cerebral cortex and amygdala of adult rats (A) and mice (B). Camera lucida drawings of 3 representative 50-μm coronal sections covering the rostral to caudal extent of the rodent cerebral cortex. The somata of PSA-NCAM immunoreactive cells with the characteristic morphology of interneurons have been represented as black dots. PSA-NCAM immunoreactive cells in the hippocampal SGZ and the SVZ have been represented as red dots and those in the paleocortex layer II in blue. Scale bar: 3.4 mm for A and 2 mm for B. The profiles of the representative sections have been modified from those in Paxinos and Watson (2007) and Paxinos and Franklin (2001).

16 PSA-NCAM expressing cells in the rat paleocortex layer II

16.1 Ultrastructural features of tangled cells

A detailed analysis of PSA-NCAM or TOAD64 (Turned On After Division)/Ulip/CRMP-4 (TUC-4), expressing somata in the paleocortex layer II showed that they had only a small rim of cytoplasm surrounding the nucleus. Many astroglial lamellae were found in close apposition to the plasma membrane and it was common to find swellings of the extracellular space adjacent to the portions of the plasmatic membrane not covered by these glial processes. In the nuclei of labeled cells, chromatin appeared slightly more compacted than in those of the neighboring non-labeled pyramidal neurons and the presence of heterochromatin clumps was also more abundant in the labeled cells. None of these immunoreactive cells had synapses on their somata or proximal processes in layer II (Fig. 16.1).

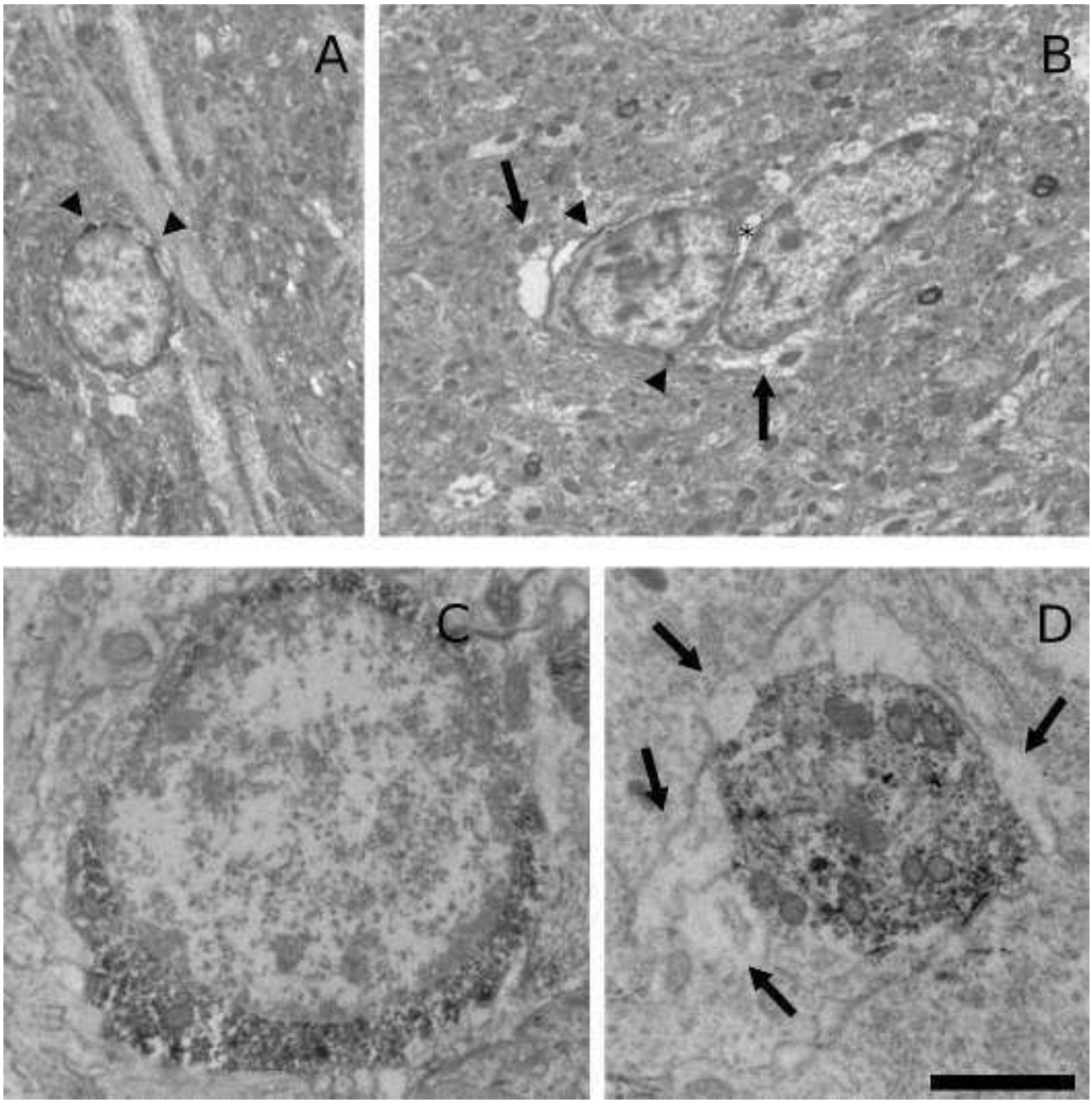

Fig. 16.1: Electron micrographs of immature neurons in the paleocortex layer II

Electron micrographs of PSA-NCAM (A, B), and TUC-4 (C, D), immunolabeled cells of the paleocortex layer II. (A, B) Somata of PSA-NCAM expressing cells. PSA-NCAM immunoreactivity is especially abundant in certain regions associated with the plasma membrane (arrowheads). Note the presence of clear structures surrounding the labeled somata (arrows), corresponding to astroglial lamellae and swellings of the extracellular space (asterisk). Several heterochromatin clumps can be observed inside the nuclei of the labeled cells. (C) Soma of a TUC-4 expressing cell showing an intensely labeled cytoplasm and a nucleus displaying abundant heterochromatin. (D) Transversal section of a proximal process from a TUC-4 expressing cell. Some mitochondria and cisternae can be observed inside the immunoreactive cytoplasm. Note that this process is also surrounded by clear structures resembling astroglial lamellae (arrows). Scale bar: 5 μm for (A), (B); 2.5 μm for (C); 1 μm for (D).

17 PSA-NCAM expressing interneurons in the hippocampus

17.1 Neurochemical phenotype of PSA-NCAM expressing cells in GIN mice

Most PSA-NCAM expressing cells coexpressed NeuN, a neuronal specific protein, indicating that they were mature neurons. Many of these cells also expressed markers of interneurons, such as glutamic acid decarboxylase 67(GAD67), calcium-binding proteins (parvalbumin (PV), calretinin (CR) and calbindin (CB)) and neuropeptides (somatostatin (SOM)). There was also a low percentage of PSA-NCAM expressing cells that coexpressed the immediate early gene c-fos (Fig 17.1 and Table 3). In addition, we analyzed the proportion of GAD67 expressing interneurons coexpressing PSA-NCAM and observed that the subpopulation of PSA-NCAM expressing interneurons represents a 34 $\pm$ 2.8% of the global interneuronal population.

Marker	Mean $\pm$ SE
NeuN	90.2 $\pm$ 4.2
GAD67	42 $\pm$ 7.1
CB	31.5 $\pm$ 6.4
CR	10.2 $\pm$ 2.2
PV	14.4 $\pm$ 6.1
SOM	41.5 $\pm$ 6.8
c-fos	15.4 $\pm$ 5

Tab. 3: Phenotypic characterization of PSA-NCAM expressing non-granule neurons in the mouse hippocampus

Numbers indicate the percentage ($\pm$ SEM) of PSA-NCAM expressing cells that co-express the different cellular markers.

Ultrastructural analysis of cortical pyramidal cells in pre-embedding PSA-NCAM immunostained sections confirmed that none of these cells expressed this molecule in the plasma membrane of their perisomatic region .

17.2 Expression of serotonin receptors in PSA-NCAM expressing interneurons

We found that interneurons expressing PSA-NCAM also expressed different types of serotonin receptors, such as type 1a, 2a, 2c and 3 in the medial prefrontal cortex (mPFC), the amygdala and the hippocampus. It has to be noted, that the serotonin type 1a receptor expression was located in the soma, although its expression was faint in PSA-NCAM expressing interneurons of the mPFC (Fig. 17.2) and the amygdala (Fig. 17.3). The serotonin type 2a receptor, was expressed mainly in the cytoplasm and the plasmatic membrane, but in addition, its expression was intense in the surrounding neuropil in the mPFC and the hippocampus (Fig. 17.4). We also identified expression of this receptor in the proximal part of dendrites emerging from the soma. Finally, the expression of

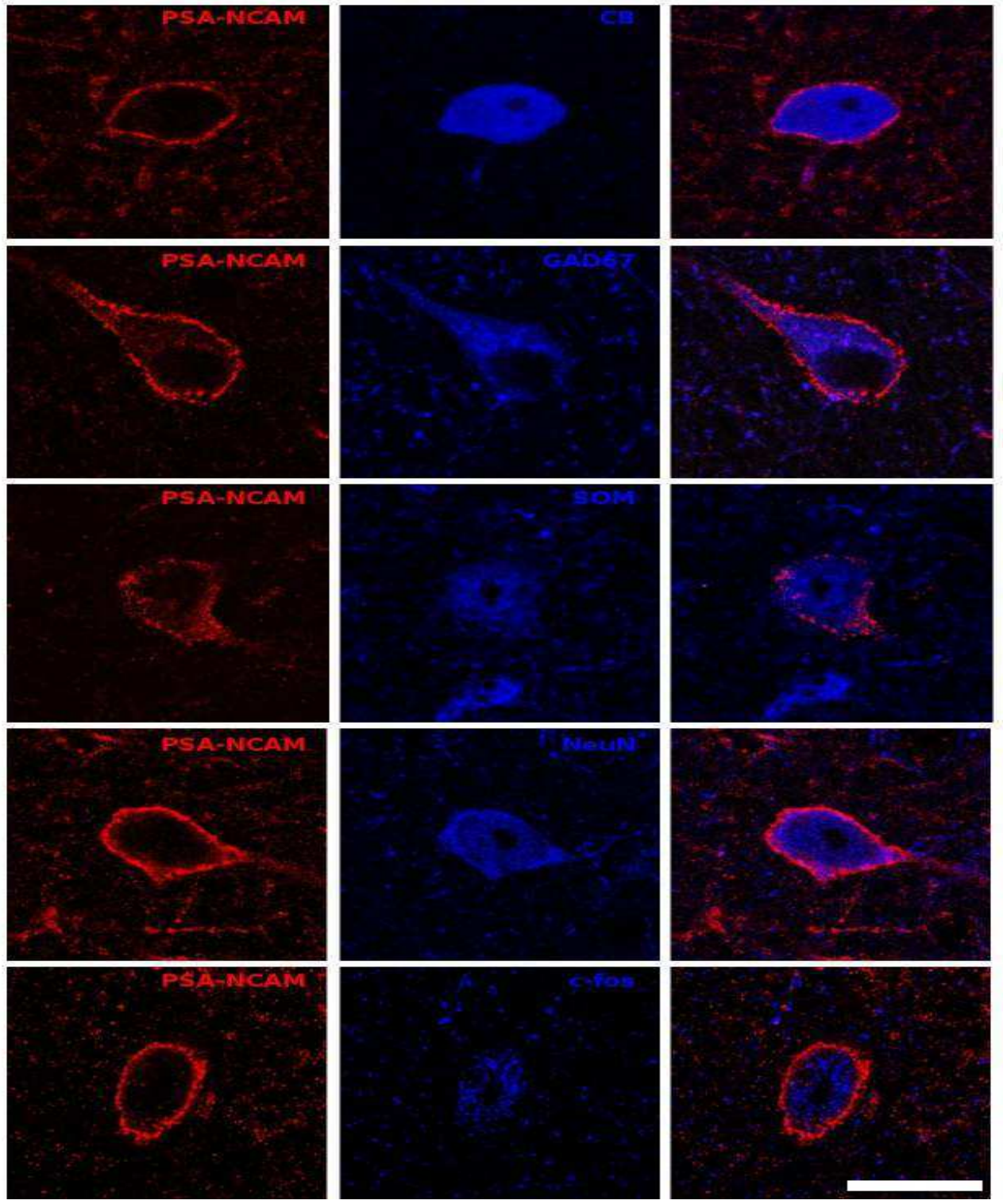

Fig. 17.1: Neurochemical phenotype of non-granule hippocampal PSA-NCAM expressing neurons

Confocal microscopic analysis of the phenotype of non-granule PSA-NCAM expressing cells in the ventral hippocampus of GIN mice. A: CB/PSA-NCAM expressing cell. B: GAD67/PSA-NCAM expressing cell. C: SOM/ PSA-NCAM expressing cell. Scale bar: 15μm. All the images in this figure are single confocal planes. GAD67: glutamate decarboxylase, isoform 67; CB: calbindin; SOM: somatostatin.

receptors type 2c and 3 was found in the cytoplasm and the membrane of PSA-NCAM expressing interneurons (see insets and figures 4, 5 and 6).

17.3 NCAM is the only polysialylated protein in interneurons

Although NCAM is the major carrier of polysialyc acid (PSA) in the vertebrate central nervous system (CNS) (Hildebrandt et al., 2010), different reports have described the presence of this complex sugar in some other proteins (Vitureira et al., 2010; Galuska et al., 2010; Zuber et al., 1992). Since the antibody used in this thesis recognizes only PSA but not the protein to which it is attached, we analyzed inhibitory elements in NCAM-deficient mice using PSA immunohistochemistry. Our study revealed the absence of PSA expression in cortical somata or neuropil elements expressing GAD67 (Fig. 17.5A and B), indicating that in inhibitory elements, PSA was exclusively associated to NCAM. Therefore, the appropriate nomenclature for the antigen recognized by our antibody is PSA-NCAM.

17.4 The expression of PSA-NCAM in interneurons is not affected by the genetic deletion of NCAM in principal cells

The analysis of PSA-NCAM expression in NCAMff+ mice (in which the NCAM gene is ablated under the control of the Ca^{2+}/ calmodulin dependent protein kinase II (CaMKII) promoter and thus absent from principal neurons) revealed very few differences when comparing these animals with their wild-type littermates. NCAMff+ mice lacked PSA-NCAM expression in their hippocampal mossy fibers, but presented several labeled cells in the SGZ of the dentate gyrus, as described previously (Bukalo et al., 2004). Typical PSA-NCAM expressing interneurons were found in all the regions studied, with similar morphology and distribution to those described before, and many of them coexpressed GAD67 (Fig. 17.5C). We estimated the number of PSA-NCAM expressing cells in the CA1 region of the entire hippocampus and there were no significant differences between the wild type (NCAMff-) (1892 ± 224.4) and NCAMff+ mice (2004 ± 70.8) (Unpaired student's t-test, $p = 0.86$). However, analysis of PSA-NCAM expressing puncta in the neuropil revealed that NCAMff+ mice showed a significant reduction in PSA-NCAM expression in the neuropil of CA1 lacunosum moleculare (wild type: 83.556 ± 7.601, NCAMff+: 28.667 ± 3.908; $p = 0.046$, Fig. 17.5E and F). This reduction was not detectable in deep layers of the infralimbic cortex (wild type: 24.443 ± 6.738, NCAMff+: 36.113 ± 10.794; $p = 0.932$, Fig. 17.5G and H).

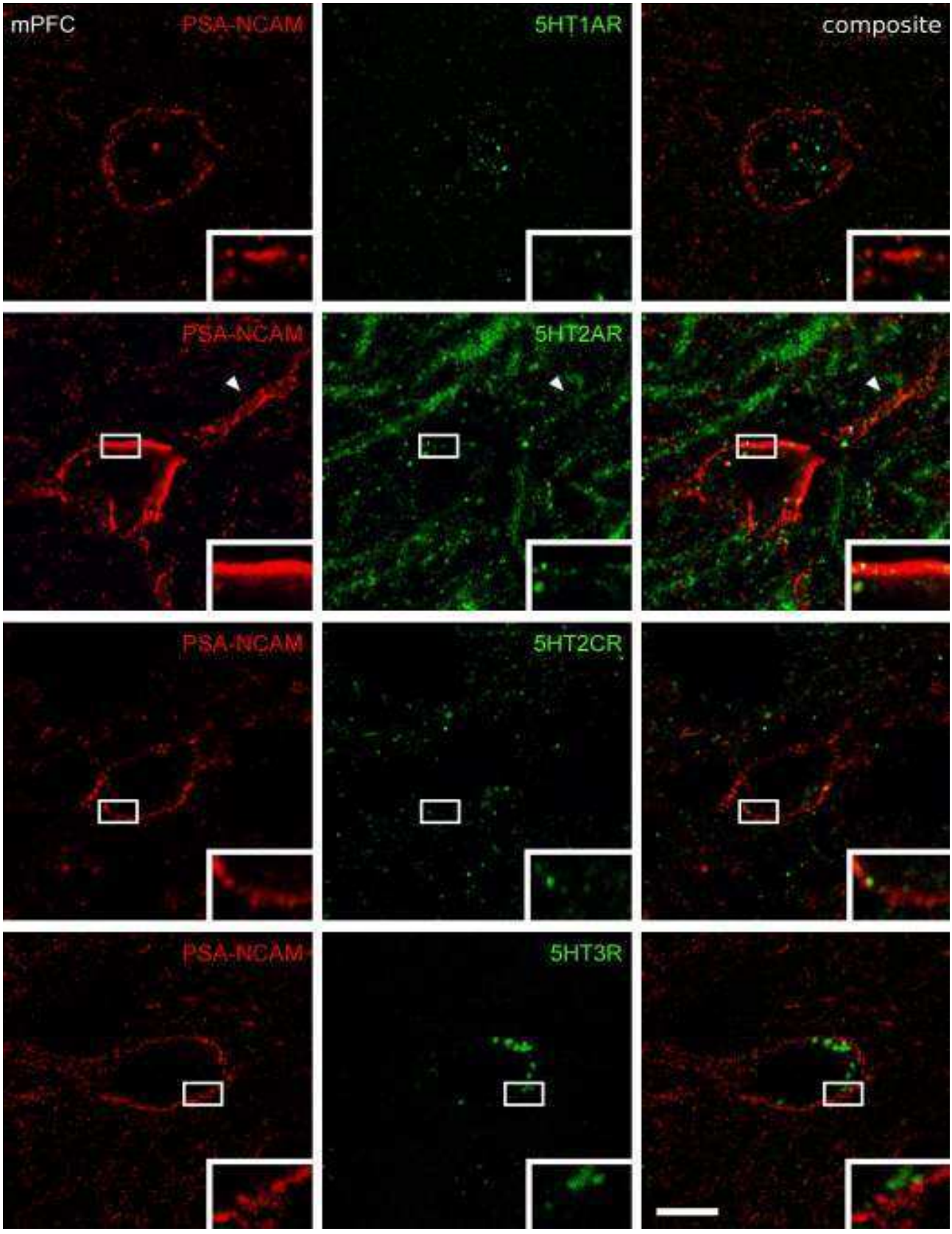

Fig. 17.2: Expression of different serotonin receptors in PSA-NCAM expressing interneurons of the mPFC

Scale bar 7 μm.

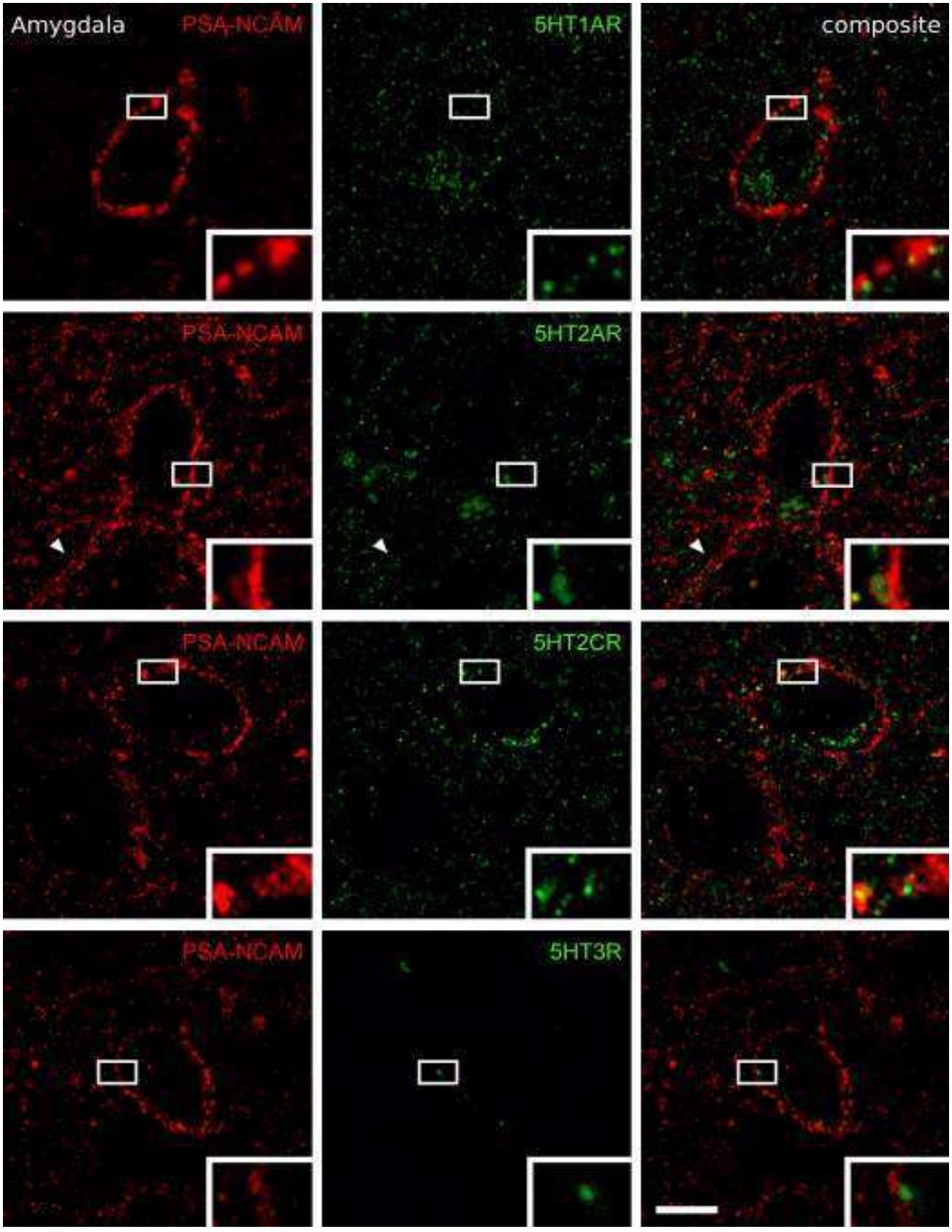

Fig. 17.3: Expression of different serotonin receptors in PSA-NCAM expressing interneurons of the amygdala

Scale bar 7 μm.

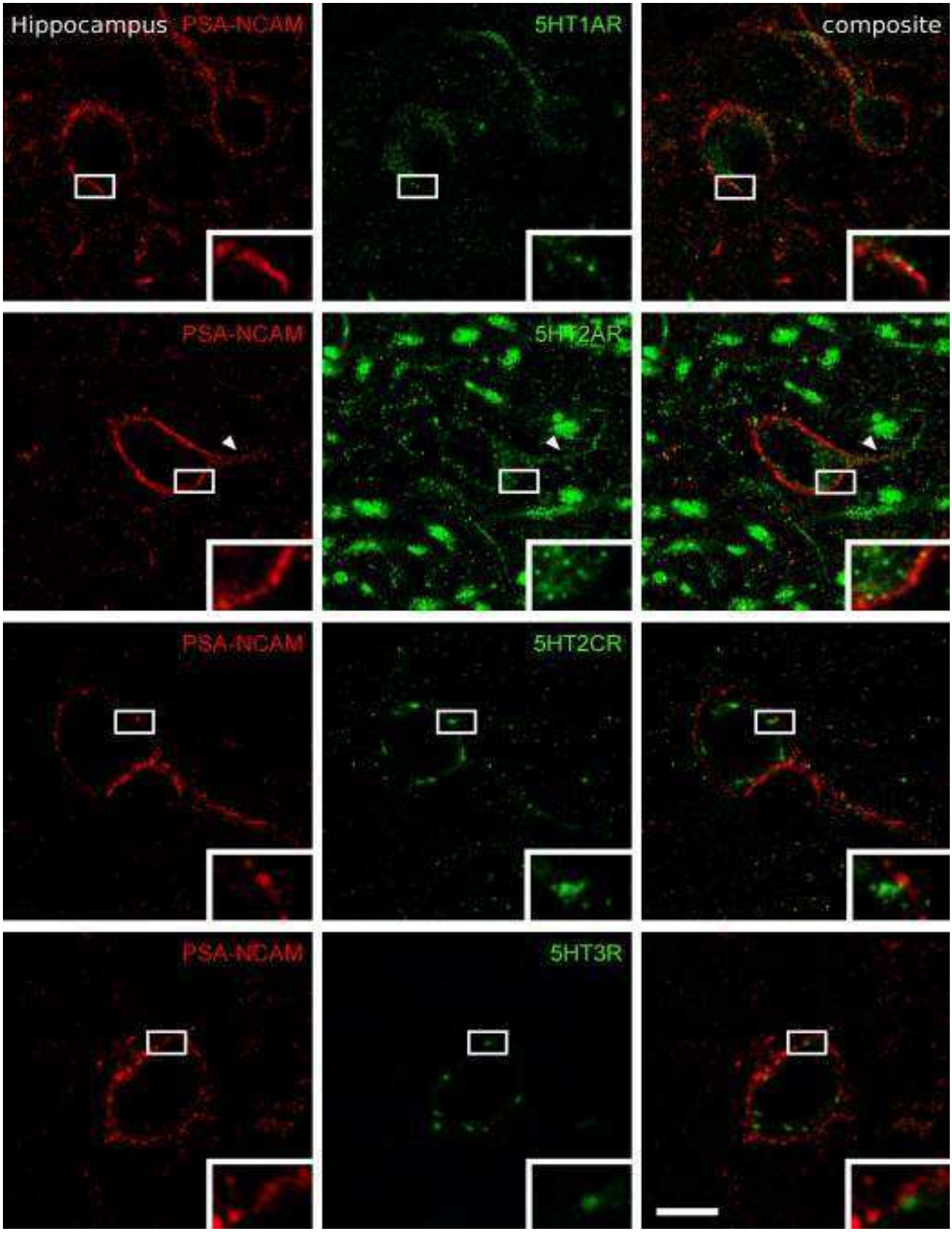

Fig. 17.4: Expression of different serotonin receptors in PSA-NCAM expressing interneurons of the hippocampus

Scale bar 7 μm.

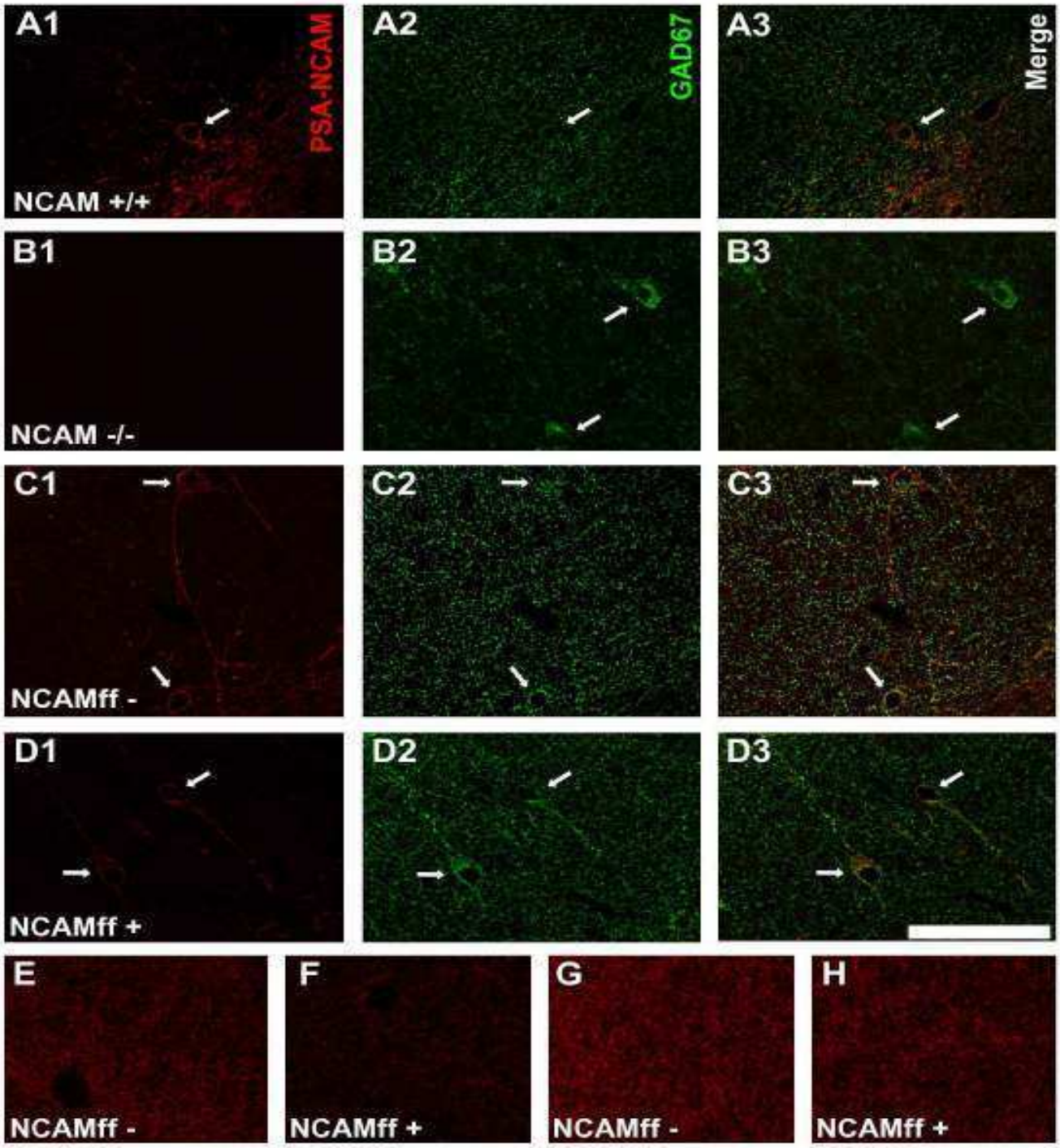

Fig. 17.5: Confocal microscopic analysis of PSA expression in inhibitory elements of NCAM-deficient mice and NCAMff mice

GAD67 and PSA-NCAM expressing interneuronal somata are indicated by arrows. (A-F) CA1 hippocampal stratum radiatum and (G and H) prelimbic cortex. (A) NCAM+/+ mice displayed PSA and GAD67 immunoreactivity in neuronal somata and the neuropil. (B) In NCAM-/- mice, although GAD67 expression is still present, PSA-NCAM labeling is completely absent. (C) NCAMff- mice show normal PSA-NCAM and GAD67 expression. (D) This expression pattern is preserved in NCAMff+ mice. (E and F) PSA-NCAM expression in the CA1 stratum lacunosum moleculare. Observe that immunoreactivity is considerably reduced in NCAMff+ mice. (G and H) PSA-NCAM expression in prelimbic cortex layer IV. No differences in immunoreactivity intensity can be observed between NCAMff- and NCAMff+ mice. All images are single confocal planes. Scale bar: 75 lm for A-D and 25 lm for E-H.

17.5 Structure of PSA-NCAM expressing interneurons

In order to analyze the structure of PSA-NCAM expressing interneurons, using GIN mice, we compared the dendritic arbor of enhanced green fluorescent protein (eGFP) labeled interneurons expressing PSA-NCAM (GFP+/PSA-NCAM+) and those lacking this molecule (GFP+/PSA-NCAM-). Prior to this analysis, we also studied this subpopulation of eGFP expressing interneurons using immunohistochemistry for different neuronal markers, in order to confirm their phenotype and the synaptic input of the dendritic spines of these interneurons.

17.5.1 Phenotype of eGFP-expressing inhibitory neurons

For the morphological studies of interneurons, we have used a strain of mice, which expresses eGFP under the GAD promoter (Oliva et al., 2000) and therefore it is expressed by a subset of interneurons. A previous study has shown that in these mice most of these interneurons correspond to the subpopulation expressing somatostatin (Oliva et al., 2000). We have analyzed the neurochemical phenotype of these eGFP expressing interneurons in our material and have confirmed that indeed most of them express somatostatin. We also found that these eGFP expressing interneurons did not coexpress other neuropeptides, such as cholecystokinin (CCK) or vasoactive intestinal peptide (VIP). However, we found a high proportion of eGFP interneurons expressing different calcium binding proteins such as calbindin, parvalbumin or calretinin (Fig. 17.6, Table 4).

Marker	Mean $\pm$ SE
PV	45.1 $\pm$ 5.4
CB	33.9 $\pm$ 0.9
CR	4 $\pm$ 1
SOM	70.7 $\pm$ 7.7
CCK	0
VIP	0

Tab. 4: Neurochemical phenotype of GFP-expressing interneurons

17.5.2 Synaptic input on eGFP-expressing neuronal spines

Another characteristic of this population of eGFP labeled interneurons is that they display dendritic spines. Therefore, we also decided to analyze the synaptic input on these spines in the hippocampus. We found that most of them (46.4% $\pm$ 4.4) were juxtaposed to vesicular glutamate transporter-1 (VGluT1) expressing puncta, while a 39.3% $\pm$ 6.7 were juxtaposed to vesicular γ-Aminobutyric acid transporter (VGAT) expressing puncta. We also found a 14.4% $\pm$ 4.2 of spines associated with both VGluT1 and VGAT expressing puncta. Finally, we found a 27.9% $\pm$ 2.5 of spines not associated with any excitatory or inhibitory marker (Fig. 17.7).

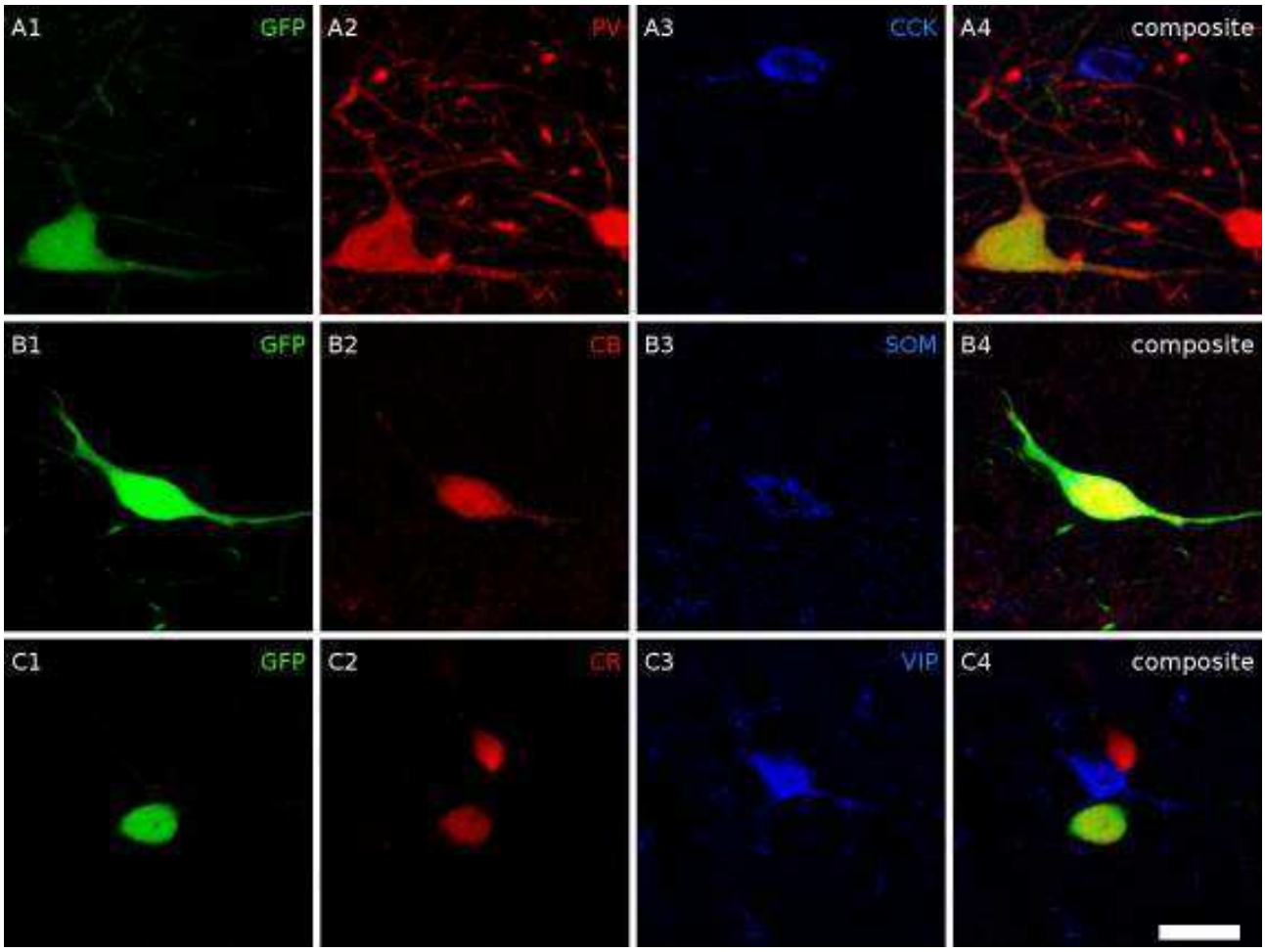

Fig. 17.6: Neurochemical phenotype of eGFP expressing interneurons in the hippocampus
Expression of different interneuronal markers in the eGFP expressing cells of the hippocampus CA1 of GIN mice. Single confocal planes showing the colocalization between eGFP (A1, B1 and C1), the calcium binding proteins parvalbumin (A2), calbindin (B2) and calretinin (C2) and different neuropeptides, such as cholecystokinin (A3), somatostatin (B3) and vasoactive intestinal peptide (C3). Scale bar: 20 μm

17.5.3 Morphologic features of PSA-NCAM interneurons

In the ventral hippocampus, Sholl analysis revealed reduced dendritic arborization in eGFP+/PSA-NCAM+ expressing interneurons when compared with eGFP+/PSA-NCAM- cells (Fig. 17.8). These differences were significant between segments 2 and 6 (i.e. in the distance between 20 and 120 μm from the soma), reaching a maximum difference in the fourth segment (between 60 and 80 μm of distance). The number of bifurcations was also significantly smaller in PSA-NCAM expressing interneurons (Fig. 17.8D).

The analysis of dendritic spine density also showed significant differences in the dendrites of PSA-NCAM expressing interneurons. The dendrites of interneurons expressing eGFP were divided into 3 segments of 60 μm. We found a significant reduction in the dendritic spine density of PSA-NCAM expressing interneurons in the 2 distal segments. This reduction was also significant when taking into account the whole length of the dendritic fragment studied (Fig. 17.9).

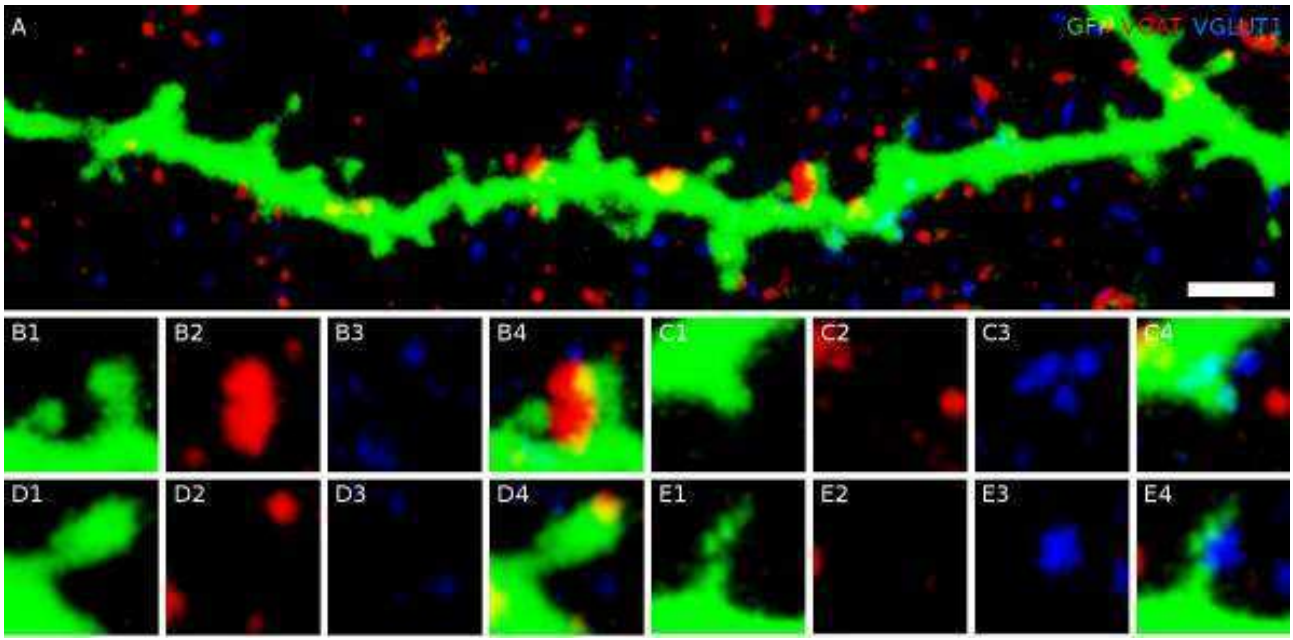

Fig. 17.7: Expression of presynaptic markers in the proximity of the dendritic spines of interneurons
Expression of presynaptic markers in the proximity of dendritic spines of interneurons. Reconstruction of a dendritic segment of a CA1 hippocampal interneuron carrying spines on its dendrites (A). Focal plane showing puncta expressing the vesicular GABA transporter (B2, D2) in close apposition to spines from an interneuron (B4, D4). Focal plane showing a dendritic spine from a interneuron (C1, E1) in close apposition with puncta expressing vesicular glutamate transporter-1 (C3, E3). Scale bar: 2 µm in A and 1.1 µm in the rest.

17.6 Ultrastructure of PSA-NCAM expressing interneurons

The ultrastructure of PSA-NCAM expressing non-granule neurons in the ventral region of the hippocampus and of interneurons in deep layers of the mPFC was studied with transmission electron microscopy (Fig. 17.10). All the cells studied showed typical interneuron features, such as a profound invagination of the nucleus, reduced soma size when compared with pyramidal neurons, and an electron-dense cytoplasm with high density of mitochondria, endoplasmic reticulum, and Golgi apparatus (Schwartzkroin and Kunkel, 1985; Babb et al., 1988). Excitatory and inhibitory synaptic contacts were observed in the perisomatic region of these interneurons. PSA-NCAM expression was found restricted to the plasma membrane and located exclusively at the extracellular surface (Fig. 17.10B and D). Although immunolabeling was present in most of the surface of the somata studied, it was never found on the surface contacting a presynaptic membrane. By contrast, pyramidal neuron somata in the hippocampus and mPFC cortex never showed PSA-NCAM expression in their plasma membrane. Since the qualitative estimation of the number of perisomatic synaptic contacts per μm of membrane in these hippocampal PSA-NCAM expressing interneurons revealed differences with those lacking PSA-NCAM expression in their vicinity (Fig. 17.10E and F), a detailed comparison of this number was made. The number of perisomatic synaptic contacts normalized to the cell perimeters sampled in PSA-NCAM expressing interneurons was significantly smaller than in those lacking expression of this molecule (Fig. 17.11).

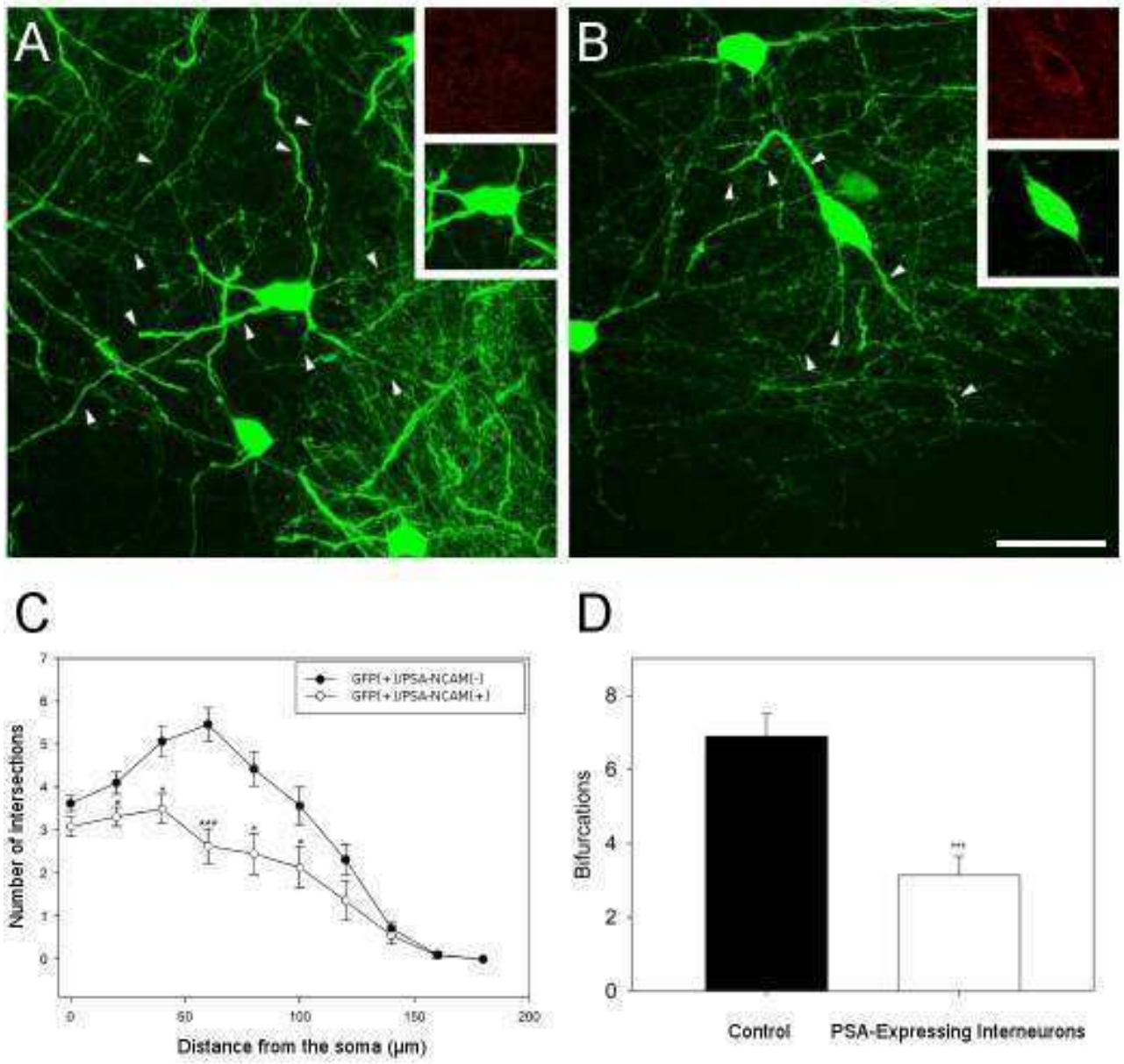

Fig. 17.8: Dendritic arborization and spine density in eGFP+/PSA-NCAM- versus eGFP+/PSA-NCAM+ expressing interneurons in the ventral hippocampus of GIN mice

3D reconstructions of GFP-expressing interneurons lacking PSA-NCAM expression (A) and coexpressing PSA-NCAM (B). Insets are views of the somata displayed in A and B showing coexpression of PSA-NCAM (up) and eGFP (bottom). Sholl analysis of eGFP-expressing interneurons, showing the intersection number per 20 μm dendritic radial unit distance from the soma (C) and bifurcation number (D). White circles (C) and bars (D) indicate interneurons lacking PSA-NCAM expression and black circles and bars correspond to PSA-NCAM expressing interneurons. Scale bar = 50 μm. Asterisks indicate statistically significant differences (* $p<0.05$, ** $p<0.01$, *** $p<0.001$). Values represent means $\pm$ standard error of the mean.

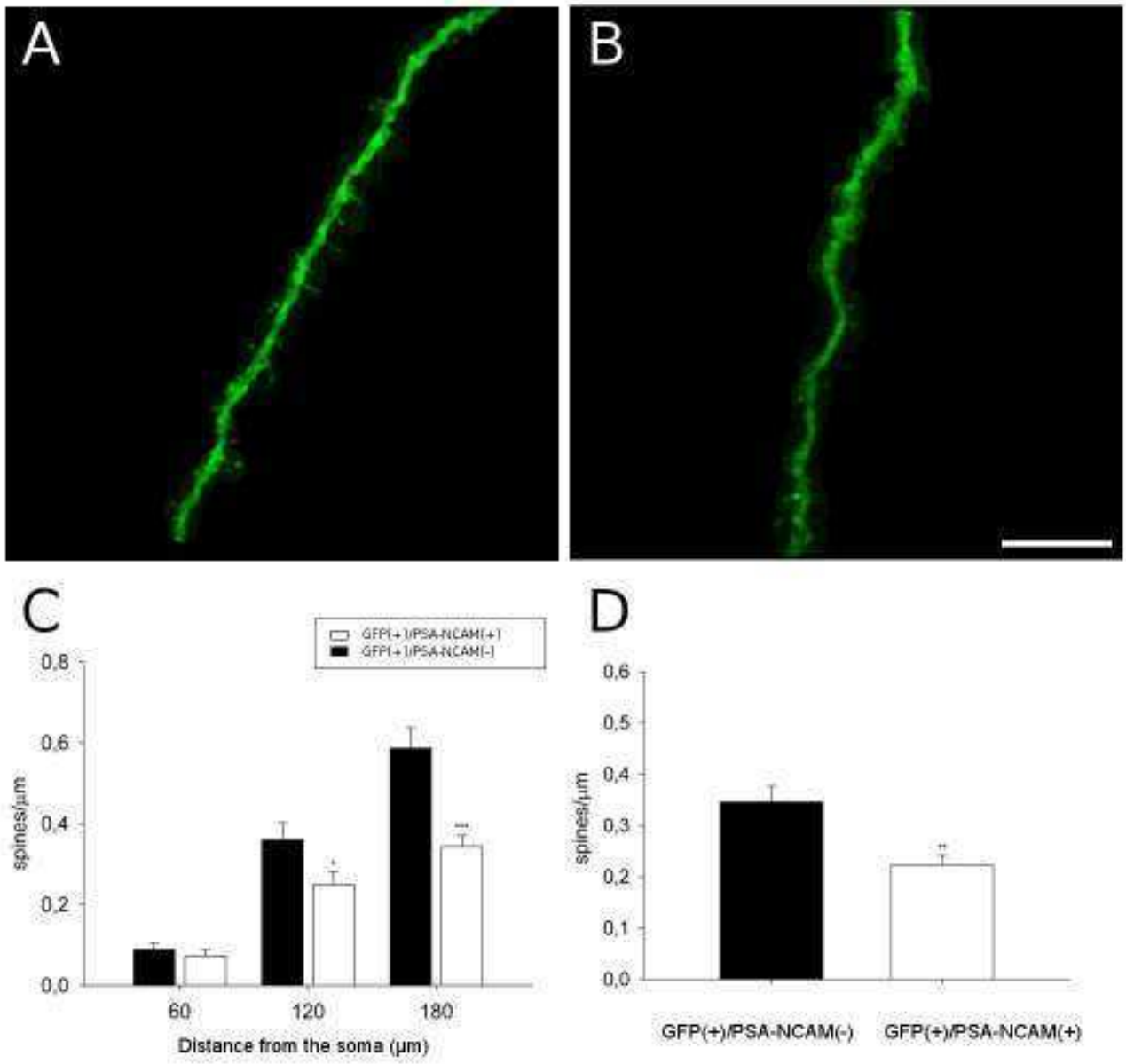

Fig. 17.9: Spine density in PSA-NCAM interneurons

Compositions, using fragments of different confocal planes, of spinous dendrites of GFP-expressing cells in interneurons expressing PSA-NCAM (A) and in interneurons lacking this molecule (B). Histograms of the differences in dendritic spine density in segments at different distances from the soma (C) and the total density of dendritic spines (D). Scale bar = 10 μm. Asterisks indicate statistically significant differences (*p<0.05, **p<0.01, ***p<0.001). Values represent means $\pm$ standard error of the mean.

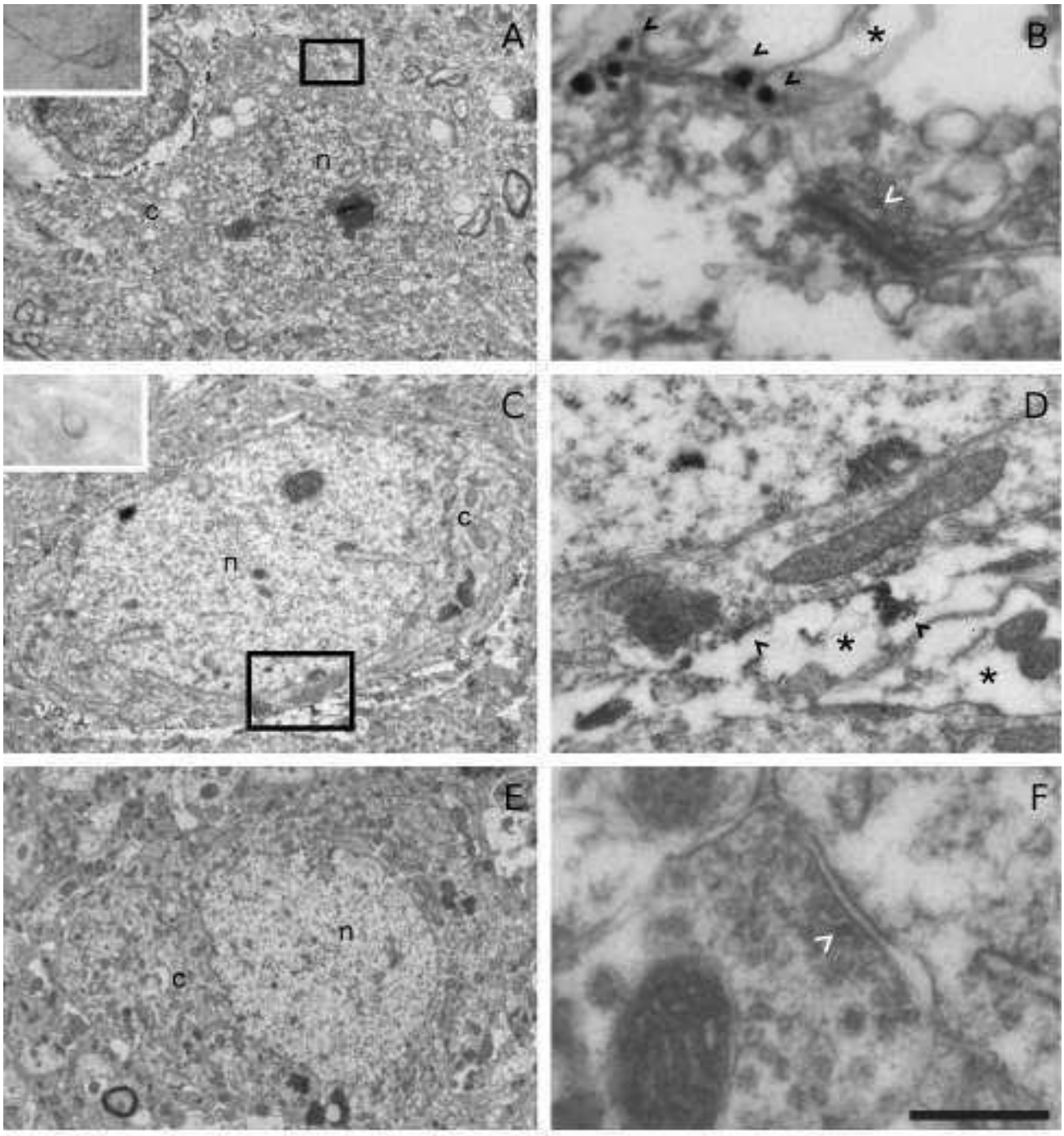

Fig. 17.10: Immunogold detection of PSA-NCAM expressing interneurons in the hippocampus
Electron micrographs of gold-immunolabeled PSA-NCAM expressing cells in the hippocampus of adult rats. (A) Panoramic view of a PSA-NCAM expressing interneuron soma. The letters "c" and "n" refer to the cytoplasm and the nucleus respectively. The small inset, in the left top of the figure, shows an optical micrograph of the PSA-NCAM expressing neuron in the resin-embedded sections from where ultrathins were obtained. (B) Detailed view of the squared area in A, showing an asymmetric synaptic contact (white arrowhead) on the surface of the cell somata. Asterisks indicate astroglial lamellae. Black arrowheads point to antigen location on the surface of the plasma membrane. Note that gold particles are found in the surroundings of the synapse but not inside it. (C) Panoramic view of a PSA-NCAM expressing interneuron soma. (D) Detailed view of the squared area in C, showing the antigen location with diaminobenzidine (DAB) precipitation (black arrowheads) and the astroglial lamellae (asterisks). (E) Panoramic view of an interneuron lacking expression of PSA-NCAM. (F) Detailed view of the squared area in E, showing an asymmetric synaptic contact. Scale bar 5 μm for A, 4.5 μm for C, 4 μm for E, 1 μm for D, 0.5 μm for B, 0.3 μm for F.

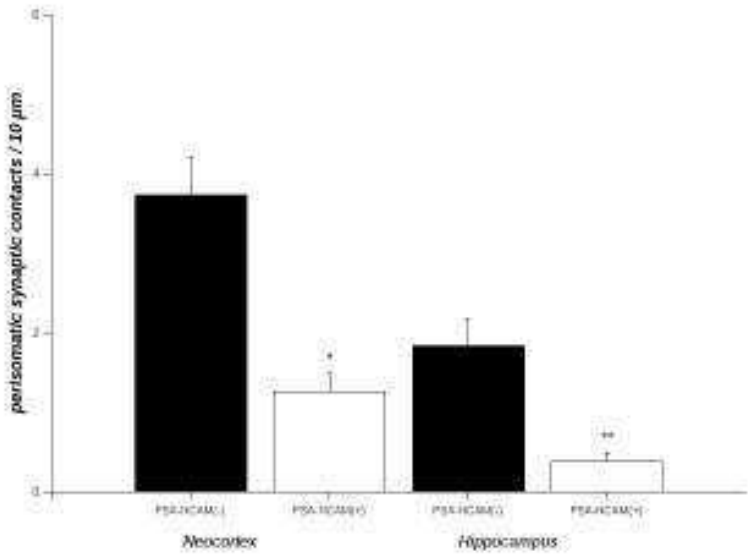

Fig. 17.11: Histogram showing differences in the number of perisomatic synapses per μm between interneurons lacking PSA-NCAM expression and those expressing this molecule

Asterisks indicate statistically significant differences (* $p<0.05$, ** $p<0.01$), and values represent means $\pm$ standard error of the mean.

18 Distribution and dynamics of gephyrin

We have described that PSA-NCAM expressing cells outside the neurogenic niches and the paleocortex layer II are mature interneurons. Interneurons make synaptic contacts on other neurons using the neurotransmitter γ-Aminobutyric acid (GABA), whose receptors are clustered by gephyrin, a scaffolding protein, which therefore is located in the postsynaptic part of the inhibitory synapse. Consequently, the dynamics of its expression should parallel the basal plasticity of inhibitory networks (Panzanelli et al., 2011). We have analyzed the distribution of gephyrin on transfected CA1 hippocampal pyramidal neurons in organotypic cultures and have observed that this protein is expressed in all the regions of the cell, including the basal and apical dendrites, the soma and the axon. In the basal dendrites, we found a mean density of 1.18 puncta per 10 μm, a similar density in the apical dendrites (1.06 puncta per 10 μm) and a higher density in the axon (2.16 puncta per 10 μm). The expression of gephyrin in the somatic region was more intense than that of other regions, where the intensity of fluorescence was lower (Fig. 18.1). We analyzed the basal turnover of gephyrin puncta on different parts of the neuron and we found similar stability rates in the apical (82%), the basal dendrites (80%) and the soma (77%). We also analyzed the apparition rate of new gephyrin puncta and we also observed similar values in the apical and basal dendrites and the soma (Fig. 18.2).

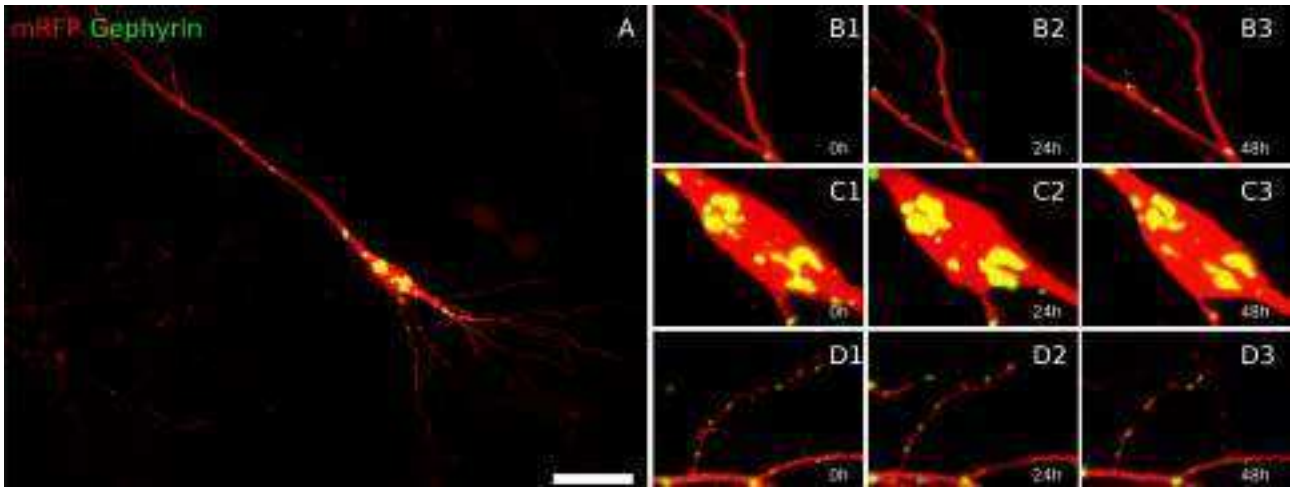

Fig. 18.1: Distribution and dynamics of gephyrin

(A) z-projection of a CA1 pyramidal neuron transfected with gephyrin, showing the distribution of gephyrin puncta in different neuronal regions. 24 hour time lapse turnover of gephyrin puncta in an apical dendrite (B1-B3), the soma (C1-C3) and a basal dendrite (D1-D3) of a pyramidal neuron. Scale bar 50 μm for A and 15 for the other images.

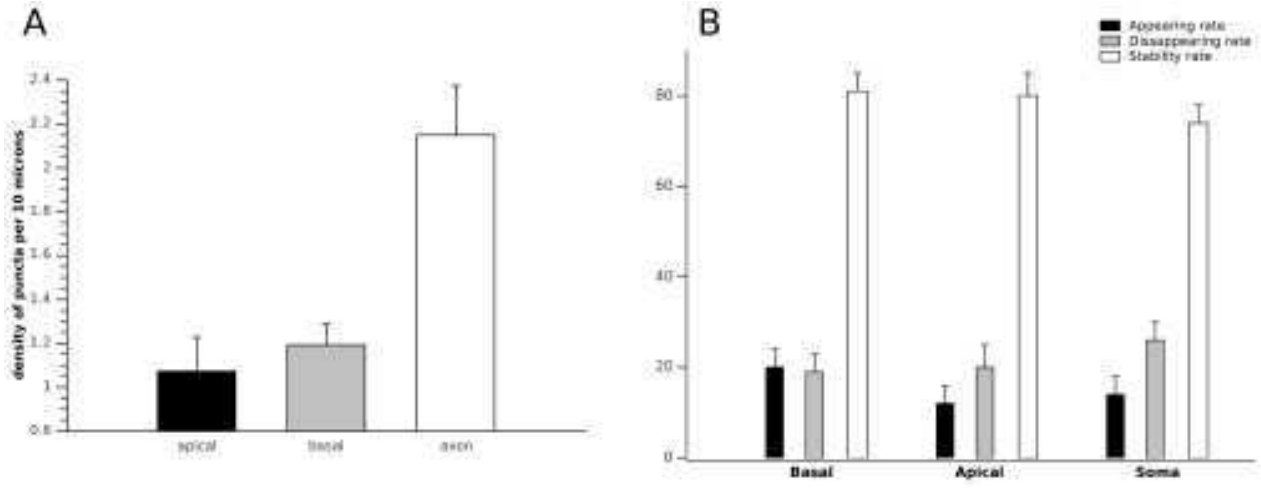

Fig. 18.2: Histograms showing the differences in the distribution and dynamics of gephyrin

(A) Density of gephyrin puncta per 10 μm in the apical and basal dendrites and the axon of a CA1 pyramidal neuron. (B) Stability, appearance and disappearance rate of gephyrin puncta in the different regions of a CA1 pyramidal neuron. Values represent means $\pm$ standard error of the mean.

Part V. Results II: Effects of the ablation of PSA-NCAM and its polysialyltransferases on neuronal structural plasticity

19 Divergent impact of ST8SiaII and ST8SiaIV on PSA-NCAM expression

19.1 Neocortex

In wild type animals PSA-NCAM expressing cells and PSA-NCAM expressing neuropil were detected in all regions of the neocortex. As shown for the cingulate cortex (Fig. 19.2), PSA-NCAM expressing cells were particularly abundant in deep layers. Similar to the situation in adult rats (Varea et al., 2005, 2007a), many of the PSA-NCAM expressing cells displayed multipolar morphologies and neuropil staining was generally more intense in deep layers, specially in the infralimbic and prelimbic cortices (Fig. 19.2A, D). This staining was entirely absent from the neocortex of ST8SiaIV knockout mice (Figs. 19.2B, E). However, as noted before (Eckhardt et al., 2000), absence of ST8SiaIV had no discernible effect on the strong PSA-NCAM labeling of neuroblasts in the SVZ/RMS (Fig. 19.2E, arrowheads). In addition, a small region of the superficial layers of dorsal peduncular, prelimbic and infralimbic cortices retained weak PSA-NCAM immunoreactivity (shown for IL in Fig. 19.2E, arrows). In contrast, distribution and morphology of PSA-NCAM expressing cells (including SVZ/RMS neuroblasts) as well as staining of the neuropil in ST8SiaII knockout mice were similar to that of wild type animals (Fig. 19.2C, F). Evaluation of the number of PSA expressing cells in the cingulate cortex revealed no significant differences between wild type and ST8SiaII knockout mice (Fig. 19.1).

19.2 Paleocortex

The paleocortex (entorhinal and piriform cortices) layer II of wildtype animals displayed an abundant population of PSA-NCAM expressing cells (Figs. 19.1B and 19.3A, D, G). As previously described in rats (Nacher et al., 2002a; Gómez-Climent et al., 2008) some of these cells showed long thick vertical processes that radially traverse the piriform cortex layer III and the deep layers of the lateral entorhinal cortex before entering the external capsule (Fig. 19.3A, J, K). Frequently, small cells were found closely apposed to these processes (Fig. 19.3K) (Nacher et al., 2002a). Compared to the wild type, ST8SiaIV-deficient mice had significantly more PSA-NCAM expressing cells in layer II (Figs. 19.1B and 19.3B, E) and in addition to the thick vertical processes, thin PSA-NCAM immunoreactive fibers were observed in layer III, which resembled typical axons with a small diameter and a beaded appearance (Fig. 19.3L, M). In contrast, the number of PSA-NCAM immunoreactive cells in paleocortex layer II was drastically reduced in ST8SiaII$-/-$ mice (Figs 19.1B and 19.3C, F)

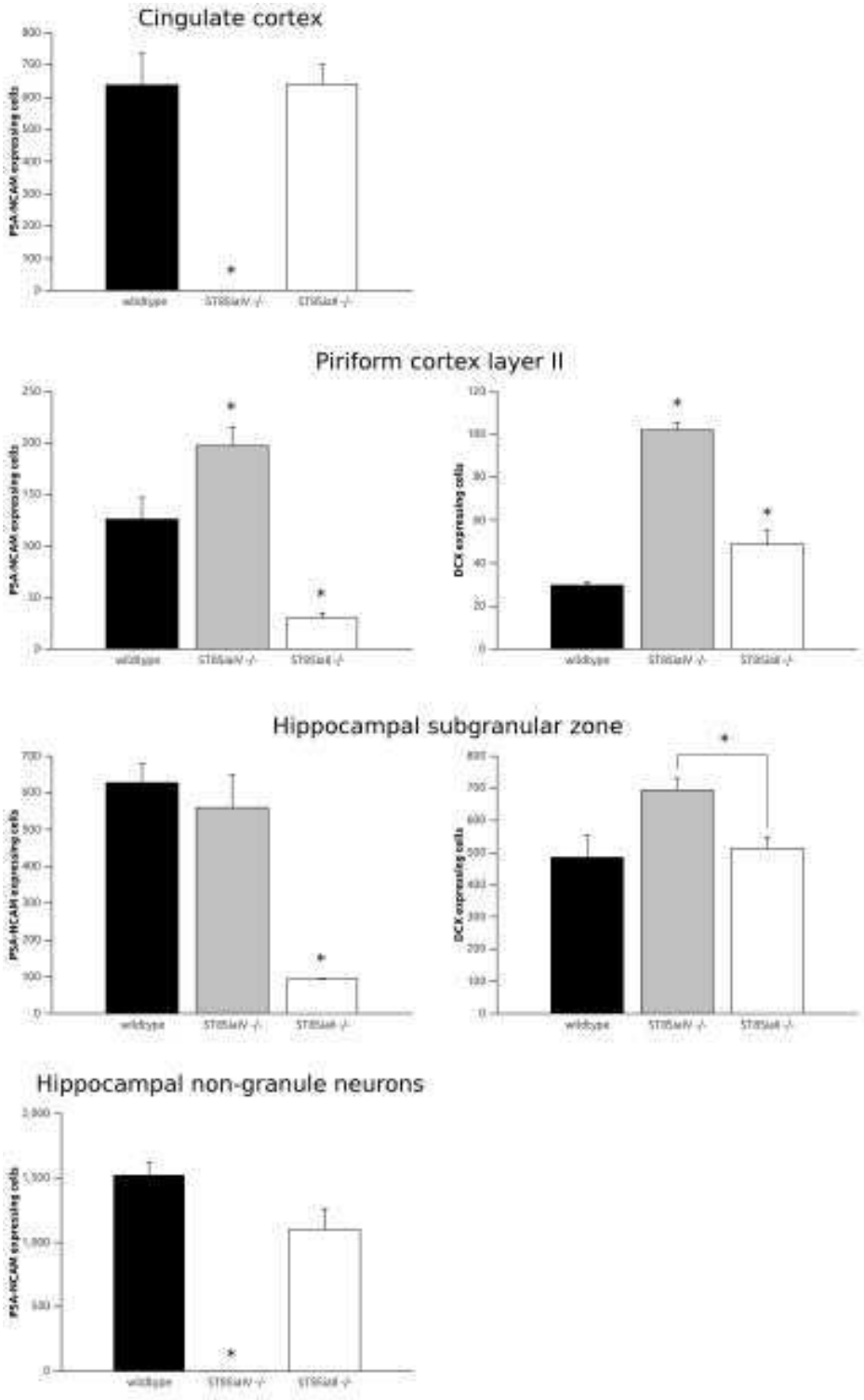

Fig. 19.1: Estimation of the total numbers of PSA-NCAM and DCX immunoreactive neurons in different regions of the cerebral cortex of adult wild type and polysialyltransferase-deficient mice

(A) PSA-NCAM expressing neurons in the cingulate cortex ($p=0.0005$). (B) PSA-NCAM expressing neurons in the piriform cortex layer II ($p=0.0005$). (C) Doublecortin (DCX) expressing neurons in the piriform cortex layer II ($p<0.0001$). (D) PSA-NCAM expressing neurons in the hippocampal SGZ ($p=0.0016$). (E) DCX expressing neurons in the hippocampal SGZ ($p=0.049$). (F) PSA expressing non-granule neurons in the hippocampus ($p=0.0005$). One-way ANOVA followed by Student–Newman–Keuls post hoc tests.

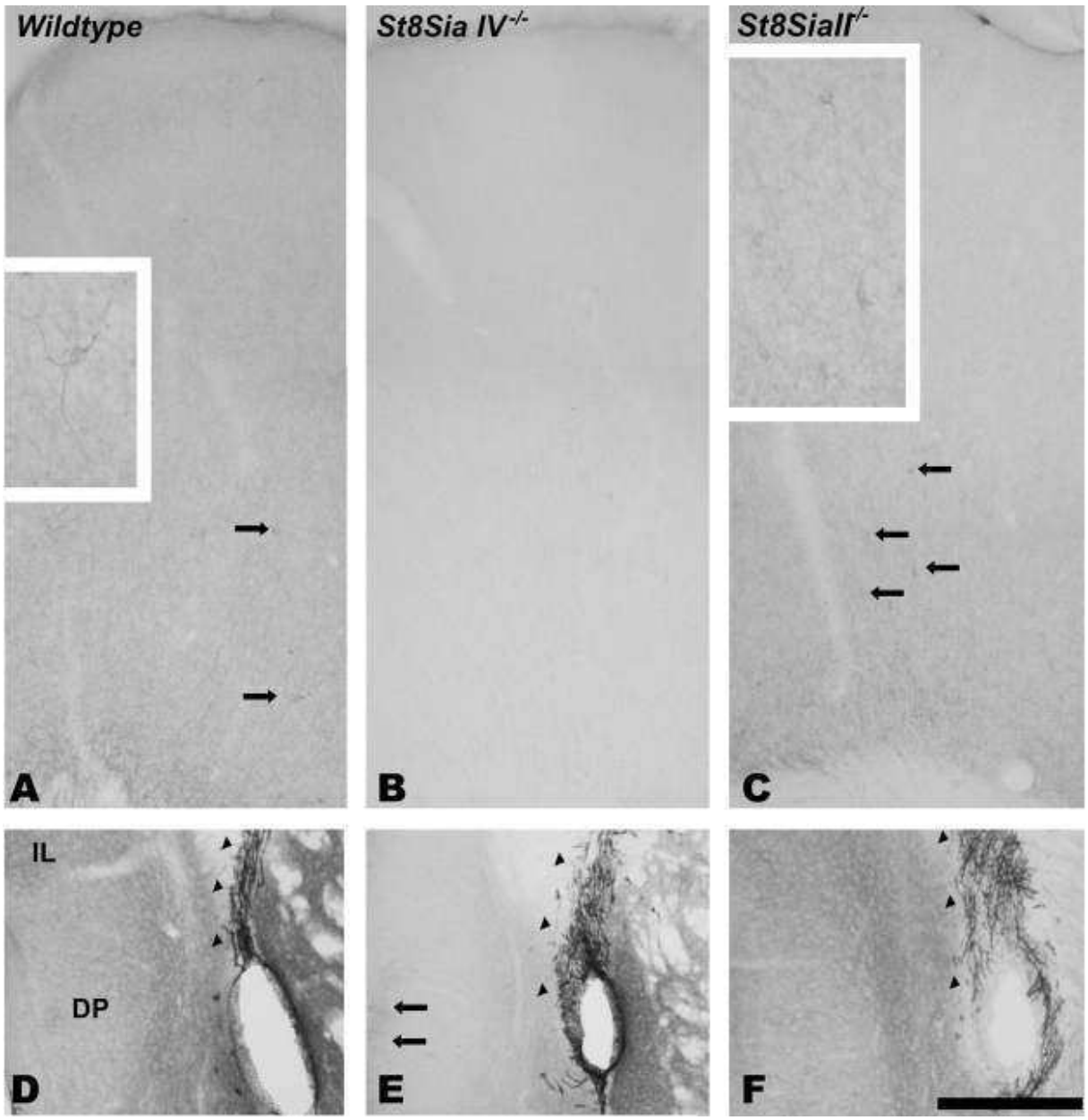

Fig. 19.2: PSA-NCAM expression in the neocortex of wild type and ST8SiaIV- and ST8SiaII-deficient mice

(A–C) PSA expressing neurons (arrows) in deep layers of the cingulate cortex. Complete absence of immunoreactivity in the neuropil and in neuronal somata, in ST8SiaIV$-/-$ mice (B). Insets show enlarged views of some of the neurons indicated by the arrows. (D–F) Infralimbic and dorsal peduncular cortices: despite the absence of PSA-NCAM immunoreactivity in most of cortical the parenchyma, a small portion of neuropil in superficial layers (arrows) displays some faint labelling. Arrowheads indicate PSA-NCAM expressing cells in the SVZ. Scale bar: 20 μm for (A–C) (10 μm for insets) and 40 μm for (D–F). IL, infralimbic cortex; DP, dorsal peduncular cortex.

and only few thick processes could be observed in layer III (Fig. 19.3N, O).

In the deep layers of the wildtype paleocortex large PSA-NCAM expressing cells were found (Fig. 19.3K), resembling those described in the neocortex (see Fig. 19.2A). These cells were present in ST8SiaII$-/-$ (Fig. 19.3N) but absent in ST8SiaIV$-/-$ mice (Fig. 19.3L, M). In wild type and ST8SiaII-deficient animals, intense immunostaining was observed in the neuropil of the endopiriform nucleus, and faint PSA expression was detected in the neuropil of all paleocortex layers (Fig. 19.3A, C). In contrast, in ST8SiaIV knockout mice these neuropil structures were completely devoid of PSA labeling (Fig. 19.3B). An abundant population of DCX expressing cells was found in the paleocortex layer II of wild type animals (Figs. 19.1C and 19.4A). In ST8SiaII- and ST8SiaIV-deficient mice the morphology of these cells appeared unaltered, but their numbers were significantly increased (Figs. 19.1C and 19.4B, C). This increase was more pronounced in the ST8SiaIV$-/-$ situation. Moreover, a small number of DCX-immunoreactive cells, with an interneuron-like multipolar morphology was detected in the paleocortex layer III of ST8SiaIV-deficient animals. (Fig. 19.4D). This type of DCX-positive cells was never observed in the wild type.

19.3 Hippocampus

The well-known pattern of strongly PSA-NCAM expressing cells in the SGZ of the dentate gyrus (Seki and Arai, 1991b) was recapitulated for wild type animals (Figs. 19.1D and 19.5A, B). Likewise, staining obtained in the neuropil of the hippocampus was mostly consistent with previous studies (Seki and Arai, 1999; Seki, 2002a; Eckhardt et al., 2000). Intense PSA-NCAM immunoreactivity was observed in the hilus and the mossy fibers of the CA3 stratum lucidum (Fig. 19.5A). The molecular layer of the dentate gyrus displayed a weaker but dense PSA-NCAM staining, with a slightly more pronounced labeling in a zone adjacent to the granule cell layer (Fig. 19.5A). Light and less compact PSA-NCAM labeling was detected throughout the stratum lacunosum-moleculare of CA1 and a plexus of markedly immunoreactive processes was found in the most dorsal region of this layer, at the limit with the stratum oriens (Fig. 19.5A, J). Moreover, a diffuse, light immunostaining was observed in the stratum pyramidale of CA1 (Fig. 19.5J).

In accordance with the previously described staining patterns of PSA-NCAM expressing cells in the SGZ of ST8SiaII- or ST8SiaIV-deficient mice (Eckhardt et al., 2000; Angata et al., 2004), a quantitative evaluation of these cells revealed a dramatic reduction in ST8SiaII$-/-$ (Figs. 19.1D and 19.5D, E), but no significant change in ST8SiaIV$-/-$ animals (Figs. 19.1D and 19.5G, H). Moreover, the few remaining PSA-NCAM expressing cells in the SGZ of ST8SiaII-deficient mice displayed only some short processes and were devoid of the pronounced vertical (apical) PSA-NCAM expressing dendrites (Fig. 19.5H). A prominent feature of the ST8SiaIV knockout mice is the reduction of PSA-NCAM immunoreactivity on mossy fibers (Eckhardt et al., 2000). Accordingly, we found that the intense labeling of mossy fibers as observed in wild type mice (Fig. 19.5A) was reduced to few thin PSA-NCAM expressing processes in the hilus and the stratum lucidum of ST8SiaIV-deficient mice (Fig. 19.5D). Some of these processes originated from PSA-NCAM

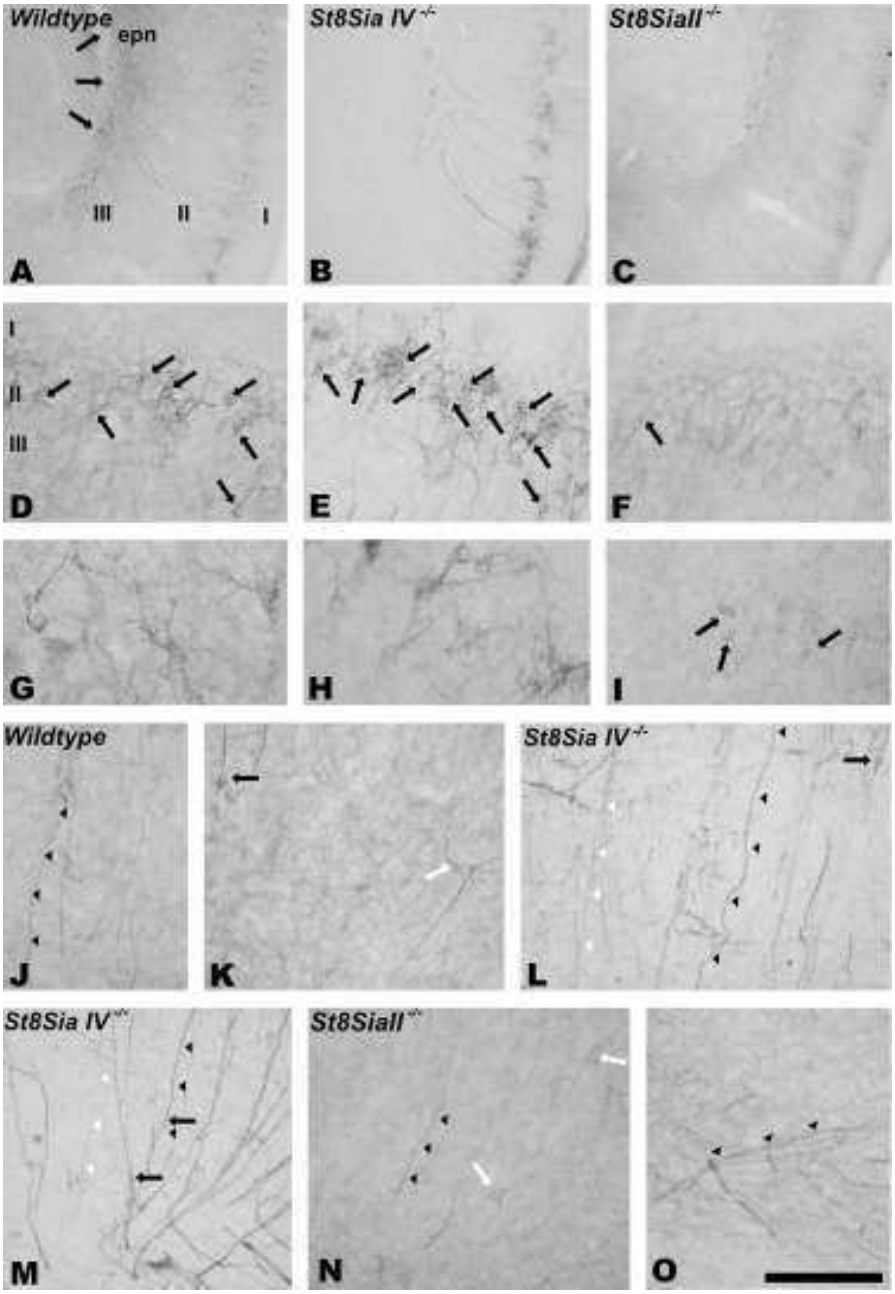

Fig. 19.3: PSA-NCAM expression in the paleocortex of wild type, ST8SiaIV- and ST8SiaII-deficient mice

(A–C) Panoramic views of piriform cortex in wildtype (A), ST8SiaIV−/− (B) and ST8SiaII−/− mice (C). Arrows indicate the end of the external capsule. (D–F) Microphotographs of piriform cortex layer II. An abundant population of PSA-NCAM immunoreactive cells (arrows) can be observed in wild type mice (D). The number of these immunoreactive cells is increased in ST8SiaIV−/− mice (E), but they are almost absent in ST8SiaII−/− mice (F). (G–I) High magnification views of PSA-NCAM expressing cells shows the reduced arborization of the scarce cells in ST8SiaII−/− mice (arrows). (J–O) Vertical immunoreactive processes can be observed in layer III of wild type (J, K), ST8SiaIV−/−(L, M) and ST8SiaII−/− mice (N, O). Black arrows indicate small cells resembling those in layer II, while white arrows indicate cells similar to hippocampal non-granule PSA-NCAM expressing neurons. In addition two types of processes were distinguished: thick vertical processes (black arrowheads) and thin fibers (white arrowheads). Scale bar: 40 μm for (A–C), 10 μm for (D–F) and (J–O), 6 μm for (G–I). epn, endopiriform nucleus.

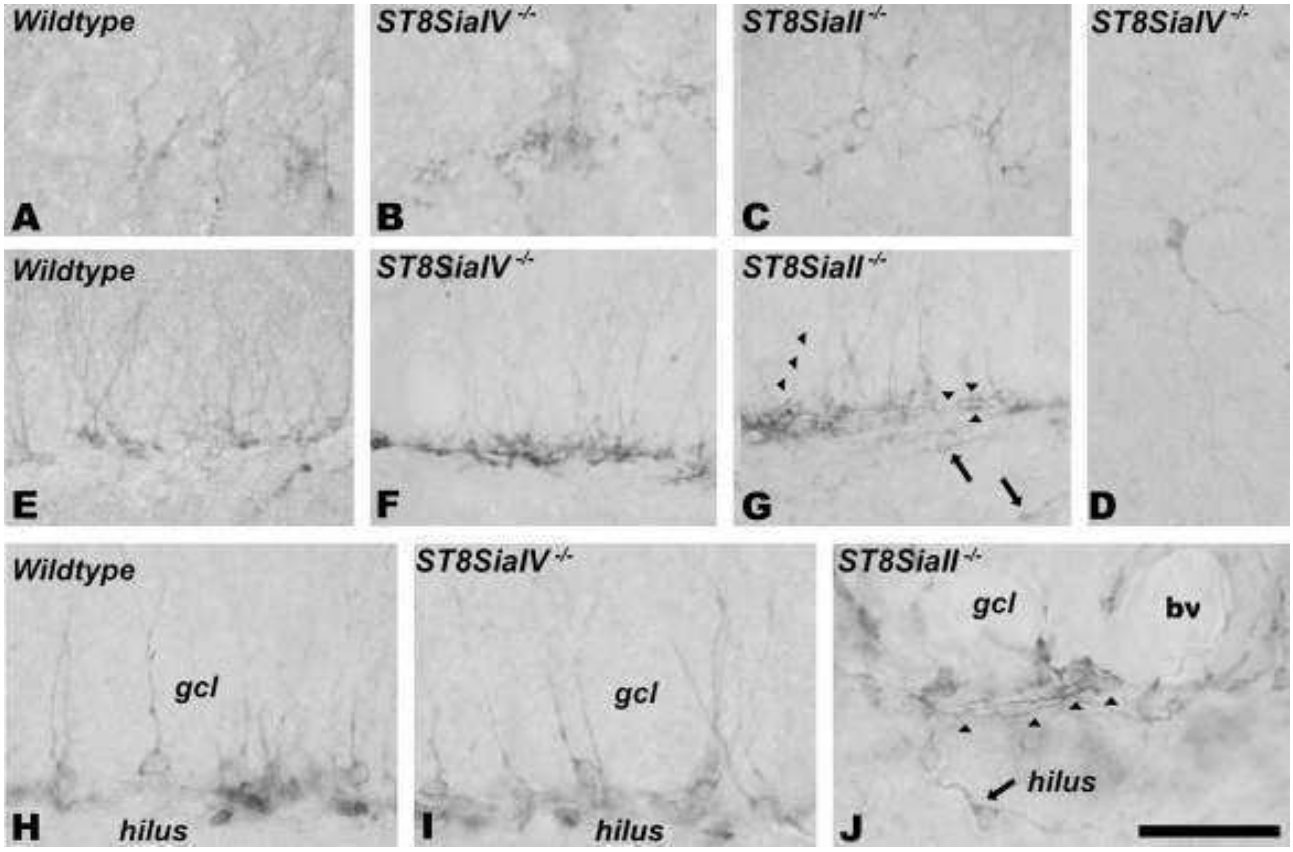

Fig. 19.4: DCX expression in the paleocortex and the SGZ of wild type, ST8SiaIV- and ST8SiaII-deficient mice

(A–C) Piriform cortex layer II. The population of DCX immunoreactive cells is more abundant in ST8SiaIV$-/-$ mice. (D) Piriform cortex layer III. DCX expressing multipolar cell resembling an interneuron. (E–G) SGZ. DCX expressing cells are more abundant in ST8SiaIV$-/-$ mice but their morphology is similar to that found in wild type mice. In ST8SiaII$-/-$ mice many of these cells had an aberrant morphology, that is, presence of short apical processes restricted to the granule cell or horizontal/basal processes restricted to the SGZ and the hilus (arrowheads). DCX expressing ectopic cells can be found in the hilus (arrows). (G–J) High magnification views of DCX expressing cells in the SGZ. Note that while the morphology of most of the cells in wild type and ST8SiaIV$-/-$ mice is typical, many cells in ST8SiaII$-/-$ animals have abnormal morphologies/orientations (arrowheads) or ectopic locations (arrow). Scale bar: 10 μm for (A–G), 6 μm for (H–J).

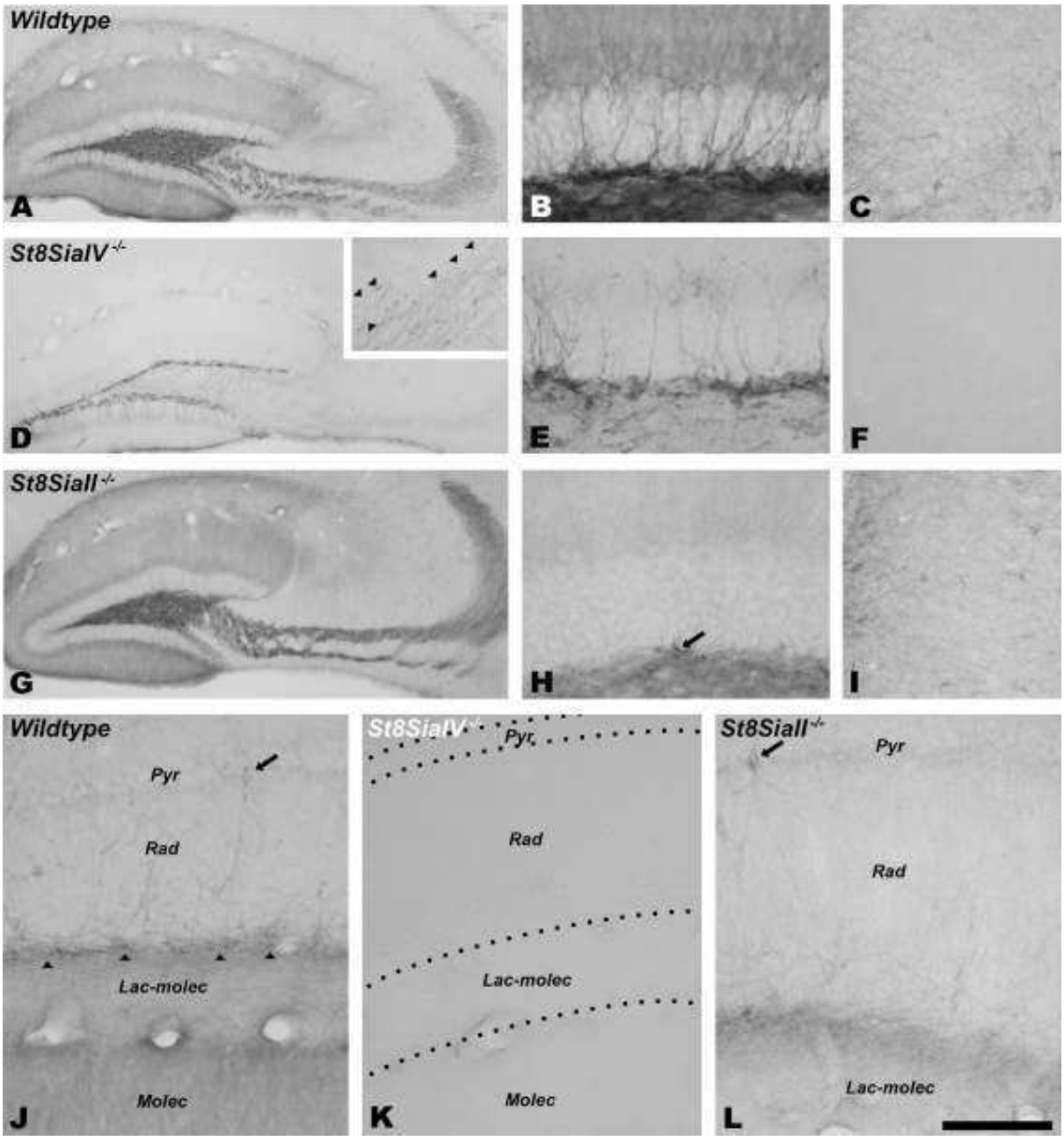

Fig. 19.5: PSA-NCAM expression in the hippocampus of wild type, ST8SiaIV- and ST8SiaII-deficient mice

(A, D, G): Dorsal hippocampus. The neuropil expression of PSA-NCA in ST8SiaIV−/− mice (D) is reduced in the molecular layer and restricted to a few thin PSA-positive processes in the hilus and the stratum lucidum (inset). (B, E, H) Dentate gyrus. Only a faint PSA immunostaining can be detected in the inner third region of the molecular layer of ST8SiaIV−/− mice (E). ST8SiaII−/− mice display neuropil PSA expression similar to that of wildtype mice. The number of labeled cell somata in the SGZ is highly reduced (H). (C, F, I) Ventral hippocampus. PSA-NCAM expressing non-granule neurons can be found in the wild type (C) and ST8SiaII−/− (I) but not in ST8SiaIV−/− mice (F). (J–L) Strata pyramidale (pyr), radiatum (rad) and lacunosum moleculare (lac-molec) of CA1. Wild type and ST8SiaII−/− mice show several PSA-NCAM immunostained cell somata resembling typical interneurons (arrows) as well as neuropil in the stratum lacunosum-moleculare (arrowheads). PSA-NCAM immunostaining is absent from the entire CA1 region of ST8SiaIV−/− mice (K). Scale bar: 40 μm for (A, D, G); 10 μm for (B, E, H); 20 μm for (C, F, I); 15 μm for (J–L).

expressing somata in the SGZ indicating that they were mossy fibers. Moreover, the entire stratum lacunosum-moleculare of the CA1 field (including the immunoreactive plexus next to the hippocampal fissure) as well as most of the molecular layer of the dentate gyrus was completely devoid of PSA-NCAM staining (Fig. 19.5D, K). Faint residual immunoreactivity, however, was detected in the inner zone of the molecular layer (Fig. 19.5D, E). In accordance with the findings of Angata et al. (2004), PSA-NCAM staining of mossy fibers in ST8SiaII knockout mice was as intense as in the wildtype and revealed the aberrant projection of the infrapyramidal mossy fibers extending to the CA3a field (Fig. 19.5G, H). In addition, we found that PSA-NCAM immunoreactivity of the other neuropil structures of the hippocampus was not affected by the absence of ST8SiaII (Fig. 19.5G, L). As described in the rat (Nacher et al., 2002b), numerous non-granule PSA expressing cells were found throughout the hippocampus of wild type mice (Fig. 19.1F), particularly in its ventral region and in the vicinity of the fimbria (Fig. 19.5C). While these cells were completely absent in mice lacking ST8SiaIV (Figs. 19.1F and 19.5F), their numbers and their morphology were unaffected in ST8SiaII knockout mice (Figs. 19.1F and 19.5I). Evaluation of DCX expressing cells in the SGZ revealed similar numbers in wild type (Figs. 19.1E and 19.4E) and ST8SiaII-deficient mice (Figs. 19.1E and 19.4G). Compared to the ST8SiaII$-/-$ situation, the amount of DCX-positive cells was significantly increased in the absence of ST8SiaIV (Figs. 19.1E and 19.4F) but most of them retained the characteristic morphology of immature granule cells as well as their position within the SGZ (Fig. 19.4E, F, I). In contrast, the appearance of many of the DCX-positive cells in the SGZ of ST8SiaII-deficient mice was aberrant. Instead of the apical dendrites typically extending into the molecular layer, some of these cells displayed short apical vertical processes that did not reach beyond the granule cell layer, or they presented horizontal or basal processes that were restricted to the SGZ or extended into the hilus. Moreover, several DCX expressing ectopic cells were found in the hilus (Fig. 19.4G, J). Some of these cells with aberrant morphology and/or ectopic locations, as described previously in control adult rats (Nacher et al., 2001) could also be found, although in reduced numbers, in ST8SiaIV-deficient and wild type mice.

19.4 Extracortical regions

PSA-NCAM expression was also studied in selected extracortical regions. As in the rat (Nacher et al., 2002c), the neuropil of the central and medial amygdaloid nuclei displayed intense immunoreactivity in wild type mice, while faint immunostaining was observed in the lateral and basolateral nuclei (Fig. 19.6A). PSA-NCAM expressing cells were detected in all amygdaloid nuclei (Fig. 19.6D). In the amygdala of ST8SiaIV knockout mice, PSA-NCAM expression was strongly reduced in the central and medial nuclei and completely absent from the basolateral and lateral nuclei (Fig. 19.6B). The number of PSA-NCAM expressing somata was reduced to a few, small immunoreactive cells mostly located within the basolateral and lateral nuclei (Fig. 19.6E). PSA-NCAM expression in the amygdala of ST8SiaII-deficient mice was indistinguishable from the wild type situation (Fig. 19.6C, F). In the neuropil of the septum PSA-NCAM expression was markedly reduced in ST8SiaIV$-/-$,

but not ST8SiaII−/− mice (Fig. 19.6G–I). In clear contrast to the PSA-NCAM positive cells in the cortex, PSA-NCAM expressing cells in the septum (Foley et al., 2003) were present in ST8SiaIV- and in ST8SiaII-deficient mice (not shown). Likewise, PSA-NCAM staining patterns of neuropil in the striatum (Fig. 19.6G–I) and the hypothalamus (Fig. 19.6J–L) were not noticeably affected by genetic deletion of either polysialyltransferase.

19.5 Phenotype of PSA-NCAM expressing cells in the ST8SiaII- and the ST8SiaIV- knockout mice

In consonance with previous results (Varea et al., 2005), none of the PSA-NCAM expressing cells analyzed outside the neurogenic regions and the paleocortex layer II of wildtype and the ST8SiaII knockout mice expressed CAMKII, a marker of excitatory neurons. In addition, none of the PSA expressing cells in the paleocortex layer II of wildtype and the ST8SiaIV expressed CAMKII (Fig. 19.7).

19.6 The expression of presynaptic markers is not affected in the ST8SiaII- and the ST8SiaIV- knockout mice

We analyzed the expression of two presynaptic markers in the layer V of the cingulate cortex, a region of the mPFC: synaptophysin (SYN), a reliable marker of synaptic transmission, and GAD6, a marker of presynaptic inhibitory synapses (The GAD6 antibody recognizes both 65 kDa and 67 kDa isoforms). We observed no change in the expression of neither SYN ($p=0.861$) nor GAD6 ($p=0.555$) (Fig. 19.8)

20 Effects of PSA removal on the structural plasticity of hippocampal interneurons

20.1 Dendritic spine density 2 and 7 days after intracerebral EndoN injection

We studied the dendritic spine density of interneurons expressing eGFP in the hippocampal CA1 region, 2 and 7 days after an intracranial injection of the Endo-N-actylneuraminidase enzyme. In all interneurons analyzed, the spine density increased with the distance from the soma to each segment (two-way ANOVA; 2 days: $p<0.0001$; 7 days: $p<0.0001$). When analyzing the different 60 μm segments 2 days after the injection, we did not observe differences in dendritic spine density between the control and the treated animals neither in the first (protected LSD $p=0.6659$) nor in the second segment, where there was a trend towards an increase ($p=0.0706$). However, we observed a significant increase in the distal segment ($p=0.0205$) in the animals injected with EndoN compared with the controls (Fig. 20.1D1 and D2). We also observed a significant increase (t-test $p=0.0256$)

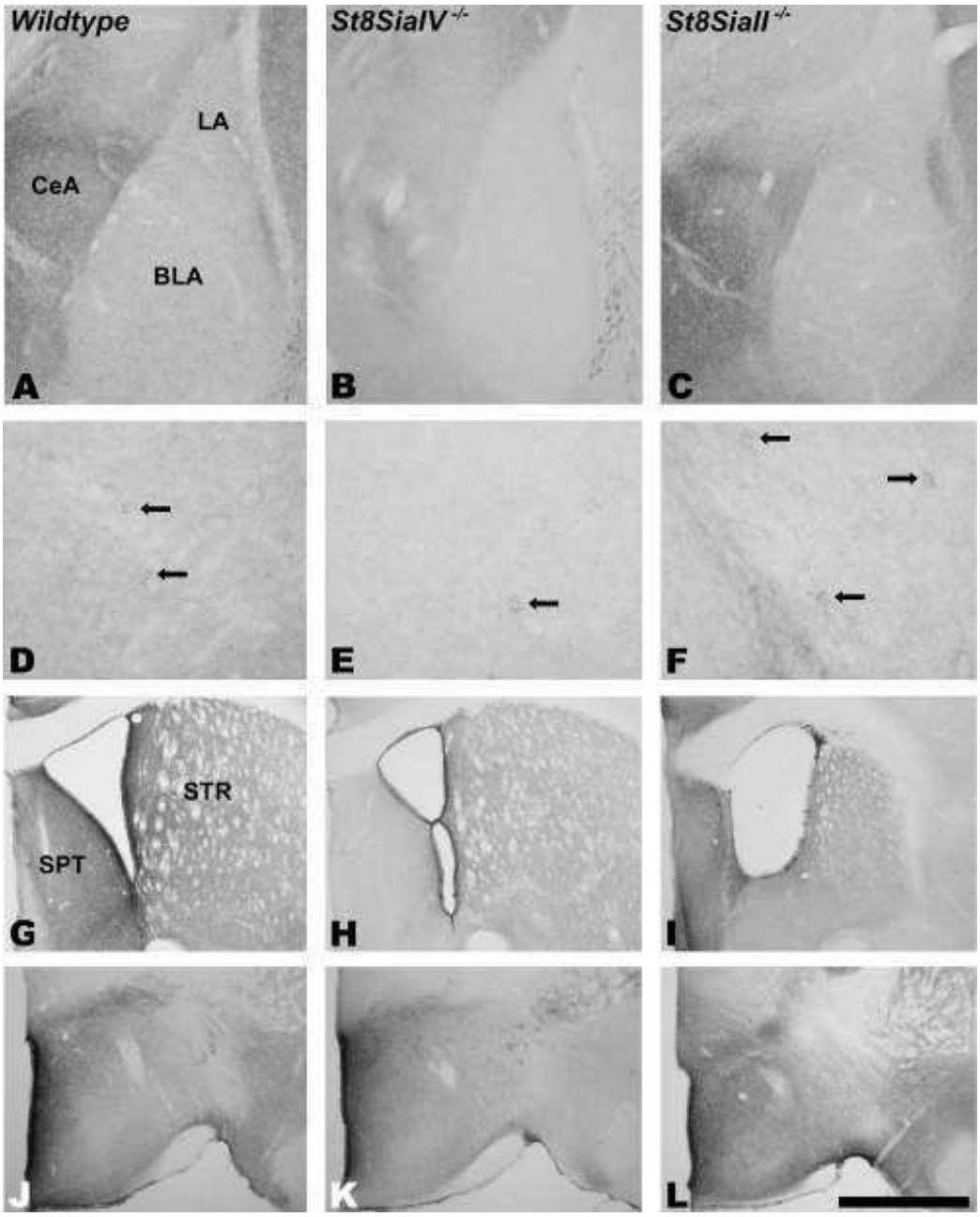

Fig. 19.6: PSA-NCAM expression in cell somata and neuropil of different extracortical regions of wild type, ST8SiaIV- and ST8SiaII-deficient mice

(A–C) Amygdala. ST8SiaIV−/− mice display a severe reduction in the general intensity of PSA-NCAM expression in the neuropil. However, some faint immunostaining can be detected in the central amygdala. (D–F) Basolateral amygdala. The number of PSA-NCAM expressing cells (black arrows) and the neuropil intensity in this amygdaloid nucleus is reduced in the ST8SiaIV−/−mice. However, some scarce small cells with faint PSA-NCAM expression can be observed in these animals. (G–I) Septum and striatum. The striatum of all the different animals studied shows a similar intensity of PSA-NCAM expression. However, a marked reduction in immunostaining can be seen in the septum of ST8SiaIV−/−mice. (J–L) Hypothalamus. No major differences in PSA-NCAM expression can be observed in the neuropil of the hypothalamic regions observed. Scale bar: 40 μm. BLA, basolateral amygdaloid nucleus; CeA, central amygdaloid nucleus; LA, lateral amygdaloid nucleus; SPT, septum; STR, striatum.

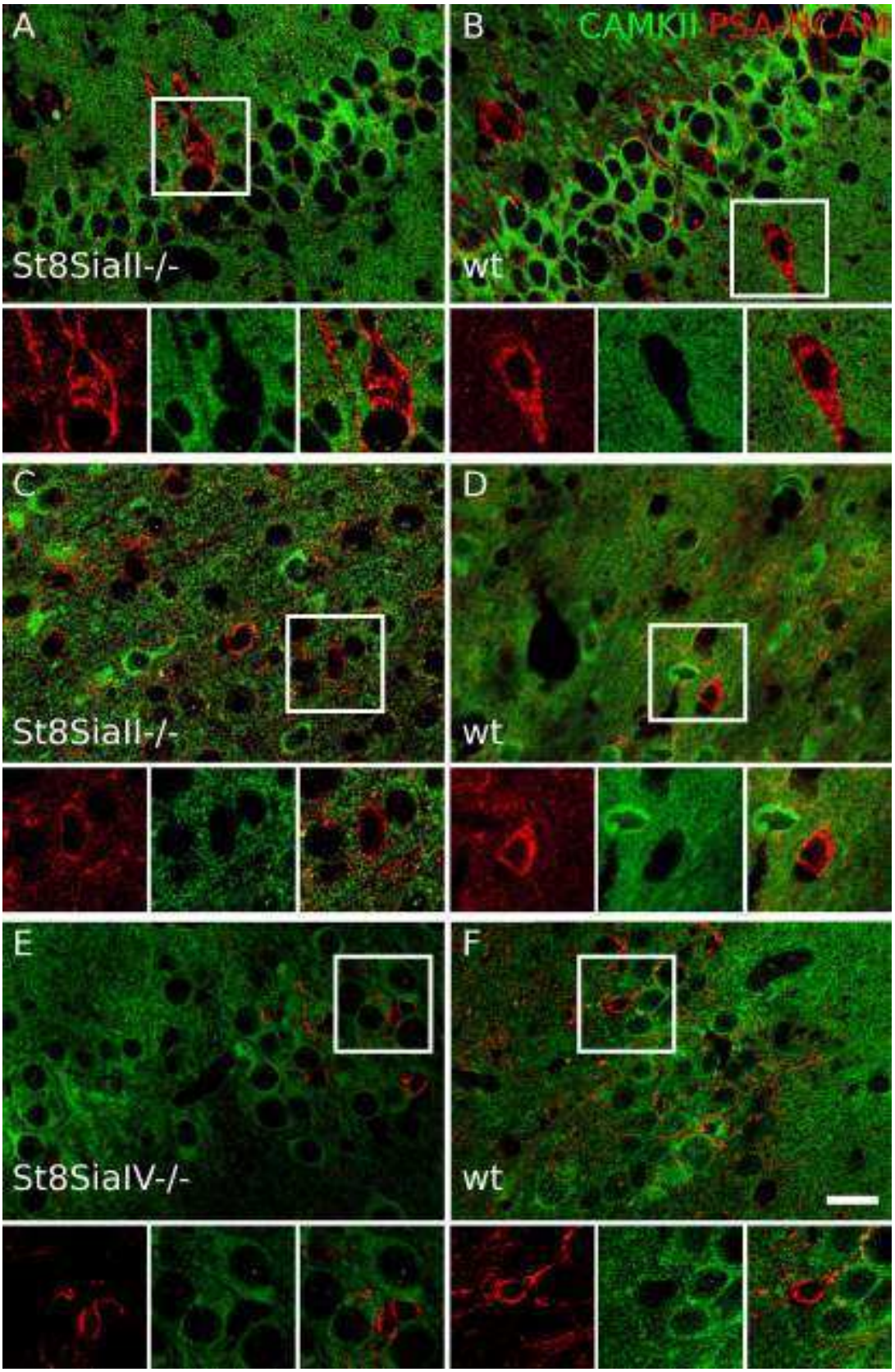

Fig. 19.7: Phenotype of PSA-NCAM expressing cells in wild type, ST8SiaII and ST8SiaIV mice
PSA-NCAM (red) and CAMKII (green) immunohistochemistry. (A, B) Hippocampal CA1 stratum radiatum in ST8SiaII-deficient mice (A) and wild type (B). Note that in both cases PSA-NCAM expressing cells lack CAMKII immunoreactivity, which, by contrast, is specially intense in the pyramidal cell layer. (C, D) Cingulate region of the mPFC of ST8SiaII-deficient (C) and wild type mice (D). (E, F) Paleocortex layer II in ST8SiaIV-deficient (E) and wild type mice (F). All images in this figure are single confocal planes. Scale bar 20 μm for (A) and (B); 12.5 μm for insets.

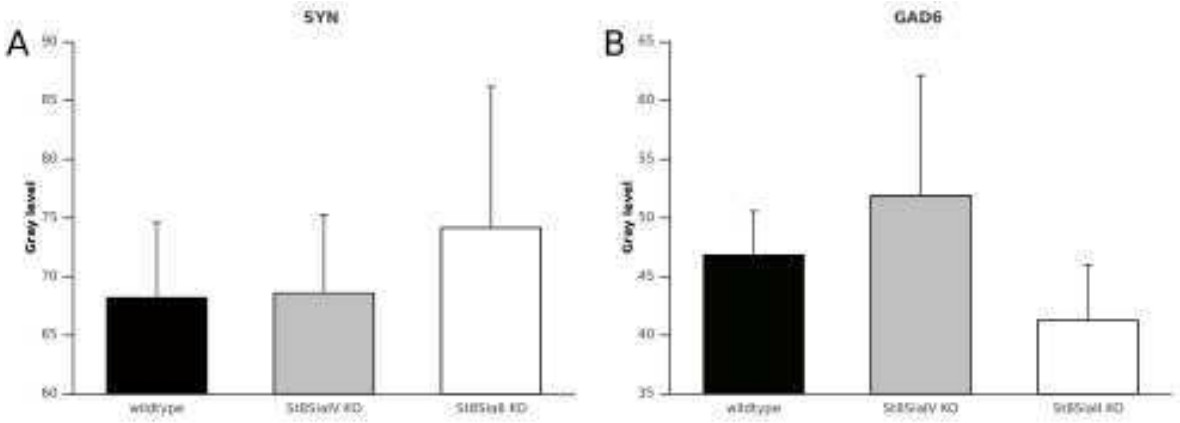

Fig. 19.8: Histograms showing the expression of presynaptic markers in the mPFC of wild type, ST8SiaII and ST8SiaIV mice

SYN (A) and GAD6 (B) expression in the mPFC of ST8SiaII and ST8SiaIV deficient mice. Values represent means ± standard error of the mean.

when considering the total number of spines in the dendrite between the animals injected with EndoN and those injected with the vehicle. Comparing the control and the EndoN treated animals 7 days after the injection in the different dendritic segments analyzed we found a decrease in spine density in the distal segment (p=0.0484) of the animals injected with EndoN compared with those injected with vehicle (Fig. 20.1E1 and E2), but we did not find significant changes in the proximal (p=0.7516) or the intermediate segments (p=0.1766). When analyzing the total density of spines we only found a tendency towards a decrease in the EndoN injected group (p=0.0892).

20.2 Effects of EndoN treatment on spine dynamics

In control conditions, in our organotypic hippocampal cultures (see methods section) the stability rate of CA1 hippocampal interneuronal spines in a 24 hour time-lapse experiment represented between 66 and 69 % of the total pre-existing spines, while the apparition rate of new interneuronal spines represented a 35% of the total of pre-existing spines (Fig. 20.2). Under experimental conditions, the apparition rate of new spines was significantly increased 24 hours after the addition of EndoN to the culture medium, when compared to either the internal (p=0.0024) or the external control (p=0.0063).

However, there was no effect of EndoN on the stability of pre-existing spines (Fig. 20.2). When analyzing the relative variation of the spine density, we observed a strong increase in the spine density in the slices treated with EndoN when compared to the internal (p=0.0003) and external controls (p=0.0008).

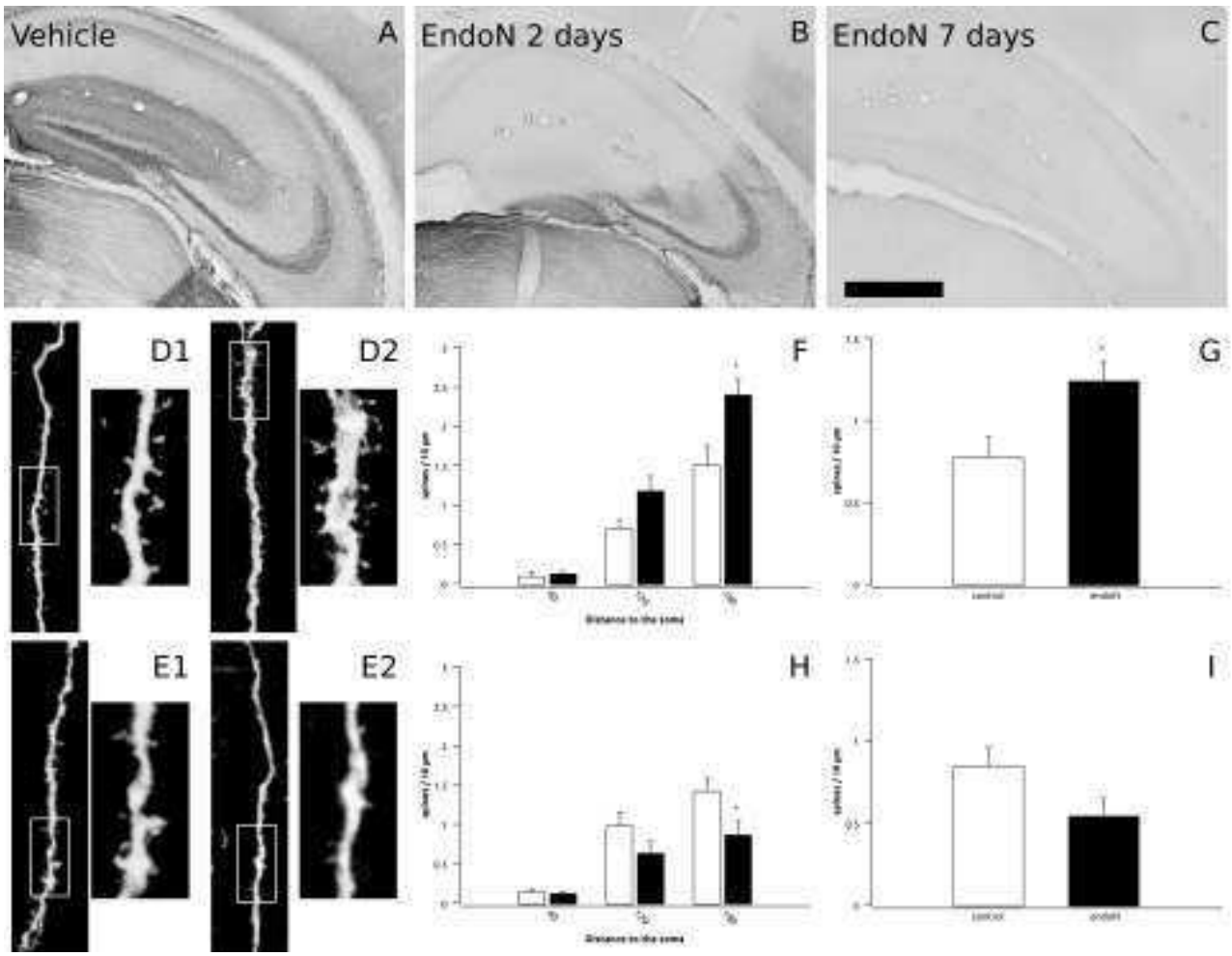

Fig. 20.1: Effects of PSA removal on the hippocampus of GIN mice

A-C: Micrographs showing the expression of PSA-NCAM in the hippocampus of mice 2 days after intracerebral injections of vehicle (A), EndoN (B) and 7 days after intracerebral injections of EndoN (C). D-E: Z-Projections of the distal portion of interneuron dendrites in CA1 showing the difference in spine density between animals injected with vehicle (D1) or EndoN (D2) sacrificed 2 days after the injection and between animals injected with vehicle (E1) or EndoN (E2) sacrificed 7 days after the injection. F-I: Graphs representing the spine density of interneuron dendrites between vehicle and EndoN injected animals per 60 μm segments (F: 2 days after the injection; H: 7 days after the injection) and the total spine density (G: 2 days after the injection; I: 7 days after the injection) at 2 days and 7 days respectively. White bars represent vehicle injected animals and black bars represent EndoN injected animals. Tendency (# $p < 0.1$) and statistically significant (* $p < 0.05$, ** $p < 0.01$, *** $p < 0.001$) student t-test. Scale bar: 500 μm for A, B and C and 15 μm for D1, D2, E1 and E2.

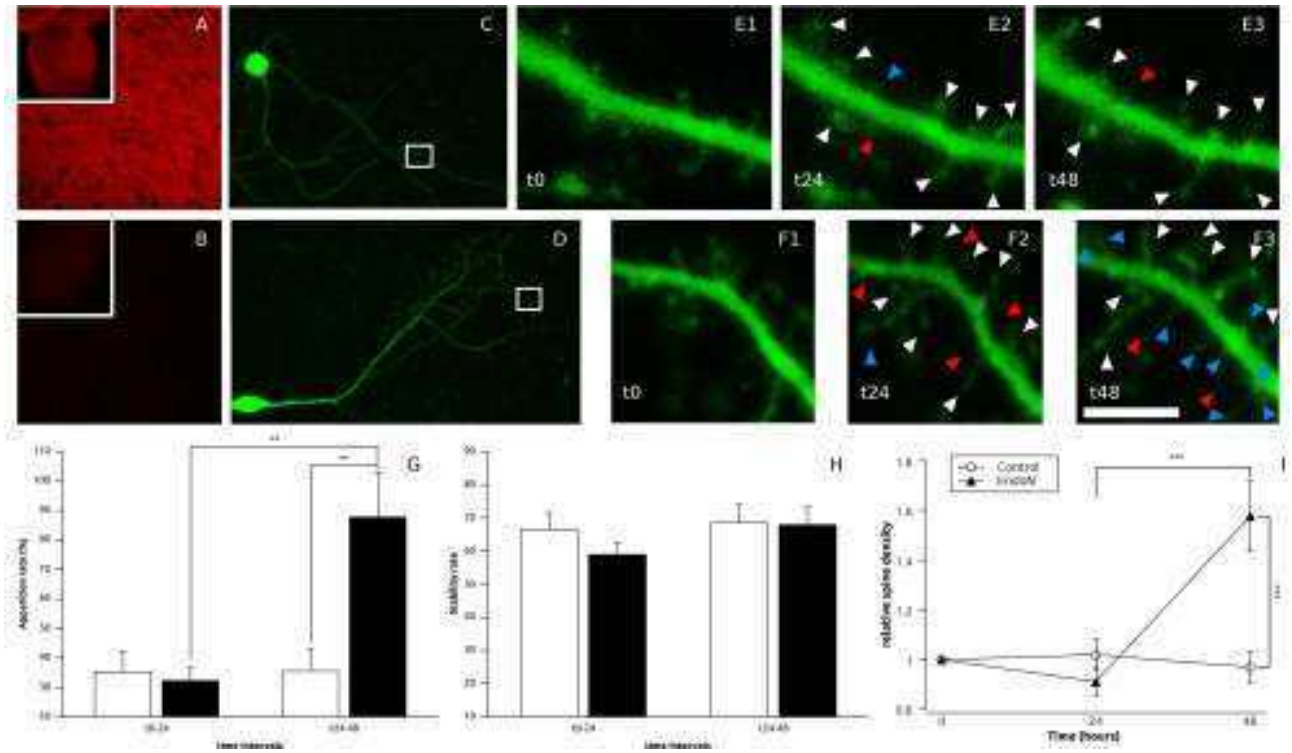

Fig. 20.2: Effects of PSA removal on organotypic hippocampal cultures

A-B: Single confocal planes showing the expression of PSA-NCAM in the cultures 24 hours after the addition of vehicle (A) or EndoN (B) in the culture medium. C-D: Z-Projections showing the complete morphology of interneurons from slices treated with vehicle (C) or EndoN (D). E-F: Turnover of interneuronal spines: external control between 0 (E1) and 24 hours (E2) and 24 hours after the addition of vehicle (E3). Internal control between 0 (F1) and 24 hours (F2) and 24 hours after the addition of EndoN (F3). Arrowheads indicate stable (white), new (blue) and lost (red) spines compared to the previous time-point. G-H: Graphs representing the apparition rate of new spines (G) and the stability rate of preexisting spines (H) during the internal control (t0-24) and the treatment with either vehicle or EndoN (t24-48). I: Graph representing the spine density relative to the original spine density at 0, 24 and 48 hours. White bars represent vehicle injected animals and black bars represent EndoN injected animals. Statistically significant (* $p < 0.05$, ** $p < 0.01$, *** $p < 0.001$) student t-test. Scale bar: 125 μm for A and B (700 μm for their insets), 75 μm for C and D and 5 μm for E1, E2, E3, F1, F2 and F3.

Part VI. Results III: Effects of the antidepressant fluoxetine on neuronal structural plasticity

21 Effects of chronic fluoxtine treatment in the somatosensory cortex of young rats

21.1 Regional activation

We have analyzed the expression of the immediate early gene c-fos, and have observed that the chronic fluoxetine treatment induced a three fold significant increase (P=0.021) in the number of c-fos immunolabeled nuclei in the primary somatosensory cortex of young rats (Fig 21.1).

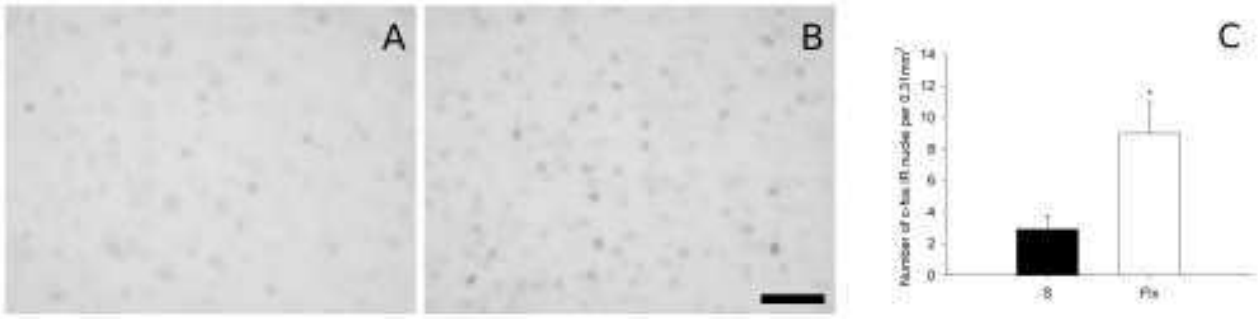

Fig. 21.1: c-fos expression in the somatosensory cortex of young rats after chronic fluoxetine treatment

A, B: Photographs showing coronal sections of c-fos immunoreactive nuclei in layers III to V of the somatosensory cortex of a control rat (A) and a rat treated for 14 days with fluoxetine (B). C: Graphs representing changes in the number of c-fos immunoreactive nuclei in the primary somatosensory cortex after chronic fluoxetine treatment. Statistically significant (* 0.01), unpaired t-test. White bar represents control animals and black bar represents fluoxetine treated animals. Scale bar: 50 μm.

21.2 Expression of plasticity-related molecules

Chronic fluoxetine treatment did not induce significant changes in GAD67 immunostaining in the neuropil of the different layers of the primary somatosensory cortex (layer II: p=0.2666; layer III: p=0.1424; layer IV: p=0.0670; layer V: p=0.0704; layer VI: p=0.1122). However, a clear trend towards an increase could be observed in all the layers (Fig 21.2). We did not observe any significant change in VGluT1 immunostaining intensity in the neuropil of the different layers of the primary somatosensory cortex (layer II: p=0.2624; layer III: p=0.9948; layer IV: p=0.6854; layer V: p=0.7260; layer VI: p=0.6264) (Fig 21.2).

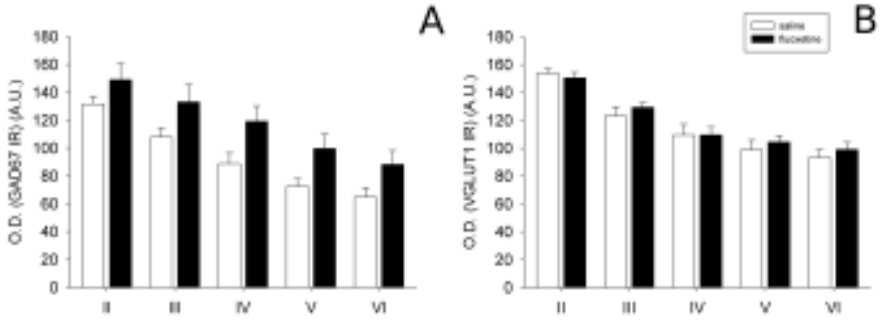

Fig. 21.2: Effect of chronic fluoxetine treatment on the expression of GAD and VGluT1 in the somatosensory cortex of young rats

Graphs represent the change in the intensity of GAD67 (A) and VGluT1 (B) in the layers II to VI of the somatosensory cortex in control animals (white bars) and animals treated with fluoxetine (black bars).

21.3 Structure of pyramidal neurons

We observed that the dendritic spine density in pyramidal neurons of the primary somatosensory cortex layers III and V was lower in the proximal segment and that it increased progressively towards the apical extreme of the principal dendrite (Figure 13A). There were significant differences in the spine density between the first and second segments ($p=0.003$), the second and the third ($p<0.0001$) and the third and the fourth ($p=0.042$), according to the distance from the soma. After 14 days of fluoxetine treatment, we did not found differences in the dendritic spine density of the proximal segments (0-50 µm). However, significant increases were observed in the second ($p=0.01$, 50-100 μm), the third ($p<0.0001$, 100-150 μm) and the forth segments ($p=0.0006$, 150-200 μm) (Fig 21.3A). We also observed significant increases in spine density when considering the entire length (0-200 μm) of the apical dendrites ($p<0.001$) (Fig 21.3B).

22 Effects of chronic fluoxetine treatment on neuronal structural plasticity in middle-aged rats

22.1 Body weight and volumetric analysis of different cerebral regions

In concordance with previous studies (McNamara et al., 2010; Thompson et al., 2004), chronic fluoxetine treatment produced a significant diminution of weight gain ($p<0.001$) after 14 days, when comparing the relation final weight/initial weight between the treated animals (0.877 ± 0.017) and the controls (1.017 ± 0.009) (Fig 22.1A).

We also analyzed the effects of chronic fluoxetine treatment on the volume of the different cerebral structures studied. We did not observe changes in the volume of the mPFC or the amygdala, but we found an increase in the volume of the hippocampus of the animals treated with fluoxetine ($p=0.001$, Fig 22.1B).

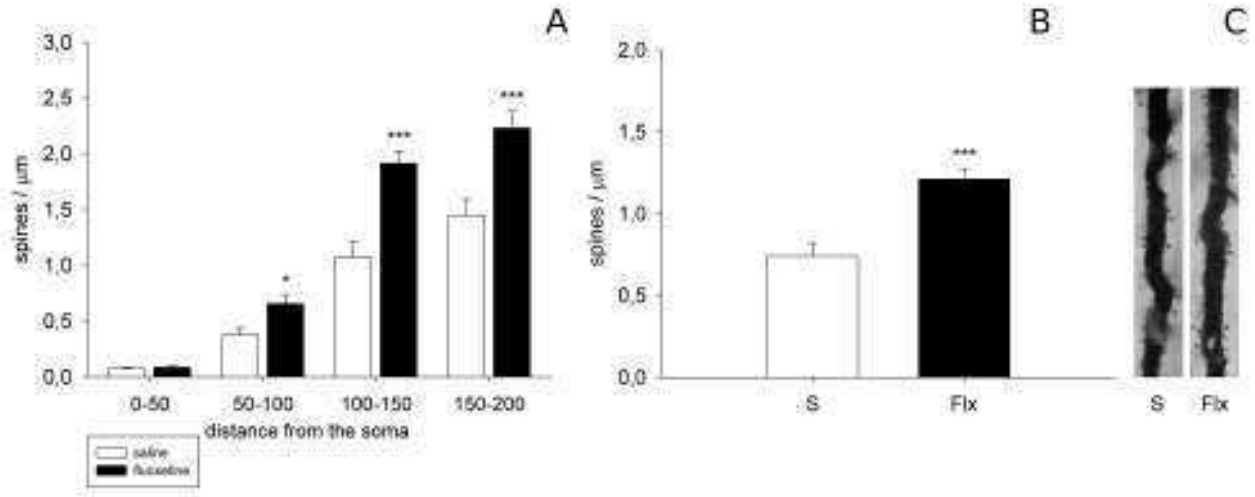

Fig. 21.3: Effect of chronic fluoxetine treatment on the spine density of pyramidal neurons of the somatosensory cortex in young rats

Changes in spine density in the principal apical dendrite of pyramidal neurons in primary somatosensory cortex layers III and V after chronic fluoxetine treatment. Spine density histograms in the different 50 μm fragments from the soma (A) and in the total length of the measured dendrite (B). Statistically significant (* $p<0.05$, ** $p<0.01$, *** $p<0.001$) unpaired t-test. White bars represent control animals and black bars represent treated animals. C: Photographs of a principal dendrite of a control animal (left) and an animal chronically treated with fluoxetine.

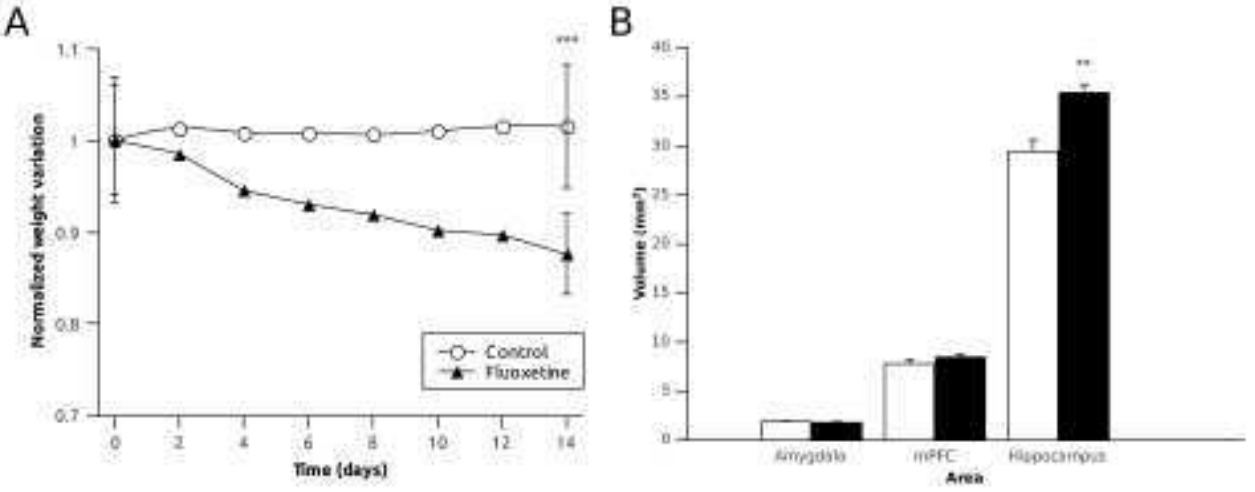

Fig. 22.1: Body weight and volume changes in different cerebral regions after chronic fluoxetine treatment in middle-aged rats

Graphs showing (A) the body weight change through the experiment for the control and fluoxetine group and (B) the effect of the chronic fluoxetine treatment on the volume of the different structures studied. Statistically significant (* $p < 0.05$, ** $p < 0.01$, *** $p < 0.001$) Student t-test.

22.2 Expression of plasticity-related molecules in the mPFC

The expression pattern of PSA-NCAM in the mPFC was similar to that described previously (Varea et al., 2005): All regions within the mPFC showed a moderate intensity of staining in layer I, nearly lack of staining in layer II, weak staining in layer III and intense staining in layers V–VI (Fig 22.2C and 22.3A and B).

In this cortical region, there was an increase in the density of PSA-NCAM expressing puncta in the fluoxetine treated animals in the dorsal cingulate cortex (Cg2) ($p=0.043$), but not in the prelimbic cortex (PrL) (Fig 22.3). No differences were found in the density of puncta expressing SYN, GAD6 or VGluT1 in any of the regions studied (Fig 22.3). We did not find changes in the density of puncta colocalizing PSA-NCAM/SYN, PSA-NCAM/GAD6 or PSANCAM/VGluT1 neither in the PrL nor in the Cg2 (Fig 22.3).

We did not find changes neither in the dot size nor in the surface covered by puncta in any of the regions and the markers analyzed (Fig 22.4).

22.3 Expression of plasticity-related molecules in the amygdala

As described previously (Nacher et al., 2002c), low levels of PSA-NCAM expression were found in the neuropil of the lateral and basolateral amygdaloid nuclei. By contrast, PSA-NCAM expression was denser and more intense in the central, medial and basomedial nuclei (Fig 22.2D and 22.5A). In the fluoxetine treated group we found significant increases in the density of PSA-NCAM expressing puncta in the central amygdaloid nucleus ($p=0.001$), of SYN expressing puncta in the lateral ($p=0.049$) and basolateral amygdaloid nuclei ($p=0.047$) and of GAD6 expressing puncta in the basolateral nucleus ($p=0.005$) (Fig 22.5). On the contrary, we found a significant decrease in the number of VGluT1 expressing puncta in the basolateral amygdaloid nucleus ($p=0.04$) (Fig 22.5). We also found an increase in PSA-NCAM/SYN ($p=0.007$) and PSANCAM/GAD6 ($p=0.041$) expressing puncta in the central amygdala. No changes in the density of these double-labeled puncta were observed in any of the other amygdaloid nuclei studied (Fig 22.5).

We also found changes similar to those described for puncta density when analyzing the dot size and the surface covered by these puncta. In the central amygdaloid nucleus we observed an increase both in the dot size and the surface covered by PSA-NCAM expressing puncta ($p=0.027$ and 0.011). In the lateral nucleus we only observed an increase in the dot size of puncta expressing SYN ($p=0.038$). By contrast, in the basolateral nucleus we found an increase in the dot size and surface covered by puncta expressing GAD6 ($p=0.011$ and 0.018) and a decrease in both, the dot size and the surface covered by puncta expressing VGluT1 ($p=0.005$ and 0.007) (Fig 22.6).

22.4 Expression of plasticity-related molecules in the hippocampus

PSA-NCAM expression in the hippocampus was similar to that described previously (Nacher et al., 2002b): briefly, the most intense expression of PSA-NCAM was located in the somata and apical

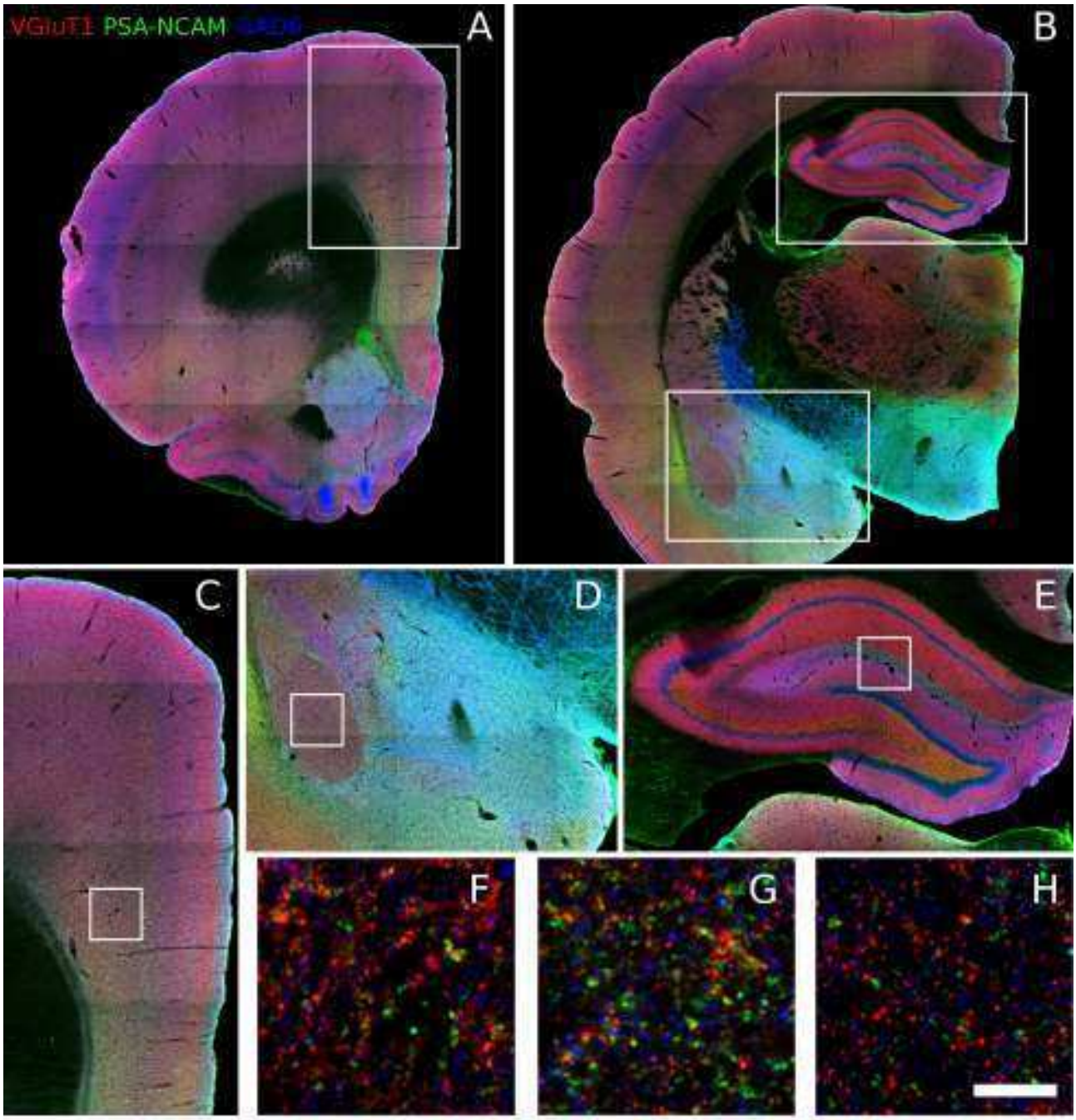

Fig. 22.2: Expression of different plasticity-related markers in the middle-aged rat brain

Confocal images showing the expression of PSA-NCAM, VGluT1 and GAD6 in the different regions of the hippocampus (B, E and H), the amygdala (B, D and G) and the mPFC (A, C and F). Scale bar = 200 μm in A and B, 100 μm in C, D and E and 1 μm in F, G and H.

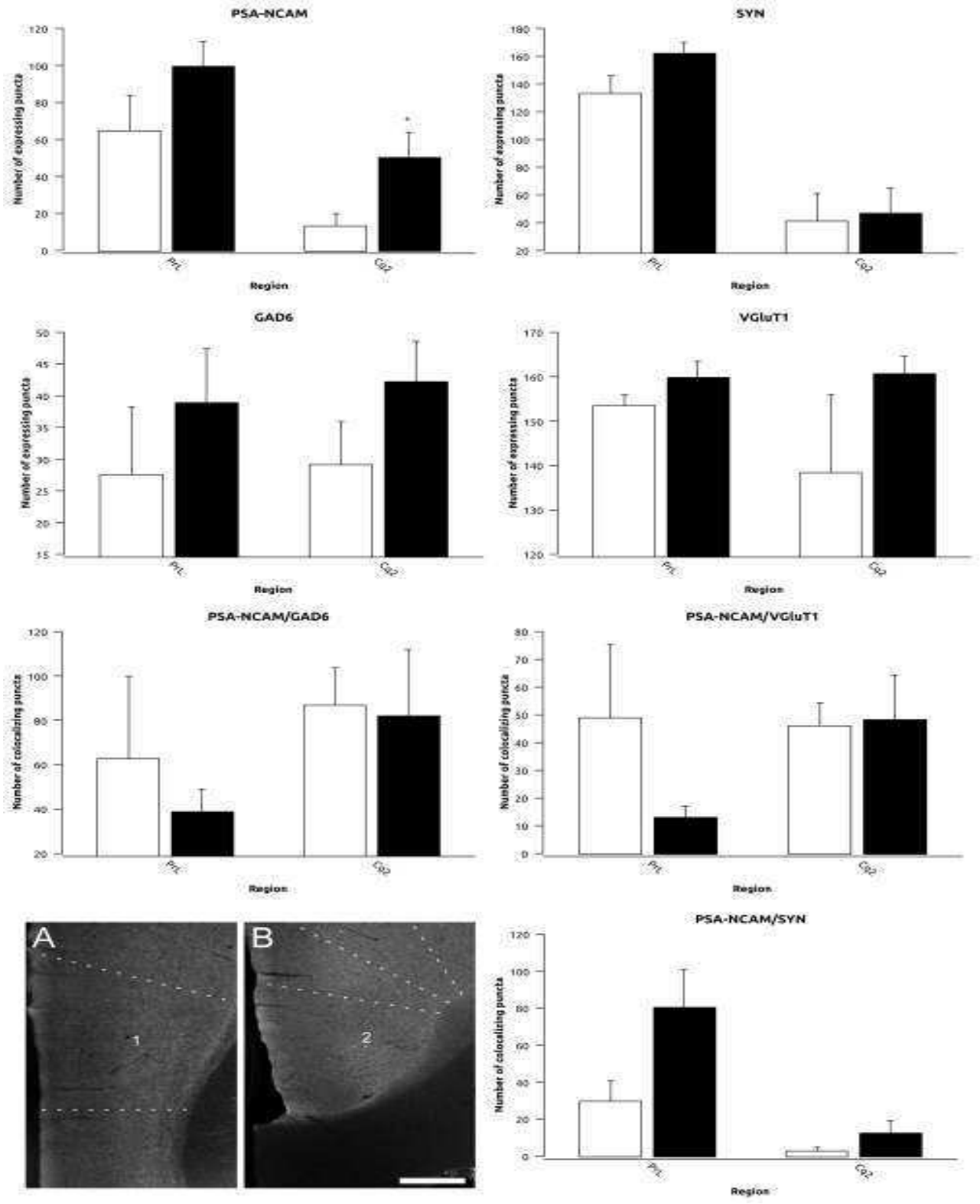

Fig. 22.3: Analysis of the density of puncta expressing different plasticity-related markers after chronic fluoxetine treatment in the mPFC of middle-aged rats

Graphs representing the density of puncta expressing different markers and its colocalization in the prelimbic and cingulate cortex of the medial prefrontal cortex. White bars represent control animals and black bars represent fluoxetine treated animals respectively. A and B are focal planes showing the expression of PSA-NCAM in (1) the prelimbic and (2) the cingulate cortex. Scale bar: 200 μm

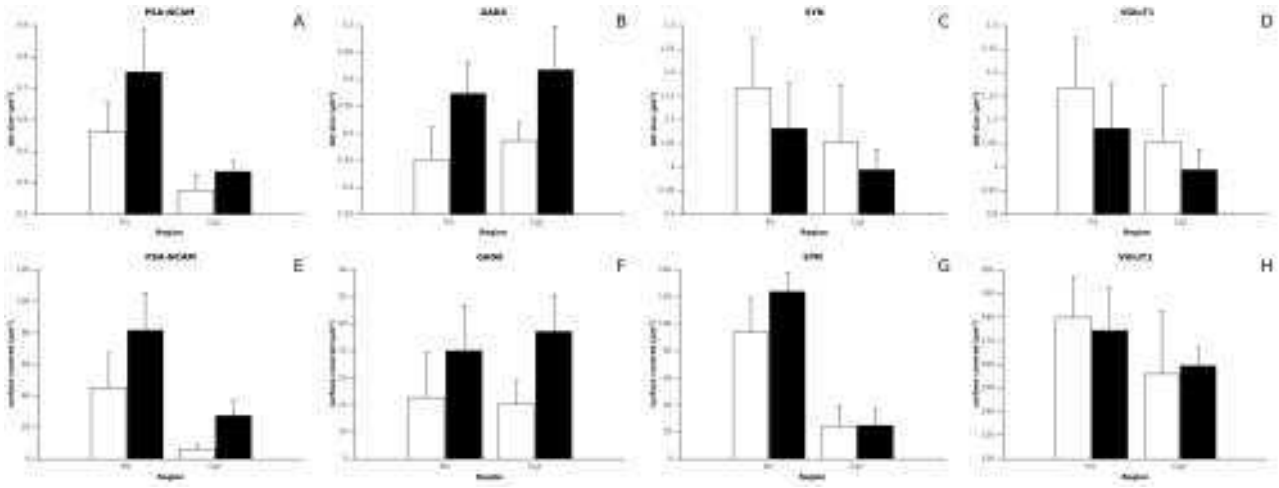

Fig. 22.4: Dot size and surface covered by puncta expressing different plasticity-related markers in the mPFC after chronic fluoxetine treatment in middle-aged rats

Graphs representing the dot size and surface covered by puncta expressing different markers in the PrL and Cg2 of the mPFC. White bars represent control animals and black bars represent fluoxetine treated animals respectively

dendrites of granule cells in the SGZ of the dentate gyrus, as well as in the neuropil of the hilus and the mossy fibers. A weaker and more diffuse expression of PSA-NCAM could be found in the neuropil of other regions of the hippocampus, such as the molecular layer of the dentate gyrus and the strata lacunosum-moleculare, radiatum and oriens of CA1 and CA3 (Figs 22.2E and 22.7A), where PSA-NCAM expressing cell somata could also be found (Nacher et al., 2002b).

After chronic fluoxetine treatment, we found significant increases in the density of PSA-NCAM expressing puncta in the molecular layer ($p=0.045$), stratum lucidum ($p=0.032$) and stratum lacunosum-moleculare ($p<0.001$) (Fig 22.8). Similar increases were found in the density of SYN expressing puncta in the strata lucidum ($p=0.012$) and lacunosum-moleculare ($p=0.038$). We also found a significant increase ($p=0.018$) in the density of GAD6 expressing puncta in the stratum lacunosum-moleculare. By contrast, we found a decrease in the density of VGluT1 expressing puncta in the strata lacunosum-moleculare ($p=0.021$) and radiatum ($p=0.030$) of CA1 (Fig 22.8). When studying the density of puncta co-expressing PSA-NCAM and each of the other markers, we observed an increase in the density of puncta co-expressing PSA-NCAM/SYN ($p=0.008$) in the stratum lacunosum-moleculare, but no change was observed in those co-expressing PSA-NCAM/GAD or PSA-NCAM/VGluT1 (Fig 22.8).

Finally, when analyzing the dot size and the surface covered by immunoreactive puncta, we also observed changes in most of the regions that showed differences in the density of puncta in these structures. In the stratum lacunosum-moleculare we observed an increase in the dot size and the surface covered by puncta expressing PSA-NCAM ($p=0.011$ and <0.001) and GAD6 ($p=0.047$ and 0.021), while there was only an increase in dot size in those expressing SYN ($p=0.044$) and a decrease in both dot size and surface covered by those expressing VGluT1 ($p=0.035$ and 0.017). We also find a decrease in both the dot size and the surface covered by puncta expressing VGluT1 in the stratum radiatum ($p=0.015$ and 0.007) (Fig 22.9).

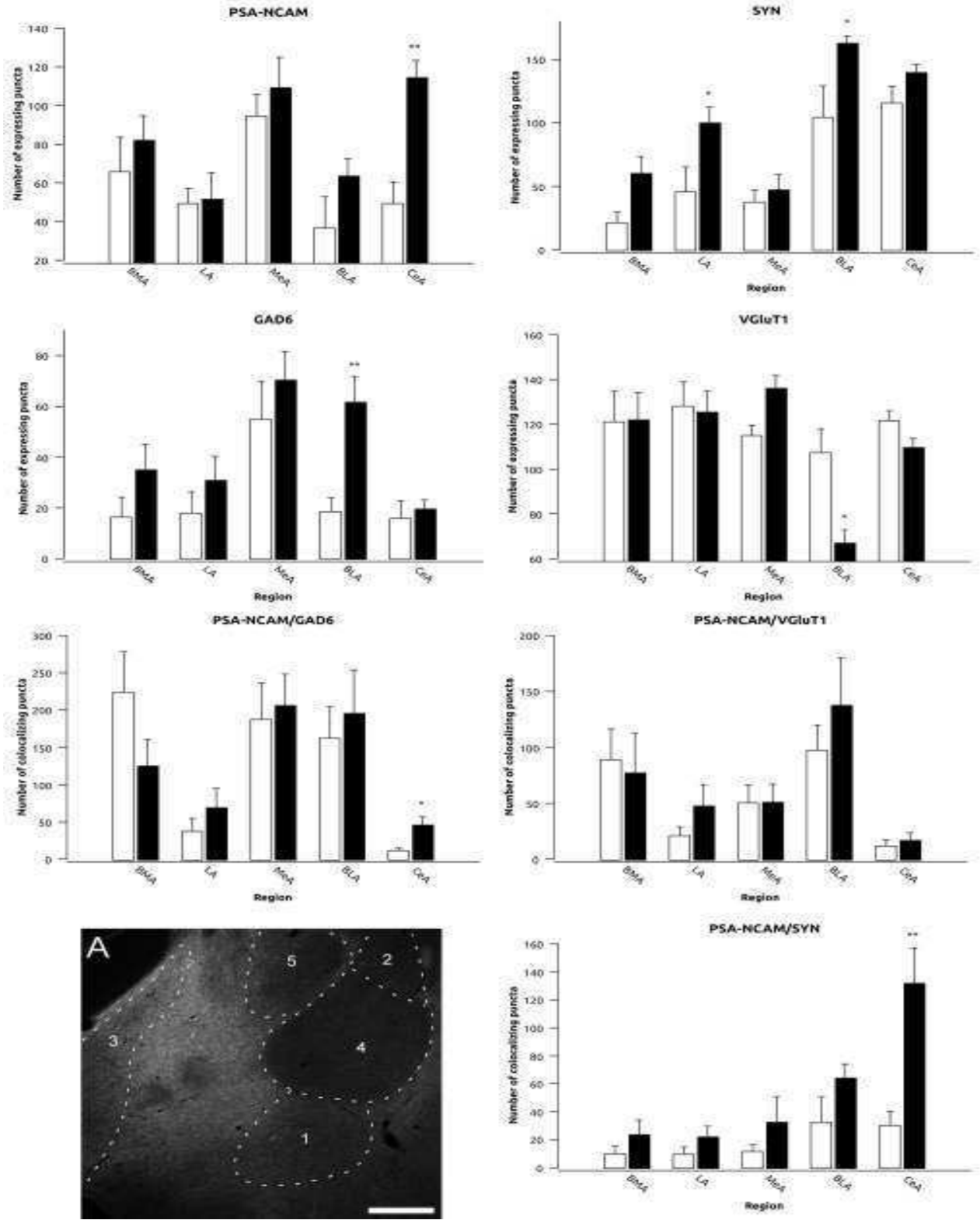

Fig. 22.5: Analysis of the density of puncta expressing different plasticity-related markers after chronic fluoxetine treatment in the amygdala of middle-aged rats

Graphs representing the density of puncta expressing different markers and its colocalization in different areas of the amygdala. White bars represent control animals and black bars represent fluoxetine treated animals respectively. A is a focal plane showing the expression of PSANCAM in the (1) basomedial (BMA) (2) lateral (LA), (3) medial (MeA), (4) basolateral (BLA) and (5) central (CeA) nuclei of the amygdala. Scale bar: 200 μm

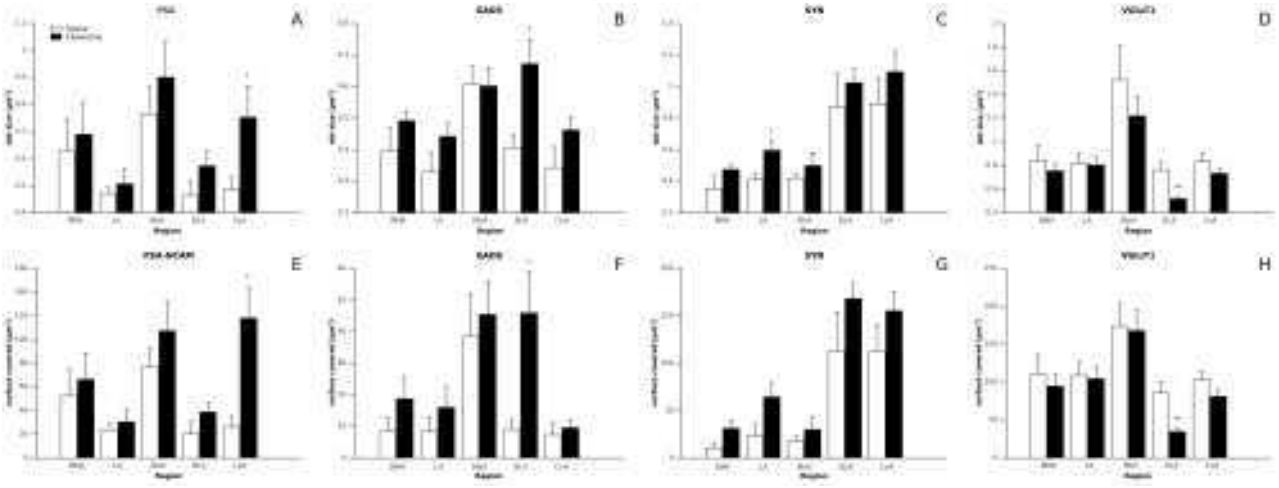

Fig. 22.6: Dot size and surface covered by puncta expressing different plasticity-related markers in the amygdala after chronic fluoxetine treatment in middle-aged rats

Graphs representing the dot size and the surface covered by puncta expressing different markers in different areas of the amygdala. White bars represent control animals and black bars represent fluoxetine treated animals respectively.

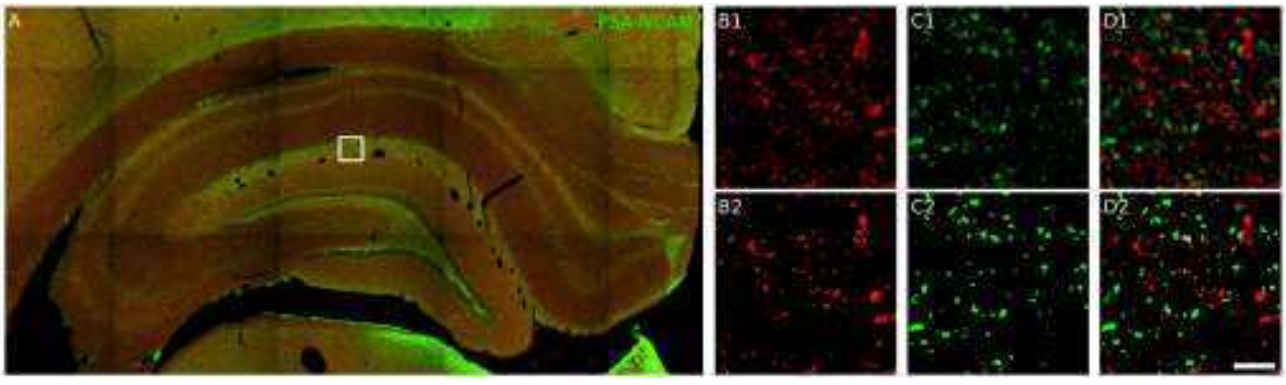

Fig. 22.7: Expression of PSA-NCAM and SYN in the hippocampus of middle aged rats

Confocal image showing the expression of PSA-NCAM and SYN in the hippocampus. Focal planes showing the original image and the processed image for the puncta analysis for (B1 and B2) PSA-NCAM, (C1 and C2) SYN and (D1 and D2) the composite image. Scale bar: 320 μm in A and 5 μm in the rest.

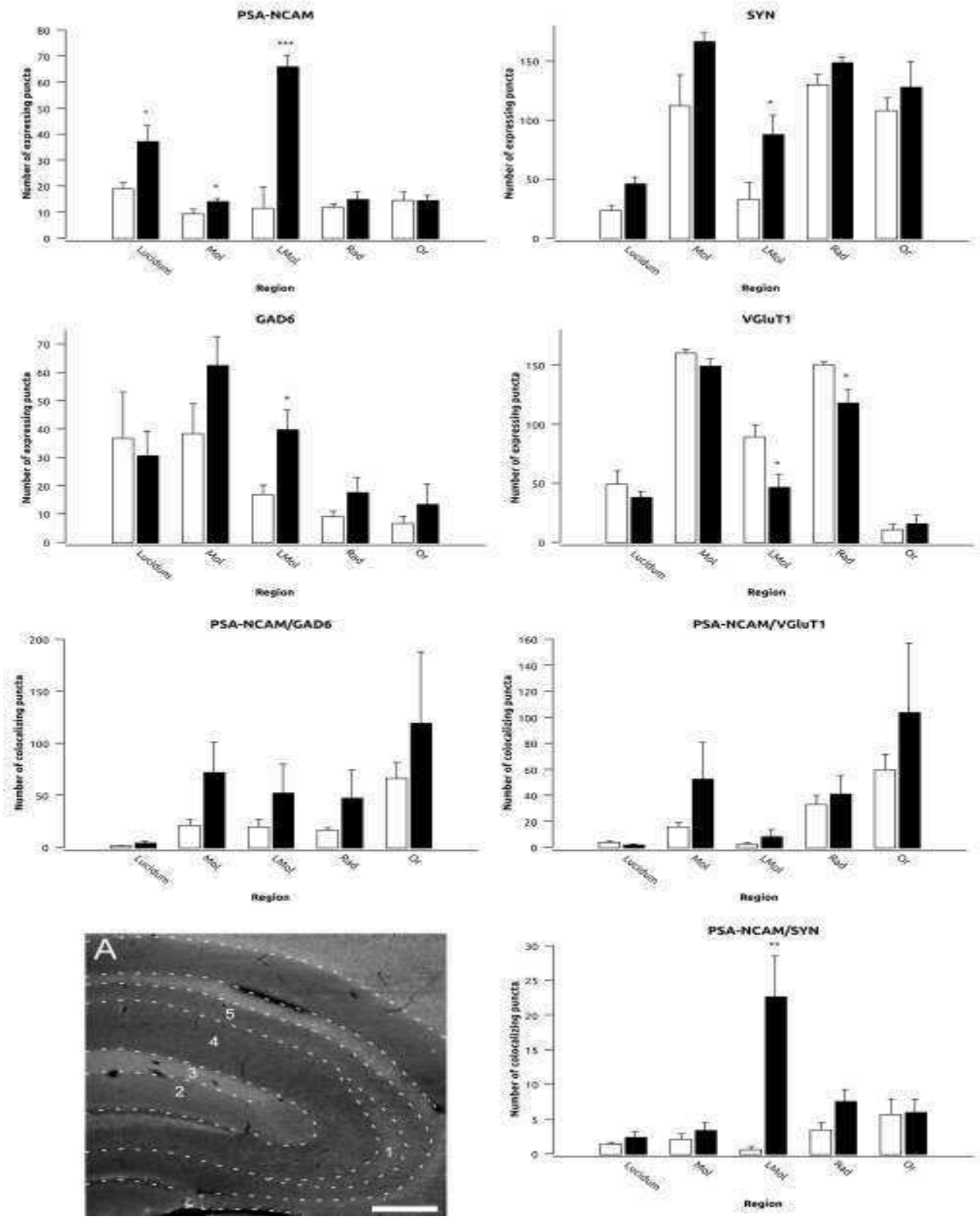

Fig. 22.8: Analysis of the density of puncta expressing different plasticity-related markers after chronic fluoxetine treatment in the hippocampus of middle-aged rats

Graphs representing the density of puncta expressing different markers and its colocalization in different areas of the hippocampus. White bars represent control animals and black bars represent fluoxetine treated animals respectively. A is a single confocal plane showing the expression of PSA-NCAM in the strata (1) lucidum, (2) moleculare (Mol), (3) lacunosum-moleculare (LMol), (4) radiatum (Rad) and (5) oriens (Or) of the hippocampus. Scale bar: 200 μm

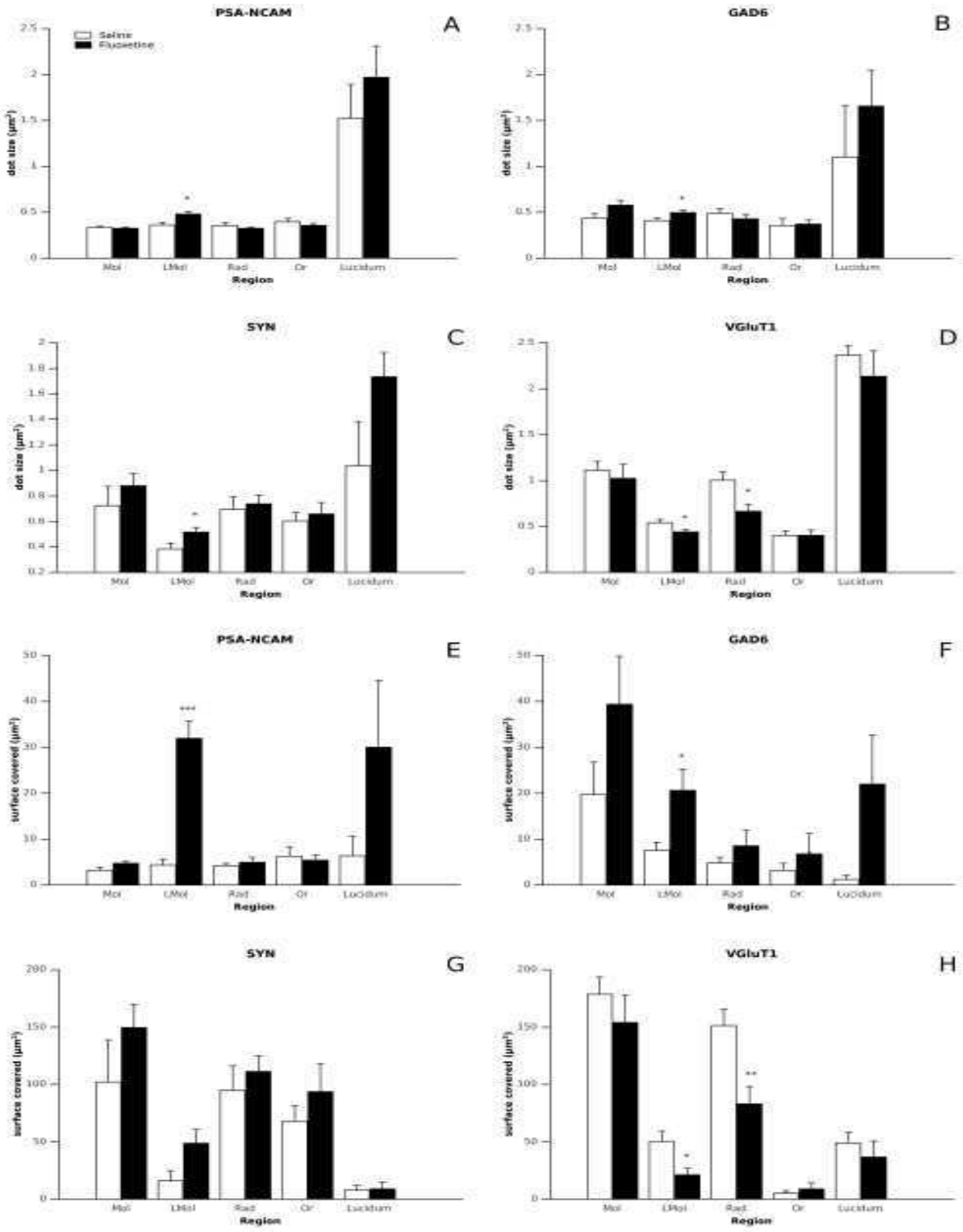

Fig. 22.9: Dot size and surface covered by puncta expressing different plasticity-related markers in the hippocampus after chronic fluoxetine treatment in middle-aged rats

Graphs representing the dot size and the surface covered by puncta expressing different markers in different areas of the hippocampus. White bars represent control animals and black bars represent fluoxetine treated animals respectively.

22.5 Neurogenesis

No change in the density of cells expressing DCX or PSA-NCAM was observed in the SGZ of the dentate gyrus after chronic fluoxetine treatment (Fig 22.10A). However, when analyzing the number of Ki67 expressing nuclei there was a trend towards a decrease in the treated group ($p=0.061$) (Fig 22.10A). In the SVZ we also failed to find changes in the expression of DCX or PSA-NCAM, but we observed a dramatic significant decrease in the number of Ki67 immunoreactive nuclei in the treated group ($p<0.001$) (Fig 22.10B).

23 Effects of chronic fluoxetine treatment on neuronal structural plasticity in young GIN mice

23.1 Expression of plasticity-related molecules in the hippocampus

The pattern of PSA-NCAM expression in the hippocampus of this strain of GIN mice (Oliva et al., 2000) was similar to that described above for young rats. After chronic fluoxetine treatment, we found significant increases in the density of PSA-NCAM expressing puncta in the strata lacunosum-moleculare ($p=0.040$), radiatum ($p=0.048$), oriens ($p=0.002$) (Fig 23.1) and in the hilus ($p=0.005$) (Fig 23.2). Similar increases were found in the density of SYN expressing puncta in the strata lucidum ($p=0.045$), moleculare ($p=0.008$), oriens ($p=0.027$) and radiatum ($p=0.016$). We also found a significant increase ($p=0.016$) in the density of GAD6 expressing puncta in the hilus. However, we did not find any change in the density of VGluT1 expressing puncta in any of the areas analyzed (Fig 23.2). When analyzing the density of puncta co-expressing these molecules, we observed an increase in the density of puncta co-expressing PSA-NCAM/GAD6 in the stratum oriens ($p=0.035$) and in the hilus ($p=0.002$) (Fig 23.2).

23.2 Perisomatic innervation of pyramidal neurons in the hippocampus

We analyzed the effects of a chronic fluoxetine treatment on the perisomatic innervation of pyramidal neurons in GIN mice, using CAMKII immunohistochemistry to delimit the profile of pyramidal neurons in the stratum pyramidale of the CA1 region of the hippocampus. Pyramidal neurons receive typically the perisomatic synaptic innervation from basket interneurons expressing parvalbumin (Freund and Buzsáki, 1996). Therefore, we analyzed the density of parvalbumin positive puncta surrounding the somata of pyramidal neurons and its colocalization with SYN (Fig 23.3). We did not observe any change in the density of PV ($p=0.708$) or SYN ($p=0.201$) expressing puncta or in that of puncta colocalizing PV and SYN ($p=0.581$) after the fluoxetine treatment (Fig 23.4).

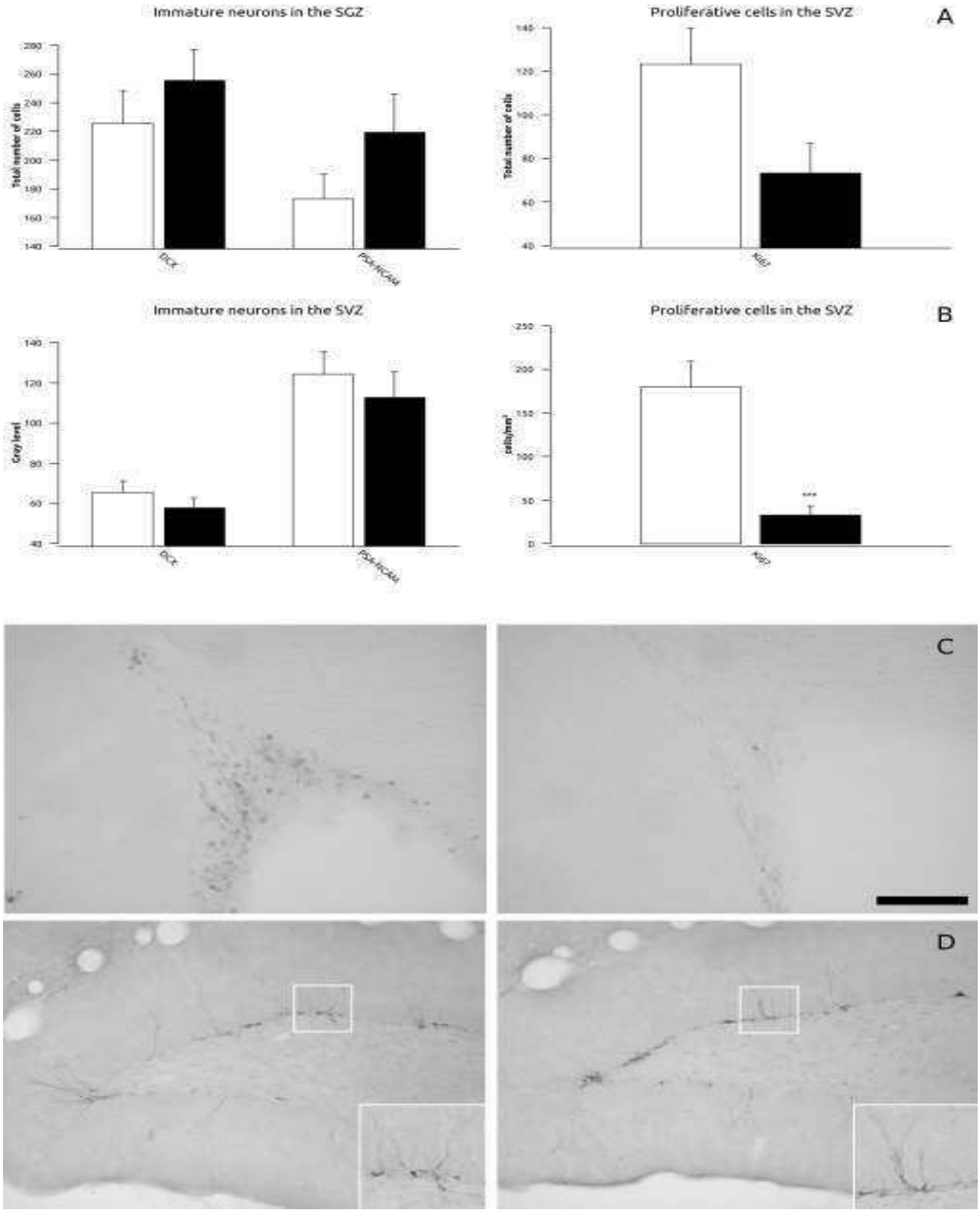

Fig. 22.10: Effects of chronic fluoxetine treatment on neurogenesis in middle-aged rats

A & B: Graphs representing (A) the total number of cells expressing immature and proliferative markers in the SGZ of the hippocampus and (B) the gray level of DCX and PSANCAM and the density of Ki67 in the SVZ. White bars represent control animals and black bars represent fluoxetine treated animals respectively. C & D: Micrographs showing the expression of Ki67 in the SVZ (C) and DCX (D) in the SGZ. Scale bar: 100 μm (C and D) and 50 μm (insets in D).

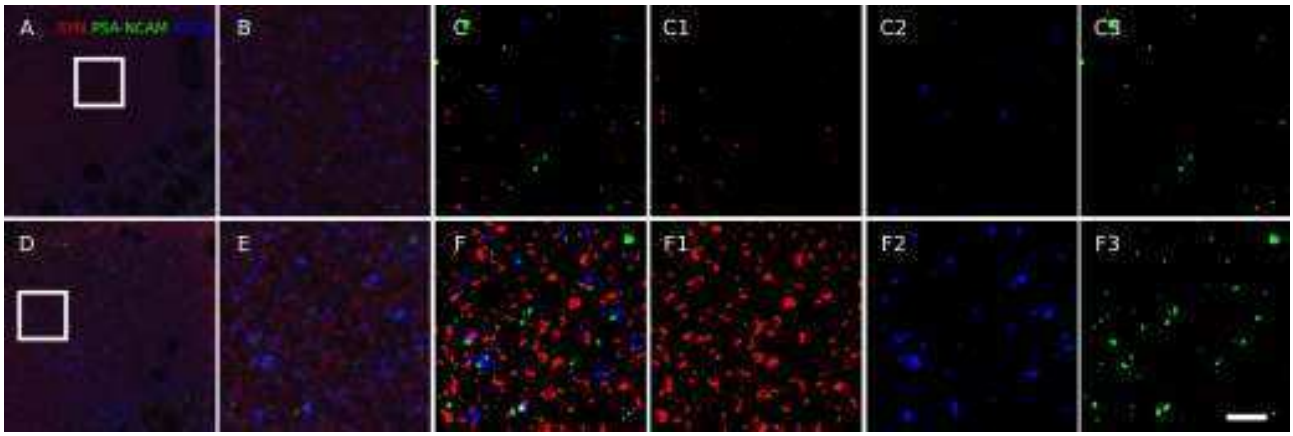

Fig. 23.1: Effects of chronic fluoxetine treatment on the expression of different plasticity-related markers in the hippocampus of GIN mice

Confocal images showing the differences in the expression of different plasticity-related molecules. (A, D) Single confocal plane of the stratum oriens of the hippocampus of saline (A) and fluoxetine (D) treated animals. (B, E) Regions squared in A and D represent a fraction of the area analyzed of saline (B) and treated (E) animals, showing the composite image with the different markers. (C, F) The images in B and E were processed for image analysis and the different channels were separated showing the puncta expressing synaptophysin (C1 and F1), GAD6 (C2, F2) and PSA-NCAM (C3, F3), for the control (C) and fluoxetine (F) groups. Scale bar = 20μm in A and D, and 4.2 for the rest of the images.

23.3 Perisomatic innervation of interneurons in the hippocampus

We analyzed the effects of a chronic fluoxetine treatment in GIN mice, which allowed us to study in detail the morphological features of a subpopulation of interneurons. We observed an increase in the density of GAD6 expressing puncta surrounding the somata of interneurons expressing eGFP in the CA1 region of the hippocampus of animals treated chronically with the antidepressant fluoxetine (p=0.015) (Fig 23.5). Although there were no changes in the density of puncta expressing SYN surrounding the somata of these interneurons (p=0.163), we found an increase in the density of perisomatic puncta co-expressing GAD6 and SYN (p=0.028) (Fig 23.6).

23.4 Structure of interneurons in the mPFC

Analyzing interneurons in GIN mice in deep layers of the prelimbic area of the mPFC, we observed that their dendritic spine density was, as it happens in pyramidal neurons, lower in the proximal segment and that it increased towards the apical extreme of the dendrite. After 14 days of fluoxetine treatment, we did not found differences in the dendritic spine density of the proximal segments (0-50 μm; p=0.070). However, significant increases in the spine density were observed in the second (p=0.006, 50-100 μm) and the third segments (p=0.008, 100-150 μm) (Fig 23.7). Significant increases were also observed when considering the entire length of the dendrite of interneurons of fluoxetine treated animals compared to the saline injected animals. (p=0.005) (Fig 23.7).

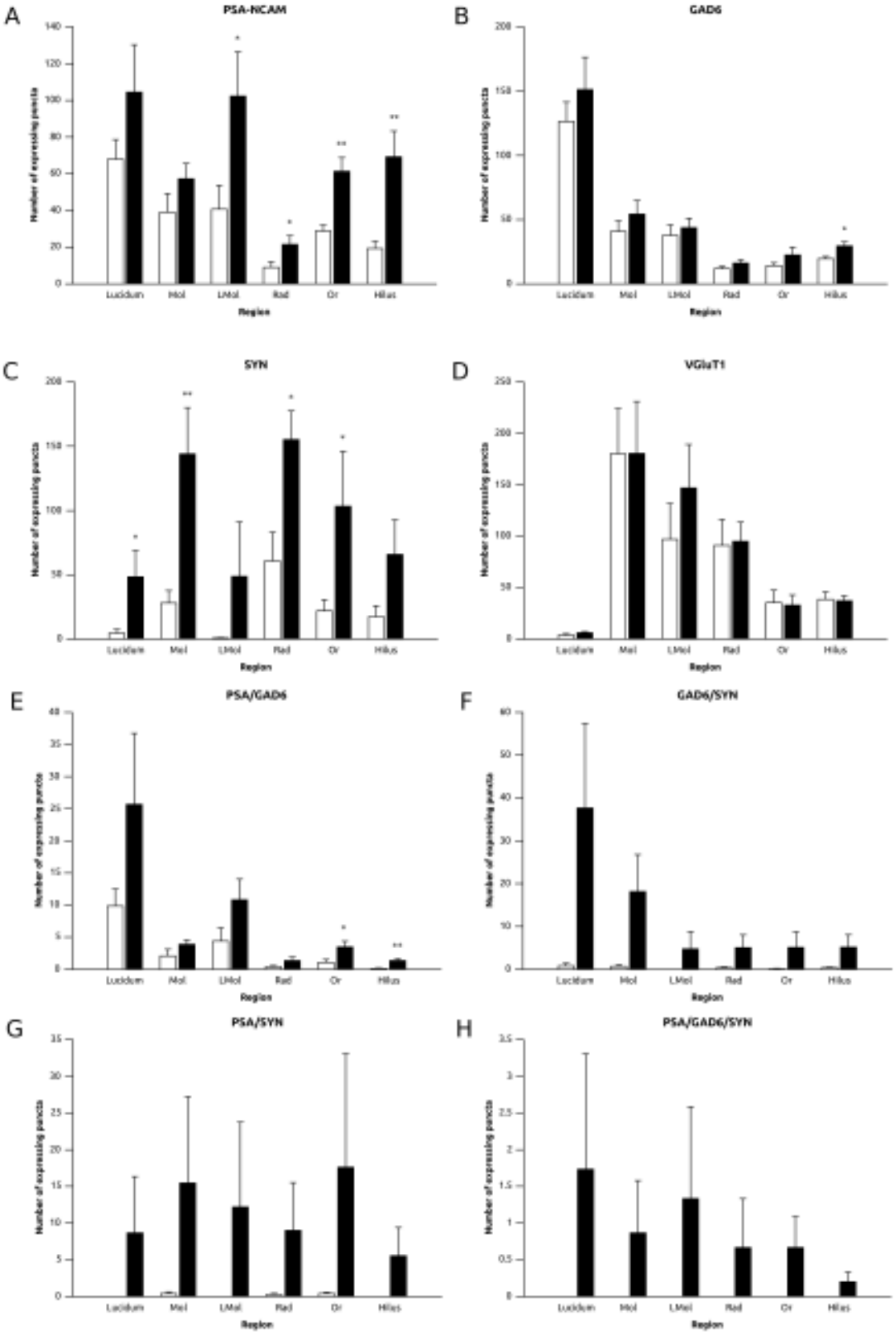

Fig. 23.2: Analysis of the density of puncta expressing different plasticity-related markers in the hippocampus of young GIN mice after chronic fluoxetine treatment

Graphs representing the density of puncta expressing the different markers and their colocalization in different areas of the hippocampus. White bars represent control animals and black bars represent fluoxetine treated animals respectively. Bars represent the mean ± the standard error of the mean.

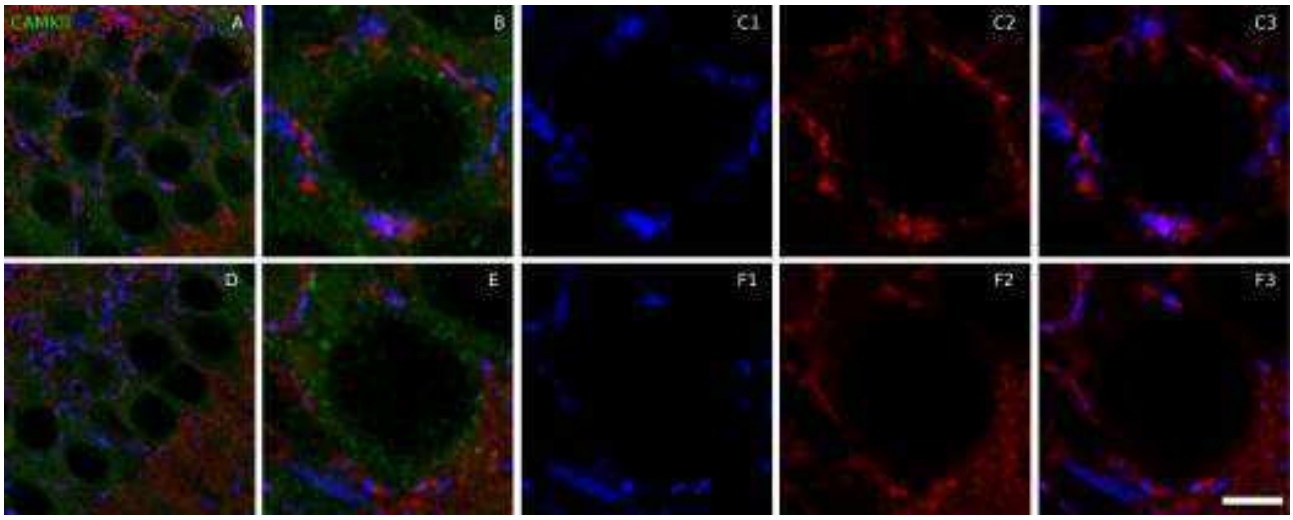

Fig. 23.3: Effects of chronic fluoxetine treatment on the perisomatic innervation in pyramidal neurons of the hippocampus of young GIN mice

Confocal images showing perisomatic puncta surrounding the somata of pyramidal neurons and expressing different markers. (A, D) Single confocal planes of the CA1 stratum pyramidale of the hippocampus showing CAMKII expressing pyramidal neuron somata (green) and perisomatic puncta expressing PV (blue) or SYN (red) in a control (A) and a fluoxetine treated (D) animal. (B, E) Single confocal planes showing PV expressing puncta surrounding the somata of a pyramidal neuron of a control (B) and a fluoxetine treated (E) animal. (C & F) Single confocal planes showing the expression of PV (1), SYN (2) and its colocalization (3) in perisomatic puncta in the control (C series) and the fluoxetine treated (F series) animals. Scale bar = 200 μm for A and D, and 63.5 μm for the rest of the images.

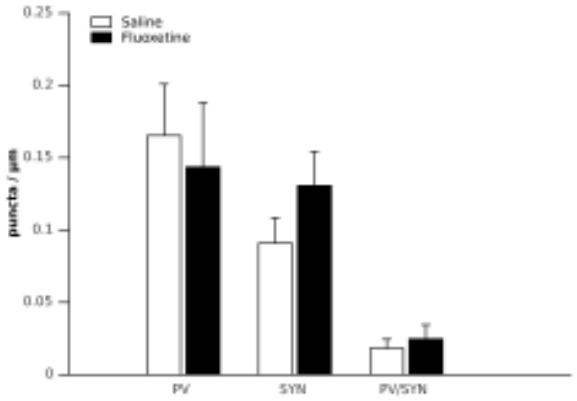

Fig. 23.4: Effects of chronic fluoxetine treatment on the density of puncta surrounding the somata of pyramidal neurons in the hippocampus of GIN mice

Graphs representing the density of puncta expressing PV, SYN and its colocalization, surrounding the somata of pyramidal neurons in the CA1 region of the hippocampus. Bars represent the mean $\pm$ the standard error of the mean.

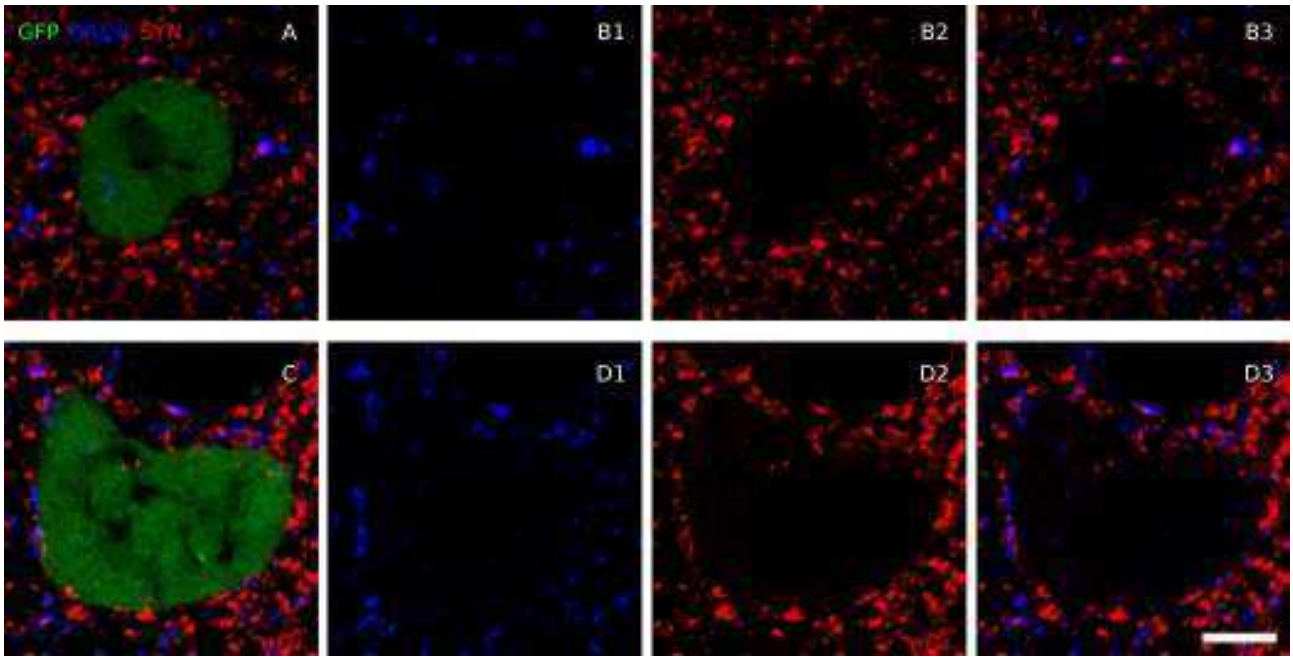

Fig. 23.5: Effects of chronic fluoxetine treatment on the perisomatic innervation of interneurons in the mPFC of young GIN mice

Confocal images showing puncta surrounding the somata of interneurons in the mPFC. (A, C) Single confocal planes of the mPFC showing the expression of eGFP in interneuron somata (green), as well as GAD6 (blue) and SYN (red) expressing perisomatic puncta in a control (A) and a fluoxetine treated (C) animal. (B, D) Single confocal planes showing perisomatic puncta expressing GAD6 (1), SYN (2) and its colocalization (3) for the control (B series) and the fluoxetine treated (D series) animals. Scale bar = 5 μm.

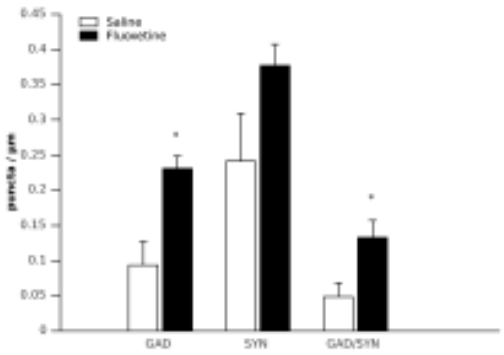

Fig. 23.6: Effects of chronic fluoxetine treatment on the density of puncta surrounding the soma of interneurons in the mPFC of GIN mice

Graphs representing the density of puncta expressing GAD6, SYN and their colocalization surrounding the somata of interneurons of the mPFC. Bars represent the mean $\pm$ the standard error of the mean.

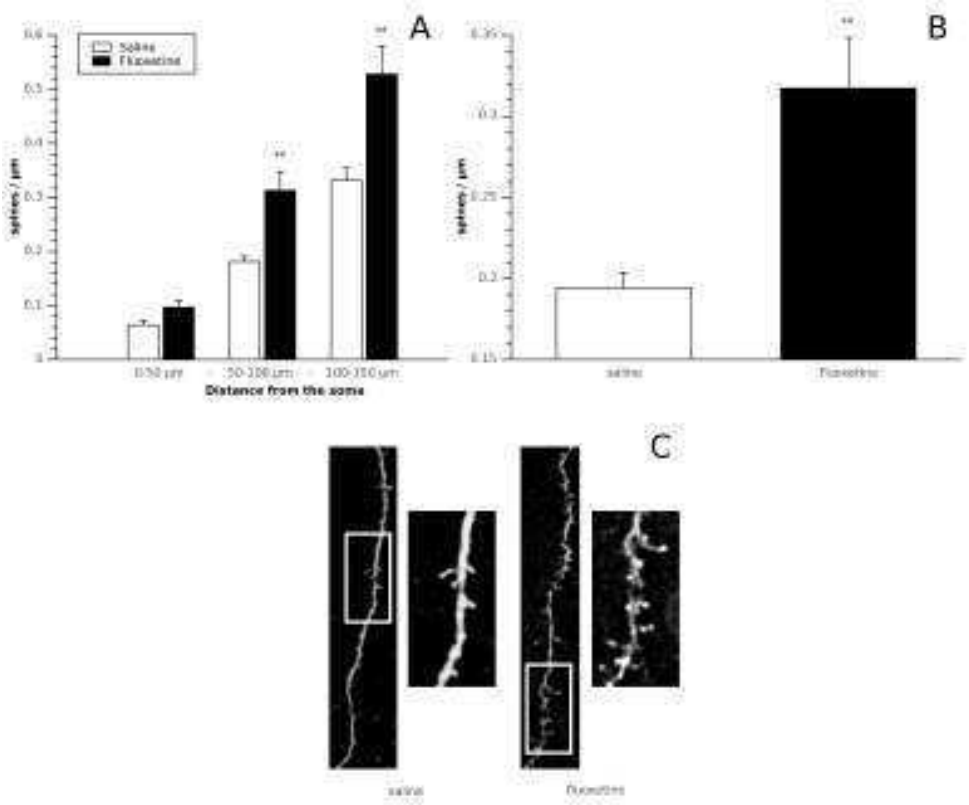

Fig. 23.7: Effects of chronic fluoxetine treatment on the spine density of interneurons in the prelimbic area of the mPFC of young GIN mice

Spine density histograms in the different 50 μm fragments from the soma (A) and in the total length of the measured dendrite (B). Statistically significant (* $p < 0.05$, ** $p < 0.01$, *** $p < 0.001$) unpaired t-test. White bars represent control animals and black bars represent treated animals. C: Reconstructions of focal planes showing the difference in dendritic spine density between the control (left) and the fluoxetine (right) groups.

Part VII. Discussion

24 Distribution of cells expressing the polysialylated form of the neural cell adhesion molecule (PSA-NCAM) in the adult rodent telencephalon

We can distinguish three different subpopulations of PSA-NCAM expressing cells regarding their origin and function: (1) the recently generated ones in the subgranular zone (SGZ), the subventricular zone (SVZ) and those of the rostral migratory stream (RMS), which will loose their PSA-NCAM expression as they mature and become integrated in the neuronal circuitry, (2) the PSA-NCAM expressing cells in the layer II of the paleocortex, which show features of immature neurons during adulthood, but were generated during embryonic developmental stages, and (3) the rest of the PSA-NCAM expressing cells throughout the dorsal telencephalon, which display features of mature interneurons. The present results describe the ultrastructural features and phenotype of PSA-NCAM expressing cells located in the paleocortex layer II, as well as many aspects of the mature interneurons expressing PSA-NCAM in different regions of the brain, specially in the medial prefrontal cortex (mPFC), the hippocampus and the amygdala. These results expand previous findings describing the existence and possible role of PSA-NCAM expressing cells in different regions of the adult rodent brain (as shown in figure 15.1), such as the hippocampus (Nacher et al., 2002b; Seki, 2002a; Bonfanti et al., 1992), the mPFC (Varea et al., 2007a), the amygdala (Nacher et al., 2002c) or the entorhinal cortex (Nacher et al., 2002a; Seki and Arai, 1991a).

25 PSA-NCAM expressing cells in the paleocortex layer II

25.1 Nomenclature

To date, there is not a consensus on the identity of the PSA-NCAM expressing cells in the paleocortex layer II. Seki and Arai (1991a) described some of them as semilunar neurons. O'Connell et al. (1997) described these PSA-NCAM expressing cells and classified most of them as small neurons (5 to 10 μm) and also acknowledged the presence of some scarce PSA-NCAM expressing neurons, which they classified as pyramidal-like neurons (10 to 20 μm). In a previous study, our laboratory has classified these cells mainly as neurogliaform neurons and pyramidal/semilunar transitional neurons respectively, although some PSA-NCAM expressing cells were found with a morphology similar to that of pyramidal neurons and fusiform cells in the paleocortex layer II (Nacher et al., 2002a). However, we have demonstrated that the abundant population of small PSA-NCAM expressing cells does not correspond to neurogliaform neurons (Gómez-Climent et al., 2008). Neurogliaform neurons are mature interneurons, which usually express γ-Aminobutyric acid (GABA), glutamate decarboxylase (GAD), or α-actinin (Price et al., 2005), and none of these markers is expressed by the small cells in layer II. Given the intricate trajectories of their processes, we have chosen to

denominate them "tangled cells." However, it has to be noted that some cells with characteristics of both tangled cells and semilunar-pyramidal transitional neurons can be found, which may indicate a transition state between these cell types. Although in rodents the distribution of PSA-NCAM expressing cells in layer II appears to be restricted to the piriform, entorhinal, and perirhinal cortex (with some scarce cells located in the adjacent agranular insular and ectorhinal cortices), in mammals with larger cerebral cortices, such as rabbits, cats or primates, there is a more widespread distribution of these cells, which can be found in layer II of most neocortical regions (Cai et al., 2009; Varea et al., 2011a; Bonfanti, 2006).

26 Ultrastructural features, phenotype and fate of PSA-NCAM expressing cells in the paleocortex layer II

But what is the phenotype of PSA-NCAM expressing cells in the adult paleocortex layer II? Our results indicate that they are early immature neurons, which apparently have detained their differentiation program and are in a "dormant" stage. Their ultrastructure gives support to this hypothesis: These cells commonly show heterochromatin clumps and they appear to be surrounded by multiple astroglial lamellae and swellings of the extracellular space adjacent to the plasma membrane, which isolate them from the surrounding nervous parenchyma. Moreover, they normally do not show synaptic contacts on their somata or proximal processes. These are 2 characteristics found in early immature neurons in the adult dentate gyrus (Seki and Arai, 1999; Shapiro et al., 2007). Moreover, the presence of astroglial processes and the absence of synapses on doublecortin (DCX) expressing cell somata in the piriform cortex layer II has also been reported (Shapiro et al., 2007). However, it appears that a subpopulation of PSA-NCAM expressing cells in the paleocortex layer II, mostly constituted by semilunar and semilunar–pyramidal transitional neurons does receive, although sparsely, excitatory synapses in its apical dendrites located in layer I (Gómez-Climent et al., 2008), suggesting that these cells are in a more differentiated state. Although we have previously suggested that the expression of PSA-NCAM (Nacher et al., 2002a) in paleocortex layer II cells was linked to neuronal structural plasticity, these results indicate that this expression together with the astroglial covering probably has an insulating role, which will prevent these cells from receiving synaptic inputs. We still do not have a plausible explanation for the expression of DCX or Turned on after division/Ulip/CRMP-4 (TUC-4) proteins in these cells, because during development these proteins are associated with a dynamic cytoskeleton, which is participating in neurite development or neuronal migration (Minturn et al., 1995). The second intriguing point arisen by our study is the fate of PSA-NCAM expressing cells in the adult paleocortex layer II. Several studies have demonstrated that the number of these cells dramatically declines during aging (Abrous et al., 1997; Murphy et al., 2001; Varea et al., 2009). There are 2 possible explanations for this reduction in the number of inmmature neurons: 1) the cells expressing these proteins are progressively dying or 2) they are differentiating into mature neurons, which lack these markers. The second possibility appears more likely, and it is tempting to think that tangled cells could mature eventually into some

of the larger PSA-NCAM expressing cells, and then into mature neurons. This is supported by the fact that intermediate cell types between tangled and larger cells are habitually found in layer II and that, as discussed above, larger cells appear more mature than tangled cells. Then PSA-NCAM expressing cells in the paleocortex layer II may constitute a "reservoir", which in different circumstances may complete its differentiation program. However, as we will discuss later, in transgenic knockout mice for the polysialyltransferases, the abscence of PSA-NCAM does not seem necessary to maintain the immature phenotype of these cells. Nevertheless, experiments that follow the fate of this cellular subpopulation after different experimental treatments and during aging will shed light on the mysterious nature of these cells.

27 PSA-NCAM expressing interneurons

27.1 Neurochemical phenotype

Although the neural cell adhesion molecule (NCAM) is not the exclusive carrier of polysialic acid (PSA) (Zuber et al., 1992; Close et al., 2000; Galuska et al., 2010; Vitureira et al., 2010), the present results strongly suggest that NCAM is its only carrier in cortical interneurons. Consequently, following the terminology used in the literature, we will refer to this molecule as PSA-NCAM.

Due to its intense expression in immature neurons, PSA-NCAM has been erroneously considered in many studies an exclusive developmental marker. However, previous works have clearly demonstrated its presence in mature neurons and its involvement in their structural plasticity (Bonfanti, 2006; Gascon et al., 2007; Rutishauser, 2008). The present thesis also argues against this incorrect view and clearly indicates that most PSA-NCAM expressing cells outside adult neurogenic regions and paleocortex layer II are mature neurons. In this thesis we provide different lines of evidence indicating that mature cortical neurons expressing PSA-NCAM constitute a subpopulation of interneurons: 1) the expression of the enzyme responsible for GABA synthesis (revealed by GAD67 immunohistochemistry and by the analysis of transgenic mice expressing the enhanced green fluorescent protein (eGFP) under the GAD67 promoter, 2) the expression of different neuropeptides and calcium-binding proteins considered markers of mature interneurons, 3) the ultrastructural characteristics and 4) the analysis of PSA-NCAM expression in transgenic mice where NCAM is absent from neurons expressing Ca2+/calmodulin dependent protein kinase II (CAMKII) (a marker of excitatory cells). The fact that many PSA-NCAM expressing cells sometimes do not appear to colocalize with inhibitory markers can be explained because none of these markers is present in all interneurons. Even the expression of GABA or their synthesizing enzymes is not found in all interneuronal somata; some interneurons, depending on their activity or the distance to their axonal terminals, may have low levels of these molecules in their somata (Freund and Buzsáki, 1996). PSA-NCAM expressing elements in the cortical neuropil also appear to belong to inhibitory neurons because they express markers associated with interneuronal neurites or synapses. Most of these elements must correspond to neurites of local interneurons, although since PSA-NCAM is expressed in interneurons of extra-

cortical regions such as the amygdala (Gilabert-Juan et al., 2011) or the septum (Foley et al., 2003), some of them may correspond to projections from extracortical origin. Moreover, the present data demonstrate that PSA-NCAM expression is clearly absent from mature principal neuron somata in the adult cerebral cortex, using electron microscopy, CAMKII immunohistochemistry, and transgenic mice. The absence of PSA-NCAM expression in principal neurons of the neocortex is supported by our analysis of NCAMff+ transgenic mice, in which NCAM is absent from excitatory neurons. However, certain mature excitatory neuronal populations in the hippocampus of wild-type rodents express PSA-NCAM only in their axons or their terminal boutons: the axons (mossy fibers) of most mature granule cells in the hilus and CA3 stratum lucidum (Seki and Arai, 1999) and the terminal boutons of axons of CA3 pyramidal neurons (Schaffer collaterals), some of which terminate in the CA1 stratum lacunosum moleculare (Muller et al., 1996; Schuster et al., 2001). This may explain the lack of PSA-NCAM expression in the mossy fibers of NCAMff+ mice (Bukalo et al., 2004) and the reduction observed in the stratum lacunosum moleculare. However, in NCAMff+ mice, not only PSA but also NCAM are ablated and, consequently, the effects observed may be NCAM dependent.

Cortical interneurons can be classified on basis of their neurochemical properties by the expression of different calcium-binding proteins and neuropeptides (Freund and Buzsáki, 1996; Markram et al., 2004; Ascoli et al., 2008). The present results indicate that cortical PSA-NCAM expressing interneurons do not belong to any of the previously described categories. It seems more likely that different subpopulations of interneurons have the possibility to express PSA-NCAM. It is also conceivable that some interneurons do not express PSA-NCAM in their somata but only in their terminal fields, as it has been recently reported for parvalbumin (PV) expressing neurons in the mPFC (Castillo-Gómez et al., 2011).

27.2 Possible dynamics of PSA-NCAM expression in interneurons

In contrast to PSA-NCAM expression in the hippocampal subgranular zone or the paleocortex layer II, which is strongly downregulated during aging (Seki and Arai 1995; Abrous et al. 1997; Varea et al. 2009), PSA-NCAM expression in cortical interneurons is stable over lifetime (both in the number of PSA-NCAM expressing cells and in the intensity of PSA-NCAM expressing neuropil) (Varea et al., 2009). However, we do not know whether PSA-NCAM is expressed always in the same subgroup of interneurons or whether different groups of interneurons can switch on and off this expression depending on synaptic activity. It is also possible that all, or a subset, of PSA-NCAM expressing interneurons retain this expression constitutively since their generation during embryonic development. In any case, our laboratory has demonstrated that different pharmacological manipulations can increase or decrease the number of PSA-NCAM expressing neurons in the adult cerebral cortex (Varea et al., 2007b,a; Castillo-Gómez et al., 2008), indicating that, at least to some extent, inhibitory neurons can stop expressing, express *de novo*, or reexpress PSA-NCAM.

28 Impact of the polysialyltransferases ST8SiaII or ST8SiaIV on PSA-NCAM expression

The comparative immunohistochemical analysis of PSA-NCAM expression in mice lacking either of the two polysialyltransferases, ST8SiaII or ST8SiaIV, provides a detailed picture of the divergent impact of the two enzymes across different regions of the mature mouse forebrain. In overview, the data demonstrate that both polysialyltransferases contribute to PSA synthesis in the mature brain, but their share is clearly different. As assessed before by real time RT-PCR and Western blot analyses of whole brain lysates, ST8SiaII is predominant during development, while ST8SiaIV is the major polysialyltransferase of the adult brain (Galuska et al., 2006; Oltmann-Norden et al., 2008; Schiff et al., 2009) (see Fig. 4.2). A direct comparison of the PSA-NCAM fraction isolated from perinatal brain of wild-type, ST8SiaII- and ST8SiaIV-deficient mice indicated clear differences in the quantity of NCAM that can be processed by the amounts of ST8SiaII or ST8SiaIV available *in vivo*, but only minor differences in the chain length pattern and number of PSA chains per N-glycosylation site (Galuska et al., 2006, 2008). Moreover, PSA produced by either enzyme is able to prevent axon tract defects caused by the complete loss of PSA indicating that both enzymes are equally able to modulate NCAM functions (Hildebrandt et al., 2009). Thus, rather than producing PSA-NCAM species with distinct properties, the difference between the two enzymes appears to be the context- and site-specific regulation of PSA-NCAM synthesis. The patterns of PSA-NCAM immunoreactivity in the forebrain of 3 month old ST8SiaII- and ST8SiaIV-deficient mice provided by the current thesis confirm this predominance of ST8SiaIV and largely corroborate comparative analyses of ST8SiaII and ST8SiaIV mRNA expression in the wildtype and of PSA-NCAM expression levels in ST8SiaII$-/-$ and ST8SiaIV$-/-$ mice (Hildebrandt et al., 1998; Ong et al., 1998; Galuska et al., 2006; Oltmann-Norden et al., 2008). More important, however, are the new insights into the allocation of the two enzymes to PSA synthesis in brain regions and cell types not studied previously.

28.1 ST8SiaIV is the major polysialyltransferase of mature interneurons in the mouse forebrain

The present results on the distribution of PSA-NCAM expressing cells in the polysialyltransferase-deficient mice are in good agreement with a previous *in situ* hybridization study detecting no ST8SiaII, but widely dispersed ST8SiaIV expression in all neocortical layers of young rats (Hildebrandt et al., 1998). In rats and mice, our laboratory has characterized PSA-NCAM positive cells as mature interneurons (Nacher et al., 2002b; Varea et al., 2005; Gilabert-Juan et al., 2011). As demonstrated for the prefrontal cortex, the PSA-NCAM positive processes or puncta also belong to inhibitory interneurons (Varea et al., 2005). The lack of PSA-NCAM expression, therefore, indicates that ST8SiaIV is solely responsible for PSA synthesis in mature cortical interneurons during adulthood. ST8SiaIV-deficient mice also lack PSA-NCAM expressing cells with an interneuron-like appearance in the deep layers of the paleocortex. Moreover, PSA-NCAM in the stratum lacunosum-moleculare

of CA1 and most of the staining in the molecular layer of the dentate gyrus depends on ST8SiaIV. Similarly, a dramatic (although not complete) reduction of PSA-NCAM positive neuropil and in the number of PSA-NCAM expressing cells has been observed in the amygdala of ST8SiaIV-deficient mice. In the wildtype, these cells have features of interneurons (Gilabert-Juan et al., 2011), suggesting that also in this region ST8SiaIV is responsible for the polysialylation of mature interneurons. Similarly, we found that PSA-NCAM expression of cells in the septum is uncompromised in both, ST8SiaIV- and in ST8SiaII-deficient mice. These cells, however, have previously been characterized as interneurons (Foley et al., 2003) indicating that both polysialyltransferases can incorporate PSA in interneurons outside of the cerebral cortex.

28.2 ST8SiaII is the major polysialyltransferase of immature neurons in the adult cerebral cortex

The present results demonstrate a predominant impact of ST8SiaII on PSA-NCAM expression of specifically immature neuron populations in the adult cerebral cortex. ST8SiaII, but not ST8SiaIV deficient animals have strongly reduced PSA-NCAM expression in the neurogenic region of the hippocampal SGZ (as described before by Angata et al. (2004)), as well as in the paleocortex layer II, a region of the brain of young rodents, in which immature cells have been described (Gómez-Climent et al., 2008). As noted before (Eckhardt et al., 2000; Angata et al., 2004), neither of the two polysialyltransferase-deficient single knockout strains displayed marked reductions of PSA-NCAM staining of neuroblasts in the SVZ/RMS system. These data imply that in the neurogenic system of the anterior SVZ both polysialyltransferases are co-expressed and that under these conditions each enzyme can compensate, at least to a certain extent, for the loss of the other. Such compensation is perfectly consistent with previous data obtained by analyses on the level of whole brain homogenates (Galuska et al., 2006). On the other hand, in almost all other forebrain areas of the 3 month-old mice investigated in the current thesis, the loss of ST8SiaIV virtually eliminates PSA-NCAM immunostaining, whereas ST8SiaII deficiency had no discernible effect. During hippocampal neurogenesis granule cell precursors within the SGZ acquire PSA-NCAM immunoreactivity at an early neuroblast-like stage, before they migrate and differentiate into granule cells with transient PSA-NCAM expression on their axonal and somato–dendritic compartments. By contrast, mature granule cells only retain PSA-NCAM expression on their mossy fiber axons (Seki and Arai, 1993a, 1999; Schuster et al., 2001). As shown in the current thesis, expression of PSA-NCAM on cell somata of granule cell precursors of the hippocampal SGZ in 3 month old mice depends mostly, but not exclusively, on the presence of ST8SiaII, while it was unaffected by the genetic ablation of ST8SiaIV. The PSA-NCAM staining in the SGZ of ST8SiaII knockout mice was found on cells with only short processes, suggesting a contribution of ST8SiaIV to polysialylation in some immature SGZ neurons. On the other hand, PSA-NCAM expression on mossy fibers was almost completely abolished in 3 months old St8siaIV$-/-$ mice. Some of the remaining thin, isolated PSA-NCAM positive processes in the hilus and in the CA3 subfield, arose from PSA-NCAM expressing granule neurons in the SGZ.

These profiles, therefore, seem to correspond to immature mossy fibers and, consequently, ST8SiaII may still contribute to PSA production during early stages of mossy fiber formation. These findings are in good agreement with the first reports on ST8SiaII- and ST8SiaIV-deficient mice (Eckhardt et al., 2000; Angata et al., 2004) and in line with earlier *in situ* hybridization data showing ST8SiaII expression in the SGZ, where new granule cells are born, but ST8SiaIV expression in most mature granule cells (Hildebrandt et al., 1998). The differential loss of PSA-NCAM in the dentate gyrus of the two polysialyltransferase knockout models, together with the expression patterns of the two enzymes, indicates that PSA is predominantly synthesized by ST8SiaII in newly generated and by ST8SiaIV in older granule cells. Thus, during adult hippocampal neurogenesis the general developmental profile of the two polysialyltransferases seems to be reproduced on the cellular level. Despite the dramatic reduction of PSA-NCAM expression, we found that the number of DCX positive cells in the SGZ of ST8SiaII-deficient mice was unaffected, suggesting the uncompromised generation of granule cell precursors. This is consistent with unaltered rates of progenitor cell proliferation in the dentate gyrus reported for either ST8SiaII-deficency or in mice depleted of PSA due to ablation of NCAM (Angata et al., 2004; Aonurm-Helm et al., 2008). However, in ST8SiaII$-/-$ mice an unusually high number of DCX positive cells was found, displaying abnormal lengths and trajectories of their dendritic trees, many of them ectopically located in the hilus, suggesting aberrant differentiation/migration of newly generated granule neurons. Significantly more immature DCX expressing cells were observed in the hippocampal SGZ of ST8SiaIV-deficient mice, as well as in the piriform cortex layer II of ST8SiaII$-/-$ and ST8SiaIV$-/-$ animals. Surprisingly, a concomitant increase of PSA-NCAM positive cells was also detected in the latter. One explanation for these increasing numbers could be that immature neurons accumulate in the absence ST8SiaIV, indicating that this enzyme is somehow necessary for the maturation of these cells and/or that its absence may prevent cell death. A defect in migration/maturation in the absence of ST8SiaIV may also explain the presence of some DCX expressing cells with multipolar morphology in piriform cortex layer III. Further experiments are needed to clarify the nature and fate of these cells. PSA-NCAM expression in the paleocortex layer II depends on the presence of ST8SiaII, but despite the dramatic reduction in PSA-NCAM expression of ST8SiaII-deficient mice, the number of immature, DCX positive neurons is preserved. Thus, PSA-NCAM does not seem necessary for maintaining the immature phenotype of these cells. However, the marked increase of DCX positive cells in layer II of the paleocortex of 3 months old ST8SiaIV-deficient mice, indicates that expression of this molecule through ST8SiaIV affects the number of immature cells, either by influencing their migration, delaying their maturation or by preventing their death. In fact, the complete absence of PSA-NCAM during development, by deletion of both polysialyltransferases, perturbs cell migration and results in increased numbers of apoptotic cells in the cerebral cortex (Angata et al., 2007). Finally, the presence of some PSA-NCAM expressing cells in the amygdala of ST8SiaIV-deficient mice coincides with a low level of adult neurogenesis in this region (Bernier et al., 2002; Shapiro et al., 2009). The few immature neurons in this region, therefore, may be polysialylated by ST8SiaII. Taken together, the increase in the number of DCX expressing cells in the SGZ of ST8SiaIV-deficient mice and in the piriform cortex

layer II of either ST8SiaIV- or, less pronounced, ST8SiaII-deficient animals, their altered morphology in the SGZ under ST8SiaII$-/-$ conditions, as well as the increase of PSANCAM expressing cells in the piriform cortex layer II points towards a prominent role of polysialylation in the development of these cell types. Thus, putative functions of these newly generated neurons in learning, memory or in the behavioral response to pharmacological treatments may be impaired under conditions of compromised polysialylation.

29 Effects of PSA depletion on the structure of interneurons

The present thesis shows the effects of PSA removal on the morphology of a subpopulation of hippocampal interneurons, most of them expressing somatostatin, which display dendritic spines. These spines receive both excitatory and inhibitory inputs. The use of hippocampal organotypic slices and intracerebral injections of the enzyme Endo-N-acetylneuraminidase (EndoN), demonstrate that these interneurons have a basal turnover of their dendritic spines and that PSA removal influences some structural features of these spines. These data demonstrate that the dendritic spines of interneurons are dynamic structures in the adult brain and suggest a novel role for PSA-NCAM in the regulation of the synaptic input of inhibitory circuits.

29.1 A subpopulation of hippocampal interneurons display dendritic spines, which receive inhibitory and excitatory inputs

A previous study on the strain of mice used in our experiments, stated that the majority of eGFP expressing cells in the CA1 region of the hippocampus were interneurons expressing somatostatin (Oliva et al., 2000). These interneurons are known to mainly project to the stratum lacunosum-moleculare, and to coexpress calbindin (CB) as well (Gulyás et al., 2003). However, the present results show that not all eGFP interneurons belong to the somatostatin expressing subpopulation of interneurons in the hippocampus, but they also appear to belong to the population expressing PV and, to a lesser extent, to that expressing calretinin (CR). Although somatostatin expressing interneurons in the neocortex are known to have dendritic spines (Kawaguchi et al., 2006), nobody to our knowledge has explored yet their synaptic input. However, a recent report has studied the synaptic input of spines in subpopulations of neocortical interneurons expressing neuropeptide Y (Keck et al., 2011); this study, using a similar approach to the one used in the present experiments, has shown that these interneuronal spines receive mostly glutamatergic input (almost 90%) and that spines receiving inhibitory input constitute around 30% (Keck et al., 2011). By contrast, the results of this thesis on the somatostatin expressing interneurons in the hippocampus CA1 show that more than 45% of their spines are closely apposed to puncta expressing the vesicular glutamate transporter-1 (VGluT1) and almost a 40% to puncta expressing vesicular GABA transporter (VGAT). This discrepancy may be due to differences in the type of interneurons studied and/or the region analyzed. The present results are also different to those observed in the dendritic spines of excitatory

neurons, most of which receive excitatory input. In these excitatory neurons the inhibitory input is normally located on the dendritic shaft or the soma (Keller, 2002). Moreover, in pyramidal neurons around 90% of the excitatory synapses are located on spines (Nimchinsky et al., 2002), while only 4.4% of spines receive an inhibitory input (Knott et al., 2002). However, both the study of Keck et al. and this thesis indicate that spines from interneurons may have a different synaptic input, since a 30-40% of their spines are in close apposition to inhibitory presynaptic puncta.

29.2 Structural dynamics of dendritic spines on interneurons

Dendritic spines of pyramidal neurons are plastic structures that have been shown to modify their morphology, density and dynamics after many different paradigms (Yuste and Bonhoeffer, 2001). In these neurons, spines represent the excitatory post-synaptic input and therefore the changes in spine density and dynamics have been associated with changes in neural acitvity (Yuste and Bonhoeffer, 2001). In addition, dendritic spines appear and disappear continuously, although only a small portion of them become stable, suggesting a stabilization mechanism driven by synaptic activity (Muller et al., 2010). In this line, previous studies on organotypic hippocampal cultures have described the turnover of dendritic spines of CA1 pyramidal neurons in similar conditions than the present experiments, showing a stability rate around 80% and an apparition rate about 20% (De Roo et al., 2008a; Mendez et al., 2010a). In addition, they have shown how different experimental conditions are able to modify this turnover (De Roo et al., 2008b; Mendez et al., 2010b). However, studies using *in vivo* imaging with cranial windows have shown a stability rate over 95% in a daily basis and around a 65% for one month period in pyramidal neurons of the somatosensory and visual cortices (Knott and Holtmaat, 2008), suggesting that there is a lower degree of spine turnover *in vivo* in the adult neocortex. Regarding interneurons, to date very few studies have explored their structural remodeling. In this line, using cranial windows in transgenic mice with fluorescent interneurons, different studies by Dr. Nedivi's laboratory have shown the elongation/retraction of dendritic branch tips *in vivo* in different neocortical regions (Lee et al., 2006; Chen et al., 2011b,a). However, only another recent study has been focused on the turnover of the dendritic spines of interneurons, and it shows a stability rate close to 98% in a 24 hours time-lapse experiment (Keck et al., 2011). These results are considerable higher than the ones we have found in hippocampal interneurons, where the stability rate is around 65%. These differences may be due to a difference in the stability of different interneuronal subpopulations, the region studied, or more likely to a major stability in *in vivo* conditions than in our organotypic hippocampal cultures. These changes in the structural plasticity of inhibitory neurons, both at the level of dendrites and spines, have been suggested to modulate neuronal connectivity within local cortical circuits (Stepanyants et al., 2002; Chen and Nedivi, 2010). Therefore, decreases in the dynamics of these structures, may be a result not only of decreased activity of interneurons, but in the local network activity (Freund, 2003).

29.3 Effects of PSA depletion on dendritic spine density and spine dynamics

The addition of EndoN (an enzyme that removes the polysialic acid) to the organotypic cultures increased the apparition rate of dendritic spines 24 hours after the delivery of the enzyme without affecting the stability of previous spines. Consequently, it increased the relative spine density, which is the same effect we observe in fixed tissue 2 days after an EndoN injection. However, we found the opposite effect 7 days after the EndoN injection. These results suggest an important role for PSA-NCAM in regulating the synaptic input of hippocampal interneurons.

After PSA removal, it has been demonstrated that there is an increased interaction between BDNF and its receptors (Burgess and Aubert, 2006). This may explain the increase of the apparition rate and the density of spines observed in the hippocampal organotypic cultures and in the fixed tissue 2 days after the injection of EndoN, as we will discuss in the next part of the discussion. However, the long-term disruption of a mechanism regulating the action of local trophic factors may reduce the correct distribution of BDNF, resulting in a decreased synaptic transmission, which may explain the decreased spine density in the interneurons observed 7 days after the EndoN injection. These putative changes in BDNF would affect not only interneurons but also excitatory neurons, and in fact, recent data from our laboratory indicates that PSA depletion also produces a decrease in the spine density of pyramidal neurons in the medial prefrontal cortex 14 days after the injection with EndoN (Castillo-Gomez E. et al, unpublished results). However, another non-excluding hypothesis is possible: PSA-NCAM may be blocking certain synapses in an interneuronal subpopulation (Castillo-Gómez et al., 2011; Di Cristo et al., 2007) and, consequently, PSA depletion may activate many of these synapses. Some of these new synapses may make contact with recently generated spines, stabilizing a greater portion of these structures (Muller et al., 2010), which could explain the increase in spine density 2 days after the injection of EndoN *in vivo* and the increase in their appearance rate in organotypic cultures after the addition of the enzyme. The long-term effects of PSA removal, i.e. 7 days after the injection *in vivo*, decreasing the density of dendritic spines are more complex to interpret. These effects may be due to a compensatory response of the local hippocampal circuits to PSA depletion. If after PSA depletion interneurons increase their spine density and, consequently, their synaptic input, this may result in an overall inhibition of these local circuits, and in a negative feedback on these interneurons.

30 Functional role of PSA-NCAM expression in interneurons

One key aspect of this thesis is the question relating to the physiological consequences for an interneuron to express PSA-NCAM on its plasma membrane. We propose two non-excluding hypotheses. First, the presence of PSA-NCAM reduces cell-to-cell and cell-to-extracellular matrix adhesion, thus allowing interneurons to remodel the structure of their neurites, spines, and/or synapses. Consequently, the morphology of PSA-NCAM expressing interneurons may be just an instantaneous

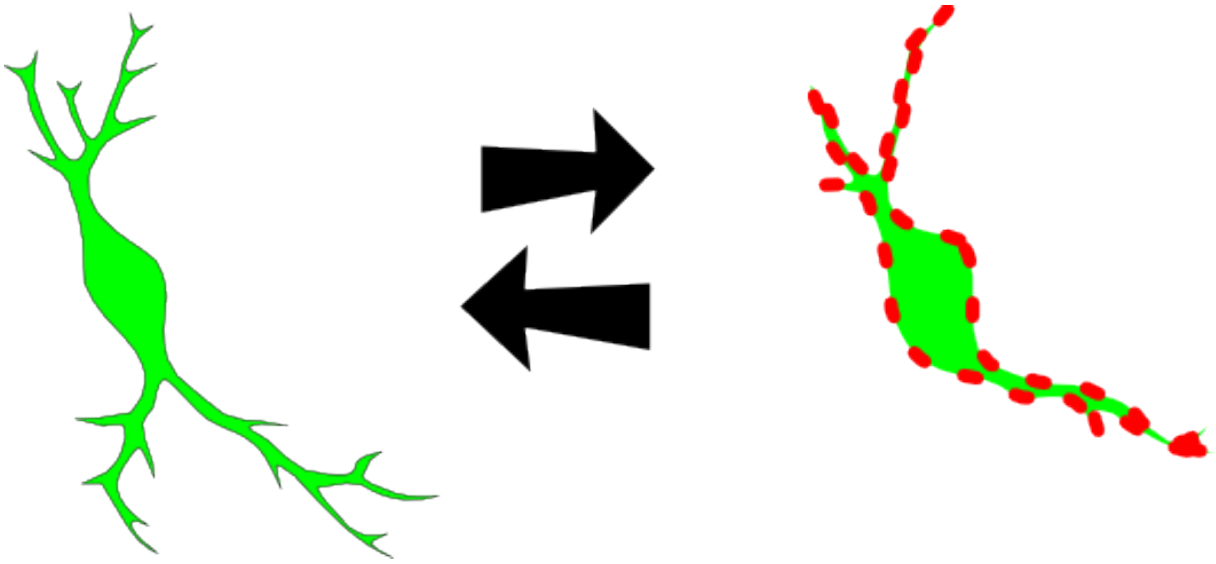

Fig. 30.1: «Insulating hypothesis» for the role of PSA-NCAM in the structural plasticity of interneurons

"picture" of a dynamic remodeling process. The second hypothesis, is the "shielding" or "insulating" hypothesis, which poses that PSA-NCAM expression may play an insulatory role, restricting the possibility of establishing synaptic contacts in the plasma membrane regions where it is present (Fig. 30.1). In fact, under the electron microscope, we have never found a synapse in a portion of surface displaying PSA-NCAM expression. In addition, previous studies have shown that the removal of PSA induces neuronal differentiation (Seidenfaden et al., 2003; Petridis et al., 2004) and increases brain-derived neurotrophic factor (BDNF) binding capacity (Burgess and Aubert, 2006). These later results led to the formulation of a "shielding" hypothesis for the action of PSA: The addition of PSA to NCAM may cover membrane receptors such as the neurotrophic tyrosine kinase receptor type 2 (TrkB) or p75 neurotrophin receptor, limiting its action on the portion of plasma membrane where PSA is expressed. Since BDNF has been shown to increase dendritic spine density (Tyler and Pozzo-Miller, 2003) and its diffusion in the nervous parenchyma is very restricted (Horch and Katz, 2002), it is possible that the expression of PSA may regulate dendritic spine density by limiting the binding of BDNF and other neurotrophins to their receptors. This is in agreement with the present results, showing that interneurons expressing PSA-NCAM have a reduced arborization pattern, decreased dendritic spine density and reduced number of perisomatic synaptic contacts than other interneurons. We have shown that immature PSA-NCAM expressing neurons in the adult paleocortex layer II are completely isolated from synaptic input, probably due to the presence of PSA-NCAM and glial processes in most of their surface (Gómez-Climent et al., 2008). By contrast, this insulation is incomplete in PSA-NCAM expressing interneurons, since we have found that some inhibitory synapses contact the perisomatic region of these interneurons. Consequently, PSA-NCAM expressing interneurons are integrated in the cortical circuits but may have reduced activity, possibly resulting in reduced dendritic arborization, decreased spine density, and low expression of cell activity markers.

It is tempting to think that PSA-NCAM expressing interneurons may constitute a reservoir, which after downregulating PSA-NCAM expression, may receive more synaptic contacts and thus become more integrated in the circuitry and that PSA-NCAM upregulation in interneurons may lead to the opposite effect. However, electrophysiology experiments need to be performed to verify this hypothesis. Finally, this thesis has demonstrated that enzymatic removal of PSA affects the structure of cortical interneurons *in vivo* (in fixed tissue of animals injected intracerebrally) and *in vitro* (using organotypic cultures). These results indicate that the polysialylation of NCAM is an important factor in the modulation of interneuronal structural plasticity and, consequently, in the connectivity of inhibitory networks. These findings may be particularly relevant to psychiatric disorders, such as schizophrenia or major depression, in which alterations in the structure of cortical inhibitory networks and in PSA-NCAM expression have been described, both in patients (Barbeau et al., 1995; Sullivan et al., 2007; Tao et al., 2007; Brennaman and Maness, 2010; Varea et al., 2011b) and in animal models of these disorders (Phillips et al., 2003; Mattson et al., 2004; Castrén, 2005; Gilabert-Juan et al., 2011).

31 Antidepressant treatment as a model for neuronal structural plasticity induction

As we have discussed previously, PSA-NCAM, due to its anti-adhesive properties, is involved in several forms of neuronal structural plasticity. In this line, our group has demonstrated that PSA-NCAM expression is sensible to antidepressants such as fluoxetine, acting through serotonin (5HT) type 3 receptors (Varea et al., 2007a). However, other serotonin receptors are also present in all the regions analyzed in this thesis and known to mediate the effects of fluoxetine; consequently, it is possible that they also mediate changes in PSA-NCAM expression (Hewlett et al., 1999; Li et al., 2003; McDonald and Mascagni, 2007; Morales et al., 1998; Puig et al., 2004; Weber and Andrade, 2010).

As it has been discussed before, many PSA-NCAM expressing structures in the cerebral cortex (Nacher et al., 2002b) and the amygdala (Gilabert-Juan et al., 2011) of rodents belong to mature interneurons and, consequently, changes in PSA-NCAM expression should primarily affect the structure of interneurons, rather than that of principal neurons. Previous reports from our laboratory using a dopamine D2 receptor agonist, which increases PSA-NCAM expression in the mPFC, also resulted in a parallel upregulation of GAD67 expression (Castillo-Gómez et al., 2008). In line with the neuroplastic hypothesis of depression, it is possible then, that changes in PSA-NCAM expression affect the connectivity of certain interneurons, regulating the ability to remodel the structure of their neurites and, consequently, their connections in response to antidepressant treatment (Fig. 31.1).

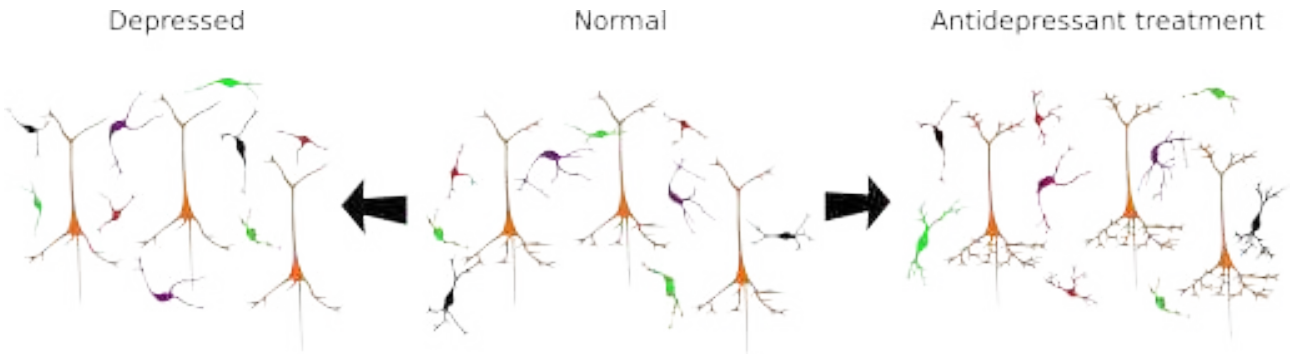

Fig. 31.1: Possible role of interneurons in the neuroplastic hypothesis of depression

31.1 Effects of fluoxetine on c-fos expression, volume of cerebral regions and animal weight

This thesis demonstrates for the first time the activation of the somatosensory cortex after chronic fluoxetine treatment in young-adult rats. In a similar way, a recent report has described effects of fluoxetine on neuronal activation and plasticity in another sensory region, the visual cortex (Maya Vetencourt et al., 2008); here, antidepressant administration restores neuronal networks involved in ocular dominance and visual function in adult amblyopic rats. This study evaluated neuronal plasticity at the electrophysiological, molecular and behavioural level, but it is very likely that structural plasticity may be also involved. The present c-fos expression study is also in consonance with previous reports using immediate early gene expression, which shown that an important number of cerebral regions become activated after chronic antidepressant treatment. Lino-de oliveira et al. (2001) demonstrated that chronic fluoxetine treatment induce a significant increase in c-fos immunoreactivity in the lateral septal nucleus, the bed nucleus of the stria terminalis, the medial amygdala, the dorsal raphe nucleus and the periaqueductal gray, while it induces a decrease in the locus coeruleus. Morinobu et al. (1997) also showed that a chronic treatment with imipramine or tranylcypromine caused a significant increase in the expression of c-fos mRNA in the frontal cortex. Our finding of an increased activation of the somatosensory cortex after chronic antidepressant treatment is also supported by some reports that have demonstrated, using different activation markers, changes in this region in animal models of depression or after antidepressant treatment (Skelin et al., 2008; Qu et al., 2003). In the present thesis, we also describe an increase in the volume of the hippocampus after chronic fluoxetine treatment in middle-aged rats. These results suggest the presence of structural changes and are in agreement with changes observed in both patients and animal models of depression, where decreases in the volume of certain cerebral regions, such as the hippocampus or the mPFC, have been described (Phillips et al., 2003; Tata and Anderson, 2010). Finally, we also describe a decrease in body weight after chronic fluoxetine treatment in middle-aged rats, similar to what has been described in younger animals (Thompson et al., 2004; McNamara et al., 2010).

31.2 Expression of PSA-NCAM and other molecules related with structural plasticity

Previous studies have described the effects of chronic treatments with antidepressants, such as fluoxetine, in the expression of PSA-NCAM and other molecules related to structural plasticity in young-adult rats (3 months-old) (Varea et al., 2007b,a). The results presented in this thesis expand this previous results to middle-aged rats and young-adult mice (3 months-old).

The present results in the mPFC of middle-aged rats showing only an increase in the density of PSA-NCAM expressing puncta in the dorsal cingulate cortex, are more restricted than those found previously in young-adult rats, which showed increases in every region and layer of the mPFC (Varea et al., 2007a). The lack of changes in the density of puncta expressing presynaptic markers is also in contrast with previous reports using young-adult rats, which showed increases in synaptophysin (SYN) expression in deep layers of the prelimbic and infralimbic cortices (Varea et al., 2007b) and of VGluT1 mRNA expression in the cingulate cortex (Tordera et al., 2005). In the hippocampus, previous studies with young-adult rats found an increase in PSA-NCAM expression in the stratum lucidum, but not in the rest of hippocampal strata studied (Varea et al., 2007b), while a general increase was found in this thesis in most of the regions analyzed both in middle-aged rats and in young mice. Since in young-adult rats antidepressants promote an increase in the density of PSA-NCAM expressing cells in the SGZ (Sairanen et al., 2007), fluoxetine may be affecting PSA-NCAM expression (in the molecular layer or the stratum lucidum) by increasing the production or accelerating the maturation of immature granule cells, some of which may have already sent PSA-NCAM expressing mossy fibers to the stratum lucidum and extended dendrites into the molecular layer (Seki and Arai, 1999). However, in middle-aged rats, the present results clearly indicate that the number of these cells (in the SGZ) is not affected by fluoxetine in middle-aged rats. Moreover, other studies in mice also indicate that fluoxetine does not increase the number of immature cells (Holick et al., 2008; Huang et al., 2008), suggesting that these changes in PSA-NCAM expression are not linked to adult neurogenesis.

In fact, the present results on middle-aged rats show that the increase of PSA-NCAM expressing puncta in the stratum lacunosum-moleculare is accompanied by an increase in the density of SYN expressing puncta and of puncta co-expressing PSA-NCAM/SYN, while in young mice the increase in PSA-NCAM expressing puncta is accompanied by an increase in the density of SYN expressing puncta in the strata radiatum and oriens, suggesting that these puncta correspond to synapses. Interestingly, in the stratum lacunosum-moleculare of middle-aged animals we also found an increase in the density of GAD6 expressing puncta and a decrease in the density of those expressing VGluT1, while in the young mice we also found an increase in the density of GAD6 expressing puncta in the stratum oriens and an increase in the number of puncta co-expressing PSA-NCAM/GAD6 in the stratum oriens and in the hilus. Altogether, these results indicate that the upregulation of PSA-NCAM expression may be linked to changes in inhibitory circuits, probably involving the formation of inhibitory synapses.

In most amygdaloid nuclei, chronic fluoxetine treatment in young-adult rats decreases PSA-NCAM and SYN expression (Varea et al., 2007b) and decreases the number of PSA-NCAM expressing neurons in this limbic region (Homberg et al., 2011). By contrast, in middle-aged rats we not only have failed to observe decreases in the density of puncta expressing PSA-NCAM or SYN, but have observed significant increases in the density of PSA-NCAM expressing puncta in the central nucleus and of those expressing SYN in the lateral and basolateral nuclei. There is, in fact, a general tendency for an increase in the density of puncta expressing PSA-NCAM, SYN and GAD6 in all the amygdaloid nuclei studied. Moreover, despite the fact that no significant changes in puncta expressing exclusively GAD6 or SYN were observed in the central amygdala, the density of puncta coexpressing PSA-NCAM and each of these two markers also increases significantly in this nucleus, suggesting that changes in PSA-NCAM expression may be associated to the generation or remodeling of inhibitory synapses in this region as well. In the basolateral amygdala, chronic fluoxetine treatment may also influence positively synaptic plasticity of inhibitory circuits, as indicated by increased densities of GAD6 and SYN expressing puncta, while the density of those expressing VGluT1 is decreased. It is possible that substantial differences in 5HT content and in the expression of its receptors, transporters, etc... occur in middle-aged animals. The levels of 5HT are generally reduced in the brain of aged rats (Homberg et al., 2011) and, although there are no studies in middle-aged animals, it is possible that they are already reduced at this age. There is also evidence indicating that the expression 5HT1A receptor, which has an important role in the antidepressant effects of 5HT reuptake inhibitors (Blier, 2010; Hensler, 2002), is lower in young-adult than in adolescent rats (Homberg et al., 2011). Additionally, other factors such as changes in inhibitory neurotransmission may also influence the effects of fluoxetine in middle-aged animals, particularly in the amygdala, where decreases in GABA concentration and hyperactivity have been described during aging (Lolova and Davidoff, 1991; Nakanishi, 1998).

31.3 Effects of fluoxetine on the perisomatic innervation of pyramidal neurons and interneurons

As discussed before, chronic antidepressant treatment increases the expression of inhibitory markers in the neuropil of certain cerebral regions, however, there is little information on the plasticity induced by antidepressants on the perisomatic innervation of both excitatory and inhibitory neurons. In the present thesis, we provide evidence of the effects of chronic fluoxetine treatment on the perisomatic innervation of pyramidal neurons and interneurons located in the CA1 region of the hippocampus of young-adult mice. Although it has been suggested that the perisomatic innervation of pyramidal neurons should not be the subject of structural remodeling (Freund, 2003), different studies have shown that this perisomatic innervation is modulated by, at least, visual deprivation in the postnatal visual cortex (Di Cristo et al., 2007) and by pharmacological treatments in the adult mPFC (Castillo-Gómez et al., 2011). Previous studies have suggested that antidepressants increase the density of parvalbumin expressing interneurons (Prince et al., 2009). However, no changes in the number of

perisomatic puncta expressing parvalbumin or SYN on hippocampal CAMKII expressing pyramidal cells were found after chronic fluoxetine treatment. On the other hand, an increase in the density of perisomatic puncta expressing GAD6 was found on interneurons expressing eGFP. Although the density of perisomatic puncta expressing SYN was unaffected, an increase in the number of puncta co-expressing GAD6 and SYN was observed. These results suggest that this subpopulation of interneurons (some of which express parvalbumin, see Fig. 17.6) may be involved in the mechanism of action of antidepressants.

31.4 Effects of fluoxetine on the structure of pyramidal neurons and interneurons

The results of this thesis indicate that antidepressant treatment promotes spine remodeling in both excitatory and inhibitory neurons. In the somatosensory cortex of young-adult rats, chronic fluoxetine treatment induces an increase in the spine density of pyramidal neurons and in young-adult mice we describe an increase in the dendritic spine density of mPFC interneurons. As discussed before, the structural remodeling of excitatory neurons has been extensively studied and the present results in the somatosensory cortex expand the repertoire of regions where antidepressants produce this sort of structural remodeling. These results are, therefore, in agreement with those shown in a previous report describing an increase in the number of spine synapses in pyramidal neurons of the hippocampus after 5 and 14 days of treatment with fluoxetine (Henn and Vollmayr, 2004). Conversely, the opposite effect has been found in different studies with animal models of depression, such as chronic stress (McEwen, 2010). Chronic stress also decreases dendritic branching and spine density in principal neurons of the mPFC Radley et al. (2004, 2005b, 2006b) and the orbitofrontal cortex (Murmu et al., 2006). Finally, in certain regions of the amygdala, chronic stress produces hypertrophy of excitatory neurons (Mitra et al., 2005; Vyas et al., 2002). However, there is little information about the structural remodeling of interneurons after antidepressant treatments or in animal models of depression. In this line, a recent study from our laboratory has shown that after chronic stress, interneurons in the amygdala display a reduced Sholl profile (Gilabert-Juan et al., 2011). In the present thesis, we describe that chronic fluoxetine treatment produces an increase in the dendritic spine density in interneurons of the mPFC. Although in other cortical areas, such as the visual cortex, it has been proven that fluoxetine produces a decrease in inhibition (Maya Vetencourt et al., 2008), in the frontal cortex fluoxetine induces an increase in the expression of the inhibitory marker GAD65 (Fatemi et al., 2009). In addition, other studies have shown that chronic stress decreases the expression of parvalbumin, a protein exclusively expressed in interneurons, and that this decrease is reverted after treatment with antidepressants such as fluoxetine (Czeh et al., 2005).

31.5 Effects of fluoxetine on adult neurogenesis

The present results on adult hippocampal neurogenesis are in agreement with previous studies showing that neither proliferation nor neuronal survival/differentiation is affected by chronic antidepressant treatment in middle-aged rodents (Couillard-Despres et al., 2009; Cowen et al., 2008). This lack of response of the SGZ in middle-aged animals must be due to changes that alter the molecular pathways by which 5HT stimulates neurogenesis. There is an age-dependent reduction in the levels of 5HT (Homberg et al., 2011) and some of its receptors (Marcusson et al., 1984) in the hippocampus, which may explain the failure of the fluoxetine treatment used in this thesis and others studies to increase neurogenesis in middle-aged and old animals. Since glucocorticoids are important modulators of adult hippocampal neurogenesis and these steroids are particularly elevated during aging (Mcewen et al., 2002), they may also influence the neurogenic response to antidepressants in middle-aged animals. In fact, glucocorticoids decrease 5HT transporter expression (Slotkin et al., 1997) and the neurogenic action of fluoxetine is blocked by a flattened corticosterone rhythm induced by artificially enhanced glucocorticoid levels (Huang and Herbert, 2006). In agreement with our study, other reports have demonstrated that stress does not produce any change in the expression of DCX or PSA-NCAM, in both the SGZ and the SVZ of marmoset monkeys (Marlatt et al., 2011). In addition, it is possible that the stress induced solely by daily injections influence neurogenesis, as in fact has been shown that daily injections induce structural changes (Seib and Wellman, 2003). Other molecules known to modulate adult neurogenesis, including neurotransmitters, such as glutamate acting on N-Methyl-D-aspartic acid (NMDA) receptors (Nacher and McEwen, 2006) and GABA (Markwardt and Overstreet-Wadiche, 2008), or trophic factors, such as BDNF (Castrén and Rantamäki, 2010), can be influenced by antidepressants such as fluoxetine (Wu and Castrén, 2009; Li et al., 2006; Saarelainen et al., 2003). Consequently, age-dependent changes in their expression or in the molecular pathways in which these molecules are involved may also lead to changes in the pro-neurogenic effects of antidepressants. In contrast to previous studies in young-adult rodents, that found increases in the number of proliferating cells in the SVZ using fluoxetine (Nasrallah et al., 2010) and 5HT receptor agonists (Banasr et al., 2004), the opposite effect has been described in this thesis. On the other hand, the present results are in agreement with a recent report describing that in young-adult mice, 3 weeks of fluoxetine treatment do not affect cell proliferation in the SVZ, but that the extension of this treatment to 6 weeks produces a significant deficit in the number of dividing cells in this region (Ohira and Miyakawa, 2011). These results indicate that the SVZ of middle-aged rodents is more sensible to fluoxetine treatment, since a significant decrease in cell proliferation can be achieved with a shorter treatment. It is possible that the lack of differences in the number of neuroblasts in the SVZ may be due to a homeostatic parallel change in the number of apoptotic cells in this region, as suggested previously (Sairanen et al., 2005). Alternatively, fluoxetine could impair neuronal migration, which may cause accumulation of neuroblasts in the SVZ.

Part VIII. Conclusions

1. PSA-NCAM expressing cells with morphological characteristics of interneurons are widely distributed throughout the telencephalon of adult rats and mice.

2. Analysis of NCAM knockout mice reveals that NCAM is the only polysialylated protein in interneurons of the adult cerebral cortex.

3. In the adult rat paleocortex layer II, PSA-NCAM expressing tangled cells show ultrastructural features of immature neurons.

4. PSA-NCAM expressing non-granule neurons in the adult mouse hippocampus express markers of interneurons and this expression persists in conditional NCAM transgenic mice, which do not express neither NCAM nor PSA in excitatory neurons.

5. In the adult mouse brain a subpopulation of interneurons, expressing mainly somatostatin and parvalbumin, carry spines on their dendrites and these spines receive in a similar proportion both excitatory and inhibitory inputs.

6. In the adult mouse brain PSA-NCAM expressing interneurons have reduced dendritic arborization and dendritic spine density than other interneurons lacking this molecule.

7. PSA-NCAM expressing interneurons receive less perisomatic synaptic contacts than other interneurons lacking this molecule in the mPFC and hippocampus of the adult rat brain.

8. Gephyrin is a dynamic molecule expressed in every part of pyramidal neurons in the CA1 region of the hippocampus, with a higher expression in cell parts associated with postsynaptic inhibitory neurotrasmission, such as the soma and the axon.

9. St8SiaII is the main responsible enzyme of the polysialylation of immature neurons and St8SiaIV for the polysialylation of mature interneurons in the adult brain.

10. The absence of each of the polysialyltransferases influences the number, the location and the structure of immature neurons in the adult brain, but not the expression of glutamic acid decarboxylase or synaptophysin.

11. The removal of PSA *in vivo* produces a time-dependent change in the structure of interneurons in the hippocampus of mice.

12. The removal of PSA *in vitro* produces an increase in the apparition turnover rate of the spines of interneurons.

13. The antidepressant fluoxetine promotes an activation of the somatosensory cortex in young rats and an increase in the dendritic spine density of pyramidal neurons in layers III and V of the same region, but not changes in the expression of glutamic acid decarboxylase or the vesicular transporter of glutamate type 1.

14. Fluoxetine induces an increase in the volume of the hippocampus in the middle-aged rat brain, as well as an increase in the expression of plasticity-related molecules such as PSA-NCAM, glutamic acid decarboxylase and synaptophysin in the hippocampus and the amygdala.

15. Fluoxetine promotes an increase in the dendritic spine density of interneurons in the medial prefrontal cortex of mice, while in the hippocampus it produces an increase in the expression of plasticity-related molecules and an increase in the density of perisomatic puncta expressing glutamic acid decarboxylase on interneurons.

Part IX. References

References

Aaron, L. I. and Chesselet, M. F. (1989). Heterogeneous distribution of polysialylated neuronal-cell adhesion molecule during post-natal development and in the adult: an immunohistochemical study in the rat brain. *Neuroscience*, 28(3):701–710.

Abrous, D. N., Montaron, M. F., Petry, K. G., Rougon, G., Darnaudéry, M., Le Moal, M., and Mayo, W. (1997). Decrease in highly polysialylated neuronal cell adhesion molecules and in spatial learning during ageing are not correlated. *Brain Research*, 744(2):285–292.

Acheson, A., Sunshine, J. L., and Rutishauser, U. (1991). NCAM polysialic acid can regulate both cell-cell and cell-substrate interactions. *The Journal of Cell Biology*, 114(1):143–153.

Aimone, J. B., Wiles, J., and Gage, F. H. (2006). Potential role for adult neurogenesis in the encoding of time in new memories. *Nature Neuroscience*, 9(6):723–727.

Akiskal, H. S., Bourgeois, M. L., Angst, J., Post, R., Möller, H., and Hirschfeld, R. (2000). Re-evaluating the prevalence of and diagnostic composition within the broad clinical spectrum of bipolar disorders. *Journal of Affective Disorders*, 59 Suppl 1(0165-0327 (Print) LA - eng PT - Journal Article PT - Review RN - 0 (Antidepressive Agents) SB - IM):S5–S30.

Alvarez-Buylla, A., Herrera, D. G., and Wichterle, H. (2000). The subventricular zone: source of neuronal precursors for brain repair. *Progress in Brain Research*, 127:1–11.

American-Psychiatric-Association (2000). *Diagnostic and statistical manual of mental disorders: DSM-IV-TR.*, volume 4th of *DIAGNOSTIC AND STATISTICAL MANUAL OF MENTAL DISORDERS*. American Psychiatric Association.

Angata, K., Huckaby, V., Ranscht, B., Terskikh, A., Marth, J. D., and Fukuda, M. (2007). Polysialic Acid-Directed Migration and Differentiation of Neural Precursors Are Essential for Mouse Brain Development. *Molecular and Cellular Biology*, 27(19):6659–6668.

Angata, K., Long, J. M., Bukalo, O., Lee, W., Dityatev, A., Wynshaw-Boris, A., Schachner, M., Fukuda, M., and Marth, J. D. (2004). Sialyltransferase ST8Sia-II assembles a subset of polysialic acid that directs hippocampal axonal targeting and promotes fear behavior. *The Journal of Biological Chemistry*, 279(31):32603–32613.

Aonurm-Helm, A., Jurgenson, M., Zharkovsky, T., Sonn, K., Berezin, V., Bock, E., and Zharkovsky, A. (2008). Depression-like behaviour in neural cell adhesion molecule (NCAM)-deficient mice and its reversal by an NCAM-derived peptide, FGL. *European Journal of Neuroscience*, 28(8):1618–1628.

Arancio, O. and Chao, M. V. (2007). Neurotrophins, synaptic plasticity and dementia. *Current Opinion in Neurobiology*, 17(3):325–330.

Ascoli, G. A., Alonso-Nanclares, L., Anderson, S. A., Barrionuevo, G., Benavides-Piccione, R., Burkhalter, A., Buzsaki, G., Cauli, B., Defelipe, J., Fairen, A., Feldmayer, D., Fishell, G., Fregnac, Y., Freund, T. F., Gardner, D., Gardner, E. P., Goldberg, J. H., Helmstaedter, M., Hestrin, S., Karube, F., Kisvarday, Z. F., Lambolez, B., Lewis, D. A., Marin, O., Markram, H., Munoz, A., Packer, A., Petersen, C. C., Rockland, K. S., Rossier, J., Rudy, B., Somogyi, P., Staiger, J. F., Tamas, G., Thomson, A. M., Toledo-Rodriguez, M., Wang, Y., West, D. C., and Yuste, R. (2008). Petilla terminology: nomenclature of features of GABAergic interneurons of the cerebral cortex. *Nature Reviews Neuroscience*, 9(7):557–68.

Babb, T. L., Pretorius, J. K., Kupfer, W. R., and Brown, W. J. (1988). Distribution of glutamate-decarboxylase-immunoreactive neurons and synapses in the rat and monkey hippocampus: light and electron microscopy. *Journal of Comparative Neurology*, 278(1):121–138.

Baier, H. and Bonhoeffer, F. (1992). Axon guidance by gradients of a target-derived component. *Science*, 255(5043):472–475.

Banasr, M., Hery, M., Printemps, R., and Daszuta, A. (2004). Serotonin-induced increases in adult cell proliferation and neurogenesis are mediated through different and common 5-HT receptor subtypes in the dentate gyrus and the subventricular zone. *Neuropsychopharmacology*, 29(3):450–60.

Barbeau, D., Liang, J. J., Robitalille, Y., Quirion, R., and Srivastava, L. K. (1995). Decreased expression of the embryonic form of the neural cell adhesion molecule in schizophrenic brains. *Proceedings of the National Academy of Sciences of the United States of America*, 92(7):2785–9.

Becker, C. G., Artola, A., Gerardy-Schahn, R., Becker, T., Welzl, H., and Schachner, M. (1996). The polysialic acid modification of the neural cell adhesion molecule is involved in spatial learning and hippocampal long-term potentiation. *Journal of neuroscience research*, 45(2):143–52.

Beggs, H. E., Baragona, S. C., Hemperly, J. J., and Maness, P. F. (1997). NCAM140 interacts with the focal adhesion kinase p125(fak) and the SRC-related tyrosine kinase p59(fyn). *The Journal of Biological Chemistry*, 272(13):8310–8319.

Ben Achour, S. and Pascual, O. (2010). Glia: the many ways to modulate synaptic plasticity. *Neurochemistry International*, 57(4):440–445.

Benes, F. M. and Berretta, S. (2001). GABAergic interneurons: implications for understanding schizophrenia and bipolar disorder. *Neuropsychopharmacology*, 25:1–27.

Berendse, H. W., Galis-De Graaf, Y., and Groenewegen, H. J. (1992). Topographical organization and relationship with ventral striatal compartments of prefrontal corticostriatal projections in the rat. *Journal of Comparative Neurology*, 316(3):314–347.

Bernier, P. J., Bedard, A., Vinet, J., Levesque, M., and Parent, A. (2002). Newly generated neurons in the amygdala and adjoining cortex of adult primates. *Proceedings of the National Academy of Sciences of the United States of America*, 99(17):11464–11469.

Bhardwaj, R. D., Curtis, M. A., Spalding, K. L., Buchholz, B. A., Fink, D., Björk-Eriksson, T., Nordborg, C., Gage, F. H., Druid, H., Eriksson, P. S., and Frisén, J. (2006). Neocortical neurogenesis in humans is restricted to development. *Proceedings of the National Academy of Sciences of the United States of America*, 103(33):12564–12568.

Bhat, S. and Silberberg, D. H. (1986). Oligodendrocyte cell adhesion molecules are related to neural cell adhesion molecule (N-CAM). *Journal of Neuroscience*, 6(11):3348–3354.

Blier, P. (2010). Altered function of the serotonin 1A autoreceptor and the antidepressant response. *Neuron*, 65(1):1–2.

Bonfanti, L. (2006). PSA-NCAM in mammalian structural plasticity and neurogenesis. *Progress in neurobiology*, 80(3):129–64.

Bonfanti, L., Olive, S., Poulain, D. A., and Theodosis, D. T. (1992). Mapping of the distribution of polysialylated neural cell adhesion molecule throughout the central nervous system of the adult rat: an immunohistochemical study. *Neuroscience*, 49(2):419–436.

Bork, K., Gagiannis, D., Orthmann, A., Weidemann, W., Kontou, M., Reutter, W., and Horstkorte, R. (2007). Experimental approaches to interfere with the polysialylation of the neural cell adhesion molecule in vitro and in vivo. *Journal of Neurochemistry*, 103 Suppl:65–71.

Brennaman, L. H. and Maness, P. F. (2010). NCAM in neuropsychiatric and neurodegenerative disorders. *Advances in experimental medicine and biology*, 663:299–317.

Bruel-Jungerman, E., Davis, S., and Laroche, S. (2007). Brain plasticity mechanisms and memory: a party of four. *Neuroscientist*, 13(5):492–505.

Brusés, J. L. and Rutishauser, U. (2001). Roles, regulation, and mechanism of polysialic acid function during neural development. *Biochimie*, 83(7):635–43.

Bukalo, O., Fentrop, N., Lee, A. Y. W., Salmen, B., Law, J. W. S., Wotjak, C. T., Schweizer, M., Dityatev, A., and Schachner, M. (2004). Conditional ablation of the neural cell adhesion molecule reduces precision of spatial learning, long-term potentiation, and depression in the CA1 subfield of mouse hippocampus. *Journal of Neuroscience*, 24(7):1565–1577.

Burgess, A. and Aubert, I. (2006). Polysialic acid limits choline acetyltransferase activity induced by brain-derived neurotrophic factor. *Journal of neurochemistry*, 99(3):797–806.

Büttner, B., Kannicht, C., Reutter, W., and Horstkorte, R. (2003). The neural cell adhesion molecule is associated with major components of the cytoskeleton. *Biochemical and Biophysical Research Communications*, 310(3):967–971.

Buzsáki, G., Kaila, K., and Raichle, M. (2007). Inhibition and brain work. *Neuron*, 56(5):771–783.

Cai, Y., Xiong, K., Chu, Y., Luo, D.-W., Luo, X.-G., Yuan, X.-Y., Struble, R. G., Clough, R. W., Spencer, D. D., Williamson, A., Kordower, J. H., Patrylo, P. R., and Yan, X.-X. (2009). Doublecortin expression in adult cat and primate cerebral cortex relates to immature neurons that develop into GABAergic subgroups. *Experimental Neurology*, 216(2):342–356.

Cambon, K., Hansen, S. M., Venero, C., Herrero, A. I., Skibo, G., Berezin, V., Bock, E., and Sandi, C. (2004). A synthetic neural cell adhesion molecule mimetic peptide promotes synaptogenesis, enhances presynaptic function, and facilitates memory consolidation. *Journal of Neuroscience*, 24(17):4197–4204.

Cameron, H. A. and Gould, E. (1994). Adult neurogenesis is regulated by adrenal steroids in the dentate gyrus. *Neuroscience*, 61(2):203–209.

Cameron, H. A., McEwen, B. S., and Gould, E. (1995). Regulation of adult neurogenesis by excitatory input and NMDA receptor activation in the dentate gyrus. *Journal of Neuroscience*, 15(6):4687–4692.

Cameron, H. A. and McKay, R. D. (1999). Restoring production of hippocampal neurons in old age. *Nature Neuroscience*, 2(10):894–897.

Castillo-Gómez, E., Gómez-Climent, M. A., Varea, E., Guirado, R., Blasco-Ibáñez, J. M., Crespo, C., Martínez-Guijarro, F. J., and Nácher, J. (2008). Dopamine acting through D2 receptors modulates the expression of PSA-NCAM, a molecule related to neuronal structural plasticity, in the medial prefrontal cortex of adult rats. *Experimental neurology*, 214(1):97–111.

Castillo-Gómez, E., Varea, E., Blasco-Ibáñez, J. M., Crespo, C., and Nacher, J. (2011). Polysialic Acid Is Required for Dopamine D2 Receptor-Mediated Plasticity Involving Inhibitory Circuits of the Rat Medial Prefrontal Cortex. *PLoS ONE*, 6(12):e29516.

Castrén, E. (2005). Is mood chemistry? *Nature reviews Neuroscience*, 6(3):241–6.

Castrén, E. and Rantamäki, T. (2010). The role of BDNF and its receptors in depression and antidepressant drug action: Reactivation of developmental plasticity. *Developmental neurobiology*, 70(5):289–97.

Chakravarthy, S., Saiepour, M. H., Bence, M., Perry, S., Hartman, R., Couey, J. J., Mansvelder, H. D., and Levelt, C. N. (2006). Postsynaptic TrkB signaling has distinct roles in spine maintenance in adult visual cortex and hippocampus. *Proceedings of the National Academy of Sciences of the United States of America*, 103(4):1071–1076.

Chance, S. A., Walker, M., and Crow, T. J. (2005). Reduced density of calbindin-immunoreactive interneurons in the planum temporale in schizophrenia. *Brain Research*, 1046(1-2):32–37.

Chen, J. L., Flanders, G. H., Lee, W.-C. A., Lin, W. C., and Nedivi, E. (2011a). Inhibitory Dendrite Dynamics as a General Feature of the Adult Cortical Microcircuit. *Journal of Neuroscience*, 31(35):12437–12443.

Chen, J. L., Lin, W. C., Cha, J. W., So, P. T., Kubota, Y., and Nedivi, E. (2011b). Structural basis for the role of inhibition in facilitating adult brain plasticity. *Nature neuroscience*, 14(5):587–94.

Chen, J. L. and Nedivi, E. (2010). Neuronal structural remodeling: is it all about access? *Current opinion in neurobiology*, 20(5):557–62.

Chothia, C. and Jones, E. Y. (1997). The molecular structure of cell adhesion molecules. *Annual Review of Biochemistry*, 66:823–862.

Cline, H. and Haas, K. (2008). The regulation of dendritic arbor development and plasticity by glutamatergic synaptic input: a review of the synaptotrophic hypothesis. *The Journal of Physiology*, 586(Pt 6):1509–1517.

Close, B. E., Tao, K., and Colley, K. J. (2000). Polysialyltransferase-1 autopolysialylation is not requisite for polysialylation of neural cell adhesion molecule. *The Journal of Biological Chemistry*, 275(6):4484–4491.

Colonnier, M. (1964). The tangential organization of the visual cortex. *Journal of Anatomy*, 98(Pt 3):327–344.3.

Cook, S. C. and Wellman, C. L. (2003). Chronic Stress Alters Dendritic Morphology in Rat Medial Prefrontal Cortex. *Journal of Neurobiology*, pages 236–248.

Couillard-Despres, S., Wuertinger, C., Kandasamy, M., Caioni, M., Stadler, K., Aigner, R., Bogdahn, U., and Aigner, L. (2009). Ageing abolishes the effects of fluoxetine on neurogenesis. *Molecular psychiatry*, 14(9):856–64.

Cowen, D. S., Takase, L. F., Fornal, C. A., and Jacobs, B. L. (2008). Age-dependent decline in hippocampal neurogenesis is not altered by chronic treatment with fluoxetine. *Brain research*, 1228:14–9.

Cremer, H., Lange, R., Christoph, A., Plomann, M., Vopper, G., Roes, J., Brown, R., Baldwin, S., Kraemer, P., Scheff, S., and Et Al. (1994). Inactivation of the N-CAM gene in mice results in size reduction of the olfactory bulb and deficits in spatial learning. *Nature*, 367(6462):455–459.

Cummins, R. A., Walsh, R. N., Budtz-Olsen, O. E., Konstantinos, T., and Horsfall, C. R. (1973). Environmentally-induced changes in the brains of elderly rats. *Nature*, 243(5409):516–518.

Czeh, B., Simon, M., Van Der Hart, M. G., Schmelting, B., Hesselink, M. B., and Fuchs, E. (2005). Chronic stress decreases the number of parvalbumin-immunoreactive interneurons in the hippocampus: prevention by treatment with a substance P receptor (NK1) antagonist. *Neuropsychopharmacology*, 30(1):67–79.

Dade, L. A., Zatorre, R. J., and Jones-Gotman, M. (2002). Olfactory learning: convergent findings from lesion and brain imaging studies in humans. *Brain*, 125(Pt 1):86–101.

Dalva, M. B., McClelland, A. C., and Kayser, M. S. (2007). Cell adhesion molecules: signalling functions at the synapse. *Nature Reviews Neuroscience*, 8(3):206–220.

Danzer, S. C., Kotloski, R. J., Walter, C., Hughes, M., and McNamara, J. O. (2008). Altered morphology of hippocampal dentate granule cell presynaptic and postsynaptic terminals following conditional deletion of TrkB. *Hippocampus*, 18(7):668–678.

Davis, A. E., Gimenez, A. M., and Therrien, B. (2001). Effects of entorhinal cortex lesions on sensory integration and spatial learning. *Nursing Research*, 50(2):77–85.

Dayer, A. G., Cleaver, K. M., Abouantoun, T., and Cameron, H. A. (2005). New GABAergic interneurons in the adult neocortex and striatum are generated from different precursors. *The Journal of Cell Biology*, 168(3):415–427.

De Castilhos, J., Forti, C. D., Achaval, M., and Rasia-Filho, A. A. (2008). Dendritic spine density of posterodorsal medial amygdala neurons can be affected by gonadectomy and sex steroid manipulations in adult rats: a Golgi study. *Brain Research*, 1240:73–81.

De Graaf-Peters, V. B. and Hadders-Algra, M. (2006). Ontogeny of the human central nervous system: what is happening when? *Early Human Development*, 82(4):257–266.

De Magalhães, J. a. P. and Sandberg, A. (2005). Cognitive aging as an extension of brain development: a model linking learning, brain plasticity, and neurodegeneration. *Mechanisms Of Ageing And Development*, 126(10):1026–1033.

De Roo, M., Klauser, P., Mendez, P., Poglia, L., and Muller, D. (2008a). Activity-dependent PSD formation and stabilization of newly formed spines in hippocampal slice cultures. *Cerebral cortex*, 18(1):151–61.

De Roo, M., Klauser, P., and Muller, D. (2008b). LTP promotes a selective long-term stabilization and clustering of dendritic spines. *PLoS biology*, 6(9):e219.

DeFelipe, J. and Farinas, I. (1992). The pyramidal neuron of the cerebral cortex: morphological and chemical characteristics of the synaptic inputs. *Progress in Neurobiology*, 39(6):563–607.

Di Cristo, G., Chattopadhyaya, B., Kuhlman, S. J., Fu, Y., Bélanger, M.-C., Wu, C. Z., Rutishauser, U., Maffei, L., and Huang, Z. J. (2007). Activity-dependent PSA expression regulates inhibitory maturation and onset of critical period plasticity. *Nature neuroscience*, 10(12):1569–77.

Diamond, M. C., Johnson, R. E., and Ingham, C. (1971). Brain plasticity induced by environment and pregnancy. *The International journal of neuroscience*, 2(4):171–178.

Diana, G., Valentini, G., Travaglione, S., Falzano, L., Pieri, M., Zona, C., Meschini, S., Fabbri, A., and Fiorentini, C. (2007). Enhancement of learning and memory after activation of cerebral Rho GTPases. *Proceedings of the National Academy of Sciences of the United States of America*, 104(2):636–641.

Dillon, C. and Goda, Y. (2005). The actin cytoskeleton: Integrating form and function at the synapse. *Annual Review of Neuroscience*, 28(1):25–55.

Dityatev, A., Bukalo, O., and Schachner, M. (2008). Modulation of synaptic transmission and plasticity by cell adhesion and repulsion molecules. *Neuron Glia Biology*, 4(3):197–209.

Dityatev, A., Dityateva, G., Sytnyk, V., Delling, M., Toni, N., Nikonenko, I., Muller, D., and Schachner, M. (2004). Polysialylated neural cell adhesion molecule promotes remodeling and formation of hippocampal synapses. *Journal of Neuroscience*, 24(42):9372–9382.

Doherty, P., Rimon, G., Mann, D. A., and Walsh, F. S. (1992). Alternative splicing of the cytoplasmic domain of neural cell adhesion molecule alters its ability to act as a substrate for neurite outgrowth. *Journal of Neurochemistry*, 58(6):2338–2341.

Drake, P. M., Nathan, J. K., Stock, C. M., Chang, P. V., Muench, M. O., Nakata, D., Reader, J. R., Gip, P., Golden, K. P. K., Weinhold, B., Gerardy-Schahn, R., Troy, F. A., and Bertozzi, C. R. (2008). Polysialic acid, a glycan with highly restricted expression, is found on human and murine leukocytes and modulates immune responses. *The Journal of Immunology*, 181(10):6850–6858.

Drake, P. M., Stock, C. M., Nathan, J. K., Gip, P., Golden, K. P. K., Weinhold, B., Gerardy-Schahn, R., and Bertozzi, C. R. (2009). Polysialic acid governs T-cell development by regulating progenitor access to the thymus. *Proceedings of the National Academy of Sciences of the United States of America*, 106(29):11995–12000.

Duman, R. S., Malberg, J., and Nakagawa, S. (2001). Regulation of adult neurogenesis by psychotropic drugs and stress. *The Journal of pharmacology and experimental therapeutics*, 299(2):401–407.

Eaton, B. A., Fetter, R. D., and Davis, G. W. (2002). Dynactin is necessary for synapse stabilization. *Neuron*, 34(5):729–41.

Eckhardt, M., Bukalo, O., Chazal, G., Wang, L., Goridis, C., Schachner, M., Gerardy-Schahn, R., Cremer, H., and Dityatev, A. (2000). Mice deficient in the polysialyltransferase ST8SiaIV/PST-1 allow discrimination of the roles of neural cell adhesion molecule protein and polysialic acid in neural development and synaptic plasticity. *Journal of Neuroscience*, 20(14):5234–5244.

Ehninger, D. and Kempermann, G. (2003). Regional effects of wheel running and environmental enrichment on cell genesis and microglia proliferation in the adult murine neocortex. *Cerebral Cortex*, 13(8):845–851.

Eichenbaum, H. (2000). Hippocampus: mapping or memory? *Current Biology*, 10(21):R785–R787.

Elmariah, S. B., Crumling, M. A., Parsons, T. D., and Balice-Gordon, R. J. (2004). Postsynaptic TrkB-mediated signaling modulates excitatory and inhibitory neurotransmitter receptor clustering at hippocampal synapses. *Journal of Neuroscience*, 24(10):2380–2393.

Enwere, E., Shingo, T., Gregg, C., Fujikawa, H., Ohta, S., and Weiss, S. (2004). Aging results in reduced epidermal growth factor receptor signaling, diminished olfactory neurogenesis, and deficits in fine olfactory discrimination. *Journal of Neuroscience*, 24(38):8354–8365.

Eyre, M. D., Richter-Levin, G., Avital, A., and Stewart, M. G. (2003). Morphological changes in hippocampal dentate gyrus synapses following spatial learning in rats are transient. *European Journal of Neuroscience*, 17(9):1973–1980.

Fan, Y., Zou, B., Ruan, Y., Pang, Z., and Xu, Z. C. (2005). In vivo demonstration of a late depolarizing postsynaptic potential in CA1 pyramidal neurons. *Journal of Neurophysiology*, 93(3):1326–1335.

Fatemi, S. H., Reutiman, T. J., and Folsom, T. D. (2009). Chronic psychotropic drug treatment causes differential expression of Reelin signaling system in frontal cortex of rats. *Schizophrenia Research*, 111(1-3):138–152.

Fava, M. and Kendler, K. S. (2000). Major depressive disorder. *Neuron*, 28(2):335–41.

Foley, A. G., Rø nn, L. C. B., Murphy, K. J., and Regan, C. M. (2003). Distribution of polysialylated neural cell adhesion molecule in rat septal nuclei and septohippocampal pathway: transient increase of polysialylated interneurons in the subtriangular septal zone during memory consolidation. *Journal of Neuroscience Research*, 74(6):807–817.

Fox, K. D. (2009). Experience-dependent plasticity mechanisms for neural rehabilitation in somatosensory cortex. *Philosophical Transactions of the Royal Society of London - Series B: Biological Sciences*, 364(1515):369–381.

Freund, T. (2003). Interneuron Diversity series: Rhythm and mood in perisomatic inhibition. *Trends in Neurosciences*, 26(9):489–495.

Freund, T. F. and Buzsáki, G. (1996). Interneurons of the hippocampus. *Hippocampus*, 6(4):347–470.

Friedlander, D. R., Grumet, M., and Edelman, G. M. (1986). Nerve growth factor enhances expression of neuron-glia cell adhesion molecule in PC12 cells. *The Journal of Cell Biology*, 102(2):413–419.

Fritschy, J.-m. and Harvey, R. J. (2008). Gephyrin: where do we stand, where do we go? *Trends in Neurosciences*, (April):257–264.

Fu, M. and Zuo, Y. (2011). Experience-dependent structural plasticity in the cortex. *Trends in neurosciences*, 34(4):177–87.

Fuster, J. M. (2008). *The prefrontal cortex*, volume 2. Raven Press.

Gabbott, P. L. A., Dickie, B. G. M., Vaid, R. R., Headlam, A. J. N., and Bacon, S. J. (1997). Local-circuit neurones in the medial prefrontal cortex (areas 25, 32 and 24b) in the rat: Morphology and quantitative distribution.

Gage, F. H., Kempermann, G., Palmer, T. D., Peterson, D. A., and Ray, J. (1998). Multipotent progenitor cells in the adult dentate gyrus. *Journal of Neurobiology*, 36(2):249–266.

Galuska, S. P., Geyer, R., Gerardy-Schahn, R., Mühlenhoff, M., and Geyer, H. (2008). Enzyme-dependent variations in the polysialylation of the neural cell adhesion molecule (NCAM) in vivo. *The Journal of Biological Chemistry*, 283(1):17–28.

Galuska, S. P., Oltmann-Norden, I., Geyer, H., Weinhold, B., Kuchelmeister, K., Hildebrandt, H., Gerardy-Schahn, R., Geyer, R., and Mühlenhoff, M. (2006). Polysialic acid profiles of mice expressing variant allelic combinations of the polysialyltransferases ST8SiaII and ST8SiaIV. *The Journal of Biological Chemistry*, 281(42):31605–31615.

Galuska, S. P., Rollenhagen, M., Kaup, M., Eggers, K., Oltmann-Norden, I., Schiff, M., Hartmann, M., Weinhold, B., Hildebrandt, H., Geyer, R., Mühlenhoff, M., and Geyer, H. (2010). Synaptic cell adhesion molecule SynCAM 1 is a target for polysialylation in postnatal mouse brain. *Proceedings of the National Academy of Sciences of the United States of America*, 107(22):10250–10255.

Gascon, E., Vutskits, L., and Kiss, J. Z. (2007). Polysialic acid-neural cell adhesion molecule in brain plasticity: From synapses to integration of new neurons. *Brain Research Reviews*, 56:101–118.

Ge, S., Pradhan, D. A., Ming, G.-L., and Song, H. (2007). GABA sets the tempo for activity-dependent adult neurogenesis. *Trends in Neurosciences*, 30(1):1–8.

Gegelashvili, G., Andersson, A. M., Schousboe, A., and Bock, E. (1990). Characterization of NCAM diversity in cultured neurons. *FEBS Letters*, 277(3):337–340.

Gelman, D. M. and Marín, O. (2010). Generation of interneuron diversity in the mouse cerebral cortex. *European Journal of Neuroscience*, 31(12):2136–2141.

Gilabert-Juan, J., Castillo-Gomez, E., Pérez-Rando, M., Moltó, M. D., and Nacher, J. (2011). Chronic stress induces changes in the structure of interneurons and in the expression of molecules related to neuronal structural plasticity and inhibitory neurotransmission in the amygdala of adult mice. *Experimental neurology*, 232(1):33–40.

Glass, J. D., Watanabe, M., Fedorkova, L., Shen, H., Ungers, G., and Rutishauser, U. (2003). Dynamic regulation of polysialylated neural cell adhesion molecule in the suprachiasmatic nucleus. *Neuroscience*, 117(1):203–211.

Gómez-Climent, M. A., Castillo-Gómez, E., Varea, E., Guirado, R., Blasco-Ibáñez, J. M., Crespo, C., Martínez-Guijarro, F. J., and Nácher, J. (2008). A population of prenatally generated cells in the rat paleocortex maintains an immature neuronal phenotype into adulthood. *Cerebral cortex*, 18(10):2229–40.

Gould, E. (2007). How widespread is adult neurogenesis in mammals? *Nature Reviews Neuroscience*, 8(6):481–488.

Gould, E., Beylin, A., Tanapat, P., Reeves, A., and Shors, T. J. (1999a). Learning enhances adult neurogenesis in the hippocampal formation. *Nature Neuroscience*, 2(3):260–265.

Gould, E., Reeves, A. J., Graziano, M. S., and Gross, C. G. (1999b). Neurogenesis in the Neocortex of Adult Primates. *Science*, 286(5439):548–552.

Gould, E., Vail, N., Wagers, M., and Gross, C. G. (2001). Adult-generated hippocampal and neocortical neurons in macaques have a transient existence. *Proceedings of the National Academy of Sciences of the United States of America*, 98(19):10910–10917.

Greenough, W. T. (1976). Enduring brain effects of differential experience and training. *Neural mechanisms of learning and memory*, pages 255–278.

Groenewegen, H. J., Wright, C. I., and Uylings, H. B. M. (1997). The anatomical relationships of the prefrontal cortex with limbic structures and the basal ganglia. *Journal of Psychopharmacology*, 11(2):99–106.

Gulyás, A. I., Hájos, N., Katona, I., and Freund, T. F. (2003). Interneurons are the local targets of hippocampal inhibitory cells which project to the medial septum. *The European journal of neuroscience*, 17(9):1861–72.

Gutierrez, H. and Davies, A. M. (2007). A fast and accurate procedure for deriving the Sholl profile in quantitative studies of neuronal morphology. *Journal of Neuroscience Methods*, 163:24–30.

Gutiérrez-Castellanos, N., Martínez-Marcos, A., Martínez-García, F., and Lanuza, E. (2010). Chemosensory function of the amygdala. *Vitamins And Hormones*, 83(10):165–196.

Haberly, L. B. (1983). Structure of the piriform cortex of the opossum. I. Description of neuron types with Golgi methods. *Journal of Comparative Neurology*, 213(2):163–187.

Haberly, L. B. and Price, J. L. (1978). Association and commissural fiber systems of the olfactory cortex of the rat. *Journal of Comparative Neurology*, 178(4):711–740.

Hajszan, T., MacLusky, N. J., and Leranth, C. (2005). Short-term treatment with the antidepressant fluoxetine triggers pyramidal dendritic spine synapse formation in rat hippocampus. *The European journal of neuroscience*, 21(5):1299–303.

Halpern, M. and Martínez-Marcos, A. (2003). Structure and function of the vomeronasal system: an update. *Progress in Neurobiology*, 70(3):245–318.

Hansson, A. C., Nixon, K., Rimondini, R., Damadzic, R., Sommer, W. H., Eskay, R., Crews, F. T., and Heilig, M. (2010). Long-term suppression of forebrain neurogenesis and loss of neuronal progenitor cells following prolonged alcohol dependence in rats. *The international journal of neuropsychopharmacology*, 13(5):583–93.

Hao, J., Rapp, P. R., Leffler, A. E., Leffler, S. R., Janssen, W. G., Lou, W., McKay, H., Roberts, J. A., Wearne, S. L., Hof, P. R., and Morrison, J. H. (2006). Estrogen alters spine number and morphology in prefrontal cortex of aged female rhesus monkeys. *Journal of Neuroscience*, 26(9):2571–8.

Henn, F. A. and Vollmayr, B. (2004). Neurogenesis and depression: etiology or epiphenomenon? *Biological psychiatry*, 56(3):146–50.

Hensch, T. K. (2004). Critical period regulation. *Annual Review of Neuroscience*, 27(1):549–579.

Hensler, J. G. (2002). Differential regulation of 5-HT1A receptor-G protein interactions in brain following chronic antidepressant administration. *Neuropsychopharmacology*, 26(5):565–73.

Hewlett, W. A., Trivedi, B. L., Zhang, Z.-J., de Paulis, T., Schmidt, D. E., Lovinger, D. M., Ansari, M. S., and Ebert, M. H. (1999). Characterization of (S)-Des-4-amino-3-[125I]iodozacopride ([125I]DAIZAC), a Selective High-Affinity Radioligand for 5-Hydroxytryptamine3 Receptors. *The Journal of pharmacology and experimental therapeutics*, 288(1):221–231.

Hildebrandt, H., Becker, C., Mürau, M., Gerardy-Schahn, R., and Rahmann, H. (1998). Heterogeneous expression of the polysialyltransferases ST8Sia II and ST8Sia IV during postnatal rat brain development. *Journal of neurochemistry*, 71(6):2339–48.

Hildebrandt, H., Mühlenhoff, M., and Gerardy-Schahn, R. (2010). Polysialylation of NCAM. *Advances in experimental medicine and biology*, 663:95–109.

Hildebrandt, H., Mühlenhoff, M., Oltmann-Norden, I., Röckle, I., Burkhardt, H., Weinhold, B., and Gerardy-Schahn, R. (2009). Imbalance of neural cell adhesion molecule and polysialyltransferase alleles causes defective brain connectivity. *Brain*, 132(Pt 10):2831–8.

Hildebrandt, H., Mühlenhoff, M., Weinhold, B., and Gerardy-Schahn, R. (2007). Dissecting polysialic acid and NCAM functions in brain development. *Journal of Neurochemistry*, 103 Suppl:56–64.

Hoffman, K. B., Larson, J., Bahr, B. A., and Lynch, G. (1998). Activation of NMDA receptors stimulates extracellular proteolysis of cell adhesion molecules in hippocampus. *Brain Research*, 811(1-2):152–5.

Hoffman, S., Sorkin, B. C., White, P. C., Brackenbury, R., Mailhammer, R., Rutishauser, U., Cunningham, B. A., and Edelman, G. M. (1982). Chemical characterization of a neural cell adhesion molecule purified from embryonic brain membranes. *The Journal of biological chemistry*, 257(13):7720–9.

Holick, K. A., Lee, D. C., Hen, R., and Dulawa, S. C. (2008). Behavioral effects of chronic fluoxetine in BALB/cJ mice do not require adult hippocampal neurogenesis or the serotonin 1A receptor. *Neuropsychopharmacology*, 33(2):406–17.

Homberg, J. R., Olivier, J. D. A., Blom, T., Arentsen, T., van Brunschot, C., Schipper, P., Korte-Bouws, G., van Luijtelaar, G., and Reneman, L. (2011). Fluoxetine exerts age-dependent effects on behavior and amygdala neuroplasticity in the rat. *PloS one*, 6(1):e16646.

Horch, H. W. and Katz, L. C. (2002). BDNF release from single cells elicits local dendritic growth in nearby neurons. *Nature neuroscience*, 5(11):1177–84.

Huang, G.-J., Bannerman, D., and Flint, J. (2008). Chronic fluoxetine treatment alters behavior, but not adult hippocampal neurogenesis, in BALB/cJ mice. *Molecular psychiatry*, 13(2):119–21.

Huang, G.-J. and Herbert, J. (2006). Stimulation of neurogenesis in the hippocampus of the adult rat by fluoxetine requires rhythmic change in corticosterone. *Biological psychiatry*, 59(7):619–24.

Huang, L., DeVries, G. J., and Bittman, E. L. (1998). Photoperiod regulates neuronal bromodeoxyuridine labeling in the brain of a seasonally breeding mammal. *Journal of Neurobiology*, 36(3):410–420.

Hume, R. I. and Purves, D. (1981). Geometry of neonatal neurones and the regulation of synapse elimination. *Nature*, 293(5832):469–471.

Isgor, C., Kabbaj, M., Akil, H., and Watson, S. J. (2004). Delayed effects of chronic variable stress during peripubertal-juvenile period on hippocampal morphology and on cognitive and stress axis functions in rats. *Hippocampus*, 14(5):636–648.

Jin, K., Sun, Y., Xie, L., Batteur, S., Mao, X. O., Smelick, C., Logvinova, A., and Greenberg, D. A. (2003). Neurogenesis and aging: FGF-2 and HB-EGF restore neurogenesis in hippocampus and subventricular zone of aged mice. *Aging Cell*, 2(3):175–183.

Johnson, C. P., Fujimoto, I., Rutishauser, U., and Leckband, D. E. (2005). Direct evidence that neural cell adhesion molecule (NCAM) polysialylation increases intermembrane repulsion and abrogates adhesion. *The Journal of Biological Chemistry*, 280(1):137–145.

Jones, E. G., Coulter, J. D., Burton, H., and Porter, R. (1977). Cells of origin and terminal distribution of corticostriatal fibers arising in the sensory-motor cortex of monkeys. *Journal of Comparative Neurology*, 173(1):53–80.

Kalus, P., Bondzio, J., Federspiel, A., Müller, T. J., and Zuschratter, W. (2002). Cell-type specific alterations of cortical interneurons in schizophrenic patients. *Neuroreport*, 13(5):713–7.

Kandel, E. R., Schwartz, J. H., and Jessell, T. M. (2000). *Principles of Neural Science*, volume 3. McGraw-Hill.

Kaplan, M. S. (1981). Neurogenesis in the 3-month-old rat visual cortex. *Journal of Comparative Neurology*, 195(2):323–338.

Katidou, M., Vidaki, M., Strigini, M., and Karagogeos, D. (2008). The immunoglobulin superfamily of neuronal cell adhesion molecules: lessons from animal models and correlation with human disease. *Biotechnology Journal*, 3(12):1564–1580.

Kawaguchi, Y., Karube, F., and Kubota, Y. (2006). Dendritic branch typing and spine expression patterns in cortical nonpyramidal cells. *Cerebral cortex*, 16(5):696–711.

Kawaguchi, Y. and Kubota, Y. (1997). GABAergic cell subtypes and their synaptic connections in rat frontal cortex. *Cerebral Cortex*, 7(6):476–486.

Keck, T., Mrsic-Flogel, T., Afonso, M., Eysel, U., Bonhoeffer, T., and Hubener, M. (2008). Massive restructuring of neuronal circuits during functional reorganization of adult visual cortex. *Nature Neuroscience*, 11(10):1162–7.

Keck, T., Scheuss, V., Jacobsen, R., Wierenga, C., Eysel, U., Bonhoeffer, T., and Hübener, M. (2011). Loss of Sensory Input Causes Rapid Structural Changes of Inhibitory Neurons in Adult Mouse Visual Cortex. *Neuron*, 71(5):869–882.

Keller, A. (2002). Use-dependent inhibition of dendritic spines. *Trends in Neurosciences*, 25(11):2260–2262.

Kempermann, G. (2002). Regulation of adult hippocampal neurogenesis - implications for novel theories of major depression. *Bipolar Disorders*, 4(1):17–33.

Kempermann, G., Kuhn, H. G., and Gage, F. H. (1997). More hippocampal neurons in adult mice living in an enriched environment. *Nature*, 386(6624):493–495.

Kiss, J. Z. and Rougon, G. (1997). Cell biology of polysialic acid.

Knott, G. and Holtmaat, A. (2008). Dendritic spine plasticity–current understanding from in vivo studies. *Brain research reviews*, 58(2):282–9.

Knott, G. W., Quairiaux, C., Genoud, C., and Welker, E. (2002). Formation of dendritic spines with GABAergic synapses induced by whisker stimulation in adult mice. *Neuron*, 34(2):265–73.

Kodama, M., Fujioka, T., and Duman, R. S. (2004). Chronic olanzapine or fluoxetine administration increases cell proliferation in hippocampus and prefrontal cortex of adult rat. *Biological Psychiatry*, 56(8):570–580.

Kojima, N., Kono, M., Yoshida, Y., Tachida, Y., Nakafuku, M., and Tsuji, S. (1996). Biosynthesis and expression of polysialic acid on the neural cell adhesion molecule is predominantly directed by ST8Sia II/STX during in vitro neuronal differentiation. *The Journal of Biological Chemistry*, 271(36):22058–62.

Kolkova, K., Novitskaya, V., Pedersen, N., Berezin, V., and Bock, E. (2000). Neural cell adhesion molecule-stimulated neurite outgrowth depends on activation of protein kinase C and the Ras-mitogen-activated protein kinase pathway. *Journal of Neuroscience*, 20(6):2238–2246.

Kornack, D. R. and Rakic, P. (2001). Cell proliferation without neurogenesis in adult primate neocortex. *Science*, 294(5549):2127–2130.

Kramer, I., Hall, H., Bleistein, U., and Schachner, M. (1997). Developmentally regulated masking of an intracellular epitope of the 180 kDa isoform of the neural cell adhesion molecule NCAM. *Journal of Neuroscience Research*, 49(2):161–175.

Kuhn, H. G., Dickinson-Anson, H., and Gage, F. H. (1996). Neurogenesis in the dentate gyrus of the adult rat: age-related decrease of neuronal progenitor proliferation. *Journal of Neuroscience*, 16(6):2027–2033.

LaBar, K. S. and LeDoux, J. E. (1996). Partial disruption of fear conditioning in rats with unilateral amygdala damage: correspondence with unilateral temporal lobectomy in humans. *Behavioral Neuroscience*, 110(5):991–997.

Lambe, E. K., Krimer, L. S., and Goldman-Rakic, P. S. (2000). Differential postnatal development of catecholamine and serotonin inputs to identified neurons in prefrontal cortex of rhesus monkey. *Journal of Neuroscience*, 20(23):8780–8787.

LeDoux, J. E. (2000). Emotion circuits in the brain. *Annual Review of Neuroscience*, 23(1):155–184.

Lee, W.-C. A., Chen, J. L., Huang, H., Leslie, J. H., Amitai, Y., So, P. T., and Nedivi, E. (2008). A dynamic zone defines interneuron remodeling in the adult neocortex. *Proceedings of the National Academy of Sciences of the United States of America*, 105(50):19968–73.

Lee, W.-c. A., Huang, H., Feng, G., Sanes, J. R., Brown, E. N., So, P. T., and Nedivi, E. (2006). Dynamic Remodeling of Dendritic Arbors in GABAergic Interneurons of Adult Visual Cortex. *Imaging*, 4(2).

Leuner, B., Falduto, J., and Shors, T. J. (2003). Associative memory formation increases the observation of dendritic spines in the hippocampus. *Journal of Neuroscience*, 23(2):659–665.

Lévesque, M. and Parent, A. (1998). Axonal arborization of corticostriatal and corticothalamic fibers arising from prelimbic cortex in the rat. *Cerebral Cortex*, 8(7):602–613.

Levi-Montalcini, R. and Cohen, S. (1956). In vitro and in vivo effects of a nerve growth-stimulating agent isolated from snake venom. *Proceedings of the National Academy of Sciences of the United States of America*, 42(9):695–699.

Li, Q., Wichems, C. H., Ma, L., Van de Kar, L. D., Garcia, F., and Murphy, D. L. (2003). Brain region-specific alterations of 5-HT 2A and 5-HT 2C receptors in serotonin transporter knockout mice. *Journal of Neurochemistry*, 84(6):1256–1265.

Li, Y.-F., Zhang, Y.-Z., Liu, Y.-Q., Wang, H.-L., Cao, J.-B., Guan, T.-T., and Luo, Z.-P. (2006). Inhibition of N-methyl-D-aspartate receptor function appears to be one of the common actions for antidepressants. *Journal of psychopharmacology*, 20(5):629–35.

Lino-de oliveira, C., Sales, A. J., Aparecida, E., Bel, D., Cristina, M., Silveira, L., and Guimara, F. S. (2001). Effects of acute and chronic fluoxetine treatments on restraint stress-induced Fos expression. *Brain Research*, 55(6):747–754.

Livingston, B. D., Jacobs, J. L., Glick, M. C., and Troy, F. A. (1988). Extended polysialic acid chains (n greater than 55) in glycoproteins from human neuroblastoma cells. *The Journal of Biological Chemistry*, 263(19):9443–9448.

Lolova, I. and Davidoff, M. (1991). Changes in GABA-immunoreactivity and GABA-transaminase activity in rat amygdaloid complex in aging. *Journal für Hirnforschung*, 32(2):231–8.

Löscher, W. and Ebert, U. (1996). The role of the piriform cortex in kindling. *Progress in Neurobiology*, 50(5-6):427–481.

Magariños, A. M., Deslandes, A., and McEwen, B. S. (1999). Effects of antidepressants and benzodiazepine treatments on the dendritic structure of CA3 pyramidal neurons after chronic stress. *European journal of pharmacology*, 371(2-3):113–22.

Magariños, A. M. and McEwen, B. S. (1995). Stress-induced atrophy of apical dendrites of hippocampal CA3c neurons: involvement of glucocorticoid secretion and excitatory amino acid receptors. *Neuroscience*, 69(1):89–98.

Mair, W. G., Warrington, E. K., and Weiskrantz, L. (1979). Memory disorder in Korsakoff's psychosis: a neuropathological and neuropsychological investigation of two cases. *Brain*, 102(4):749–783.

Maness, P. F., Beggs, H. E., Klinz, S. G., and Morse, W. R. (1996). Selective neural cell adhesion molecule signaling by Src family tyrosine kinases and tyrosine phosphatases. *Perspectives on Developmental Neurobiology*, 4(2-3):169–181.

Maness, P. F. and Schachner, M. (2007). Neural recognition molecules of the immunoglobulin superfamily: signaling transducers of axon guidance and neuronal migration. *Nature Neuroscience*, 10(1):19–26.

Marcusson, J., Morgan, D., Winblad, B., and Finch, C. (1984). Serotonin-2 binding sites in human frontal cortex and hippocampus. Selective loss of S-2A sites with age. *Brain Research*, 311(1):51–56.

Markham, J. A. and Greenough, W. T. (2004). Experience-driven brain plasticity: beyond the synapse. *Neuron Glia Biology*, 1(4):351–363.

Markham, J. A. and Juraska, J. M. (2002). Aging and sex influence the anatomy of the rat anterior cingulate cortex. *Neurobiology of Aging*, 23(4):579–588.

Markham, J. A., McKian, K. P., Stroup, T. S., and Juraska, J. M. (2005). Sexually dimorphic aging of dendritic morphology in CA1 of hippocampus. *Hippocampus*, 15(1):97–103.

Markham, J. A., Pych, J. C., and Juraska, J. M. (2002). Ovarian hormone replacement to aged ovariectomized female rats benefits acquisition of the morris water maze. *Hormones and Behavior*, 42(3):284–293.

Markram, H., Toledo-rodriguez, M., Wang, Y., Gupta, A., Silberberg, G., and Wu, C. (2004). Interneurons of the neocortical inhibitory system. *Nature Reviews Neuroscience*, 5:793–807.

Markwardt, S. and Overstreet-Wadiche, L. (2008). GABAergic signalling to adult-generated neurons. *The Journal of physiology*, 586(16):3745–9.

Marlatt, M. W., Lucassen, P. J., and van Praag, H. (2010). Comparison of neurogenic effects of fluoxetine, duloxetine and running in mice. *Brain research*, 1341:93–9.

Marlatt, M. W., Philippens, I., Manders, E., Czéh, B., Joels, M., Krugers, H., and Lucassen, P. J. (2011). Distinct structural plasticity in the hippocampus and amygdala of the middle-aged common marmoset (Callithrix jacchus). *Experimental neurology*, 230(2):291–301.

Mattson, M. P. (2008). Glutamate and neurotrophic factors in neuronal plasticity and disease. *Annals of The New York Academy of Sciences*, 1144(1):97–112.

Mattson, M. P., Maudsley, S., and Martin, B. (2004). BDNF and 5-HT: a dynamic duo in age-related neuronal plasticity and neurodegenerative disorders. *Trends in neurosciences*, 27(10):589–94.

Maya Vetencourt, J. F., Sale, A., Viegi, A., Baroncelli, L., De Pasquale, R., O'Leary, O. F., Castrén, E., and Maffei, L. (2008). The antidepressant fluoxetine restores plasticity in the adult visual cortex. *Science*, 320(5874):385–8.

McDonald, A. J. and Mascagni, F. (2007). Neuronal localization of 5-HT type 2A receptor immunoreactivity in the rat basolateral amygdala. *Neuroscience*, 146(1):306–20.

McEwen, B. S. (1999). Stress and hippocampal plasticity. *Annual Review of Neuroscience*, 22(1):105–122.

McEwen, B. S. (2000a). Effects of adverse experiences for brain structure and function. *Biological psychiatry*, 48(8):721–31.

McEwen, B. S. (2000b). The neurobiology of stress: from serendipity to clinical relevance. *Brain research*, 886(1-2):172–189.

McEwen, B. S. (2005). Glucocorticoids , depression , and mood disorders : structural remodeling in the brain. *Molecular Brain Research*, 54(Suppl 1):20–23.

McEwen, B. S. (2008). Central effects of stress hormones in health and disease: Understanding the protective and damaging effects of stress and stress mediators. *European Journal of Pharmacology*, 583(2-3):171–179.

McEwen, B. S. (2010). Stress, sex, and neural adaptation to a changing environment: mechanisms of neuronal remodeling. *Annals of the New York Academy of Sciences*, 1204 Suppl:E38–59.

McEwen, B. S. and Gianaros, P. J. (2011). Stress- and allostasis-induced brain plasticity. *Annual Review of Medicine*, 62(August 2010):431–445.

Mcewen, B. S., Magarinos, A. M., and Reagan, L. P. (2002). Structural plasticity and tianeptine: cellular and molecular targets. *Psychiatry: Interpersonal and Biological Processes*, (October):5–9.

McNamara, R. K., Able, J. A., Rider, T., Tso, P., and Jandacek, R. (2010). Effect of chronic fluoxetine treatment on male and female rat erythrocyte and prefrontal cortex fatty acid composition. *Progress in neuro-psychopharmacology & biological psychiatry*, 34(7):1317–21.

Mendez, P., De Roo, M., Poglia, L., Klauser, P., and Muller, D. (2010a). N-cadherin mediates plasticity-induced long-term spine stabilization. *The Journal of cell biology*, 189(3):589–600.

Mendez, P., Garcia-Segura, L. M., and Muller, D. (2010b). Estradiol promotes spine growth and synapse formation without affecting pre-established networks. *Hippocampus*, 21(12):1263–7.

Meyer, G. and Feldman, E. L. (2002). Signaling mechanisms that regulate actin-based motility processes in the nervous system. *Journal of Neurochemistry*, 83(3):490–503.

Ming, G.-l. and Song, H. (2005). Adult neurogenesis in the mammalian central nervous system. *Annual Review of Neuroscience*, 28(1):223–250.

Minturn, J. E., Geschwind, D. H., Fryer, H. J., and Hockfield, S. (1995). Early postmitotic neurons transiently express TOAD-64, a neural specific protein. *Journal of Comparative Neurology*, 355(3):369–379.

Mitra, R., Jadhav, S., McEwen, B. S., Vyas, A., and Chattarji, S. (2005). Stress duration modulates the spatiotemporal patterns of spine formation in the basolateral amygdala. *Proceedings of the National Academy of Sciences of the United States of America*, 102(26):9371–6.

Miyahara, R., Tanaka, F., Nakagawa, T., Matsuoka, K., Isii, K., and Wada, H. (2001). Expression of neural cell adhesion molecules (polysialylated form of neural cell adhesion molecule and L1-cell adhesion molecule) on resected small cell lung cancer specimens: in relation to proliferation state. *Journal of Surgical Oncology*, 77(1):49–54.

Morales, M., Battenberg, E., and Bloom, F. E. (1998). Distribution of neurons expressing immunoreactivity for the 5HT3 receptor subtype in the rat brain and spinal cord. *The Journal of comparative neurology*, 402(3):385–401.

Morinobu, S., Strausbaugh, H., Terwilliger, R., and Duman, R. S. (1997). Regulation of c-Fos and NGF1-A by antidepressant treatments. *Synapse*, 25(4):313–20.

Morris, R. (1984). Developments of a water-maze procedure for studying spatial learning in the rat. *Journal of Neuroscience Methods*, 11(1):47–60.

Moult, P. R. and Harvey, J. (2008). Hormonal regulation of hippocampal dendritic morphology and synaptic plasticity. *Cell adhesion migration*, 2(4):269–275.

Mountcastle, V. B., Talbot, W. H., Darian-Smith, I., and Kornhuber, H. H. (1967). Neural basis of the sense of flutter-vibration. *Science*, 155(762):597–600.

Mukherjee, J., Kretschmannova, K., Gouzer, G., Maric, H. M., Ramsden, S., Tretter, V., Harvey, K., Davies, P. A., Triller, A., Schindelin, H., and Moss, S. J. (2011). The Residence Time of GABAARs at Inhibitory Synapses Is Determined by Direct Binding of the Receptor Â 1 Subunit to Gephyrin. *Journal of Neuroscience*, 31(41):14677–14687.

Muller, D., Djebbara-Hannas, Z., Jourdain, P., Vutskits, L., Durbec, P., Rougon, G., and Kiss, J. Z. (2000a). Brain-derived neurotrophic factor restores long-term potentiation in polysialic acid-neural cell adhesion molecule-deficient hippocampus. *Proceedings of the National Academy of Sciences of the United States of America*, 97(8):4315–4320.

Muller, D., Mendez, P., Deroo, M., Klauser, P., Steen, S., and Poglia, L. (2010). Role of NCAM in spine dynamics and synaptogenesis. *Advances in experimental medicine and biology*, 663:245–56.

Muller, D., Toni, N., and Buchs, P. A. (2000b). Spine changes associated with long-term potentiation. *Hippocampus*, 10(5):596–604.

Muller, D., Wang, C., Skibo, G., Toni, N., Cremer, H., Calaora, V., Rougon, G., and Kiss, J. Z. (1996). PSA-NCAM is required for activity-induced synaptic plasticity. *Neuron*, 17(3):413–422.

Murase, S. and Schuman, E. M. (1999). The role of cell adhesion molecules in synaptic plasticity and memory.

Murmu, M. S., Salomon, S., Biala, Y., Weinstock, M., Braun, K., and Bock, J. (2006). Changes of spine density and dendritic complexity in the prefrontal cortex in offspring of mothers exposed to stress during pregnancy. *European Journal of Neuroscience*, 24(5):1477–87.

Murphy, K. J., Fox, G. B., Foley, A. G., Gallagher, H. C., O'Connell, A., Griffin, A. M., Nau, H., and Regan, C. M. (2001). Pentyl-4-yn-valproic acid enhances both spatial and avoidance learning, and attenuates age-related NCAM-mediated neuroplastic decline within the rat medial temporal lobe. *Journal of Neurochemistry*, 78(4):704–714.

Nacher, J., Alonso-Llosa, G., Rosell, D., and McEwen, B. (2002a). PSA-NCAM expression in the piriform cortex of the adult rat. Modulation by NMDA receptor antagonist administration. *Brain Research*, 927(2):111–121.

Nacher, J., Alonso-Llosa, G., Rosell, D. R., and McEwen, B. S. (2003). NMDA receptor antagonist treatment increases the production of new neurons in the aged rat hippocampus. *Neurobiology of Aging*, 24(2):273–284.

Nacher, J., Blasco-Ibáñez, J. M., and McEwen, B. S. (2002b). Non-granule PSA-NCAM immunoreactive neurons in the rat hippocampus. *Brain research*, 930(1-2):1–11.

Nacher, J., Crespo, C., and McEwen, B. S. (2001). Doublecortin expression in the adult rat telencephalon.

Nacher, J., Lanuza, E., and McEwen, B. S. (2002c). Distribution of PSA-NCAM expression in the amygdala of the adult rat. *Neuroscience*, 113(3):479–84.

Nacher, J. and McEwen, B. S. (2006). The role of N-methyl-D-asparate receptors in neurogenesis. *Hippocampus*, 16(3):267–70.

Nacher, J., Rosell, D. R., and McEwen, B. S. (2000). Widespread expression of rat collapsin response-mediated protein 4 in the telencephalon and other areas of the adult rat central nervous system. *The Journal of comparative neurology*, 424(4):628–39.

Nakanishi, H. (1998). Hyperexcitability of amygdala neurons of Senescence-Accelerated Mouse revealed by electrical and optical recordings in an in vitro slice preparation. *Brain Research*, 812(1-2):142–149.

Nakayama, J. and Fukuda, M. (1996). A human polysialyltransferase directs in vitro synthesis of polysialic acid. *The Journal of Biological Chemistry*, 271(4):1829–1832.

Nasrallah, H. A., Hopkins, T., and Pixley, S. K. (2010). Differential effects of antipsychotic and antidepressant drugs on neurogenic regions in rats. *Brain research*, 1354:23–9.

Navailles, S., Hof, P. R., and Schmauss, C. (2008). Antidepressant drug-induced stimulation of mouse hippocampal neurogenesis is age-dependent and altered by early life stress. *The Journal of comparative neurology*, 509(4):372–81.

Nemeroff, C. B. (2007). The burden of severe depression: a review of diagnostic challenges and treatment alternatives. *Journal of Psychiatric Research*, 41(3-4):189–206.

Nestler, E. J. (1998). Antidepressant treatments in the 21st century. *Biological Psychiatry*, 44(7):526–533.

Nestler, E. J., Barrot, M., DiLeone, R. J., Eisch, A. J., Gold, S. J., and Monteggia, L. M. (2002). Neurobiology of depression. *The New England Journal of Medicine*, 49(1):13–25.

Nimchinsky, E. A., Sabatini, B. L., and Svoboda, K. (2002). Structure and function of dendritic spines. *Annual review of physiology*, 64:313–53.

O'Connell, A. W., Fox, G. B., Barry, T., Murphy, K. J., Fichera, G., Foley, A. G., Kelly, J., and Regan, C. M. (1997). Spatial learning activates neural cell adhesion molecule polysialylation in a corticohippocampal pathway within the medial temporal lobe. *Journal of Neurochemistry*, 68(6):2538–2546.

Ohira, K. and Miyakawa, T. (2011). Chronic treatment with fluoxetine for more than 6 weeks decreases neurogenesis in the subventricular zone of adult mice. *Molecular brain*, 4(1):10.

Oliva, A. A., Jiang, M., Lam, T., Smith, K. L., and Swann, J. W. (2000). Novel hippocampal interneuronal subtypes identified using transgenic mice that express green fluorescent protein in GABAergic interneurons. *Journal of neuroscience*, 20(9):3354–68.

Olsen, M., Krog, L., Edvardsen, K., Skovgaard, L. T., and Bock, E. (1993). Intact transmembrane isoforms of the neural cell adhesion molecule are released from the plasma membrane. *The Biochemical journal*, 295 (Pt 3(Pt 3):833–840.

Oltmann-Norden, I., Galuska, S. P., Hildebrandt, H., Geyer, R., Gerardy-Schahn, R., Geyer, H., and Mühlenhoff, M. (2008). Impact of the polysialyltransferases ST8SiaII and ST8SiaIV on polysialic acid synthesis during postnatal mouse brain development. *The Journal of biological chemistry*, 283(3):1463–71.

O'Malley, A., O'Connell, C., Murphy, K. J., and Regan, C. M. (2000). Transient spine density increases in the mid-molecular layer of hippocampal dentate gyrus accompany consolidation of a spatial learning task in the rodent. *Neuroscience*, 99(2):229–232.

O'Malley, A., O'Connell, C., and Regan, C. M. (1998). Ultrastructural analysis reveals avoidance conditioning to induce a transient increase in hippocampal dentate spine density in the 6 hour post-training period of consolidation. *Neuroscience*, 87(3):607–613.

Ong, E., Nakayama, J., Angata, K., Reyes, L., Katsuyama, T., Arai, Y., and Fukuda, M. (1998). Developmental regulation of polysialic acid synthesis in mouse directed by two polysialyltransferases, PST and STX. *Glycobiology*, 8(4):415–424.

Panzanelli, P., Gunn, B. G., Schlatter, M. C., Benke, D., Tyagarajan, S. K., Scheiffele, P., Belelli, D., Lambert, J. J., Rudolph, U., and Fritschy, J.-M. (2011). Distinct mechanisms regulate GABAA receptor and gephyrin clustering at perisomatic and axo-axonic synapses on CA1 pyramidal cells. *The Journal of Physiology*, 20(20):4959–4980.

Paxinos, G. and Franklin, K. B. J. (2001). *The mouse brain in stereotaxic coordinates*, volume 28. Academic Press.

Paxinos, G. and Watson, C. (2007). *The rat brain in stereotaxic coordinates*, volume Second. Academic Press.

Pekcec, A., Löscher, W., and Potschka, H. (2006). Neurogenesis in the adult rat piriform cortex. *NeuroReport*, 17(6):571–574.

Penfield, W. and Rasmussen, T. (1950). *The Cerebral Cortex of Man*, volume 40. Macmillan.

Perera, T. D., Park, S., and Nemirovskaya, Y. (2008). Cognitive role of neurogenesis in depression and antidepressant treatment. *Neuroscientist*, 14(4):326–338.

Perez-Cruz, C., Simon, M., Czéh, B., Flügge, G., and Fuchs, E. (2009). Hemispheric differences in basilar dendrites and spines of pyramidal neurons in the rat prelimbic cortex: activity- and stress-induced changes. *European Journal of Neuroscience*, 29(4):738–747.

Persohn, E., Pollerberg, G. E., and Schachner, M. (1989). Immunoelectron-microscopic localization of the 180 kD component of the neural cell adhesion molecule N-CAM in postsynaptic membranes. *Journal of Comparative Neurology*, 288(1):92–100.

Peters, A., Sethares, C., and Luebke, J. I. (2008). Synapses are lost during aging in the primate prefrontal cortex. *Neuroscience*, 152(4):970–981.

Petridis, A. K., El-Maarouf, A., and Rutishauser, U. (2004). Polysialic acid regulates cell contact-dependent neuronal differentiation of progenitor cells from the subventricular zone. *Developmental dynamics : an official publication of the American Association of Anatomists*, 230(4):675–84.

Phillips, M. L., Drevets, W. C., Rauch, S. L., and Lane, R. (2003). Neurobiology of emotion perception II: Implications for major psychiatric disorders. *Biological psychiatry*, 54(5):515–28.

Pittenger, C. and Duman, R. S. (2008). Stress, depression, and neuroplasticity: a convergence of mechanisms. *Neuropsychopharmacology*, 33(1):88–109.

Price, C. J., Cauli, B., Kovacs, E. R., Kulik, A., Lambolez, B., Shigemoto, R., and Capogna, M. (2005). Neurogliaform neurons form a novel inhibitory network in the hippocampal CA1 area. *Journal of Neuroscience*, 25(29):6775–6786.

Prince, D. A., Parada, I., Scalise, K., Graber, K., Jin, X., and Shen, F. (2009). Epilepsy following cortical injury: cellular and molecular mechanisms as targets for potential prophylaxis. *Epilepsia*, 50 Suppl 2:30–40.

Puig, M. V., Santana, N., Celada, P., Mengod, G., and Artigas, F. (2004). In vivo excitation of GABA interneurons in the medial prefrontal cortex through 5-HT3 receptors. *Cerebral cortex*, 14(12):1365–75.

Purves, D., Brannon, E. M., Cabeza, R., Huettel, S. A., LaBar, K. S., Platt, M. L., and Woldorff, M. G. (2008). *Principles of cognitive neuroscience*, volume 83. Sinauer Associates.

Qu, Y., Chang, L., Klaff, J., Seemann, R., and Rapoport, S. I. (2003). Imaging brain phospholipase A2-mediated signal transduction in response to acute fluoxetine administration in unanesthetized rats. *Neuropsychopharmacology*, 28(7):1219–1226.

Quartu, M., Serra, M. P., Boi, M., Ibba, V., Melis, T., and Del Fiacco, M. (2008). Polysialylated-neural cell adhesion molecule (PSA-NCAM) in the human trigeminal ganglion and brainstem at prenatal and adult ages. *BMC Neuroscience*, 9:108.

Radley, J., Rocher, A., Janssen, W., Hof, P., McEwen, B., and Morrison, J. (2005a). Reversibility of apical dendritic retraction in the rat medial prefrontal cortex following repeated stress. *Experimental neurology*, 196(1):199–203.

Radley, J. J., Johnson, L. R., Janssen, W. G. M., Martino, J., Lamprecht, R., Hof, P. R., LeDoux, J. E., and Morrison, J. H. (2006a). Associative Pavlovian conditioning leads to an increase in spinophilin-immunoreactive dendritic spines in the lateral amygdala. *European Journal of Neuroscience*, 24(3):876–884.

Radley, J. J., Rocher, A. B., Janssen, W. G. M., Hof, P. R., McEwen, B. S., and Morrison, J. H. (2005b). Reversibility of apical dendritic retraction in the rat medial prefrontal cortex following repeated stress. *Experimental Neurology*, 196(1):199–203.

Radley, J. J., Rocher, A. B., Miller, M., Janssen, W. G. M., Liston, C., Hof, P. R., McEwen, B. S., and Morrison, J. H. (2006b). Repeated stress induces dendritic spine loss in the rat medial prefrontal cortex. *Cerebral cortex*, 16(3):313–20.

Radley, J. J., Sisti, H. M., Hao, J., Rocher, A. B., McCall, T., Hof, P. R., McEwen, B. S., and Morrison, J. H. (2004). Chronic behavioral stress induces apical dendritic reorganization in pyramidal neurons of the medial prefrontal cortex. *Neuroscience*, 125(1):1–6.

Rakic, P. (1985). Limits of neurogenesis in primates. *Science*, 227(4690):1054–1056.

Ramon Y Cajal, S. (1913). *Degeneration and regeneration of the nervous system*. Hafner.

Renner, M., Specht, C. G., and Triller, A. (2008). Molecular dynamics of postsynaptic receptors and scaffold proteins. *Current Opinion in Neurobiology*, 18(5):532–540.

Roberts, N., Puddephat, M. J., and McNulty, V. (2000). The benefit of stereology for quantitative radiology. *The British journal of radiology*, 73(871):679–697.

Roos, J., Hummel, T., Ng, N., Klämbt, C., and Davis, G. W. (2000). Drosophila Futsch regulates synaptic microtubule organization and is necessary for synaptic growth. *Neuron*, 26(2):371–82.

Rosenzweig, E. S. and Barnes, C. A. (2003). Impact of aging on hippocampal function: plasticity, network dynamics, and cognition. *Progress in Neurobiology*, 69(3):143–179.

Rougon, G., Nédélec, J., Malapert, P., Goridis, C., and Chesselet, M. F. (1990). Post-translation modifications of neural cell surface molecules. *Acta histochemica Supplementband*, 38:51–57.

Rousselot, P., Lois, C., and Alvarez-Buylla, A. (1995). Embryonic (PSA) N-CAM reveals chains of migrating neuroblasts between the lateral ventricle and the olfactory bulb of adult mice. *The Journal of comparative neurology*, 351(1):51–61.

Rubinow, M. J., Drogos, L. L., and Juraska, J. M. (2009). Age-related dendritic hypertrophy and sexual dimorphism in rat basolateral amygdala. *Neurobiology of Aging*, 30(1):137–146.

Russo, S. J., Mazei-robison, M. S., Ables, J. L., and Nestler, E. J. (2009). Neurotrophic factors and structural plasticity in addiction. *Neuropharmacology*, 56:73–82.

Rutishauser, U. (1996). Polysialic acid and the regulation of cell interactions. *Current Opinion in Cell Biology*, pages 679–684.

Rutishauser, U. (2008). Polysialic acid in the plasticity of the developing and adult vertebrate nervous system. *Nature reviews Neuroscience*, 9(1):26–35.

Rutishauser, U. and Landmesser, L. (1996). Polysialic acid in the vertebrate nervous system: a promoter of plasticity in cell-cell interactions. *Trends in Neurosciences*, 19(10):422–427.

Saarelainen, T., Hendolin, P., Lucas, G., Koponen, E., Sairanen, M., MacDonald, E., Agerman, K., Haapasalo, A., Nawa, H., Aloyz, R., Ernfors, P., and Castren, E. (2003). Activation of the TrkB Neurotrophin Receptor Is Induced by Antidepressant Drugs and Is Required for Antidepressant-Induced Behavioral Effects. *Journal of Neuroscience*, 23(1):349–357.

Sabel, B. A. (2008). Plasticity and restoration of vision after visual system damage: an update. *Restorative Neurology and Neuroscience*, 26(4-5):243–247.

Sairanen, M., Lucas, G., Ernfors, P., Castrén, M., and Castrén, E. (2005). Brain-derived neurotrophic factor and antidepressant drugs have different but coordinated effects on neuronal turnover, proliferation, and survival in the adult dentate gyrus. *Journal of neuroscience*, 25(5):1089–94.

Sairanen, M., O'Leary, O. F., Knuuttila, J. E., and Castrén, E. (2007). Chronic antidepressant treatment selectively increases expression of plasticity-related proteins in the hippocampus and medial prefrontal cortex of the rat. *Neuroscience*, 144(1):368–74.

Sandi, C. and Loscertales, M. (1999). Opposite effects on NCAM expression in the rat frontal cortex induced by acute vs. chronic corticosterone treatments. *Brain Research*, 828(1-2):127–134.

Sandi, C., Merino, J. J., Cordero, M. I., Kruyt, N. D., Murphy, K. J., and Regan, C. M. (2003). Modulation of hippocampal NCAM polysialylation and spatial memory consolidation by fear conditioning. *Biological Psychiatry*, 54(6):599–607.

Santarelli, L., Saxe, M., Gross, C., Surget, A., Battaglia, F., Dulawa, S., Weisstaub, N., Lee, J., Duman, R., Arancio, O., Belzung, C., and Hen, R. (2003). Requirement of hippocampal neurogenesis for the behavioral effects of antidepressants. *Science*, 301(5634):805–9.

Sawaguchi, A., Idate, Y., Ide, S., Kawano, J. I., Nagaike, R., Oinuma, T., and Suganuma, T. (1999). Multistratified expression of polysialic acid and its relationship to VAChT-containing neurons in the inner plexiform layer of adult rat retina. *The journal of histochemistry and cytochemistry*, 47(7):919–928.

Schaeffer, K. (1892). Beitrag zur histologie der Ammons Hornformation. *Archiv für Mikroscopische Anatomie*, 39(1):611–632.

Schiff, M., Weinhold, B., Grothe, C., and Hildebrandt, H. (2009). NCAM and polysialyltransferase profiles match dopaminergic marker gene expression but polysialic acid is dispensable for development of the midbrain dopamine system. *Journal of Neurochemistry*, 110(5):1661–1673.

Schuster, T., Krug, M., Stalder, M., Hackel, N., Gerardy-Schahn, R., and Schachner, M. (2001). Immunoelectron microscopic localization of the neural recognition molecules L1, NCAM, and its

isoform NCAM180, the NCAM-associated polysialic acid, beta1 integrin and the extracellular matrix molecule tenascin-R in synapses of the adult rat hippocampus. *Journal of Neurobiology*, 49(2):142–158.

Schwartzkroin, P. A. and Kunkel, D. D. (1985). Morphology of identified interneurons in the CA1 regions of guinea pig hippocampus. *Journal of Comparative Neurology*, 232(2):205–218.

Seamans, J. K., Lapish, C. C., and Durstewitz, D. (2008). Comparing the prefrontal cortex of rats and primates: insights from electrophysiology. *Neurotoxicity Research*, 14(2-3):249–62.

Seib, L. M. and Wellman, C. L. (2003). Daily injections alter spine density in rat medial prefrontal cortex. *Neuroscience letters*, 337(1):29–32.

Seidenfaden, R., Krauter, A., Schertzinger, F., Gerardy-Schahn, R., and Hildebrandt, H. (2003). Polysialic acid directs tumor cell growth by controlling heterophilic neural cell adhesion molecule interactions. *Molecular and cellular biology*, 23(16):5908–18.

Seki, T. (2002a). Expression patterns of immature neuronal markers PSA-NCAM, CRMP-4 and NeuroD in the hippocampus of young adult and aged rodents. *Journal of neuroscience research*, 70(3):327–34.

Seki, T. (2002b). Hippocampal adult neurogenesis occurs in a microenvironment provided by PSA-NCAM-expressing immature neurons. *Journal of neuroscience research*, 69(6):772–83.

Seki, T. and Arai, Y. (1991a). Expression of highly polysialylated NCAM in the neocortex and piriform cortex of the developing and the adult rat. *Anatomy and Embryology*, 184(4):395–401.

Seki, T. and Arai, Y. (1991b). The persistent expression of a highly polysialylated NCAM in the dentate gyrus of the adult rat. *Neuroscience research*, 12(4):503–13.

Seki, T. and Arai, Y. (1993a). Distribution and possible roles of the highly polysialylated neural cell adhesion molecule (NCAM-H) in the developing and adult central nervous system. *Neuroscience research*, 17(4):265–90.

Seki, T. and Arai, Y. (1993b). Highly polysialylated NCAM expression in the developing and adult rat spinal cord. *Brain research Developmental brain research*, 73(1):141–145.

Seki, T. and Arai, Y. (1999). Different polysialic acid-neural cell adhesion molecule expression patterns in distinct types of mossy fiber boutons in the adult hippocampus. *The Journal of comparative neurology*, 410(1):115–25.

Shapiro, L. A., Ng, K., Zhou, Q.-Y., and Ribak, C. E. (2009). Subventricular zone-derived, newly generated neurons populate several olfactory and limbic forebrain regions. *Epilepsy behavior EB*, 14 Suppl 1(1):74–80.

Shapiro, L. A., Ng, K. L., Kinyamu, R., Whitaker-Azmitia, P., Geisert, E. E., Blurton-Jones, M., Zhou, Q.-Y., and Ribak, C. E. (2007). Origin, migration and fate of newly generated neurons in the adult rodent piriform cortex. *Brain structure function*, 212(2):133–148.

Shimizu, E. (2000). NMDA Receptor-Dependent Synaptic Reinforcement as a Crucial Process for Memory Consolidation. *Science*, 290(5494):1170–1174.

Sizonenko, S. V., Bednarek, N., and Gressens, P. (2007). Growth factors and plasticity. *Seminars in fetal neonatal medicine*, 12(4):241–249.

Skelin, I., Sato, H., and Diksic, M. (2008). Olfactory bulbectomy reduces cerebral glucose utilization: 2-[14C]deoxyglucose autoradiographic study. *Brain Research Bulletin*, 76(5):485–492.

Slotkin, T. A., McCook, E. C., Ritchie, J. C., Carroll, B. J., and Seidler, F. J. (1997). Serotonin transporter expression in rat brain regions and blood platelets: aging and glucocorticoid effects. *Biological psychiatry*, 41(2):172–83.

Sousa, N., Lukoyanov, N. V., Madeira, M. D., Almeida, O. F., and Paula-Barbosa, M. M. (2000). Reorganization of the morphology of hippocampal neurites and synapses after stress-induced damage correlates with behavioral improvement. *Neuroscience*, 97(2):253–266.

Stepanyants, A., Hof, P. R., and Chklovskii, D. B. (2002). Geometry and structural plasticity of synaptic connectivity. *Neuron*, 34(2):275–88.

Stewart, M., Popov, V., Medvedev, N., Gabbott, P., Corbett, N., Kraev, I., and Davies, H. (2010). Dendritic Spine and Synapse Morphological Alterations Induced by a Neural Cell Adhesion Molecule (NCAM) Mimetic. *Advances in experimental medicine and biology*, 663:373–383.

Sullivan, P. F., Keefe, R. S. E., Lange, L. A., Lange, E. M., Stroup, T. S., Lieberman, J., and Maness, P. F. (2007). NCAM1 and neurocognition in schizophrenia. *Biological psychiatry*, 61(7):902–10.

Sutton, M. A. and Schuman, E. M. (2006). Dendritic protein synthesis, synaptic plasticity, and memory. *Cell*, 127(1):49–58.

Suzuki, M., Suzuki, M., Nakayama, J., Suzuki, A., Angata, K., Chen, S., Sakai, K., Hagihara, K., Yamaguchi, Y., and Fukuda, M. (2005). Polysialic acid facilitates tumor invasion by glioma cells. *Glycobiology*, 15(9):887–894.

Swanson, L. W. and Petrovich, G. D. (1998). What is the amygdala? *Trends in Neurosciences*, 21(8):323–331.

Sytnyk, V., Leshchyns'ka, I., Delling, M., Dityateva, G., Dityatev, A., and Schachner, M. (2002). Neural cell adhesion molecule promotes accumulation of TGN organelles at sites of neuron-to-neuron contacts. *The Journal of Cell Biology*, 159(4):649–661.

Sytnyk, V., Leshchyns'ka, I., Nikonenko, A. G., and Schachner, M. (2006). NCAM promotes assembly and activity-dependent remodeling of the postsynaptic signaling complex. *The Journal of Cell Biology*, 174(7):1071–1085.

Szele, F. G., Dowling, J. J., Gonzales, C., Theveniau, M., Rougon, G., and Chesselet, M. F. (1994). Pattern of expression of highly polysialylated neural cell adhesion molecule in the developing and adult rat striatum. *Neuroscience*, 60(1):133–144.

Tao, R., Li, C., Zheng, Y., Qin, W., Zhang, J., Li, X., Xu, Y., Shi, Y. Y., Feng, G., and He, L. (2007). Positive association between SIAT8B and schizophrenia in the Chinese Han population. *Schizophrenia research*, 90(1-3):108–14.

Tata, D. A. and Anderson, B. J. (2010). The effects of chronic glucocorticoid exposure on dendritic length, synapse numbers and glial volume in animal models: implications for hippocampal volume reductions in depression. *Physiology & behavior*, 99(2):186–93.

Theodosis, D. T., Rougon, G., and Poulain, D. A. (1991). Retention of embryonic features by an adult neuronal system capable of plasticity: polysialylated neural cell adhesion molecule in the hypothalamo-neurohypophysial system. *Proceedings of the National Academy of Sciences of the United States of America*, 88(13):5494–5498.

Thompson, M. R., Li, K. M., Clemens, K. J., Gurtman, C. G., Hunt, G. E., Cornish, J. L., and McGregor, I. S. (2004). Chronic fluoxetine treatment partly attenuates the long-term anxiety and depressive symptoms induced by MDMA ('Ecstasy') in rats. *Neuropsychopharmacology*, 29(4):694–704.

Tordera, R. M., Pei, Q., and Sharp, T. (2005). Evidence for increased expression of the vesicular glutamate transporter, VGLUT1, by a course of antidepressant treatment. *Journal of neurochemistry*, 94(4):875–83.

Trachtenberg, J. T., Chen, B. E., Knott, G. W., Feng, G., Sanes, J. R., Welker, E., and Svoboda, K. (2002). Long-term in vivo imaging of experience-dependent synaptic plasticity in adult cortex. *Nature*, 420(6917):788–94.

Tyler, W. J. and Pozzo-Miller, L. (2003). Miniature synaptic transmission and BDNF modulate dendritic spine growth and form in rat CA1 neurones. *The Journal of physiology*, 553(Pt 2):497–509.

Uno, H., Eisele, S., Sakai, A., Shelton, S., Baker, E., DeJesus, O., and Holden, J. (1994). Neurotoxicity of glucocorticoids in the primate brain.

Uylings, H. B. and Van Eden, C. G. (1990). Qualitative and quantitative comparison of the prefrontal cortex in rat and in primates, including humans. *Progress in Brain Research*, 85:31–62.

Vaithianathan, T., Matthias, K., Bahr, B., Schachner, M., Suppiramaniam, V., Dityatev, A., and Steinhaüser, C. (2004). Neural cell adhesion molecule-associated polysialic acid potentiates alpha-amino-3-hydroxy-5-methylisoxazole-4-propionic acid receptor currents. *The Journal of Biological Chemistry*, 279(46):47975–47984.

Van Praag, H., Christie, B. R., Sejnowski, T. J., and Gage, F. H. (1999). Running enhances neurogenesis, learning, and long-term potentiation in mice. *Proceedings of the National Academy of Sciences of the United States of America*, 96(23):13427–13431.

Varea, E., Belles, M., Vidueira, S., Blasco-Ibáñez, J. M., Crespo, C., Pastorand, A. M., and Nacher, J. (2011a). PSA-NCAM is Expressed in Immature, but not Recently Generated, Neurons in the Adult Cat Cerebral Cortex Layer II. *Frontiers in neuroscience*, 5:9.

Varea, E., Blasco-Ibáñez, J. M., Gómez-Climent, M. A., Castillo-Gómez, E., Crespo, C., Martínez-Guijarro, F. J., and Nácher, J. (2007a). Chronic fluoxetine treatment increases the expression of PSA-NCAM in the medial prefrontal cortex. *Neuropsychopharmacology*, 32(4):803–12.

Varea, E., Castillo-Gómez, E., Gómez-Climent, M. A., Blasco-Ibáñez, J. M., Crespo, C., Martínez-Guijarro, F. J., and Nàcher, J. (2007b). Chronic antidepressant treatment induces contrasting patterns of synaptophysin and PSA-NCAM expression in different regions of the adult rat telencephalon. *European neuropsychopharmacology : the journal of the European College of Neuropsychopharmacology*, 17(8):546–57.

Varea, E., Castillo-Gómez, E., Gómez-Climent, M. A., Blasco-Ibáñez, J. M., Crespo, C., Martínez-Guijarro, F. J., and Nàcher, J. (2007c). PSA-NCAM expression in the human prefrontal cortex. *Journal of chemical neuroanatomy*, 33(4):202–9.

Varea, E., Castillo-Gómez, E., Gómez-Climent, M. A., Guirado, R., Blasco-Ibáñez, J. M., Crespo, C., Martínez-Guijarro, F. J., and Nácher, J. (2009). Differential evolution of PSA-NCAM expression during aging of the rat telencephalon. *Neurobiology of aging*, 30(5):808–18.

Varea, E., Guirado, R., Gilabert-Juan, J., Martí, U., Castillo-Gomez, E., Blasco-Ibáñez, J. M., Crespo, C., and Nacher, J. (2011b). Expression of PSA-NCAM and synaptic proteins in the amygdala of psychiatric disorder patients. *Journal of psychiatric research*.

Varea, E., Nácher, J., Blasco-Ibáñez, J. M., Gómez-Climent, M. A., Castillo-Gómez, E., Crespo, C., and Martínez-Guijarro, F. J. (2005). PSA-NCAM expression in the rat medial prefrontal cortex. *Neuroscience*, 136(2):435–43.

Venero, C., Herrero, A. I., Touyarot, K., Cambon, K., López-Fernández, M. A., Berezin, V., Bock, E., and Sandi, C. (2006). Hippocampal up-regulation of NCAM expression and polysialylation plays a key role on spatial memory. *European Journal of Neuroscience*, 23(6):1585–1595.

Vitureira, N., Andrés, R., Pérez-Martínez, E., Martínez, A., Bribián, A., Blasi, J., Chelliah, S., López-Doménech, G., De Castro, F., Burgaya, F., McNagny, K., and Soriano, E. (2010). Podocalyxin Is a Novel Polysialylated Neural Adhesion Protein with Multiple Roles in Neural Development and Synapse Formation. *PLoS ONE*, 5(8):16.

Vyas, A., Mitra, R., Shankaranarayana Rao, B. S., and Chattarji, S. (2002). Chronic stress induces contrasting patterns of dendritic remodeling in hippocampal and amygdaloid neurons. *Journal of Neuroscience*, 22(15):6810–6818.

Vyas, A., Pillai, A. G., and Chattarji, S. (2004). Recovery after chronic stress fails to reverse amygdaloid neuronal hypertrophy and enhanced anxiety-like behavior. *Neuroscience*, 128(4):667–673.

Wallace, M., Luine, V., Arellanos, A., and Frankfurt, M. (2006). Ovariectomized rats show decreased recognition memory and spine density in the hippocampus and prefrontal cortex. *Brain Research*, 1126(1):176–182.

Walmod, P. S., Kolkova, K., Berezin, V., and Bock, E. (2004). Zippers make signals: NCAM-mediated molecular interactions and signal transduction. *Neurochemical Research*, 29(11):2015–2035.

Walsh, F. S. and Doherty, P. (1997). Neural cell adhesion molecules of the immunoglobulin superfamily: role in axon growth and guidance. *Annual Review of Cell and Developmental Biology*, 13(1):425–56.

Watanabe, Y., Gould, E., Daniels, D. C., Cameron, H., and McEwen, B. S. (1992). Tianeptine attenuates stress-induced morphological changes in the hippocampus. *European Journal of Pharmacology*, 222(1):157–162.

Weber, E. T. and Andrade, R. (2010). Htr2a Gene and 5-HT(2A) Receptor Expression in the Cerebral Cortex Studied Using Genetically Modified Mice. *Frontiers in neuroscience*, 4.

Wechsler, A. and Teichberg, V. I. (1998). Brain spectrin binding to the NMDA receptor is regulated by phosphorylation, calcium and calmodulin. *The European Molecular Biology Organization Journal*, 17(14):3931–3939.

Williams, R. K., Goridis, C., and Akeson, R. (1985). Individual neural cell types express immunologically distinct N-CAM forms. *The Journal of Cell Biology*, 101(1):36–42.

Williams, S. R. and Atkinson, S. E. (2008). Dendritic synaptic integration in central neurons. *Current Biology*, 18(22):R1045–R1047.

Willner, P. (1997). Validity, reliability and utility of the chronic mild stress model of depression: a 10-year review and evaluation. *Psychopharmacology*, 134(4):319–329.

Wong, W. T., Faulkner-Jones, B. E., Sanes, J. R., and Wong, R. O. (2000). Rapid dendritic remodeling in the developing retina: dependence on neurotransmission and reciprocal regulation by Rac and Rho. *Journal of Neuroscience*, 20(13):5024–5036.

Woolley, S. and Mcewen, S. (1992). Estradiol Mediates during the Estrous. *Spine*, 12(July).

Wu, X. and Castrén, E. (2009). Co-treatment with diazepam prevents the effects of fluoxetine on the proliferation and survival of hippocampal dentate granule cells. *Biological psychiatry*, 66(1):5–8.

Wysocki, C. J., Meredith, M., Finger, T. E., and Silver, W. L. (1991). Vomeronasal system. *Science*, pages 601–601.

Xerri, C. (2008). Imprinting of idiosyncratic experience in cortical sensory maps: neural substrates of representational remodeling and correlative perceptual changes. *Behavioural brain research*, 192(1):26–41.

Yamada, S. and Nelson, W. J. (2007). Synapses: sites of cell recognition, adhesion, and functional specification. *Annual Review of Biochemistry*, 76(1):267–94.

Yang, P., Yin, X., and Rutishauser, U. (1992). Intercellular space is affected by the polysialic acid content of NCAM. *The Journal of Cell Biology*, 116(6):1487–1496.

Yoshida, K., Rutishauser, U., Crandall, J. E., and Schwarting, G. A. (1999). Polysialic acid facilitates migration of luteinizing hormone-releasing hormone neurons on vomeronasal axons. *Journal of Neuroscience*, 19(2):794–801.

Yuste, R. and Bonhoeffer, T. (2001). Morphological changes in dendritic spines associated with long-term synaptic plasticity. *Annual review of neuroscience*, 24:1071–89.

Zuber, C., Lackie, P. M., Catterall, W. A., and Roth, J. (1992). Polysialic acid is associated with sodium channels and the neural cell adhesion molecule N-CAM in adult rat brain. *The Journal of Biological Chemistry*, 267(14):9965–9971.

Zucker, R. S. and Regehr, W. G. (2002). Short-term synaptic plasticity. *Annual Review of Physiology*, 64(1):355–405.

Part X. Appendix: Publications derived from the thesis

Cerebral Cortex October 2008;18:2229–2240
doi:10.1093/cercor/bhm255
Advance Access publication January 31, 2008

FEATURE ARTICLE

A Population of Prenatally Generated Cells in the Rat Paleocortex Maintains an Immature Neuronal Phenotype into Adulthood

María Ángeles Gómez-Climent, Esther Castillo-Gómez, Emilio Varea, Ramón Guirado, José Miguel Blasco-Ibáñez, Carlos Crespo, Francisco José Martínez-Guijarro and Juan Nácher

Neurobiology Unit and Program in Basic and Applied Neurosciences, Cell Biology Dpt., Universitat de València, Spain

New neurons in the adult brain transiently express molecules related to neuronal development, such as the polysialylated form of neural cell adhesion molecule, or doublecortin (DCX). These molecules are also expressed by a cell population in the rat paleocortex layer II, whose origin, phenotype, and function are not clearly understood. We have classified most of these cells as a new cell type termed tangled cell. Some cells with the morphology of semilunar–pyramidal transitional neurons were also found among this population, as well as some scarce cells resembling semilunar, pyramidal. and fusiform neurons. We have found that none of these cells in layer II express markers of glial cells, mature, inhibitory, or principal neurons. They appear to be in a prolonged immature state, confirmed by the coexpression of DCX, TOAD/Ulip/CRMP-4, A3 subunit of the cyclic nucleotide-gated channel, or phosphorylated cyclic adenosine monophosphate response element–binding protein. Moreover, most of them lack synaptic contacts, are covered by astroglial lamellae, and fail to express cellular activity markers, such as c-Fos or Arc, and N-methyl-d-aspartate or glucocorticoid receptors. We have found that none of these cells appear to be generated during adulthood or early youth and that most of them have been generated during embryonic development, mainly in E15.5.

Keywords: adult neurogenesis, doublecortin, entorhinal cortex, piriform cortex, PSA-NCAM

Introduction

Neuronal production persists in discrete regions of the adult central nervous system (CNS). New neurons are incorporated to the granule layer of the dentate gyrus and to the olfactory bulb after being generated in the subventricular zone (SVZ) (Kempermann 2005). Recent studies have indicated the presence of neurogenesis in the adult neocortex and other brain regions, although this is still a matter of debate (please see Nowakowski and Hayes 2000; Rakic 2002b; Gould 2007 for review). Newly generated neurons can be identified by the coexpression of different molecules related to neuronal development. Immature neurons generated during adulthood express molecules related to cytoskeletal dynamics, such as doublecortin (DCX) or TOAD/Ulip/CRMP-4 (TUC-4) (rCRMP4, TOAD64) (Minturn, Geschwind, et al. 1995; Gleeson et al. 1999). These cells also express the polysialylated form of the neural cell adhesion molecule (PSA-NCAM), which is related to different neurodevelopmental processes (Seki and Arai 1993). Different reports have described a population of cells in the layer II of the paleocortex of adult rodents, specially in the piriform and lateral entorhinal cortices, which expresses PSA-NCAM, DCX, and TUC-4 (Seki and Arai 1991; Nacher et al. 2000; Fox et al. 2000; Nacher, Crespo, McEwen, et al. 2001; Varea, Castillo-Gomez, Gomez-Climent, Guirado, et al. 2007). A previous study demonstrated that many of these cells in layer II do not express the mature neuronal marker NeuN, suggesting an immature state, although no quantification was performed (Nacher et al. 2002a). Moreover, there is discrepancy on the time of origin of these cells. Although some reports have failed to find adult neurogenesis in this region (Nacher et al. 2002a; Bonfanti 2006), 3 recent studies have described the presence of newly generated neurons in the adult paleocortex (Pekcec et al. 2006; Shapiro, Ng, Kinyamu, et al. 2007; Shapiro, Ng, Zhou, Ribak, et al. 2007). In order to investigate in detail the phenotype of these putative immature cells in the paleocortex layer II, we have analyzed the expression of molecules commonly found in recently generated neurons and neuronal progenitor cells in the adult CNS, such as those found in the dentate gyrus and SVZ/olfactory bulb. We have also checked whether these cells expressed typical markers of mature neurons and specific markers of principal neurons and interneurons. The glial nature of these cells has also been studied using markers of astrocytes, oligodendrocytes, and microglia. Using electron microscopy we have observed the ultrastructural characteristics of these cells and the presence of synaptic contacts on them. Additionally, using 5′bromodeoxyuridine (BrdU) pulse-chase experiments we have analyzed whether these cells were proliferating and whether they were generated during adulthood, during early youth or during embryogenesis. We have also explored whether these cells were functional, studying the expression of molecules related to cellular activity. Because the number of cells expressing PSA-NCAM in the paleocortex layer II is regulated by N-methyl-d-aspartate (NMDA) receptors and glucocorticoids (Nacher et al. 2002a, 2004), we have also studied the expression of glucocorticoid and NMDA receptors, in order to understand whether excitatory amino acids and adrenal steroids could act directly on these cells.

Material and Methods

Animals and Treatments

Forty-three young-adult male Sprague–Dawley (SD) rats (3 months old, 300 ± 15 g, Harlan Iberica, Barcelona, Spain) were separated in different groups. 1) Eight rats were used to study PSA-NCAM expression and its colocalization with several cellular markers using immunohistochemistry. 2) Thirty rats were used to study whether PSA-NCAM immunoreactive cells in the paleocortex layer II were generated during adulthood using double PSA-NCAM/BrdU immunohistochemistry. All the rats in this group received 4 intraperitoneal (ip) injections, 1 each 12 h, of BrdU (Sigma, St Louis, MO; 50 mg/kg, in sterile saline) and were sacrificed 2, 4, 7, 14, 21, or 30 days after the last injection ($n = 5$ per group). 3) Five rats were used to study whether any of the PSA-NCAM immunoreactive cells in the paleocortex layer II was proliferating. These animals received an ip injection of BrdU (200 mg/kg, in sterile saline) and were sacrificed 2 h later.

A second set of 5 SD rats (45 days old, 280 ± 10 g, Harlan Iberica, Barcelona, Spain) was used to explore the possibility that PSA-NCAM

expressing cells in paleocortex layer II were generated during early youth. These animals were also injected with BrdU (4 ip injections, 1 each 12 h, 50 mg/kg, in sterile saline) and were sacrificed 60 days after the last injection.

Six pregnant SD rats (Harlan Iberica) received 2 ip injections of 5′BrdU (50 mg/kg), 8 h apart, on the following days after coupling: E11.5, E13.5, E15.5 ($n = 2$ per group). The first 24 h after coupling were designated as embryonic day 0 (E0). Four males (3 months old, 306 ± 32 g) were selected from each offspring and processed for double PSA-NCAM/BrdU immunohistochemistry, in order to identify whether these cells in the paleocortex layer II were generated during embryogenesis.

Four CD1 mice (3 months old, 30 ± 5 g, Harlan Iberica) were used for double PSA-NCAM/calretinin (CR) fluorescence immunohistochemistry as described below.

Six SD rats (3 months old, 300 ± 50 g, Harlan Iberica) were used for PSA-NCAM, TUC-4, or CNGA-3 preembedding immunohistochemistry for electron microscopy.

Histological Procedures

Rats destined for light microscopy studies were perfused transcardially under deep chloral hydrate anesthesia, with saline and then 4% paraformaldehyde in sodium phosphate buffer 0.1 M, pH 7.4 (PB). Brains for fluorescence immunohistochemistry were cut with a vibratome (Leica VT 1000E, Leica, Nussloch, Germany) and 50-μm-thick transverse sections were collected and kept in cold PB (4 °C) before processing. Brains for conventional immunohistochemistry were cryoprotected with 30% sucrose in PB, coronal sections (50 μm) were obtained with a sliding freezing microtome (Leica SM2000R) and stored at −20 °C in 30% glycerol, 30% ethylene glycol in PB until used.

The rats processed for electron microscopy were perfused transcardially under deep chloral hydrate anesthesia, first with saline for 1 min, followed by 50 mL of 3.8% acrolein (Fluka AG, Busch, Switzerland) and then by 450 mL of 3% paraformaldehyde in PB. Brains were extracted and sliced with a vibratome as described above.

All animal experimentation was conducted in accordance with the European Communities Council Directive of 24 November 1986 (86/609/EEC) and was approved by the Committee on Bioethics of the Universitat de València. Every effort was made to minimize the number of animals used and their suffering.

Immunohistochemistry for Conventional Light Microscopy

Tissue was processed "free-floating" for immunohistochemistry as follows. Briefly, sections were incubated for 1 min in an antigen unmasking solution (0.01 M citrate buffer, pH 6) at 100 °C. After cooling down the sections to room temperature they were incubated with 10% methanol, 0.003% H_2O_2 in phosphate buffered saline (PBS) for 10 min to block endogenous peroxidase activity. After this, sections were treated for 1 h with 5% normal donkey serum (NDS) (Jackson ImmunoResearch Laboratories, West Grove, PA) in PBS with 0.2% Triton-X-100 (Sigma-Aldrich, St Louis, MO) and were incubated overnight at room temperature in anti-PSA-NCAM or anti-γ-aminobutyric acid (GABA) antibodies (please see Table1). After washing, sections were incubated for 1 h with donkey anti-mouse IgM or donkey anti-rabbit IgG biotinylated antibodies (1:250; Jackson ImmunoResearch Laboratories, West Grove, PA), followed by an avidin–biotin–peroxidase complex (ABC; Vector Laboratories, Peterborough, UK) for 30 min in PBS. Color development was achieved by incubating with 3,3′-diaminobenzidine tetrahydrochloride (Sigma-Aldrich) and 0.033% hydrogen peroxide in PB for 4 min. PBS containing 0.2% Triton-X-100 and 3% NDS was used for primary and secondary antibodies dilution.

Double Fluorescence Immunohistochemistry

In order to characterize the phenotype of PSA-NCAM immunoreactive cells, we have performed double immunohistochemistry using an anti-PSA-NCAM antibody and antibodies against different markers of immature neurons, mature neurons, interneurons, astrocytes, oligodendrocytes, microglia, and proteins related to neuronal activity (please see Table 1). Sections were processed as described above, but the endogenous peroxidase block was omitted. The first day, sections were incubated overnight at room temperature with mouse monoclonal IgM anti-PSA-NCAM antibody and 1 of the above-mentioned antibodies. The second day sections were washed and incubated for 1 h with donkey anti-mouse IgM, donkey anti-goat IgG, or donkey anti-rabbit IgG secondary antibodies conjugated with Alexa 488 or Alexa 555 (1:200; Molecular Probes, Eugene, OR) in PBS containing 0.2% Triton-X-100 and 3% NDS.

In order to convert monoclonal mouse primary antibodies into a species different from that of the anti-PSA-NCAM primary antibody (Lewis Carl et al. 1993) sections were incubated for 2 h with an excess

Table 1
Primary antibodies[a]

Name	Abbreviation	Dilution	Company
Monoclonal mouse anti-α-actinin (Sarcomeric)	Anti-α-actinin	1:500	Sigma-Aldrich
Polyclonal goat for activity-regulated cytoskeleton-associated protein	Anti-Arc	1:500	Santa Cruz Biotechnology, Inc.
Polyclonal rabbit anti-γ-aminobutyric acid	Anti-GABA	1:5000	Sigma-Aldrich
Monoclonal rat anti-5′bromodeoxyuridine	Anti-5′BrdU	1:200	Immunological Direct, Oxford Biotechnology
Monoclonal mouse anti-Ca^2+/calmodulin dependent protein kinase II	Anti-CaMKII	1:200	Chemicon Int., Inc.
Polyclonal rabbit anti-calbindin-D28K	Anti-CB	1:2.000	SWANT
Polyclonal rabbit anti-calretinin	Anti-CR	1:2.000	SWANT
Polyclonal rabbit c-Fos antibody	Anti-c-Fos	1:2.000	Santa Cruz Biotechnology, Inc.
Monoclonal mouse anti-cholecystokinin	Anti-CCK	1:1.000	CURE
Polyclonal rabbit anti-cyclic nucleotide-gated cation channel	[b]Anti-CNGA-3	1:500	Alomone Labs; IL
Polyclonal goat anti-doublecortin (C-18)	Anti-DCX	1:250	Santa Cruz Biotechnology, Inc.
Polyclonal rabbit anti-glial fibrillar acidic protein	Anti-GFAP	1:500	Sigma-Aldrich
Polyclonal rabbit anti-glucocorticoid receptor	Anti-GR	1:50	ABCAM
Monoclonal mouse anti-glutamate decarboxylase, isoform 67	Anti-GAD-67	1:500	Developmental Studies Hybridoma Bank
Monoclonal mouse anti-microtubule associated protein2	Anti-MAP2	1:1000	Sigma-Aldrich
Polyclonal rabbit anti-NG2 chondroitin sulfate proteoglycan	Anti-NG2	1:250	Chemicon Int., Inc.
Polyclonal rat anti-Nestin 401	Anti-Nestin	1:500	DSHB
Monoclonal mouse anti-neuronal nuclear antigen	Anti-NeuN	1:100	Chemicon Int., Inc.
Polyclonal rabbit anti-neuropeptide Y	Anti-NPY	1:1000	Provided by Dr T. J. Görcs
Polyclonal rabbit anti-N-methyl-d-aspartate1 receptor	Anti-NMDAR1	1:100	Chemicon Int., Inc.
Polyclonal rabbit anti-parvalbumin	Anti-PV	1:2.000	SWANT
Polyclonal rabbit anti-Pax6 (C-17)	Anti-Pax6	1:3.000	Provided by Dr Grant S. Mastick
Polyclonal rabbit anti-phospho-CREB (Ser133)	Anti-p-CREB	1:500	Upstate, New York, USA
Monoclonal mouse rip antibody	Anti-RIP	1:1.000	Developmental Studies Hybridoma Bank
Monoclonal mouse anti-polysialylated form of the neural cell adhesion molecule	Anti-PSA-NCAM	1:1400	Abcys, Paris, FR
Polyclonal rabbit anti-somatostatin	Anti-SST	1:200	Provided by Dr T. J. Görcs
Polyclonal rabbit anti-TUC-4/rCRMP-4	Anti-TUC-4/rCRMP4	1:1.000	Chemicon Int., Inc.
Polyclonal rabbit anti-vasoactive intestinal peptide	Anti-VIP	1:1.000	Provided by Dr T. J. Görcs

[a]Alphabetic order by name.
[b]Other abbreviations: CNG3, CNGα2, CCNC1.

of unconjugated goat anti-mouse IgG Fab fragments (1:100; Jackson ImmunoResearch Laboratories, West Grove, PA). Then, sections were washed and incubated in fluorescent secondary antibodies as described above.

N-methyl-D-aspartate 1 receptor (NR1) immunohistochemistry requires a pretreatment, which usually affects PSA-NCAM antigeneicity. For these reason, we have decided to investigate NR1 expression in DCX immunoreactive cells, as described earlier (Nacher et al. 2007). Briefly, the sections were pretreated as those used for BrdU immunohistochemistry and incubated for 48 h at 4 °C with a mixture containing anti-DCX and anti-NR1 primary antibodies (please see Table 1). Then, secondary fluorochrome-conjugated antibodies were applied as described above.

Mirror Technique

In order to analyze the coexistence of PSA-NCAM with GABA in paleocortex layer II cells, we employed the mirror technique (Kosaka et al. 1985) using alternate series of vibratome sections. The tissue was immunostained as described above, using primary antibodies against PSA-NCAM and GABA (please see Table 1) for each 2 alternate subseries. Then the sections were treated with 1% OsO4, 7% glucose in PB for 1 h, dehydrated with ascending alcohols, flat mounted with Durcupan resin (Fluka, Sigma-Aldrich), and coverslipped. PSA-NCAM immunoreactive perikarya cut in half at the surface of the sections, as well as nearby capillaries, were drawn with a camera lucida under 40× immersion oil objective. The other halves of the immunoreactive somata were located on the corresponding surface of the adjacent section (processed for GABA immunohistochemistry) using the capillaries as landmarks. Only those cells in which the 2 halves (immunoreactive or not) could be identified with the aid of interferential contrast, were evaluated (Kosaka et al. 1985).

PSA-NCAM/ BrdU Immunohistochemistry

Sections from alternate series were treated for 60 min at 60 °C in PB and denaturation of DNA was achieved by treating for 30 min with 2 M HCl in PB at room temperature. Then, sections were processed for immunohistochemistry as described above, using monoclonal rat IgG anti-BrdU in combination with anti-PSA-NCAM monoclonal mouse antibody (see Table 1). Secondary antibodies were anti-mouse IgM and anti-rat IgG secondary antibodies generated in donkey and conjugated with Alexa 488 and Alexa 555, respectively.

Observation and Quantification of Double-Labeled Cells

All sections processed for fluorescent immunohistochemistry were mounted on slides and coverslipped using DakoCytomation fluorescent mounting medium (Dako North America, Inc., Carpinteria, CA). Then the sections were observed under a confocal microscope (Leica TCS-SP). Z-series of optical sections (1 μm apart) were obtained using sequential scanning mode. These stacks were processed with LSM 5 Image Browser software. A one in 10 series of telencephalic sections from each animal was double-labeled as described. Fifty immunoreactive cells were analyzed in each case to determine the coexpression of PSA-NCAM and the markers described before.

Immunohistochemistry for Electron Microscopy

In this procedure, sections were incubated with sodium borohydride 1% in ddH_2O for 10 min. Then, sections were washed in PB and the endogenous peroxidase activity was blocked as described above, without methanol. Free aldehydes were quenched using Tris buffer 0.5 N, pH 7.2 for 30 min. Subsequently, nonspecific binding sites were blocked with NDS 10% in PB with glycine 0.2% and lysine 0.2%. After washing, sections were processed using primary antibodies against PSA-NCAM, TUC-4, or CNGA-3, (please see Table 1), as described for conventional immunohistochemistry. Immunolabeling was intensified treating the sections with 1% osmium tetroxide (EMS, Hatfield, PA) in PB for 60 min, protected from light. After each step, sections were carefully rinsed in PB. Sections were dehydrated through increasing graded series of ethanol baths (30–100%, 10 min each step) and dyed with 1% uranyl acetate in 70% ethanol bath during the process of dehydration. Finally, sections were cleared in propylene oxide and flat-embedded in Durcupan. After the analysis of the sections under the light microscope, some cells were re-embedded in Durcupan, and 60-nm-thick ultrathin sections were cut with an ultramicrotome. Ultrathin sections were serially collected on formvar-coated single-slot copper grids and stained using lead citrate. Selected cells were observed and partially reconstructed from serial sections under a JEOL JEM-1010 electron microscope.

Results

Distribution and Morphology of PSA-NCAM Expressing Cells in the Paleocortex Layer II

The distribution of PSA-NCAM expressing cells in the piriform and entorhinal cortices layer II was identical to that described earlier (Nacher et al. 2002a; Varea, Castillo-Gomez, Gomez-Climent, Guirado, et al. 2007). Scattered PSA-NCAM expressing cells were also found in the layer II of the perirhinal cortex and the most ventral region of the agranular insular and ectorhinal cortices.

In the paleocortex layer II, the majority of PSA-NCAM immunoreactive cells were small (soma diameter: 8.9 ± 0.96 μm) and showed processes with highly irregular trajectories, usually restricted to layer II, although some of these processes with vertical trajectories were also found in layer I. Most of these cells appeared frequently in clusters of 2–5 and closely resembled those described previously as neurogliaform neurons (Haberly 1983) (Fig. 1*A*,*B*). However, although we have previously classified these small cells as neurogliaform neurons (Nacher et al. 2002a), we have found that none of them expressed GABA, glutamate decarboxylase, isoform 67 (GAD67), or α-actinin (please see Mature Neuronal Markers section below), which are commonly expressed by neurogliaform neurons (Price et al. 2005). In consequence, we have chosen to denominate them "tangled cells" due to their intricate neuritic trajectories.

Some cells resembling the semilunar–pyramidal transitional neurons described by (Haberly 1983) in the paleocortex layer II were also PSA-NCAM immunoreactive, although they appeared absent from the most rostral region of the piriform cortex. They were larger than the tangled cells (soma diameter: 14.8 ± 1.59 μm), they showed 1 or 2 long dendrites expanding into layer I and some thin basal processes (Fig. 1*B*). Occasionally, we have also found some PSA-NCAM expressing cells resembling semilunar neurons, in which only a thin process resembling an axon could be observed (Fig. 1*C*). Some scarce cells with the characteristic morphology of pyramidal neurons and some displaying fusiform morphology can be found also in the paleocortex layer II (Fig. 1*D*). Additionally, some small bipolar cells with short processes oriented vertically were observed in piriform cortex layer III, endopiriform nucleus and the deep layers of the lateral entorhinal cortex. These small immunolabeled cells were usually located adjacent to long immunoreactive processes that traverse vertically both layers. These vertical prolongations appeared to arise from PSA-NCAM expressing somata in layer II (Fig. 1*D*).

Expression of Glial Markers

Double immunohistochemistry using an anti-PSA-NCAM antibody in combination with anti-glial fibrilar acidic protein (GFAP), anti-Rip, or anti-OX42 antibodies revealed that none of PSA-NCAM expressing cells in layer II of the paleocortex of adult rats could be classified as an astrocyte, an oligodendrocyte or a microglial cell (Supplemental Fig. 1*A*–*C*).

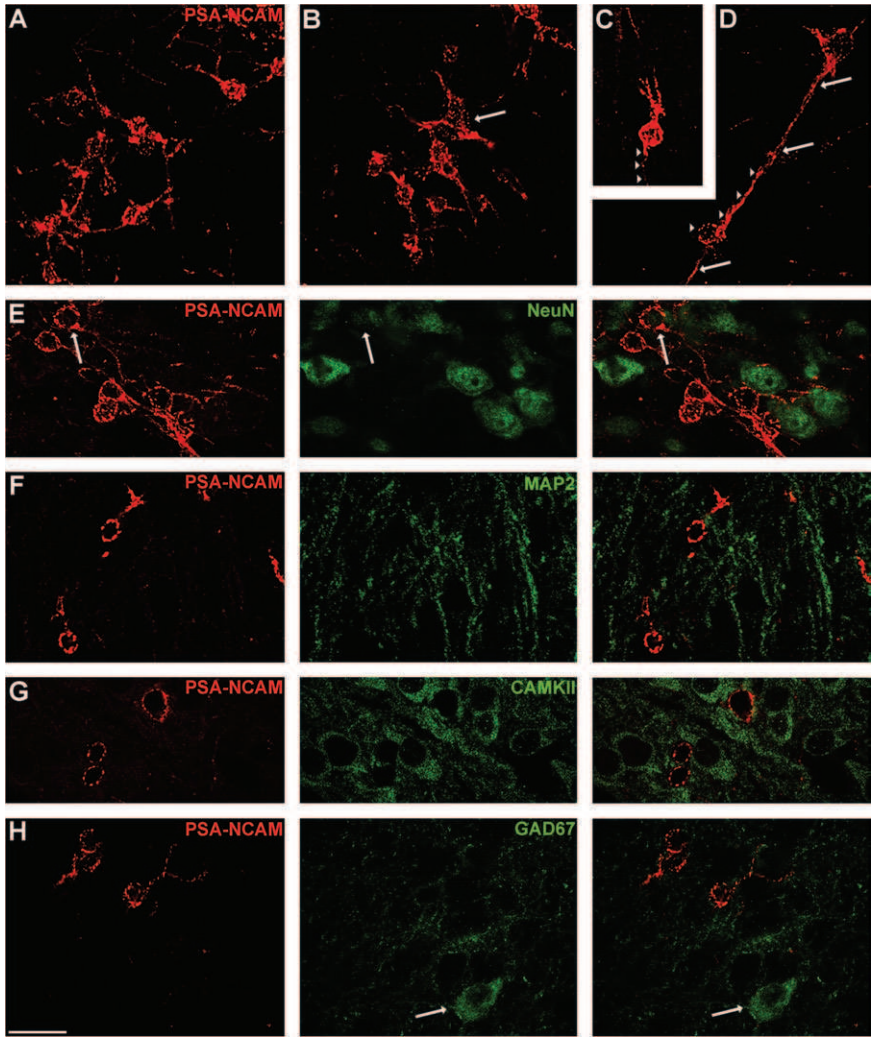

Figure 1. Confocal microscopic analysis of PSA-NCAM immunoreactive cells in the paleocortex layer II. (*A*) PSA-NCAM immunohistochemistry in the piriform cortex layer II. Note the high density of tangled cells. (*B*) PSA-NCAM immunohistochemistry in the entorhinal cortex layer II. A semilunar–pyramidal transition neuron can be observed (arrow) among the abundant smaller tangled cells. (*C*) Example of a PSA-NCAM immunolabeled semilunar cell displaying a basal process resembling an axon (arrowhead). (*D*) Detail of an inverted pyramidal PSA-NCAM immunoreactive cell. Note its single process directed to layer III (arrows), to which another PSA-NCAM expressing cell is attached (arrowheads). (*E*) Most PSA-NCAM immunoreactive tangled cells lack NeuN expression in their nuclei. However, some of these cells display faint NeuN expression in their nuclei (arrow). (*F*) PSA-NCAM expressing cells lacking MAP2 expression in their somata and dendrites. (*G*) PSA-NCAM expressing cells lacking CAMKII expression. (*H*) PSA-NCAM expressing cells lacking GAD67 expression in their somata. Note a GAD67 positive cell (arrow) which lacks PSA-NCAM expression. All the images in this figure are taken from unique confocal planes, except (*C*) and (*D*), which are 2D projections of reconstructions of 3 consecutive confocal planes located 1 μm apart. Scale bar: 20 μm. NeuN: neuronal nuclear antigen; MAP2: microtubule associated protein2; CAMKII: Ca^2+/calmodulin dependent protein kinase II.

Expression of Markers of Mature Neurons

PSA-NCAM expressing cells in paleocortex layer II rarely expressed NeuN (14 ± 1.93%, Fig. 1*E*). Moreover, in most of these scarce immunoreactive nuclei this expression was faint, especially in those corresponding to tangled cells. NeuN immunoreactivity was usually more intense in the nuclei of the larger PSA-NCAM expressing cell types (semilunar–pyramidal transitional, semilunar, pyramidal, and fusiform neurons). Tangled cells lack expression of MAP2 (Fig. 1*F*). However, faint MAP2 labeling could be found in some semilunar–pyramidal transitional neurons.

PSA-NCAM expressing cells in the paleocortex layer II did not express markers of principal neurons, such as Ca(2+)/CaM-dependent protein kinase II (CAMKII, Fig. 1*G*) or interneurons, such as GABA, GAD67, calbindin, parvalbumin, CR, somatostatin, neuropeptide Y, cholecystokinin, or vasointestinal peptide (Fig. 1*H*). Abundant cells expressing these markers can be found in the paleocortex, especially in deep layers (Supplemental Fig. 1*D–J*).

In order to unequivocally identify the neurogliaform phenotype of PSA-NCAM expressing cells in layer II of the adult paleocortex of rats (Nacher et al. 2002a), we performed double PSA-NCAM/α-actinin immunohistochemistry. Although some cells scattered in layers II and III expressed α-actinin, the expression of this protein was never found in any of the PSA-NCAM expressing cells in layer II (Supplemental Fig. 1*K*).

Expression of Markers of Immature Neurons and Neuronal Progenitor Cells

Many PSA-NCAM expressing cells, including all the subpopulations described in the precedent section, were also immunoreactive for DCX (87.4 ± 3.28%, Fig. 2*A*) and TUC-4

(68.7 ± 3.7%, Fig. 2*G*), as previously described (Nacher et al. 2000; Nacher, Crespo, McEwen, et al. 2001). Both proteins are intracytoplasmic and, consequently, allow a detailed observation of the cell morphology (Fig. 2*B–F*). The processes of tangled cells were usually devoid of spines or excrescences, but in some of the dendrites of semilunar and semilunar–pyramidal transition neurons, located in layer I, occasional bead-like swellings, protrusions resembling thin dendritic spines, or typical spines could be observed (Fig. 2*E,F*). DCX immunostaining also allowed the identification of basal thin processes in these large cells, which resembled an axon (Fig. 2*B–D*). Most, if not all, PSA-NCAM expressing cells also expressed the A3 subunit of the cyclic nucleotide-gated ion channel (CNGA-3; 97.6 ± 1.2%. Fig. 2*H*), which is strongly expressed by migrating neuroblasts of the rostral migratory stream (RMS) (Gutierrez-Mecinas et al. 2007). Moreover, most of PSA-NCAM expressing cells in the paleocortex layer II expressed phosphorylated cyclic adenosine monophosphate response element–binding protein (p-CREB) in their nuclei (94.6 ± 1.83%, Fig. 2*I*), a molecule expressed transiently in differentiating granule neurons of the adult

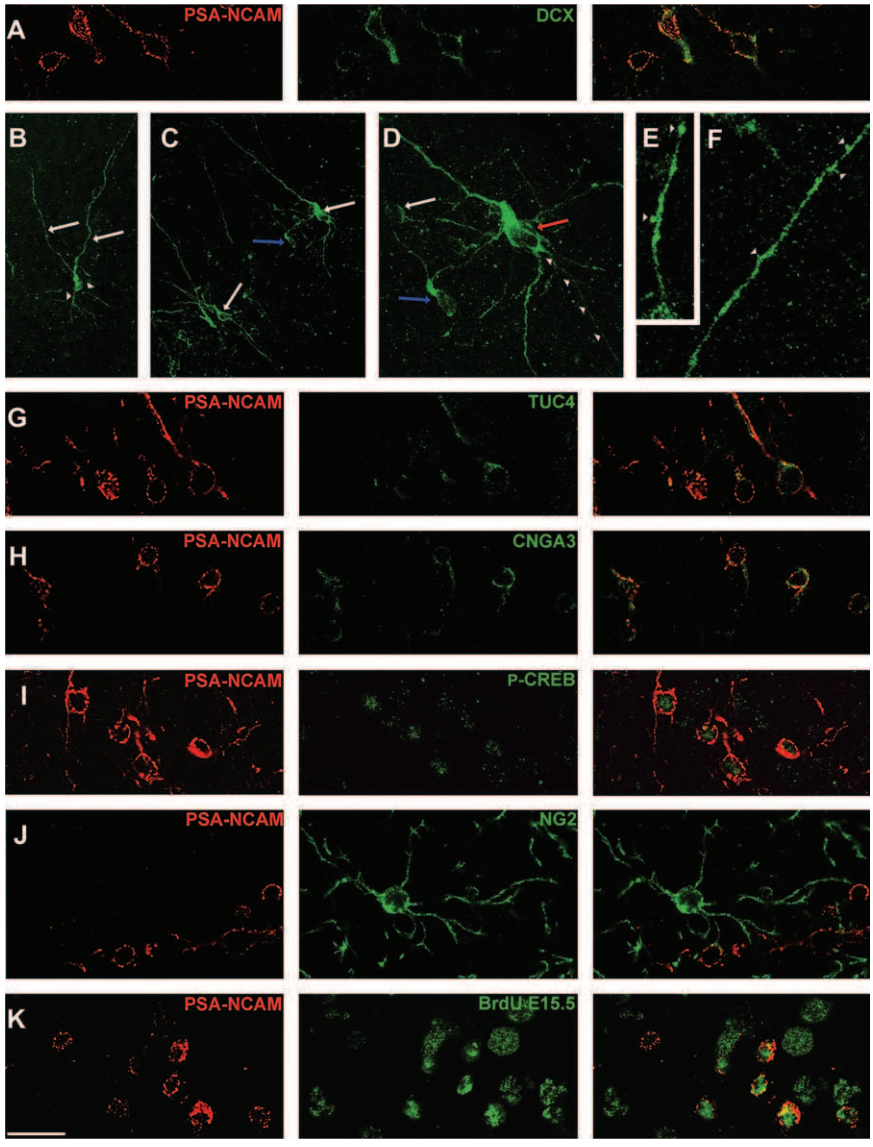

Figure 2. Confocal microscopic analysis of PSA-NCAM immunoreactive cells in the paleocortex layer II. (*A*) Cells coexpressing PSA-NCAM and DCX. (*B–F*) DCX expressing cells in the paleocortex layer II. (*B*) Typical semilunar–pyramidal transitional neuron. Observe the 2 apical dendrites (arrows) and the presence of a basal dendritic tree (arrowheads). (*C*) A couple of semilunar–pyramidal transition neurons (white arrows) in entorhinal cortex layer II. The blue arrow points to a tangled cell showing some characteristics of a semilunar neuron, such as the presence of 2 apical dendrites. (*D*) Detailed view of the cells shown on the right side of Fig. 3*C*. Note the presence of thick basal processes resembling dendrites and a thin process resembling an axon (arrowheads). Two typical tangled cells can be observed, one of them closely apposed to the semilunar–pyramidal transition neuron (red arrow) and the other located in the left margin of the figure (white arrow). (*E*, *F*) Entorhinal cortex layer I. High magnification view of dendritic processes from semilunar–pyramidal transition neurons. Observe the presence of several swellings, and protrusions resembling dendritic spines (arrowheads). (*G*) PSA-NCAM/TUC-4 immunoreactive cells. (*H*) Cells coexpressing PSA-NCAM and CNGA-3. (*I*) PSA-NCAM expressing cells displaying p-CREB expression in their nuclei. (*J*) Double PSA-NCAM/NG2 immunohistochemistry. Observe the absence of NG2 immunoreactivity in PSA-NCAM expressing cells. Some NG2 expressing processes can be observed in close apposition to PSA-NCAM expressing cell somata. (*K*) PSA-NCAM expressing cells containing BrdU immunoreactive nuclei in the piriform cortex of an adult rat injected with BrdU at E15.5. (*B*), (C), (D), (E), and (*F*) are 2D projections of reconstructions of 3 (*B–D*) or 2 (*A*, *B*) focal planes located 1 μm apart. Scale bar: 20 μm for (*A–D*) and (*G–J*). 10 μm for (*E*) and (*F*). DCX: doublecortin (C-18); TUC-4 (TOAD64 [Turned On After Division]/Ulip/CRMP); p-CREB: phospho-CREB (Ser133).

hippocampus (Nakagawa et al. 2002). Because immature neurons in the dentate gyrus of adult mice and olfactory bulb of adult mice expressed CR (Dominguez et al. 2003; Brandt et al. 2003), we have also analyzed the expression of this calcium binding protein in PSA-NCAM expressing cells of the paleocortex layer II of adult mice. None of these cells coexpressed CR.

PSA-NCAM expressing cells in paleocortex layer II did not coexpress proteins commonly found in neuronal precursor cells of the adult CNS, such as nestin (Doetsch et al. 1997; Nacher, Rosell, et al. 2001) (Supplemental Fig. 1*M*) or Pax6 (Nacher et al. 2005; Maekawa et al. 2005; Hack et al. 2005) (Supplemental Fig. 1*N*). Most PSA-NCAM expressing cells in layer II lack NG2 expression (99 ± 0.57%, Fig. 2*J*). However, occasionally we have found cells in which partial colocalization of PSA-NCAM and NG2 could be observed (Supplemental Fig. 2). Interestingly, some NG2 processes were found in close apposition to the somata of PSA-NCAM expressing cells (Fig. 2*J*).

BrdU Labeling

Proliferating Cells

In adult animals injected with BrdU and sacrificed 2 h later, some BrdU-labeled nuclei could be found scattered in layer II. However, none of these nuclei were found inside a PSA-NCAM expressing perikaryon.

Adult Neurogenesis

Although in all the groups (adult rats injected with BrdU and sacrificed 2, 4, 7, 14, 21, or 30 days later) some scarce BrdU-labeled nuclei were found in layers II and III (many of them appeared in pairs), we never found any of them located inside a PSA-NCAM expressing soma. PSA-NCAM immunoreactive cells displaying a BrdU-labeled nucleus could be found in areas with known adult neurogenetic activity (Supplemental Fig. 1*O*).

Neurogenesis during Early Youth

Some BrdU-labeled nuclei were found in the paleocortex layer II of animals injected with BrdU when they were 45 days old and sacrificed when they were 105 days old, but none of them appeared inside a PSA-NCAM expressing somata.

Embryonic Neurogenesis

In the adult rats which received BrdU at E11.5, only 2 ± 1.41% of PSA-NCAM expressing somata in the paleocortex layer II displayed BrdU labeled nuclei. In animals injected at E13.5, 23.5 ± 4.5% of PSA-NCAM expressing somata contained BrdU labeled nuclei. When BrdU was administered at E15.5, 74.75 ± 4.2% of PSA-NCAM expressing cells displayed BrdU labeled nuclei (Figs 2*K* and 3, Supplemental Fig. 3). Big BrdU-labeled nuclei lacking peripheral PSA-NCAM expression and resembling those of pyramidal neurons, usually showed a dispersed chromatin pattern, whereas the small labeled nuclei located inside PSA-NCAM expressing somata normally showed a more condensed pattern.

Electron Microscopy

A detailed analysis of PSA-NCAM, TUC-4, or CNG3A expressing somata in the paleocortex layer II showed that they had only a small rim of cytoplasm surrounding the nucleus (Fig. 4*A–C*, *F* and *G*). Many astroglial lamellae were found in close apposition to the plasma membrane both in the somata (Fig. 4*A–C*, *F*, and *G*), as well as in their processes (Fig. 4*D*,*J*). It was common to find swellings of the extracellular space adjacent to the portions of the plasmatic membrane not covered by these glial processes (Fig. 4*B*,*G*). In the nuclei of labeled cells, chromatin appeared slightly more compacted than in that of the neighboring nonlabeled pyramidal neurons and the presence of heterochromatin clumps was also more abundant in the labeled cells (Fig. 4*A–C*, *F*, and *G*). None of these immunoreactive cells had synapses on their somata or proximal processes in layer II. However, in layer I we found some very scarce asymmetric synapses with round clear vesicles contacting some of the labeled dendrites belonging to semilunar–pyramidal transitional cells (Fig. 4*H*,*I*).

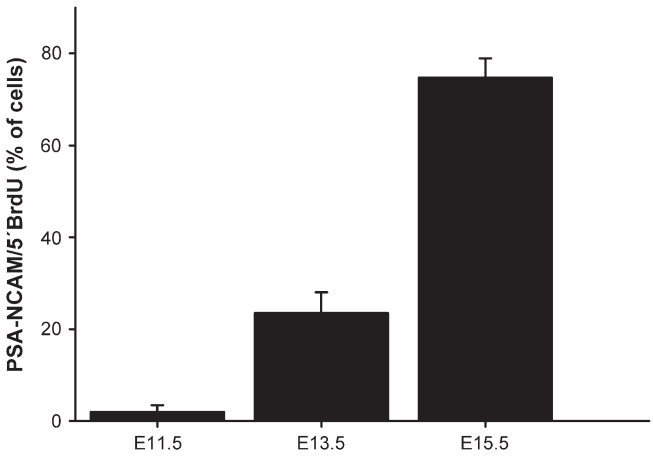

Figure 3. Graph representing the percentage of PSA-NCAM/5′BrdU double-labeled cells in the adult rats which received BrdU at E11.5, E13.5, and E15.5, respectively.

Markers of Cellular Activity

None of the PSA-NCAM expressing cells studied in the paleocortex layer II expressed c-Fos (Fig. 5*A*). Arc expression was also virtually absent from these cells (1 ± 0.36%) (Fig. 5*B*).

Expression of Glucocorticoid and NMDA Receptors

PSA-NCAM expressing cells in layer II of the paleocortex of adult rats did not coexpress glucocorticoid receptor (Fig. 5*C*). There were differences among the expression of NR1 subunit of the NMDA receptor among different cell types in the paleocortex layer II. Although none of the DCX expressing tangled cells studied expressed this receptor (Fig. 5*D*), the vast majority of larger cells (semilunar–pyramidal transition, semilunar, pyramidal, and fusiform neurons) expressed NR1 (92 ± 4%) (Fig. 5*E*).

Discussion

On the Nomenclature of PSA-NCAM Expressing Cells in the Paleocortex Layer II

To date there is not a consensus on the identity of the PSA-NCAM expressing cells in the paleocortex layer II. Seki and Arai (1991) described some of them as semilunar neurons (Seki and Arai 1991). O'Connell et al. (1997) described most of them as small neurons and also acknowledged the presence of some

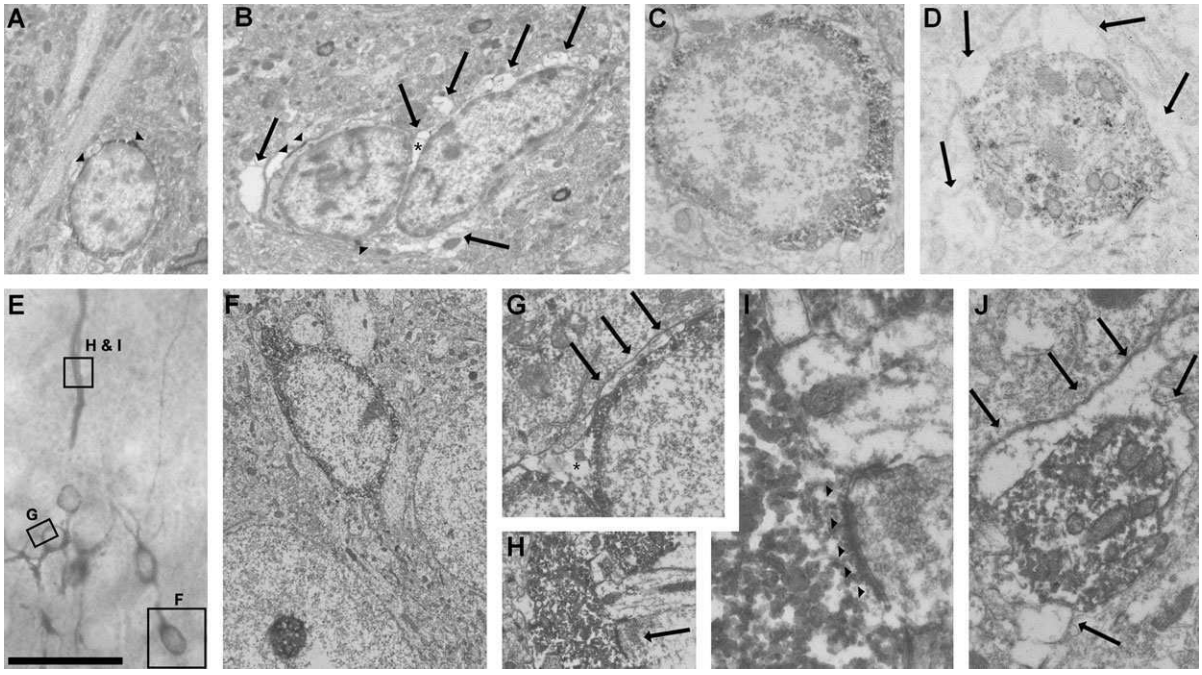

Figure 4. Electron micrographs of PSA-NCAM– (*A*, *B*), TUC-4– (*C*, *D*), and CNGA-3–immunolabeled cells (*E–I*) of the paleocortex layer II. (*A*, *B*) Somata of PSA-NCAM expressing cells. The couple of cells in panel B are intimately associated. PSA-NCAM immunoreactivity is especially abundant in certain regions associated with the plasma membrane (arrowheads). Note the presence of clear structures surrounding the labeled somata (arrows), corresponding to astroglial lamellae and swellings of the extracellular space (asterisk). Several heterochromatin clumps can be observed inside the nuclei of the labeled cells. (*C*) Soma of a TUC-4 expressing cell showing an intensely labeled cytoplasm and a nucleus displaying abundant heterochromatin. (*D*) Transversal section of a proximal process from a TUC-4 expressing cell. Some mitochondria and cisternae can be observed inside the immunoreactive cytoplasm. Note that this process is also surrounded by clear structures resembling astroglial lamellae (arrows). (*E*) View of the resin-embedded section from which the ultrathin sections shown in (*F–I*; squared areas) were obtained. (*F*) CNGA-3 immunoreactive cell surrounded by 2 unlabeled somata, probably corresponding to pyramidal neurons. (*G*) Detail of a couple of closely apposed tangled cells, in which the 2 nuclei, as well as the labeled cytoplasms, can be discerned. Note the presence of a swelling of the extracellular space (asterisk) and an astroglial lamella located closely to the plasma membrane (arrows). (*H*) Asymmetric synaptic contact (arrow) onto a CNGA-3 immunoreactive dendrite in layer I, corresponding to a semilunar–pyramidal transition neuron. (*I*) Detailed view of the synaptic contact (arrowheads) shown in (*H*). (*J*) Transversal section of a proximal process from a CNGA-3 immunoreactive cell surrounded by astroglial lamellae (arrows). Scale bar: 5 μm for (*A*), (*B*), and (*F*); 2.5 μm for (*C*) and (*G*); 1 μm for (*D*); 50 μm for (*E*); 1.5 μm for (*H*), 0.37 μm for (*I*) and (*J*). TUC-4 (TOAD64 [Turned On After Division]/Ulip/CRMP).

scarce PSA-NCAM expressing pyramidal neurons. In a previous study we have classified these cells mainly as neurogliaform neurons and pyramidal/semilunar transitional neurons, although we also found some PSA-NCAM expressing cells with the morphology of pyramidal neurons and fusiform cells in the paleocortex layer II (Nacher et al. 2002a). The present report has confirmed these previous results. However, we demonstrate that the abundant population of small PSA-NCAM expressing cells does not correspond to neurogliaform neurons. Neurogliaform neurons are mature interneurons, which usually express GABA, GAD, or α-actinin (Price et al. 2005), and none of these markers are expressed by the small cells in layer II. Given the intricate trajectories of their processes we have chosen to denominate them "tangled cells." It has to be noted, however, that some cells with characteristics of both tangled cells and semilunar neurons can be found, which may indicate a transition between these cell types. Although in rodents the distribution of PSA-NCAM–expressing cells in layer II appears to be restricted to the piriform, entorhinal, and perirhinal cortex (with some scarce cells located in the adjacent agranular insular and ectorhinal cortices), in mammals with larger cerebral cortices, such as rabbits (Bonfanti 2006), cats (E Varea and J Nacher, unpublished results), or primates (Kornack et al. 2005), there is a more widespread distribution of these cells, which can be found in layer II of most neocortical regions.

PSA-NCAM Expressing Cells in the Paleocortex Layer II are Immature Neurons

The present study provides evidence that the cells expressing PSA-NCAM in the paleocortex layer II are immature neurons. This evidence is based on 3 groups of experimental findings: 1) these cells do not express markers of mature neurons, 2) these cells express markers of immature neurons, and 3) their ultrastructural characteristics are typical of immature neurons.

Most of these cells lack expression of NeuN, a nuclear protein found in most mature neurons (Mullen et al. 1992), which is absent from immature neurons in the CNS neurogenic regions. It has to be noted, however, that certain mature neuronal populations, such as Purkinje cells, do not express NeuN (Mullen et al. 1992). However, none of the PSA-NCAM expressing cells in the paleocortex layer II express typical markers of interneurons or principal cells, thus excluding the possibility that they were mature but NeuN negative. The possibility that these cells were glia had to be investigated, because certain astrocytes (Theodosis et al. 1991; Shen et al. 1999) and oligodendrocyte precursors (Ben-Hur et al. 1998) express PSA-NCAM. However, the lack of expression of astroglial, oligodendroglial, and microglial markers completely excludes this hypothesis.

Despite its clear involvement in several neurodevelopmental events (see Bruses and Rutishauser 2001; Bonfanti 2006 for review), PSA-NCAM expression is not a sufficient criterion to

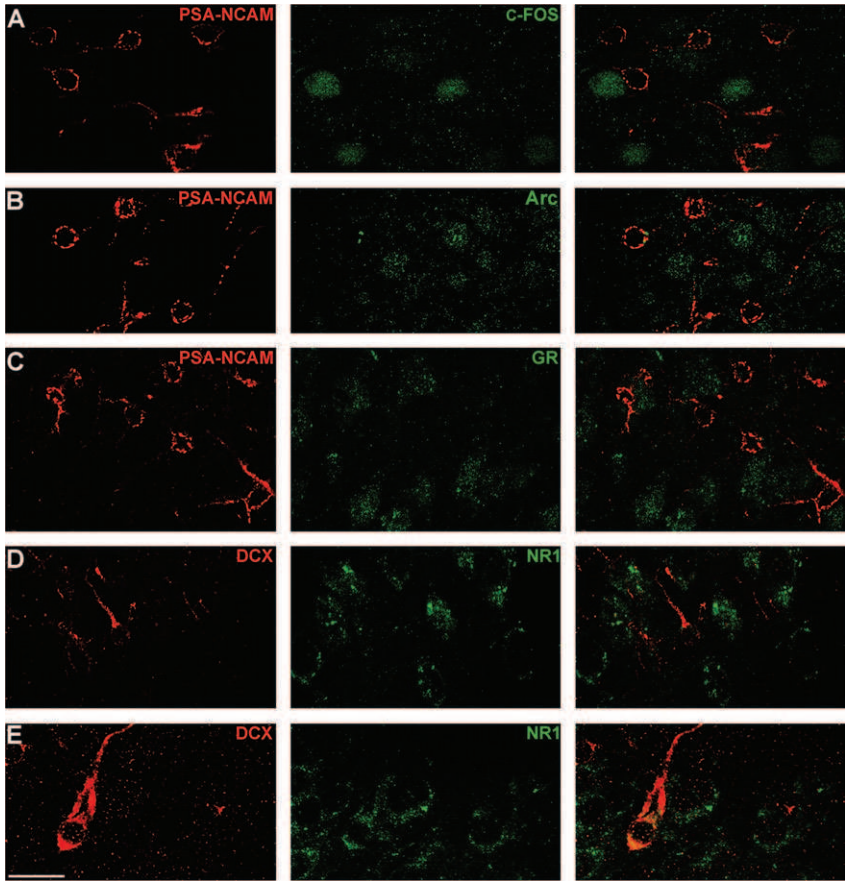

Figure 5. Confocal microscopic analysis of different markers on PSA-NCAM and DCX expressing cells in the paleocortex layer II. (*A*) PSA-NCAM expressing cells lacking c-Fos expression in their nuclei. (*B*) PSA-NCAM expressing cells lacking Arc expression in their nuclei. (*C*) PSA-NCAM immunoreactive cells lacking GR expression in their nuclei. (*D*) DCX expressing tangled cell lacking NR1 expression. (*E*) DCX expressing semilunar neuron expressing NR1 in its somata and proximal apical dendrite. All photographs in this figure correspond to single optical sections taken from z-stacks. Scale bar: 20 μm. Arc: activity-regulated cytoskeleton-associated protein.

classify a cell as an immature neuron, because some mature neurons do express this molecule in regions such as the neocortex and the hippocampus (Nacher et al. 2002a; Nacher, Blasco-Ibáñez, et al. 2002; Varea et al. 2005; Varea, Castillo-Gomez, Gomez-Climent, Blasco-Ibanez, et al. 2007). For this reason, we have investigated the expression of different proteins that are found in recently generated neurons during adulthood, both in the dentate gyrus and in the SVZ/RMS/olfactory bulb. DCX is a microtubule-associated protein expressed by migrating neuroblasts during embryonic development, which is also found in certain transiently amplifying progenitors and immature neurons in the granule cell layer and the SVZ/RMS/olfactory bulb (Brown et al. 2003). This molecule is also found in some cells in the striatum, located close to the lateral ventricle wall (Nacher, Crespo, McEwen, et al. 2001). Recent reports have clearly indicated that these cells are recently generated immature neurons, probably migrating from the SVZ (Yang et al. 2004; Dayer et al. 2005). The only other telencephalic region in which DCX-expressing cells can be found is the paleocortex layer II, indicating that these cells, also, should be considered immature neurons. In fact a recent report indicates that DCX is a protein exclusively expressed by progenitor cells or by cells restricted to the neuronal lineage (Walker et al. 2007). TUC-4 is also expressed by immature neurons during embryonic development (Minturn, Geschwind, et al. 1995) and is found in immature neurons of the adult dentate gyrus (Seki 2002) and SVZ (Bedard et al. 2002). However, this molecule is also found in other telencephalic regions where no evidence of adult neurogenesis has been found, such as the hypothalamus, and it is also present in a subset of oligodendrocytes in the adult CNS (Nacher et al. 2000). A recent report has described the presence of the CNGA-3 in migrating neuroblasts of the RMS (Gutierrez-Mecinas et al. 2007). p-CREB is also intensely expressed, although not exclusively, by immature neurons in the adult CNS (Nakagawa et al. 2002; Giachino et al. 2005).

Despite all the cautions that have to be taken into account regarding the expression of PSA-NCAM, TUC-4, CNGA-3, or p-CREB as exclusive markers of immature neurons, it is true that the coexpression of all these molecules has only been found in immature neurons of the neurogenic regions of the adult brain. In these neurogenic regions, up to 6 different cell types representing successive neurodevelopmental milestones can be identified. Following Kempermann's classification for the adult hippocampus (Kempermann et al. 2004): there is a multipotential precursor cell (type-1), which expresses nestin and GFAP. This precursor gives rise to 3 putative transiently amplifying progenitor cells, all of them lacking GFAP expression: type-2a cells express nestin alone, type-2b express nestin and DCX, and type-3 cells express DCX alone. These progenitors generate immature neurons, which retain DCX expression and start to express NeuN. These neuroblasts

progressively differentiate into mature neurons, which express NeuN and lack DCX expression. If we consider these neurodevelopmental milestones, the PSA-NCAM/DCX expressing cells in the adult paleocortex layer II can only correspond to type-3 cells or to immature neurons, because they do not express GFAP or nestin, they express DCX and PSA-NCAM and only a minor portion express NeuN. However, immature neurons in mice express CR (Jankovski and Sotelo 1996; Dominguez et al. 2003; Brandt et al. 2003) and we have not found the expression of this calcium binding protein in the PSA-NCAM/DCX expressing cells of adult mice paleocortex layer II. These cells cannot, however, be considered truly type-3 progenitors, because we have found that they do not proliferate. We believe that the PSA-NCAM/DCX expressing cells in the adult paleocortex layer II are in an intermediate stage between type-3 cells and differentiating neurons. They have been generated during embryonic development, abandoned their mitotic activity and migrated to their final destination. Once there, they seem to enter a "dormant" stage and show features of early immature neurons, although they (or most of them) do not appear to have entered the final phase of their neuronal differentiation program.

Adult Neurogenesis in the Paleocortex Layer II?

Two recent studies have reported the presence of adult neurogenesis in the piriform cortex of mice (Shapiro, Ng, Zhou, Ribak, et al. 2007) and rats (Pekcec et al. 2006) and a previous report indicated the existence of newly generated neurons in the paleocortex of adult primates (Bernier et al. 2002). Additionally, during the review process of the present study, a new report on adult neurogenesis in the rodent piriform cortex has been published by Ribak's group (Shapiro, Ng, Kinyamu, et al. 2007). A previous study has described the presence of individual SVZ-derived neurons in the anterior olfactory nucleus and anterior olfactory cortex of perinatal mice (De Marchis et al. 2004). However, these cells appear to be absent from the posterior piriform cortex, where more abundant PSA-NCAM expressing cells exist. De Marchis et al. did not find evidence of such cells in the olfactory cortex of adult animals. Although we have not studied perinatal animals, our present results indicate that, if some neurogenesis exists in olfactory cortical structures during early postnatal development, this phenomenon does not continue in young animals.

Although the existence of adult neurogenesis in the cerebral cortex is still a matter of debate (see Rakic 2002a; Gould 2007 for review), different reports have failed to find evidence that DCX, TUC-4, or PSA-NCAM expressing neurons in the paleocortex layer II of adult rats and mice (Nacher et al. 2002a; Fontana et al. 2005), rabbits (Luzzati et al. 2003), or primates (Kornack et al. 2005) are being generated during adulthood. In fact, the number of recently generated neurons found in the adult paleocortex (Pekcec et al. 2006; Shapiro, Ng, Kinyamu, et al. 2007; Shapiro, Ng, Zhou, Ribak, et al. 2007) is very low when compared with the number of DCX or PSA-NCAM cells present in this region and this may be the cause by which some studies did not find evidence of adult neurogenesis. Additionally, there is reason to believe that claims of adult cortical neurogenesis outside the dentate gyrus may be based on data misinterpretation (Nowakowski and Hayes 2000; Rakic 2002b). Moreover, the presence of newly generated neurons in the entorhinal cortex, where an extremely abundant population of PSA-NCAM expressing cells exists, has not been described in the adult rodent brain. It is also important to note that the previous reports on adult neurogenesis in the rodent piriform cortex do not explicitly indicate or quantify the presence of 5′BrdU labeled cells expressing DCX or NeuN in layer II (Pekcec et al. 2006; Shapiro, Ng, Kinyamu, et al. 2007; Shapiro, Ng, Zhou, Ribak, et al. 2007).

A recent report has described the presence of DCX/NG2 expressing cells in layer II of the piriform and entorhinal cortices of adult rats (Tamura et al. 2007). Although these authors did not find evidence PSA-NCAM expression in these cells, we have observed, that a very small subpopulation of tangled cells coexpresses NG2 and PSA-NCAM. It is interesting to note that we found that all DCX expressing cells in the paleocortex layer II also express PSA-NCAM (Nacher, Crespo, McEwen, et al. 2001) and that identical results have been found in our present material, using a different anti-DCX antibody. Tamura et al. have also shown that, in the cerebral cortex, some of these DCX expressing cells may be proliferating or have been recently generated. We have not found evidence of such dividing or recently generated cells in the paleocortex layer II of our samples. Tamura et al. state, however, that these cells are very faintly labeled with DCX immunohistochemistry and, consequently, we may have missed them. In any case, our results demonstrate that most of PSA-NCAM expressing cells in the paleocortex layer II are generated during embryonic development, in a stage that appears to coincide with, or to occur slightly before, that of most layer II neurons in this region (Bayer 1986).

Although the doses of BrdU used in our study are considered nontoxic in adult animals (Cameron and McKay 2001), some possible toxic effects of BrdU cannot be totally excluded (Taupin 2007), especially in the embryos.

Are PSA-NCAM Expressing Cells in the Paleocortex Layer II Functional?

A critical question arising from our study is what the function is of PSA-NCAM expressing cells in the adult paleocortex layer II. Our double labeling experiments indicate that they are early immature neurons, which apparently have detained their differentiation program and are in a "dormant" stage. The fact that these cells never expressed activity-related molecules, such as the immediate early genes c-Fos and Arc, may be also indicative of this "dormant" stage. Their ultrastructure also gives support to this hypothesis: These cells commonly show heterochromatin clumps and they appear to be surrounded by multiple astroglial lamellae and swellings of the extracellular space adjacent to the plasmatic membrane, which isolate them from the surrounding nervous parenchyma. Moreover, they normally do not show synaptic contacts on their somata or proximal processes. These are 2 characteristics found in early immature neurons in the adult dentate gyrus (Seki and Arai 1999; Shapiro et al. 2005). Moreover, the presence of astroglial processes and the absence of synapses on DCX expressing cell somata in the piriform cortex layer II has been reported during the review process of the present study (Shapiro, Ng, Kinyamu, et al. 2007). However, it appears that a subpopulation of PSA-NCAM expressing cells in the paleocortex layer II, mostly constituted by semilunar and semilunar–pyramidal transitional neurons does receive, although sparsely, excitatory synapses in its apical dendrites located in layer I, suggesting that these cells are in a more differentiated state. Moreover, these cells show dendritic protrusions resembling spines and thin basal

processes resembling axons. The fact that NeuN expression is more intense in these larger cells than in tangled cells also gives support to the hypothesis that large PSA-NCAM expressing cells in layer II are more mature than tangled cells, because similar increases in NeuN expression have been found during neuronal differentiation in the adult dentate gyrus (Kempermann et al. 2004; Marques-Mari et al. 2007). The fact that these larger cells also expressed the NR1 subunit of the NMDA receptor also supports this view, because this receptor is not expressed in early differentiating granule neurons in the adult dentate gyrus (Nacher et al. 2007). Although we have previously suggested that the expression of PSA-NCAM (Nacher et al. 2002a) in paleocortex layer II cells was linked to neuronal structural plasticity, our present results suggest that this expression, together with the astroglial covering, probably has an insulating role, which will prevent these cells from receiving synaptic inputs. We still do not have a plausible explanation for the expression of DCX or TUC-4 proteins in these cells, because during development these proteins are associated with a dynamic cytoskeleton, which is participating in neurite development or neuronal migration (Minturn, Fryer, et al. 1995; Francis et al. 1999).

The second intriguing point arisen by our study is the fate of PSA-NCAM expressing cells in the adult paleocortex layer II. Several studies have demonstrated that the number of these cells dramatically declines during aging (Abrous et al. 1997; Murphy et al. 2001; Varea, Castillo-Gomez, Gomez-Climent, Guirado, et al. 2007). This reduction is also observed when analyzing DCX or TUC-4 expression (J Nacher, unpublished observations). There are 2 possible explanations for this reduction in the expression of immature neuronal markers: 1) the cells expressing these proteins are progressively dying or 2) they are differentiating into mature neurons, which lack these markers. Both explanations are plausible. However, when observing the paleocortex layer II of 6-, 12-, or 24-month-old rats we have failed to find substantial numbers of pyknotic nuclei (J Nacher, unpublished observations). The second possibility appears more likely, and it is tempting to think that tangled cells could mature eventually into some of the larger PSA-NCAM expressing cells and then into mature neurons. This is supported by the fact that intermediate cell types between tangled and larger cells are habitually found in layer II and that, as discussed above, larger cells appear more mature than tangled cells. Then PSA-NCAM expressing cells in the paleocortex layer II may constitute a "reservoir," which in different circumstances may complete its differentiation program. These modulations of PSA-NCAM expression in the paleocortex layer II are probably mediated by glucocorticoids (Nacher et al. 2004) and excitatory amino acids acting on NMDA receptors (Nacher et al. 2002a). However, a direct effect has to be excluded, because, as we have shown, PSA-NCAM expressing cells in layer II rarely express glucocorticoid or NMDA receptors. We still do not know the significance of these changes in PSA-NCAM expression. Although the number of PSA-NCAM expressing cells in the piriform cortex layer II increases 21 days after a single injection of NMDA receptor antagonist (Nacher et al. 2002b), we have not observed incorporation of newly generated neurons after this treatment (J Nacher, unpublished results). This suggests that PSA-NCAM expression upregulation occurs in preexisting cells, either in cells in which PSA-NCAM was already expressed, although at undetectable levels, or in cells that did not express PSA-NCAM before the treatment. Experiments that follow the fate of PSA-NCAM expressing cells after different experimental treatments and during aging will shed light on the mysterious nature of these cells.

Supplementary Material

Supplementary material can be found at: http://www.cercor.oxfordjournals.org/.

Funding

GV04A-134, GV04A-076, GVACOMP07/169, MEC2006-BFU07313/BFI, Foundation Jerome Lejeune; and MEC BFU2004-00931. Postdoctoral fellowship for stays in Research Excellence Centers located in the Comunitat Valenciana from the Generalitat Valenciana to E.V.; predoctoral fellowships (FPU) from the Spanish Ministry of Education and Science to M.A.G.-C. and E.C.-G.; and predoctoral fellowship (FPI) from the Spanish Ministry of Education and Science to R.G.

Notes

The authors are grateful to Dr Bruce McEwen and Dr Tatsunori Seki for their comments on the manuscript. *Conflict of Interest*: None declared.

Address correspondence to Dr Juan Nàcher, Neurobiology Unit and Program in Basic and Applied Neurosciences, Cell Biology Dpt., Universitat de València, Dr. Moliner, 50, Burjassot 46100, Spain. Email: nacher@uv.es.

References

Abrous DN, Montaron MF, Petry KG, Rougon G, Darnaudery M, Le Moal M, Mayo W. 1997. Decrease in highly polysialylated neuronal cell adhesion molecules and in spatial learning during ageing are not correlated. Brain Res. 744:285–292.

Bayer SA. 1986. Neurogenesis in the rat primary olfactory cortex. Int J Dev Neurosci. 4:251–271.

Bedard A, Levesque M, Bernier PJ, Parent A. 2002. The rostral migratory stream in adult squirrel monkeys: contribution of new neurons to the olfactory tubercle and involvement of the antiapoptotic protein Bcl-2. Eur J Neurosci. 16:1917–1924.

Ben-Hur T, Rogister B, Murray K, Rougon G, Dubois-Dalcq M. 1998. Growth and fate of PSA-NCAM+ precursors of the postnatal brain. J Neurosci. 18:5777–5788.

Bernier PJ, Bedard A, Vinet J, Levesque M, Parent A. 2002. Newly generated neurons in the amygdala and adjoining cortex of adult primates. Proc Natl Acad Sci USA. 20(99):11464–11469.

Bonfanti L. 2006. PSA-NCAM in mammalian structural plasticity and neurogenesis. Prog Neurobiol. 80:129–164.

Brandt MD, Jessberger S, Steiner B, Kronenberg G, Reuter K, Bick-Sander A, von der BW, Kempermann G. 2003. Transient calretinin expression defines early postmitotic step of neuronal differentiation in adult hippocampal neurogenesis of mice. Mol Cell Neurosci. 24:603–613.

Brown JP, Couillard-Despres S, Cooper-Kuhn CM, Winkler J, Aigner L, Kuhn HG. 2003. Transient expression of doublecortin during adult neurogenesis. J Comp Neurol. 467:1–10.

Bruses JL, Rutishauser U. 2001. Roles, regulation, and mechanism of polysialic acid function during neural development. Biochimie. 83:635–643.

Cameron HA, McKay RDG. 2001. Adult neurogenesis produces a large pool of new granule cells in the dentate gyrus. J Comp Neurol. 435:406–417.

Dayer AG, Cleaver KM, Abouantoun T, Cameron HA. 2005. New GABAergic interneurons in the adult neocortex and striatum are generated from different precursors. J Cell Biol. 168:415–427.

De Marchis S, Fasolo A, Puche AC. 2004. Subventricular zone-derived neuronal progenitors migrate into the subcortical forebrain of postnatal mice. J Comp Neurol. 476:290–300.

Doetsch F, Garciá-Verdugo JM, Alvarez-Buylla A. 1997. Cellular composition and three-dimensional organization of the subventricular germinal zone in the adult mammalian brain. J Neurosci. 17:5046–5061.
Dominguez MI, Blasco-Ibanez JM, Crespo C, Marques-Mari AI, Martinez-Guijarro FJ. 2003. Calretinin/PSA-NCAM immunoreactive granule cells after hippocampal damage produced by kainic acid and DEDTC treatment in mouse. Brain Res. 966:206–217.
Fontana X, Nacher J, Soriano E, Del Rio JA. 2005. Cell proliferation in the adult hippocampal formation of rodents and its modulation by entorhinal and Fimbria-Fornix afferents. Cereb Cortex. 16:301–12.
Fox GB, Fichera G, Barry T, O' CA, Gallagher HC, Murphy KJ, Regan CM. 2000. Consolidation of passive avoidance learning is associated with transient increases of polysialylated neurons in layer II of the rat medial temporal cortex. J Neurobiol. 45:135–141.
Francis F, Koulakoff A, Boucher D, Chafey P, Schaar B, Vinet MC, Friocourt G, McDonnell N, Reiner O, Kahn A, et al. 1999. Doublecortin is a developmentally regulated, microtubule-associated protein expressed in migrating and differentiating neurons. Neuron. 23:247–256.
Giachino C, De Marchis S, Giampietro C, Parlato R, Perroteau I, Schutz G, Fasolo A, Peretto P. 2005. cAMP response element-binding protein regulates differentiation and survival of newborn neurons in the olfactory bulb. J Neurosci. 25:10105–10118.
Gleeson JG, Lin PT, Flanagan LA, Walsh CA. 1999. Doublecortin is a microtubule-associated protein and is expressed widely by migrating neurons. Neuron. 23:257–271.
Gould E. 2007. How widespread is adult neurogenesis in mammals? Nat Rev Neurosci. 8:481–488.
Gutierrez-Mecinas M, Crespo C, Blasco-Ibanez JM, Nacher J, Varea E, Martinez-Guijarro FJ. 2007. Migrating neuroblasts of the rostral migratory stream are putative targets for the action of nitric oxide. Eur J Neurosci. 26:392–402.
Haberly LB. 1983. Structure of the piriform cortex of the opossum. I. Description of neuron types with Golgi methods. J Comp Neurol. 213:163–187.
Hack MA, Saghatelyan A, de Chevigny A, Pfeifer A, Ashery-Padan R, Lledo PM, Gotz M. 2005. Neuronal fate determinants of adult olfactory bulb neurogenesis. Nat Neurosci. 8:865–872.
Jankovski A, Sotelo C. 1996. Subventricular zone-olfactory bulb migratory pathway in the adult mouse: cellular composition and specificity as determined by heterochronic and heterotopic transplantation. J Comp Neurol. 371:376–396.
Kempermann G. 2005. Adult neurogenesis. Oxford: Oxford University Press.
Kempermann G, Jessberger S, Steiner B, Kronenberg G. 2004. Milestones of neuronal development in the adult hippocampus. Trends Neurosci. 27:447–452.
Kornack DR, Kelly EA, Shannon DE. 2005. Persistent doublecortin expression identifies a novel neuronal population in adult primate neocortex. Program No. 143.10.2005 Abstract Viewer/Itinerary Planner. Washington (DC): Society for Neuroscience.
Kosaka T, Kosaka K, Tateishi K, Hamaoka Y, Yanaihara N, Wu JY, Hama K. 1985. GABAergic neurons containing CCK-8-like and/or VIP-like immunoreactivities in the rat hippocampus and dentate gyrus. J Comp Neurol. 239:420–430.
Lewis Carl SA, Gillete-Ferguson I, Ferguson DG. 1993. An indirect immunofluorescence procedure for staining the same cryosection with two mouse monoclonal primary antibodies. J Histochem Cytochem. 41:1273–1278.
Luzzati F, Peretto P, Aimar P, Ponti G, Fasolo A, Bonfanti L. 2003. Glia-independent chains of neuroblasts through the subcortical parenchyma of the adult rabbit brain. Proc Natl Acad Sci USA. 100:13036–13041.
Maekawa M, Takashima N, Arai Y, Nomura T, Inokuchi K, Yuasa S, Osumi N. 2005. Pax6 is required for production and maintenance of progenitor cells in postnatal hippocampal neurogenesis. Genes Cells. 10:1001–1014.
Marques-Mari AI, Nacher J, Crespo C, Gutierrez-Mecinas M, Martinez-Guijarro FJ, Blasco-Ibanez JM. 2007. Loss of input from the mossy cells blocks maturation of newly generated granule cells. Hippocampus. 17:510–524.
Minturn JE, Fryer HJ, Geschwind DH, Hockfield S. 1995. TOAD-64, a gene expressed early in neuronal differentiation in the rat, is related to unc-33, a C. elegans gene involved in axon outgrowth. J Neurosci. 15:6757–6766.
Minturn JE, Geschwind DH, Fryer HJ, Hockfield S. 1995. Early postmitotic neurons transiently express TOAD-64, a neural specific protein. J Comp Neurol. 355:369–379.
Mullen RJ, Buck CR, Smith AM. 1992. NeuN, a neuronal specific nuclear protein in vertebrates. Development. 116:201–211.
Murphy KJ, Fox GB, Foley AG, Gallagher HC, O'Connell A, Griffin AM, Nau H, Regan CM. 2001. Pentyl-4-yn-valproic acid enhances both spatial and avoidance learning, and attenuates age-related NCAM-mediated neuroplastic decline within the rat medial temporal lobe. J Neurochem. 78:704–714.
Nacher J, Alonso-Llosa G, Rosell D, McEwen B. 2002a. PSA-NCAM expression in the piriform cortex of the adult rat. Modulation by NMDA receptor antagonist administration. Brain Res. 927: 111–121.
Nacher J, Alonso-Llosa G, Rosell DR, McEwen BS. 2002b. PSA-NCAM expression in the piriform cortex of the adult rat. Modulation by NMDA receptor antagonist administration. Brain Res. 927:111–121.
Nacher J, Blasco-Ibáñez JM, McEwen BS. 2002. Non-granule PSA-NCAM immunoreactive neurons in the rat hippocampus. Brain Res. 930:1–11.
Nacher J, Crespo C, McEwen BS. 2001. Doublecortin expression in the adult rat telencephalon. Eur J Neurosci. 14:629–644.
Nacher J, Pham K, Gil-Fernandez V, McEwen BS. 2004. Chronic restraint stress and chronic corticosterone treatment modulate differentially the expression of molecules related to structural plasticity in the adult rat piriform cortex. Neuroscience. 26:503–509.
Nacher J, Rosell DR, Alonso-Llosa G, McEwen BS. 2001. NMDA receptor antagonist treatment induces a long lasting increase in the number of proliferating cells, PSA-NCAM immunoreactive granule neurons and radial glia in the adult rat dentate gyrus. Eur J Neurosci. 13:512–520.
Nacher J, Rosell DR, McEwen BS. 2000. Widespread expression of rat collapsin response-mediated protein 4 in the telencephalon and other areas of the adult rat central nervous system. J Comp Neurol. 424:628–639.
Nacher J, Varea E, Blasco-Ibanez JM, Castillo-Gomez E, Crespo C, Martinez-Guijarro FJ, McEwen BS. 2005. Expression of the transcription factor Pax 6 in the adult rat dentate gyrus. J Neurosci Res. 81:753–761.
Nacher J, Varea E, Miguel Blasco-Ibanez J, Gomez-Climent MA, Castillo-Gomez E, Crespo C, Martinez-Guijarro FJ, McEwen BS. 2007. N-methyl-d-aspartate receptor expression during adult neurogenesis in the rat dentate gyrus. Neuroscience. 144:855–864.
Nakagawa S, Kim JE, Lee R, Chen J, Fujioka T, Malberg J, Tsuji S, Duman RS. 2002. Localization of phosphorylated cAMP response element-binding protein in immature neurons of adult hippocampus. J Neurosci. 22:9868–9876.
Nowakowski RS, Hayes NL. 2000. New neurons: extraordinary evidence or extraordinary conclusion? Science. 288:771.
O'Connell AW, Fox GB, Barry T, Murphy KJ, Fichera G, Foley AG, Kelly J, Regan CM. 1997. Spatial learning activates neural cell adhesion molecule polysialylation in a corticohippocampal pathway within the medial temporal lobe. J Neurochem. 68:2538–2546.
Pekcec A, Loscher W, Potschka H. 2006. Neurogenesis in the adult rat piriform cortex. Neuroreport. 17:571–574.
Price CJ, Cauli B, Kovacs ER, Kulik A, Lambolez B, Shigemoto R, Capogna M. 2005. Neurogliaform neurons form a novel inhibitory network in the hippocampal CA1 area. J Neurosci. 25:6775–6786.
Rakic P. 2002a. Adult neurogenesis in mammals: an identity crisis. J Neurosci. 22:614–618.
Rakic P. 2002b. Neurogenesis in adult primate neocortex: an evaluation of the evidence. Nat Rev Neurosci. 3:65–71.
Seki T. 2002. Expression patterns of immature neuronal markers PSA-NCAM, CRMP-4 and NeuroD in the hippocampus of young adult and aged rodents. J Neurosci Res. 70:327–334.

Seki T, Arai Y. 1991. Expression of highly polysialylated NCAM in the neocortex and piriform cortex of the developing and the adult rat. Anat Embryol Berl. 184:395–401.
Seki T, Arai Y. 1993. Distribution and possible roles of the highly polysialylated neural cell adhesion molecule (NCAM-H) in the developing and adult central nervous system. Neurosci Res. 17:265–290.
Seki T, Arai Y. 1999. Temporal and spatial relationships between PSA-NCAM-expressing, newly generated granule cells, and radial glia-like cells in the adult dentate gyrus. J Comp Neurol. 410:503–513.
Shapiro LA, Korn MJ, Shan Z, Ribak CE. 2005. GFAP-expressing radial glia-like cell bodies are involved in a one-to-one relationship with doublecortin-immunolabeled newborn neurons in the adult dentate gyrus. Brain Res. 1040:81–91.
Shapiro LA, Ng KL, Kinyamu R, Whitaker-Azmitia P, Geisert EE, Blurton-Jones M, Zhou QY, Ribak CE. 2007. Origin, migration and fate of newly generated neurons in the adult rodent piriform cortex. Brain Struct Funct. 212:133–148.
Shapiro LA, Ng KL, Zhou QY, Ribak CE. 2007. Olfactory enrichment enhances the survival of newly born cortical neurons in adult mice. Neuroreport. 18:981–985.
Shen H, Glass JD, Seki T, Watanabe M. 1999. Ultrastructural analysis of polysialylated neural cell adhesion molecule in the suprachiasmatic nuclei of the adult mouse. Anat Rec. 256:448–457.
Tamura Y, Kataoka Y, Cui Y, Takamori Y, Watanabe Y, Yamada H. 2007. Multi-directional differentiation of doublecortin- and NG2-immunopositive progenitor cells in the adult rat neocortex in vivo. Eur J Neurosci. 25:3489–3498.
Taupin P. 2007. BrdU immunohistochemistry for studying adult neurogenesis: paradigms, pitfalls, limitations, and validation. Brain Res Rev. 53:198–214.
Theodosis DT, Rougon G, Poulain DA. 1991. Retention of embryonic features by an adult neuronal system capable of plasticity: polysialylated neural cell adhesion molecule in the hypothalamo-neurohypophysial system. Proc Natl Acad Sci USA. 88:5494–5498.
Varea E, Castillo-Gomez E, Gomez-Climent MA, Blasco-Ibanez JM, Crespo C, Martinez-Guijarro FJ, Nacher J. 2007. PSA-NCAM expression in the human prefrontal cortex. J Chem Neuroanat. 33:202–209.
Varea E, Castillo-Gomez E, Gomez-Climent MA, Guirado R, Blasco-Ibáñez JM, Crespo C, Martínez-Guijarro FJ, Nacher J. 2007. Differential evolution of PSA-NCAM expression during aging of the rat telencephalon. Neurobiol Aging. [Epub ahead of print].
Varea E, Nacher J, Blasco-Ibanez JM, Gomez-Climent MA, Castillo-Gomez E, Crespo C, Martinez-Guijarro FJ. 2005. PSA-NCAM expression in the rat medial prefrontal cortex. Neuroscience. 136:435–443.
Walker TL, Yasuda T, Adams DJ, Bartlett PF. 2007. The doublecortin-expressing population in the developing and adult brain contains multipotential precursors in addition to neuronal-lineage cells. J Neurosci. 27:3734–3742.
Yang HK, Sundholm-Peters NL, Goings GE, Walker AS, Hyland K, Szele FG. 2004. Distribution of doublecortin expressing cells near the lateral ventricles in the adult mouse brain. J Neurosci Res. 76:282–295.

Neuroscience Letters 457 (2009) 12–15

Contents lists available at ScienceDirect

Neuroscience Letters

journal homepage: www.elsevier.com/locate/neulet

Effects of chronic fluoxetine treatment on the rat somatosensory cortex: Activation and induction of neuronal structural plasticity

R. Guirado, E. Varea, E. Castillo-Gómez, M.A. Gómez-Climent, L. Rovira-Esteban, J.M. Blasco-Ibáñez, C. Crespo, F.J. Martínez-Guijarro, J. Nàcher*

Neurobiology Unit and Program in Basic and Applied Neurosciences, Cell Biology Dpt., Universitat de València., Spain

ARTICLE INFO

Article history:
Received 3 February 2009
Received in revised form 27 March 2009
Accepted 30 March 2009

Keywords:
Spine density
Structural plasticity
c-fos
GAD67
Antidepressant
PSA-NCAM

ABSTRACT

Recent hypotheses support the idea that disruption of normal neuronal plasticity mechanisms underlies depression and other psychiatric disorders, and that antidepressant treatment may counteract these changes. In a previous report we found that chronic fluoxetine treatment increases the expression of the polysialylated form of the neural cell adhesion molecule (PSA-NCAM), a molecule involved in neuronal structural plasticity, in the somatosensory cortex. In the present study we intended to find whether, in fact, cell activation and neuronal structural remodeling occur in parallel to changes in the expression of this molecule. Using immunohistochemistry, we found that chronic fluoxetine treatment caused an increase in the expression of the early expression gene c-fos. Golgi staining revealed that this treatment also increased spine density in the principal apical dendrite of pyramidal neurons. These results indicate that, apart from the medial prefrontal cortex or the hippocampus, other cortical regions can respond to chronic antidepressant treatment undergoing neuronal structural plasticity.

Although the neurobiological bases of depression are not well understood, it has been proposed that dysfunction of the mechanisms of neuronal plasticity may be involved [3,6]. Moreover, antidepressant drugs may act by normalizing this neural plasticity [6,5,13]. Structural plastic processes, such as dendritic or spine remodelling, have been observed in animal models of depression [12,37] and after antidepressant treatment [10], specially in the amygdala, the hippocampus and the medial prefrontal cortex (mPFC) (see [24] for review). This structural remodelling may be mediated by changes in the expression of cytoskeletal proteins or cell adhesion molecules, such as the polysialylated form of the neural cell adhesion molecule (PSA-NCAM) [2,8,30]. In fact, the antidepressant fluoxetine, a serotonin reuptake inhibitor, increases the expression of PSA-NCAM in the mPFC, the hippocampal CA3 stratum lucidum and the visual and somatosensory cortices [38,39].

To date, there is no direct evidence that the somatosensory cortex is affected by depression, although animal models of this mental disorder show alterations in the physiology of this cortical region [35] and antidepressants modulate somatosensory-related functions when administered locally [15]. The finding of an altered expression of PSA-NCAM in the somatosensory cortex after chronic treatment with fluoxetine [39] has prompted us to study whether the structure and activity of this cortical region is also modified after antidepressant treatment.

We have used twelve male Sprague–Dawley rats (4 months old, 320 ± 50 g, Harlan Iberica), which were chronically injected intraperitoneally either with the antidepressant fluoxetine ($n = 6$, 10 mg/kg), or with saline solution ($n = 6$), during 14 days (once daily at 10.00 am). All animal experimentation was conducted in accordance with the European Communities Council Directive of 24 November 1986 (86/609/EEC). Rats were perfused transcardially under deep chloral hydrate anaesthesia (chloral hydrate at 4%, 1 mL/100 g) with saline and then 4% paraformaldehyde in sodium phosphate buffer (PB 0.1 M, pH 7.4). After perfusion, the brains were extracted and stored in PB until used.

In order to study cellular activation in the somatosensory cortex the left hemisphere was cut into 50 μm thick sections with a freezing sliding microtome and immunohistochemically stained for the immediate early gene c-fos. Briefly, sections were incubated with 5% normal donkey serum (NDS) (Abcys) in PBS with 0.2% Triton-X100 (Sigma) for 1 h, and then overnight with rabbit polyclonal anti-c-fos K25 (1:2000; Santa Cruz Biotechnology, Inc.). After washing, sections were incubated for 30 min with biotinilated donkey anti-rabbit IgG (1:200; Jackson Immunoresearch), followed by an avidin-biotin-peroxidase complex (ABC, Vector Laboratories) for 30 min in PBS. Color development was achieved by incubating with 3,3′-diaminobenzidine tetrahydrochloride (DAB, Sigma) for 4 min. All the sections were coded to avoid any bias and,

* Corresponding author at: Neurobiology, Cell Biology Dpt., Universitat de València, Dr. Moliner, 50, Burjassot, 46100, Valencia, Spain. Tel.: +34 96 354 3241; fax: +34 96 354 3404.
E-mail address: nacher@uv.es (J. Nàcher).

0304-3940/$ – see front matter © 2009 Elsevier Ireland Ltd. All rights reserved.
doi:10.1016/j.neulet.2009.03.104

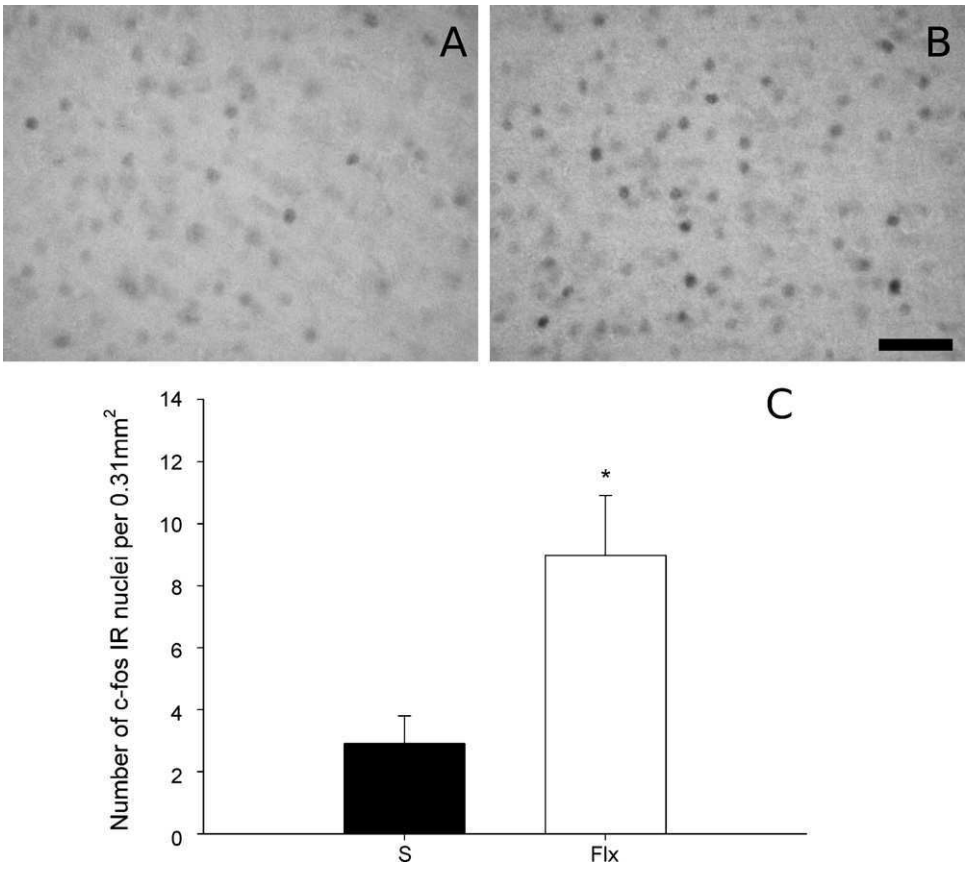

Fig. 1. A, B: Photographs showing coronal sections of c-fos immunoreactive nuclei in layers III to V of the somatosensory cortex of a control rat (A) and a rat treated for 14 days with fluoxetine (B). C: Graphs representing changes in the number of c-fos immunoreactivity nuclei in the primary somatosensory cortex after chronic fluoxetine treatment. Statistically significant (* 0.01), unpaired *t*-test. White bar represents control animals and black bar represents fluoxetine treated animals. Scale bar: 50 μm.

when processed, passed through all procedures simultaneously to minimize any difference from immunohistochemical staining itself. c-fos immunoreactive nuclei quantification was performed in two different sections containing the primary somatosensory cortex (between Bregma −2.80 mm and Bregma −3.10) in layers III, IV and V. Images were captured with a 40× objective under bright-field illumination, homogeneously lighted and digitalized using a CCD camera attached to the microscope. After background subtraction and histogram normalization, the region was selected using systematic criteria, and analyzing the whole image for the automated counting. Then the pictures were analyzed with Image J software (NIH) with a protocol for automated counting of stained nuclei based on the one described by [40]. Briefly, images were binarized using the same value of the gray histogram for all the images. Then the images were eroded and dilated. Objects smaller than 400 pixels were discarded.

In order to study spine density in pyramidal cells, the right hemisphere was processed for Golgi method. Tissue blocks (2.5–3 mm) were fixed with 3% potassium dichromate and 5% glutaraldehyde during 7 days and then impregnated with silver nitrate solution (0.75%) for 48 h. Then, the brains were cut into 150 μm-thick sections with a vibratome immersed in 70% ethanol, dehydrated with 100% ethanol and mounted with epoxy resin between two coverslips. To avoid any bias in the analysis, the slides were coded, and the code was not broken until the analysis was completed. Spine quantification was carried out in each animal in six pyramidal neurons from layers III, IV and V, which were randomly selected inside somatosensory primary cortex (S1) area. A total of 48 neurons were analyzed. In order to be suitable for dendritic spine analysis, neurons should follow these features: (i) they must display complete Golgi impregnation of the principal apical dendrite, (ii) the cell type must be identifiable and (iii) the minimum length of the apical dendrite must be 200 μm from the soma. The spine density was calculated in fragments of 50 μm length beginning from the soma.

In the somatosensory cortex c-fos expressing nuclei were widely distributed across all the layers, although they appeared to be less abundant in layer IV. This expression pattern is similar to that observed in other adjacent neocortical regions, although in these areas layer IV appeared more populated. Chronic fluoxetine treatment induced a, three fold, statistically significant increase ($p = 0.021$) in the number of c-fos immunolabeled nuclei in the primary somatosensory cortex (Fig. 1).

In both control and fluoxetine treated animals we observed that the dendritic spine density was lower in the proximal segment and that it increased progressively towards the apical extreme of the principal dendrite (Fig. 2A). There were significant differences in the spine density between the first and second segments ($p = 0.003$), the second and the third ($p < 0.0001$) and the third and the forth ($p = 0.042$), according to the distance from the soma.

After 14 days of fluoxetine treatment, we did not found differences in the dendritic spine density of the proximal segments (0–50 μm). However, significant differences were observed in the second ($p = 0.01$, 50–100 μm), the third ($p < 0.0001$, 100–150 μm) and the fourth segments ($p = 0.0006$, 150–200 μm) (Fig. 2A). Significant increases were also observed when considering the entire length of apical dendrites of pyramidal neurons in the primary somatosensory cortex ($p < 0.001$) (Fig. 2B).

The present results indicate that antidepressant treatment activates the somatosensory cortex and induces dendritic spine remodelling of pyramidal neurons in this cortical region, thus

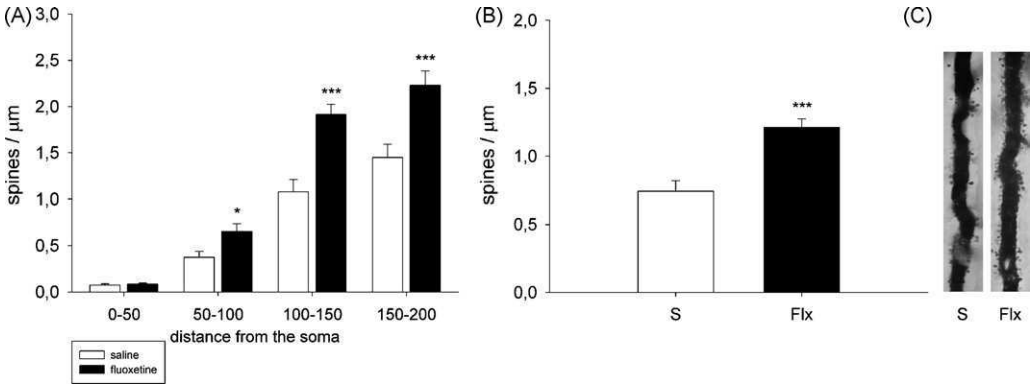

Fig. 2. Changes in spine density in the principal apical dendrite of pyramidal neurons in primary somatosensory cortex layers III and V after chronic fluoxetine treatment. Spine density histograms in the different 50 μm fragments from the soma (A) and in the total length of the measured dendrite (B). Statistically significant (* 0.05, ** 0.01, *** 0.001) unpaired *t*-test. White bars represent control animals and black bars represent treated animals. C: Photographs of a principal dendrite of a control animal (left) and an animal chronically treated with fluoxetine.

expanding the repertoire of regions that respond to these pharmacological compounds with structural plasticity.

The increase of in spine density that we have found may be related to a parallel increase in PSA-NCAM expression in this area [39], since the expression of this molecule, through its anti-adhesive properties, facilitates structural plastic events, such as neurite or spine remodeling and synaptogenesis (see [2,8,30] for review).

These results of the present study are similar to those shown in a previous report describing an increase in the number of spine synapses in pyramidal neurons of the hippocampus after 5 and 14 days of treatment with fluoxetine [10], a region in which chronic antidepressant treatment also increases PSA-NCAM expression [31,39]. Conversely, the opposite effect has been found in different studies with animal models of depression, such as chronic stress or olfactory bulbectomy. Chronic stress decreases dendritic branching and spine density in principal neurons of the medial prefrontal cortex (mPFC) pyramidal neurons [4,26,27] and the hippocampus [12,37]. Reduction of spine density is also observed in all hippocampal fields after olfactory bulbectomy [22]. Interestingly, these effects on neuronal structure, at least in the hippocampus, are reverted by antidepressant treatment. Apparently, these changes in spine density do not imply a parallel increase in the density of synapses, because the expression of synaptophysin, a reliable index of synaptic density [7,14], did not change in the somatosensory cortex after chronic fluoxetine treatment [39]. It is, however, possible that the changes in synaptophysin were under the detection limits of the methodology employed. An alternative explanation is that, after the treatment, many synapses making contact with dendritic shafts may have been transferred to the newly generated spines.

Our study demonstrates for the first time the activation of the somatosensory cortex after chronic fluoxetine treatment. In a similar way, a recent report has described effects of fluoxetine on neuronal activation and plasticity in another sensory region, the visual cortex [16]. Here antidepressant administration restores neuronal networks involved in ocular dominance and visual function in adult amblyopic rats. This study evaluated neuronal plasticity at the electrophysiological, molecular and behavioural level, but it is very likely that structural plasticity may be also involved. The present c-fos expression study is also in consonance with previous reports using immediate early gene expression, which shown that an important number of cerebral regions become activated after chronic antidepressant treatment. Lino de Oliveira et al. [11] demonstrated that chronic fluoxetine treatment induce a significant increase in c-fos immunoreactivity in the lateral septal nucleus, the bed nucleus of the stria terminalis, the medial amygdala, the dorsal raphe nucleus and the periaqueductal gray, while it induces a decrease in the locus coeruleus. Morinobu et al. [18] also showed that a chronic treatment with imipramine or tranylcypromine caused a significant increase in the expression of c-fos mRNA in the frontal cortex. Our finding of an increased activation of the somatosensory cortex after chronic antidepressant treatment is also supported by some reports that have demonstrated, using different activation markers, changes in this region in animal models of depression or after antidepressant treatment. Olfactory bulbectomy reduces regional cerebral glucose utilization in the somatosensory cortex [35]. By contrast, acute fluoxetine treatment appears to activate this region by inducing phospholipase A2-mediated signal transduction [25]. The sensitivity of the somatosensory cortex to antidepressants has also been shown using the serotonin reuptake inhibitor paroxetine: When this antidepressant is microinjected into the primary somatosensory cortex it significantly attenuates thermal hyperalgesia [15]. Psychomotor symptoms such as agitation and retardation, which may be related to somatosensory cortex activation, are present in depressed patients and are reverted after antidepressant treatment [32,36]. It may be possible that structural changes in somatosensory cortex neurons underlie these symptoms and the recovery of normal function after antidepressant treatments.

Acknowledgements

This study was supported by the following grants: Spanish Ministry of Education and Science (MEC-FEDER) BFU2004-00931 and BFU2006-07313/BFI; Generalitat Valenciana ACOMP06/093; and the Foundation Jerome Lejeune. Castillo-Gómez E. and Gómez-Climent M.A. have FPU predoctoral fellowships from the Spanish Ministry of Education and Science (AP2006-01953 and AP2005-4672). Guirado R. has a FPI predoctoral fellowship from the Spanish Ministry of Education and Science (BES 2007-15757).

References

[2] L. Bonfanti, PSA-NCAM in mammalian structural plasticity and neurogenesis, Prog. Neurobiol. 80 (2006) 129–164.
[3] E. Castren, Is mood chemistry? Nat. Rev. Neurosci. 6 (2005) 241–246.
[4] S.C. Cook, C.L. Wellman, Chronic stress alters dendritic morphology in rat medial prefrontal cortex, J. Neurobiol. 60 (2004) 236–248.
[5] R.S. Duman, Pathophysiology of depression: the concept of synaptic plasticity, Eur. Psychiatry 17 (2002) 306–310.
[6] R.S. Duman, J. Malberg, J. Thome, Neural plasticity to stress and antidepressant treatment, Biol. Psychiatry 46 (1999) 1181–1191.
[7] S.L. Eastwood, P.J. Harrison, Synaptic pathology in the anterior cingulate cortex in schizophrenia and mood disorders. A review and a Western blot study of synaptophysin, GAP-43 and the complexins, Brain Res. Bull. 55 (2001) 569–578.
[8] E. Gascon, L. Vutskits, J.Z. Kiss, Polysialic acid-neural cell adhesion molecule in brain plasticity: from synapses to integration of new neurons, Brain Res. Rev. 56 (2007) 101–118.

[10] T. Hajszan, N.J. MacLusky, C. Leranth, Short-term treatment with the antidepressant fluoxetine triggers pyramidal dendritic spine synapse formation in rat hippocampus, Eur. J. Neurosci. 21 (2005) 1299–1303.
[11] C. Lino de Oliveira, A.J. Sales, E.A. Del Bel, M.C. Silveira, F.S. Guimaraes, Effects of acute and chronic fluoxetine treatments on restraint stress-induced Fos expression, Brain Res. Bull. 55 (2001) 747–754.
[12] A.M. Magarinos, B.S. McEwen, Stress-induced atrophy of apical dendrites of hippocampal CA3c neurons: involvement of glucocorticoid secretion and excitatory amino acid receptors, Neuroscience 69 (1995) 89–98.
[13] H.K. Manji, W.C. Drevets, D.S. Charney, The cellular neurobiology of depression, Nat. Med. 7 (2001) 541–547.
[14] E. Masliah, R.D. Terry, M. Alford, R. DeTeresa, Quantitative immunohistochemistry of synaptophysin in human neocortex: an alternative method to estimate density of presynaptic terminals in paraffin sections, J. Histochem. Cytochem. 38 (1990) 837–844.
[15] K. Matsuzawa-Yanagida, M. Narita, M. Nakajima, N. Kuzumaki, K. Niikura, H. Nozaki, T. Takagi, E. Tamai, N. Hareyama, M. Terada, M. Yamazaki, T. Suzuki, Usefulness of antidepressants for improving the neuropathic pain-like state and pain-induced anxiety through actions at different brain sites, Neuropsychopharmacology 33 (2008) 1952–1965.
[16] J.F. Maya Vetencourt, A. Sale, A. Viegi, L. Baroncelli, R. De Pasquale, O.F. O'Leary, E. Castrén, L. Maffei, The antidepressant fluoxetine restores plasticity in the adult visual cortex, Science 320 (2008) 385–388.
[18] S. Morinobu, H. Strausbaugh, R. Terwilliger, R.S. Duman, Regulation of c-Fos and NGF1-A by antidepressant treatments, Synapse 25 (1997) 313–320.
[22] S.D. Norrholm, C.C. Ouimet, Altered dendritic spine density in animal models of depression and in response to antidepressant treatment, Synapse 42 (2001) 151–163.
[24] M.L. Phillips, W.C. Drevets, S.L. Rauch, R. Lane, Neurobiology of emotion perception II: Implications for major psychiatric disorders, Biol. Psychiatry 54 (2003) 515–528.
[25] Y. Qu, L. Chang, J. Klaff, R. Seemann, S.I. Rapoport, Imaging brain phospholipase A2-mediated signal transduction in response to acute fluoxetine administration in unanesthetized rats, Neuropsychopharmacology 28 (2003) 1219–1226.
[26] J.J. Radley, A.B. Rocher, M. Miller, W.G. Janssen, C. Liston, P.R. Hof, B.S. McEwen, J.H. Morrison, Repeated stress induces dendritic spine loss in the rat medial prefrontal cortex, Cereb. Cortex 16 (2005) 313–320.
[27] J.J. Radley, H.M. Sisti, J. Hao, A.B. Rocher, T. McCall, P.R. Hof, B.S. McEwen, J.H. Morrison, Chronic behavioral stress induces apical dendritic reorganization in pyramidal neurons of the medial prefrontal cortex, Neuroscience 125 (2004) 1–6.
[30] U. Rutishauser, Polysialic acid in the plasticity of the developing and adult vertebrate nervous system, Nat. Rev. Neurosci. 9 (2008) 26–35.
[31] M. Sairanen, O.F. O'Leary, J.E. Knuuttila, E. Castren, Chronic antidepressant treatment selectively increases expression of plasticity-related proteins in the hippocampus and medial prefrontal cortex of the rat, Neuroscience 144 (2007) 368–374.
[32] D. Schrijvers, W. Hulstijn, B.G. Sabbe, Psychomotor symptoms in depression: a diagnostic, pathophysiological and therapeutic tool, J. Affect. Disord. 109 (2008) 1–20.
[35] I. Skelin, H. Sato, M. Diksic, Olfactory bulbectomy reduces cerebral glucose utilization: 2-[^{14}C]deoxyglucose autoradiographic study, Brain Res. Bull. 76 (2008) 485–492.
[36] C. Sobin, H.A. Sackeim, Psychomotor symptoms of depression, Am. J. Psychiatry 154 (1997) 4–17.
[37] N. Sousa, N.V. Lukoyanov, M.D. Madeira, O.F. Almeida, M.M. Paula-Barbosa, Reorganization of the morphology of hippocampal neurites and synapses after stress-induced damage correlates with behavioral improvement, Neuroscience 97 (2000) 253–266.
[38] E. Varea, J.M. Blasco-Ibanez, M.A. Gomez-Climent, E. Castillo-Gomez, C. Crespo, F.J. Martinez-Guijarro, J. Nacher, Chronic fluoxetine treatment increases the expression of PSA-NCAM in the medial prefrontal cortex, Neuropsychopharmacology 32 (2007) 803–812.
[39] E. Varea, E. Castillo-Gomez, M.A. Gomez-Climent, J.M. Blasco-Ibanez, C. Crespo, F.J. Martinez-Guijarro, J. Nacher, Chronic antidepressant treatment induces contrasting patterns of synaptophysin and PSA-NCAM expression in different regions of the adult rat telencephalon, Eur. Neuropsychopharmacol. 17 (2007) 546–557.
[40] H. Wan, E.C. Barburton, P. Kusmierek, J.P. Aggleton, D.M. Kowalska, M.W. Brown, Fos imaging reveals differential neuronal activation of areas of rat temporal cortex by novel and familiar sounds, Eur. J. Neurosci. 14 (2001) 118–124.

Neuroscience 167 (2010) 825–837

DIVERGENT IMPACT OF THE POLYSIALYLTRANSFERASES ST8SiaII AND ST8SiaIV ON POLYSIALIC ACID EXPRESSION IN IMMATURE NEURONS AND INTERNEURONS OF THE ADULT CEREBRAL CORTEX

J. NACHER,[a]* R. GUIRADO,[a] E. VAREA,[a] G. ALONSO-LLOSA,[a] I. RÖCKLE[b] AND H. HILDEBRANDT[b]

[a]*Neurobiology Unit and Program in Basic and Applied Neurosciences, Cell Biology Department, Universitat de València, Dr. Moliner, 50, Burjassot, 46100, Spain*

[b]*Institute of Cellular Chemistry (4330), Hannover Medical School, Carl-Neuberg-Street 1, 30625 Hannover, Germany*

Abstract—Polysialic acid (PSA) is a negatively charged carbohydrate polymer, which confers antiadhesive properties to the neural cell adhesion molecule NCAM and facilitates cellular plasticity during brain development. In mice, PSA expression decreases drastically during the first postnatal weeks and it gets confined to immature neurons and regions displaying structural plasticity during adulthood. In the brain, PSA is exclusively synthesized by the two polysialyltransferases ST8SiaII and ST8SiaIV. To study their individual contribution to polysialylation in the adult, we analyzed PSA expression in mice deficient for either polysialyltransferase. Focusing on the cerebral cortex, our results indicate that ST8SiaIV is solely responsible for PSA expression in mature interneurons and in most regions of cortical neuropil. By contrast, ST8SiaII is the major polysialyltransferase in immature neurons of the paleocortex layer II and the hippocampal subgranular zone. The numbers of cells expressing PSA or doublecortin, another marker of immature neurons, were increased in the paleocortex layer II of ST8SiaIV-deficient mice, indicating altered differentiation of these cells. Analysis of doublecortin expression also indicated that the production of new granule neurons in the subgranular zone of ST8SiaII-deficient mice is not affected. However, many of the immature granule neurons showed aberrant locations and morphology, suggesting a role of ST8SiaII in their terminal differentiation.

Key words: structural plasticity, adult neurogenesis, doublecortin, neuronal differentiation.

The neural cell adhesion molecule (NCAM) has the ability of incorporating long polymeric chains of the sugar sialic acid (polysialic acid, PSA). PSA chains are negatively charged and highly hydrated and thus produce a steric impediment for homotypic and heterotypic interactions of NCAM and other cell adhesion molecules (Rutishauser, 2008). The anti-adhesive properties of PSA facilitate structural plasticity in the CNS (see; Bonfanti, 2006; Gascon et al., 2007; Rutishauser, 2008 for review). During development there is a massive and widespread expression of PSA, which mediates cell migration, neurite outgrowth and synaptogenesis. Postnatally, PSA expression is dramatically reduced, but retained in some regions of persistent plasticity. In the adult brain, the presence of PSA has been related to neurogenesis as well as to remodeling of neurites and synapses (see; Theodosis et al., 2004; Bonfanti, 2006; Gascon et al., 2007; Rutishauser, 2008 for review). In the neurogenic niches of the dentate gyrus (DG) and the subventricular zone/rostral migratory stream/olfactory bulb (SVZ/RMS/OB) system PSA is transiently expressed by immature neurons (Bonfanti et al., 1992). In addition, high levels of PSA expression were found in a population of neurons located in the paleocortex layer II (Seki and Arai, 1991; Nacher et al., 2002a; Bonfanti, 2006). As shown in the rat, these cells are generated prenatally but retain an immature neuronal phenotype into adulthood (Gomez-Climent et al., 2008). Furthermore, adult PSA expression has been described in different neocortical regions (Varea et al., 2005, 2007b,c), the hippocampus (Bonfanti et al., 1992; Seki and Arai, 1993a; Nacher et al., 2002b), the septum (Foley et al., 2003) and the amygdala (Nacher et al., 2002c). In these regions many of the PSA expressing somata and neuropil structures belong to inhibitory neurons (Nacher et al., 2002b; Foley et al., 2003; Varea et al., 2005, 2007c).

The addition of PSA to NCAM is mediated by two Golgi-resident polysialyltransferases, ST8SiaII (STX) and ST8SiaIV (PST) (see Hildebrandt et al. (2007) for review). *In vitro*, each enzyme independently is capable of synthesizing PSA on NCAM. During brain development, both enzymes are expressed with partially overlapping distribution but distinct time course (Hildebrandt et al., 2007). ST8SiaII expression is prominent in embryonic and perinatal stages, but subsequently, its level decreases rapidly and remains low in young and adult animals. By contrast, the level of ST8SiaIV expression, although reduced as well, remains higher and more persistent after early postnatal development (Hildebrandt et al., 1998; Ong et al., 1998; Oltmann-Norden et al., 2008). To understand the impact of ST8SiaII and ST8SiaIV *in vivo*, mice deficient for either polysialyltransferase have been generated (Eckhardt et al., 2000; Angata et al., 2004). Each of the two single knockout lines retained considerable amounts of PSA expression and simultaneous deletion of both genes

*Corresponding author. Tel: +34-96-354-3241; fax: +34-96-354-3404.
E-mail address: nacher@uv.es (J. Nacher).
Abbreviations: DCX, doublecortin; NCAM, neural cell adhesion molecule; PSA, polysialic acid; RMS, rostral migratory stream; SVZ, subventricular zone.

0306-4522/10 $ - see front matter © 2010 IBRO. Published by Elsevier Ltd. All rights reserved.
doi:10.1016/j.neuroscience.2010.02.067

was needed to completely ablate PSA (Weinhold et al., 2005; Angata et al., 2007; Oltmann-Norden et al., 2008). Consistent with the developmental pattern, a comparative analysis of whole brain lysates by Western blot revealed that PSA levels in adult ST8SiaIV knockout mice were lower than in ST8SiaII-deficient animals (Oltmann-Norden et al., 2008). Dramatically reduced PSA expression was observed in olfactory bulb, hippocampus, neocortex and amygdala, as well as in hypothalamus and medulla oblongata of 4 and 6 month old ST8SiaIV-defcient mice (Eckhardt et al., 2000; Markram et al., 2007). By Western blot analyses of 8 week old ST8Sia-II-deficient mice Angata et al. (2004) found lower levels of PSA in olfactory bulb and cerebral cortex, but not in hippocampus or hypothalamus. PSA–positive cells, however, were diminished in the subgranular zone (SGZ) of the DG as well as in the posterior part of the SVZ (Angata et al., 2004).

Despite the various pieces of information provided by the aforementioned studies, the contributions of ST8SiaII and ST8SiaIV to PSA expression on neuron somata and neuropil structures of the adult cortex are unresolved. With particular focus on cortical interneurons and on the population of immature neurons located in paleocortex layer II, we here provide a detailed comparative analysis of PSA expression in adult ST8SiaII- and ST8SiaIV-deficient mice. In order to detect changes in immature neuron populations, we also studied expression of doublecortin (DCX) a microtubule associated protein, which is intensely expressed by recently generated hippocampal granule neurons (Brown et al., 2003) and the population of immature cells in the paleocortex layer II (Nacher et al., 2005; Gomez-Climent et al., 2008). Our results provide strong evidence that ST8SiaIV is solely responsible for PSA expression on mature cortical interneurons, while ST8SiaII is restricted to immature neurons in the hippocampal SGZ and the paleocortex layer II of adult mice.

EXPERIMENTAL PROCEDURES

St8siaII and *St8siaIV* knock out strains (Eckhardt et al., 2000; Angata et al., 2004) were backcrossed with C57BL/6J mice for six generations and mice heterozygous for the mutant polysialyltransferase alleles were interbred to obtain wildtype or knockout offspring (*St8siaII*$^{-/-}$, *St8siaIV*$^{-/-}$). Of each genotype, five males at the age of 3 month were used in this study. All animal experimentation was conducted in accordance with the European Communities Council Directive of November 24, 1986 (86/609/EEC). Every effort was made to minimize the number of animals used and their suffering.

Mice were deeply anesthetized with 20 ml/kg 1.0% ketamine, 0.04% xylazine (Sigma) in normal saline (0.9% NaCl) and transcardially perfused with 4% paraformaldehyde in 0.1 M phosphate buffer, pH 7.4, before brains were removed and postfixed overnight. Fixed brains were sliced coronally at 50 μm with a vibratome and the sections were collected in six subseries. Tissue was processed "free-floating" for PSA or DCX immunohistochemistry as follows: Briefly, a subseries of sections from all the groups of animals studied was incubated for 1 min in an antigen unmasking solution (0.01 M citrate buffer, pH 6) at 100 °C. After cooling down the sections to room temperature, they were extensively washed and endogenous peroxidase activity was blocked with 10% methanol, 3% hydrogen peroxide in phosphate buffered saline (PBS). After this, non specific binding was blocked with 10% Normal Donkey Serum (NDS) for 30 min and sections were incubated 48 h at 4 °C in mouse IgM anti-PSA antibody (1:1400) (Abcys SA, Paris, France) or goat IgG anti-DCX antibody (1:250) (C-18, Santa Cruz Biotechnology, Inc., Santa Cruz, CA, USA). Sections were then incubated for 30 min in donkey secondary biotinylated antibodies against mouse IgM or against goat IgG (Jackson Laboratories, 1:500) and then in Avidin–Biotin–Peroxidase complex (ABC, Vector Laboratories, West Grove, PA, USA) for 30 min. Color development was achieved by incubating with diaminobenzidine tetrahydrochloryde (DAB, Sigma). PBS with 0.2% Triton X-100 was used for washing and antisera dilution. Pretreatment of the anti-PSA antibody with α-2,8-linked sialic polymer (Colominic acid, Sigma) overnight, pretreatment of the anti-DCX antibody with its peptide, or the primary antibody omission during the immunohistochemistry prevented all the labeling in every telencephalic region studied. All of the sections studied passed through all procedures simultaneously, to standardize immunohistochemical staining. All slides were coded prior to analysis and the codes were not broken until the experiment was finished.

In order to exclude the possibility that PSA expressing cells outside the neurogenic regions and the paleocortex layer II were principal cells, we have performed double fluorescence immunohistochemistry using an anti-PSA antibody and a mouse monoclonal antibody (Chemicon/Millipore) against CAMKII, a marker of principal neurons. In general, sections were processed as described above, but the endogenous peroxidase block was omitted. The sections were incubated overnight with primary antibodies and, after washing, they were incubated with donkey anti-mouse IgM and donkey anti-mouse IgG secondary antibodies conjugated with Alexa 488 or Alexa 555 (Molecular Probes, 1:200). Then, the sections were mounted on slides and coverslipped using Dako-Cytomation fluorescent mounting medium (Dako, North America, Inc, Carpinteria, CA, USA) and observed under a confocal microscope (Leica TCS SPE) using a 63× oil objective. Z-series of optical sections (1 μm apart) were obtained using the sequential scanning mode. These stacks were processed with LSM 5 image software. One in six series of telencephalic sections from each animal was double-labeled as described. Fifty randomly-selected immunoreactive cells were analyzed in each case to determine the co-expression of PSA and CAMKII. This study was performed in piriform cortex layer III, in the non-granule cells of hippocampus and in the medial prefrontal cortex (mPFC).

A different subseries of sections adjacent to those used for immunohistochemistry was stained with Toluidine Blue in order to define the cytoarchitectonic boundaries of the areas analyzed.

The number of PSA-NCAM expressing neurons in the different regions studied was estimated as described before (Nacher et al., 2002a). Briefly, sections were selected by a 1:6 fractionator sampling covering the whole rostral to caudal extension of each structure and on each section all labeled cells within the region of interest were counted. Cell somata were identified and counted with a 40× objective using an Olympus CX41 microscope. Cells appearing in the upper focal plane were omitted to prevent counting cell caps. The volume of the different areas analyzed was determined for each animal using the Cavalieri's principle. Means were determined for each animal group and the data were subjected to one-way ANOVAs followed by Student–Newman–Keuls post hoc tests.

RESULTS

Neocortex

In wild type animals PSA expressing cells and PSA-positive neuropil were detected in all regions of the neocortex. As exemplarily shown for the cingulate cortex (Figs. 1A and 2A), PSA-positive cells were particularly abundant in

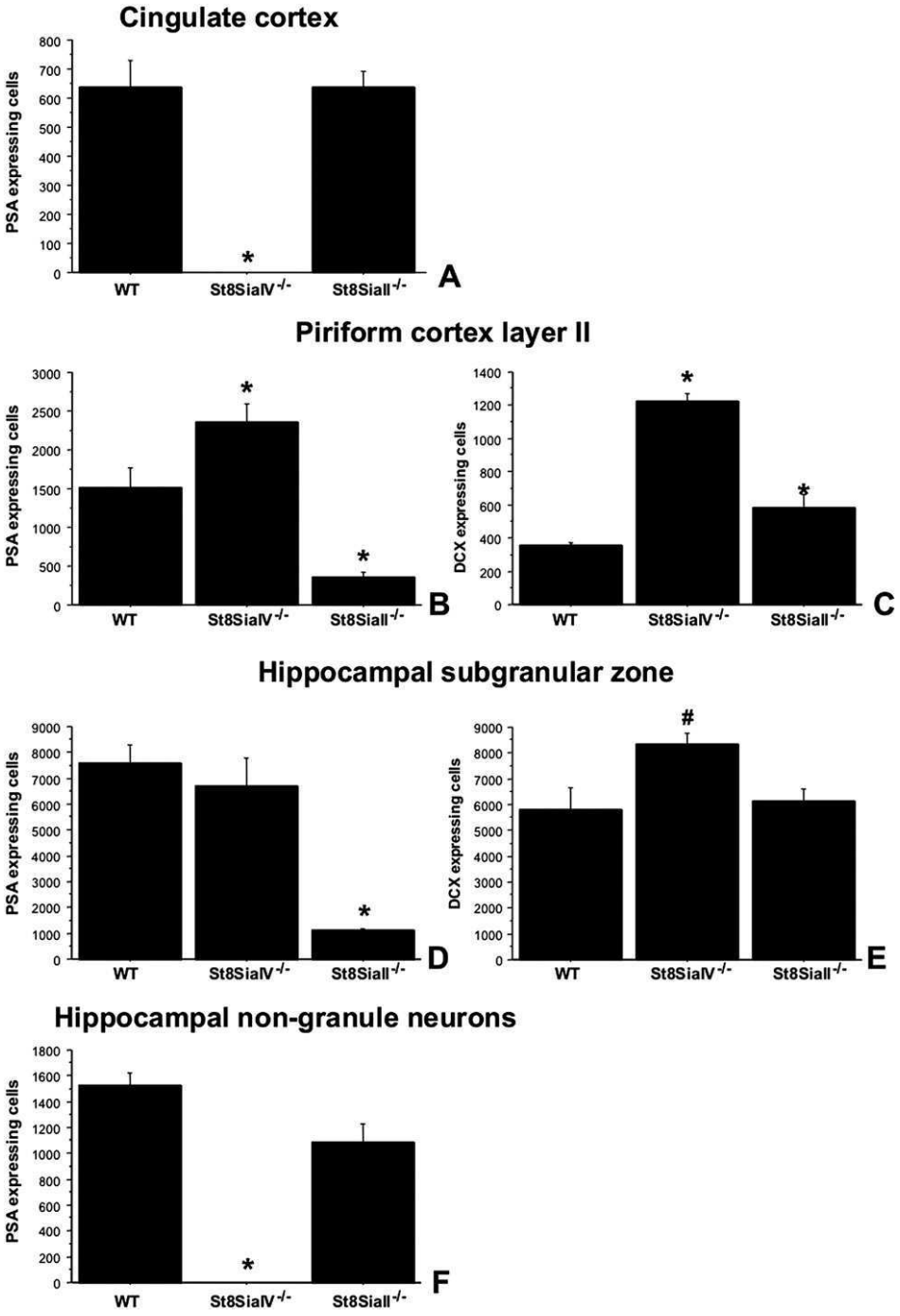

Fig. 1. Estimation of the total numbers of PSA and DCX immunoreactive neurons in different regions of the cerebral cortex of adult wild type and polysialyltransferase-deficient mice. (A) PSA expressing neurons in the cingulate cortex ($F_{2,6}$=34.53, P=0.0005). (B) PSA expressing neurons in the piriform cortex layer II ($F_{2,9}$=19.56, P=0.0005). (C) DCX expressing neurons in the piriform cortex layer II ($F_{2,6}$=68.53, P<0.0001). (D) PSA expressing neurons in the hippocampal subgranular zone ($F_{2,6}$=22.49, P=0.0016). (E) DCX expressing neurons in the hippocampal subgranular zone ($F_{2,6}$=5.18, P=0.049). (F) PSA expressing non-granule neurons in the hippocampus ($F_{2,9}$=19.56, P=0.0005). One-way ANOVA followed by Student–Newman–Keuls post hoc tests. * Significantly different from all other groups, # significantly different from ST8SiaII-deficient mice.

deep layers. Similar to the situation in adult rats (Varea et al., 2005, 2007a) many of the PSA-positive cells displayed multipolar morphologies and neuropil staining was generally more intense in deep layers, specially in the infralimbic and prelimbic cortices (Fig. 2A, D). This staining was entirely absent from the neocortex of ST8SiaIV knockout mice (Figs. 1A and 2B, E). However, as noted before (Eckhardt et al., 2000), absence of ST8SiaIV had no discernible effect on the strong PSA labeling of neuroblasts in the SVZ/RMS (Fig. 2E, arrowheads). In addition, a small

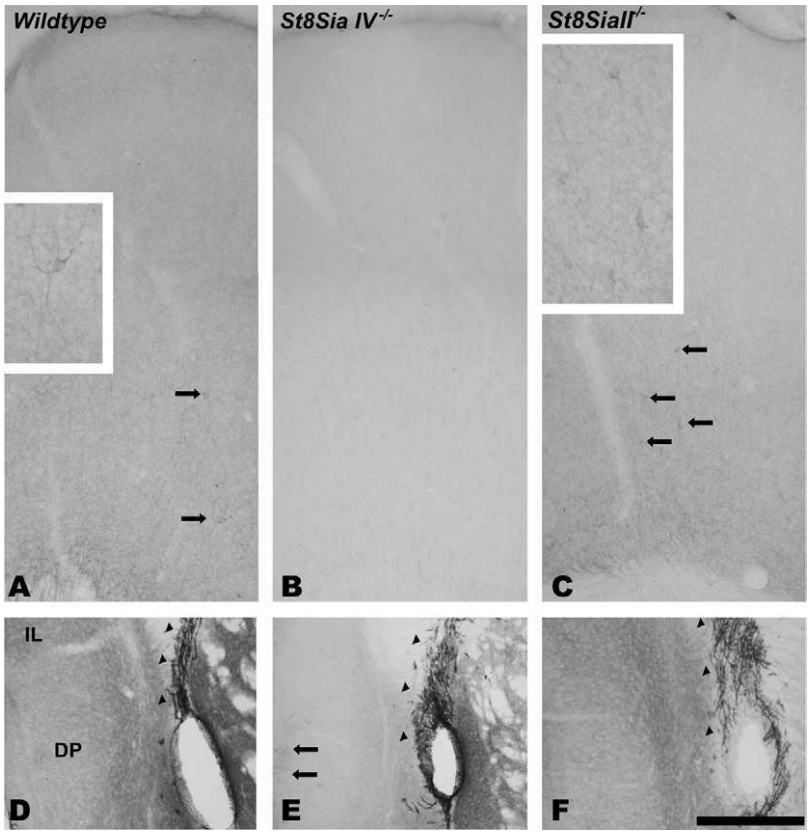

Fig. 2. PSA expression in the neocortex of wild type, ST8SiaIV- and ST8SiaII-deficient mice. (A–C) PSA expressing neurons (arrows) in deep layers of the cingulate cortex. Please note the complete absence of immunoreactivity, both in the neuropil and in neuronal somata, in *St8siaIV*$^{-/-}$ mice (B). Insets show enlarged views of some of the neurons indicated by the arrows. (D–F) Infralimbic and dorsal peduncular cortices. Note that, despite the absence of PSA immunoreactivity in most of cortical the parenchyma, a small portion of neuropil in superficial layers (arrows) displays some faint labelling. Arrowheads indicate PSA expressing cells in the subventricular zone. Scale bar: 20 μm for (A–C) (10 μm for insets) and 40 μm for (D–F). IL, infralimbic cortex; DP, dorsal peduncular cortex.

region of the superficial layers of dorsal peduncular, prelimbic and infralimbic cortices retained weak PSA immunoreactivity (shown for IL in Fig. 2E, arrows). In contrast, distribution and morphology of PSA-positive cells (including SVZ/RMS neuroblasts) as well as staining of the neuropil in ST8SiaII knockout mice were similar to that of wild type animals (Fig. 2C, F). Evaluation of the number of PSA expressing cells in the cingulate cortex revealed no significant differences between wild type and ST8SiaII knockout mice (Fig. 1A).

Paleocortex

The paleocortex (entorhinal and piriform cortices) layer II of wildtype animals displayed an abundant population of PSA expressing cells (Figs. 1B and 3A, D, G). As previously described in rats (Nacher et al., 2002a; Gomez-Climent et al., 2008) some of these cells showed long thick vertical processes that radially traverse the piriform cortex layer III and the deep layers of the lateral entorhinal cortex before entering the external capsule (Fig. 3A, J, K). Frequently, small cells were found closely apposed to these processes (Fig. 3K) (Nacher et al., 2002a). Compared to the wild type, ST8SiaIV-deficient mice had significantly more PSA expressing cells in layer II (Figs. 1B and 3B, E) and in addition to the thick vertical processes, thin PSA immunoreactive fibers were observed in layer III, which resembled typical axons with a small diameter and a beaded appearance (Fig. 3L, M). In contrast, the number of PSA-immunoreactive cells in paleocortex layer II was drastically reduced in *St8siaII*$^{-/-}$ mice (Figs. 1B and 3C, F) and only few thick processes could be observed in layer III (Fig. 3N, O).

In the deep layers of the wildtype paleocortex large PSA expressing cells were found (Fig. 3K), resembling those described in the neocortex (see Fig. 2A). These cells were present in *St8siaII*$^{-/-}$ (Fig. 3N) but absent in *St8siaIV*$^{-/-}$ mice (Fig. 3L, M). In wild type and ST8SiaII-deficient animals, intense immunostaining was observed in the neuropil of the endopiriform nucleus, and faint PSA expression was detected in the neuropil of all paleocortex layers (Fig. 3A, C). In contrast, in ST8SiaIV knockout mice these neuropil structures were completely devoid of PSA labeling (Fig. 3B).

An abundant population of DCX expressing cells was found in the paleocortex layer II of wild type animals (Figs. 1C and 4A). In ST8SiaII- and ST8SiaIV-deficient mice the morphology of these cells appeared unaltered, but their numbers were significantly increased (Figs. 1C and 4B, C).

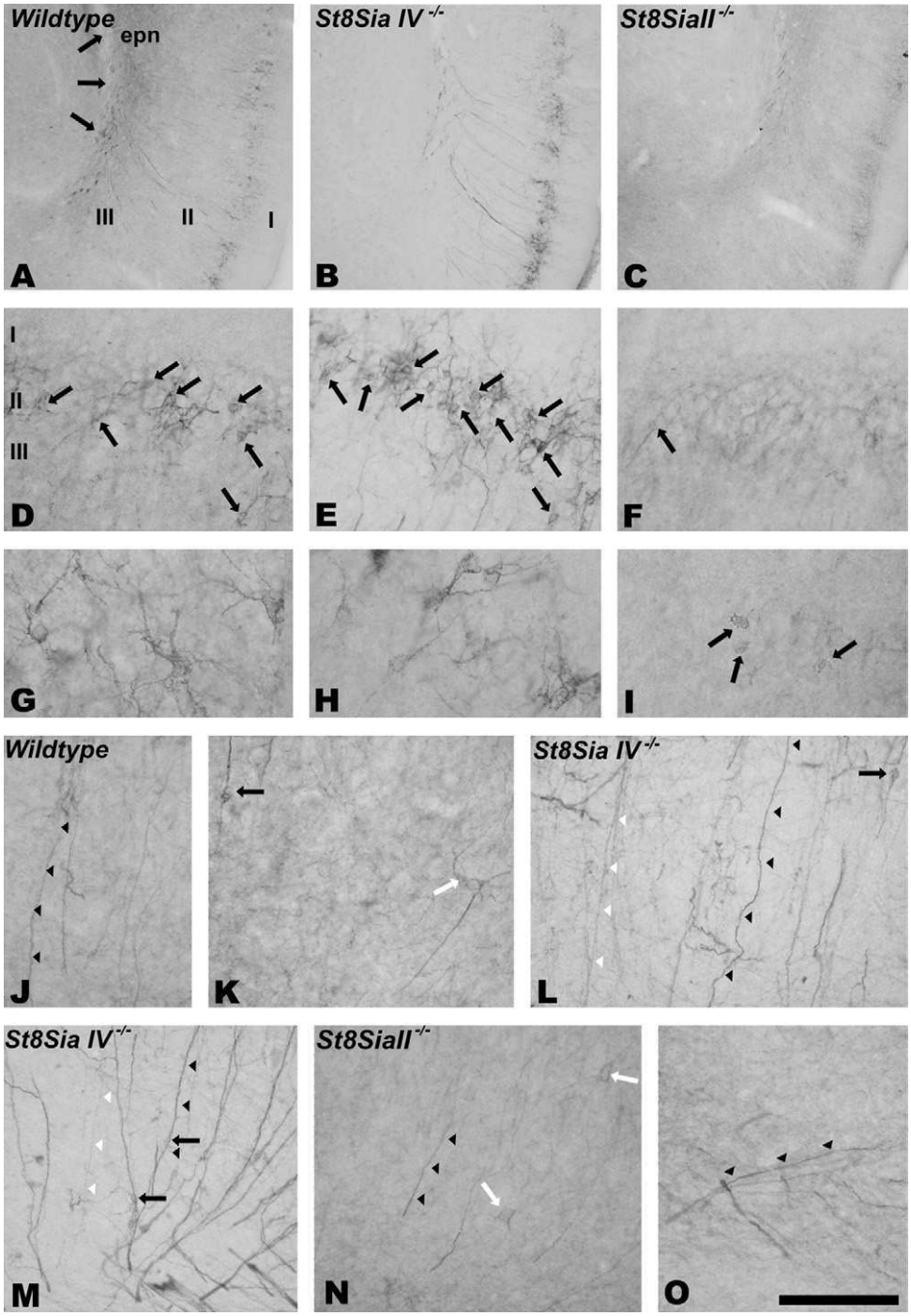

Fig. 3. PSA expression in the paleocortex of wild type, ST8SiaIV- and ST8SiaII-deficient mice. (A–C) Panoramic views of piriform cortex. Please note that populations of immunoreactive cells in layer II and of vertical processes in layer III are more abundant in *St8siaIV*$^{-/-}$ (B), but dramatically reduced in *St8siaII*$^{-/-}$ mice (C). By contrast, the immunostaining in the neuropil of layer III and the endopiriform nucleus is absent in *St8siaIV*$^{-/-}$ mice (B) and appears similar to that of wildtypes in *St8siaII*$^{-/-}$ mice (C). Arrows indicate the end of the external capsule. (D–F) Microphotographs of piriform cortex layer II. An abundant population of PSA immunoreactive cells (arrows) can be observed in wild type mice (D). The number of these immunoreactive cells is increased in *St8siaIV*$^{-/-}$ mice (E), but they are almost absent in *St8siaII*$^{-/-}$ mice (F). (G–I) High magnification views of PSA immunoreactive cells in piriform cortex layer II. Note the reduced arborization of the scarce cells in *St8siaII*$^{-/-}$ mice (arrows). (J–O) Piriform cortex layer III. Vertical immunoreactive processes can be observed in this layer in wild type (J, K), *St8siaIV*$^{-/-}$ (L, M) and *St8siaII*$^{-/-}$ mice (N, O). These processes are more abundant in *St8siaIV*$^{-/-}$ mice and, different to the wildtype, two morphological subtypes can be distinguished: thick vertical processes (black arrowheads) and thin fibers (white arrowheads). In the wildtype two different cell types expressing PSA can be observed in layer III: small cells resembling those in layer II (black arrows), which are sometimes attached to vertical processes, and larger cells resembling hippocampal non-granule PSA expressing neurons (white arrows). In the layer III of *St8siaIV*$^{-/-}$ mice, only small cells can be observed. On the contrary, only large cells can be observed in *St8siaII*$^{-/-}$ knockout mice. Scale bar: 40 μm for (A–C), 10 μm for (D–F) and (J–O), 6 μm for (G–I). epn, endopiriform nucleus.

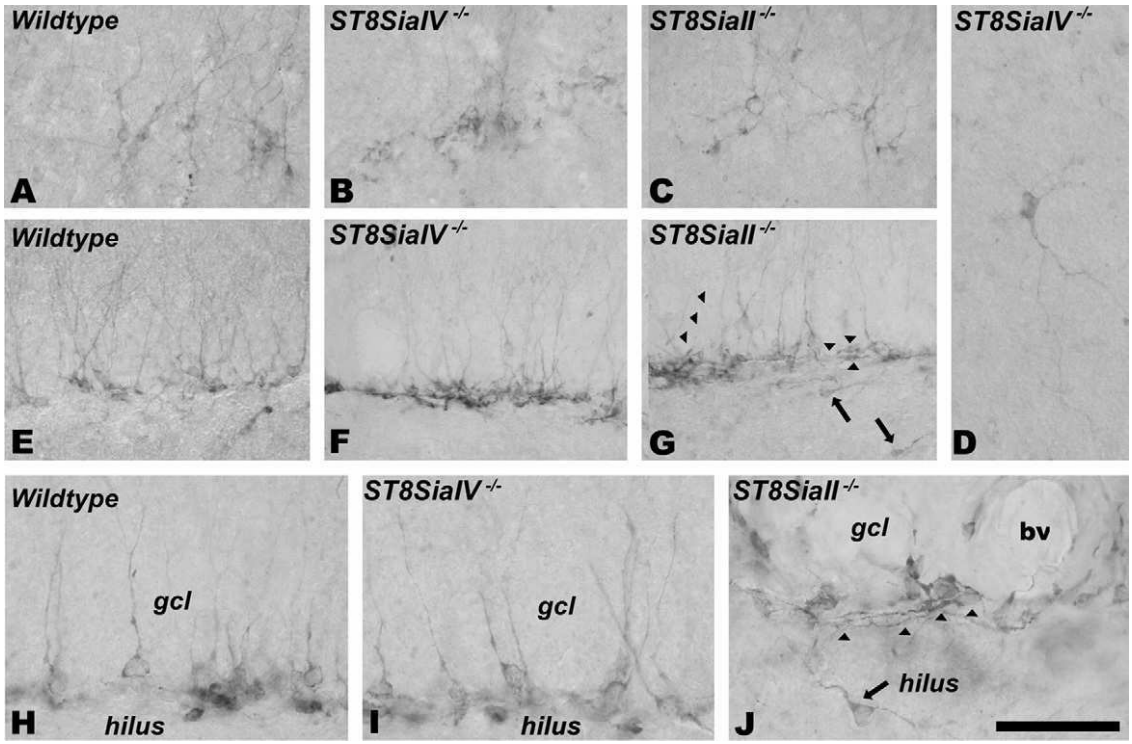

Fig. 4. Doublecortin (DCX) expression in the paleocortex and the hippocampal subgranular zone (SGZ) of wild type, ST8SiaIV- and ST8SiaII-deficient mice. (A–C) Piriform cortex layer II. The population of DCX immunoreactive cells is more abundant in *St8siaIV*$^{-/-}$ mice. (D) Piriform cortex layer III. DCX expressing multipolar cell resembling an interneuron. (E–G) SGZ. DCX expressing cells are more abundant in *St8siaIV*$^{-/-}$ mice but their morphology is similar to that found in wildtype mice. In *St8siaII*$^{-/-}$ mice many of these cells had an aberrant morphology, that is presence of short apical processes restricted to the granule cell or horizontal/basal processes restricted to the SGZ and the hilus (arrowheads). DCX expressing ectopic cells can be found in the hilus (arrows). (G–J) High magnification views of DCX expressing cells in the SGZ. Note that while the morphology of most of the cells in wild type and *St8siaIV*$^{-/-}$ mice is typical, many cells in *St8siaII*$^{-/-}$ animals have abnormal morphologies/orientations (arrowheads) or ectopic locations (arrow). Scale bar: 10 μm for (A–G), 6 μm for (H–J).

This increase was more pronounced in the *St8siaIV*$^{-/-}$ situation. Moreover, a small number of DCX-immunoreactive cells, with an interneuron-like multipolar morphology was detected in the paleocortex layer III of ST8SiaIV-deficient animals. (Fig. 4D). This type of DCX-positive cells was never observed in the wild type.

Hippocampus

The well-known pattern of strongly PSA-positive cells in the SGZ of the dentate gyrus (see e.g. (Seki, 2002)) was recapitulated for wild type animals (Figs. 1D and 5A, B). Likewise, staining obtained in the neuropil of the hippocampus was mostly consistent with previous studies (Seki and Rutishauser, 1998; Eckhardt et al., 2000; Angata et al., 2004). Intense PSA immunoreactivity was observed in the hilus and on the mossy fibers of the CA3 stratum lucidum (Fig. 5A). The molecular layer of the dentate gyrus displayed a weaker but dense PSA staining, with a slightly more pronounced labeling in a zone adjacent to the granule cell layer (Fig. 5A). Light and less compact PSA labeling was detected throughout the stratum lacunosum-moleculare of CA1 and a plexus of markedly immunoreactive processes was found in the most dorsal region of this layer, at the limit with the stratum oriens (Fig. 5A, J). Moreover, a diffuse, light immunostaining was observed in the stratum pyramidale of CA1 (Fig. 5J).

In accordance with the previously described staining patterns of PSA-positive cells in the SGZ of ST8SiaII- or ST8SiaIV-deficient mice (Eckhardt et al., 2000; Angata et al., 2004), a quantitative evaluation of these cells revealed a dramatic reduction in *St8siaII*$^{-/-}$ (Figs. 1D and 5D, E), but no significant change in *St8siaIV*$^{-/-}$ animals (Figs. 1D and 5G, H). Moreover, the few remaining PSA-positive cells in the SGZ of ST8SiaII-deficient mice displayed only some short processes and were devoid of the pronounced vertical (apical) PSA-positive dendrites (Fig. 5H).

A prominent feature of the ST8SiaIV knockout mice is the reduction of PSA-immunoreactivity on mossy fibers (Eckhardt et al., 2000). Staining is still considerable in 6 week-old animals but virtually absent at the age of 6 months. Accordingly, we found that the intense labeling of mossy fibers as observed in wild type mice (Fig. 5A) was reduced to few thin PSA-positive processes in the hilus and the stratum lucidum of ST8SiaIV-deficient mice (Fig. 5D). Some of these processes originated from PSA expressing somata in the SGZ indicating that they were mossy fibers. Moreover, the entire stratum lacunosum-moleculare of the CA1 field (including the immunoreactive plexus next to the hippocampal fissure) as well as most of the molecular layer of the dentate gyrus was completely devoid of PSA staining (Fig. 5D, K). Faint residual immunoreactivity, however, was detected in the inner zone of

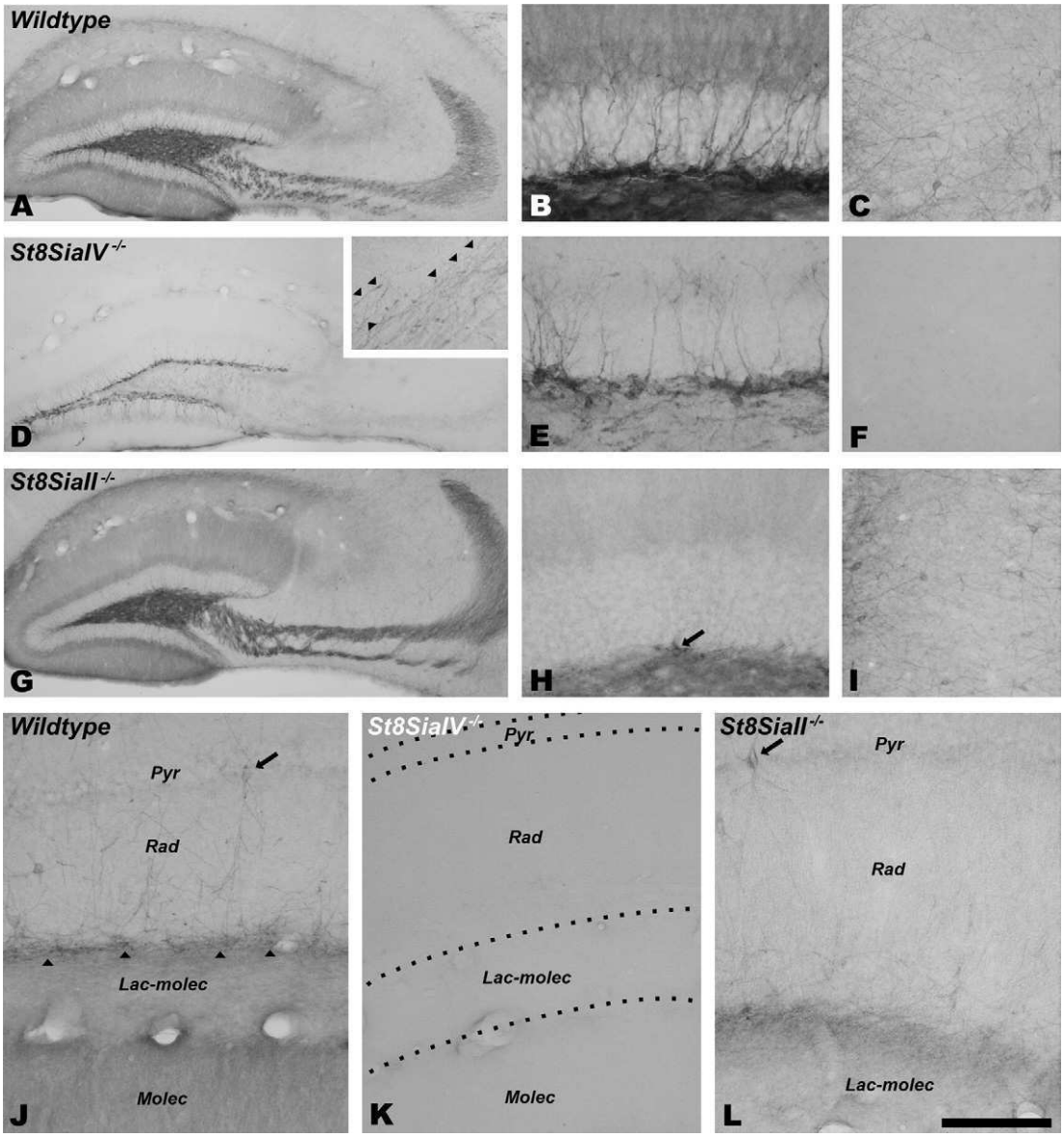

Fig. 5. PSA expression in the hippocampus of wild type, St8SiaIV- and St8SiaII-deficient mice. (A, D, G): Dorsal hippocampus. Please note that in the neuropil of *St8siaIV*$^{-/-}$ mice (D) expression is strongly reduced in the molecular layer and restricted to a few thin PSA-positive processes in the hilus and the stratum lucidum (inset). (B, E, H) Dentate gyrus. Please note that only a faint PSA immunostaining can be detected in the inner third region of the molecular layer of *St8siaIV*$^{-/-}$ mice (E). *St8siaII*$^{-/-}$ mice display neuropil PSA expression similar to that of wildtype mice. However, the number of labeled cell somata in the subgranular zone is dramatically reduced (H). In contrast to the wild type, remaining PSA-positive cells of the SGZ usually do not show apical dendrites traversing the granule cell layer or the molecular layer (arrow in H). (C, F, I) Ventral hippocampus. Several PSA expressing non-granule neurons can be found in the CA3 stratum radiatum of the ventral hippocampus of wild type (C) and *St8siaII*$^{-/-}$ (I) but not in *St8siaIV*$^{-/-}$ mice (F). (J–L) Strata pyramidale (pyr), radiatum (rad) and lacunosum moleculare (lac-molec) of CA1. Wild type and *St8siaII*$^{-/-}$ mice show several PSA immunostained cell somata resembling typical interneurons in the stratum radiatum (arrows in J and L) as well as abundant neuropil immunostaining in the stratum lacunosum-moleculare and in a plexus of markedly immunoreactive processes at the limit with the stratum oriens (arrowheads). PSA immunostaining is absent from the entire CA1 region of *St8siaIV*$^{-/-}$ mice (K). Stratum moleculare is not shown in (L) because the hippocampus is expanded in the ventral-dorsal axis in *St8siaII*$^{-/-}$ mice. Scale bar: 40 μm for (A, D, G); 10 μm for (B, E, H); 20 μm for (C, F, I); 15 μm for (J–L).

the molecular layer (Fig. 5D, E). In accordance with the findings of Angata et al. (2004), PSA-staining of mossy fibers in ST8SiaII knockout mice was as intense as in the wildtype and revealed the aberrant projection of the infrapyramidal mossy fibers extending to the CA3a field (Fig. 5G, H). In addition we found that PSA-immunoreactivity of the other neuropil structures of the hippocampus was not affected by the absence of ST8SiaII (Fig. 5G, L).

As described in the rat (Nacher et al., 2002b), numerous non-granule PSA expressing interneurons were found throughout the hippocampus of wild type mice (Fig. 1F), particularly in its ventral region and in the vicinity of the

fimbria (Fig. 5C). While these cells were completely absent in mice lacking ST8SiaIV (Figs. 1F and 5F), their numbers and their morphology were unaffected in ST8SiaII knockout mice (Figs. 1F and 5I).

Evaluation of DCX expressing cells in the SGZ revealed similar numbers in wild type (Figs. 1E and 4E) and ST8SiaII-deficient mice (Figs. 1E and 4G). Compared to the *St8siaII*$^{-/-}$ situation, the amount of DCX-positive cells was significantly increased in the absence of ST8SiaIV (Figs. 1E and 4F) but most of them retained the characteristic morphology of immature granule cells as well as their position within the SGZ (Fig. 4E, F, I). In contrast, the appearance of many of the DCX-positive cells in the SGZ of ST8SiaII-deficient mice was aberrant. Instead of the apical dendrites typically extending into the molecular layer, some of these cells displayed short apical vertical processes that did not reach beyond the granule cell layer, or they presented horizontal or basal processes that were restricted to the SGZ or extended into the hilus. Moreover, several DCX expressing ectopic cells were found in the hilus (Fig. 4G, J). Some of these cells with aberrant morphology and/or ectopic locations, as described previously in control adult rats (Nacher et al., 2001) could also be found, although in reduced numbers, in ST8SiaIV-deficient and wild type mice.

Extracortical regions

PSA expression was also studied in selected extracortical regions. As in the rat (Nacher et al., 2002c; Cordero et al., 2005) the neuropil of the central and medial amygdaloid nuclei displayed intense immunoreactivity in wild type mice, while faint immunostaining was observed in the lateral and basolateral nuclei (Fig. 6A). PSA expressing cells were detected in all amygdaloid nuclei (Fig. 6D). In the amygdala of ST8SiaIV knockout mice, PSA expression was strongly reduced in the central and medial nuclei and completely absent from the basolateral and lateral nuclei (Fig. 6B). The number of PSA expressing somata was reduced to a few, small immunoreactive cells mostly located within the basolateral and lateral nuclei (Fig. 6E). PSA expression in the amygdala of ST8SiaII-deficient mice was indistinguishable from the wild type situation (Fig. 6C, F).

In the neuropil of the septum PSA expression was markedly reduced in *St8siaIV*$^{-/-}$, but not *St8siaII*$^{-/-}$ mice (Fig. 6G–I). In clear contrast to the PSA-positive cells in the cortex, PSA expressing cells in the septum (Foley et al., 2003) were present in ST8SiaIV- and in ST8SiaII-deficient mice (not shown). Likewise, PSA staining patterns of neuropil in the striatum (Fig. 6G–I) and the hypothalamus (Fig. 6J–L) were not noticeably affected by genetic deletion of either polysialyltransferase.

Phenotype of mature PSA expressing cells

In consonance with previous results in rats (Varea et al., 2005; Gomez-Climent et al., 2008), none of the PSA expressing cells analyzed outside the neurogenic regions and the paleocortex layer II of wildtype and knockout mice expressed CAMKII. This result was obtained in all the regions studied in the present work: piriform cortex layer III, all the regions of the mPFC and the non-granule cells of hippocampus (Fig. 7).

DISCUSSION

The comparative immunohistochemical analysis of residual PSA expression in mice lacking either of the two polysialyltransferases, ST8SiaII or ST8SiaIV, provides a detailed picture of the divergent impact of the two enzymes across different regions of the mature mouse forebrain. In overview, the data demonstrate that both polysialyltransferases contribute to PSA synthesis in the mature brain but their share is clearly different. As assessed before by real time RT-PCR and Western blot analyses of whole brain lysates, ST8SiaII is predominant during development, while ST8SiaIV is the major polysialyltransferase of the adult brain (Galuska et al., 2006; Oltmann-Norden et al., 2008; Schiff et al., 2009). A direct comparison of the PSA-NCAM fraction isolated from perinatal brain of wild-type, ST8SiaII- and ST8SiaIV-deficient mice indicated clear differences in the quantity of NCAM that can be processed by the amounts of ST8SiaII or ST8SiaIV available *in vivo*, but only minor differences in the quality of PSA produced by the individual enzyme, that is the chain length pattern and number of PSA chains per *N*-glycosylation site (Galuska et al., 2006, 2008). Moreover, PSA produced by either enzyme is able to prevent axon tract defects caused by the complete loss of PSA indicating that both enzymes are equally able to modulate NCAM functions (Hildebrandt et al., 2009). Thus, rather than producing PSA species with distinct properties, the difference between the two enzymes appears to be the context- and site-specific regulation of PSA synthesis.

The patterns of PSA immunoreactivity in the forebrain of 3 month old ST8SiaII- and ST8SiaIV-deficient mice provided by the current study confirm this predominance of ST8SiaIV and largely corroborate comparative analyses of ST8SiaII and ST8SiaIV mRNA expression in the wildtype and of PSA expression levels in *St8siaII*$^{-/-}$ and *St8siaIV*$^{-/-}$ mice (Hildebrandt et al., 1998; Ong et al., 1998; Galuska et al., 2006; Oltmann-Norden et al., 2008). More important, however, are the new insights into the allocation of the two enzymes to PSA synthesis in brain regions and cell types not studied previously.

ST8SiaIV is the major polysialyltransferase of mature interneurons in the mouse forebrain

The present results on the distribution of PSA-NCAM expressing cells in the polysialyltransferase-deficient mice are in good agreement with a previous *in situ* hybridization study detecting no ST8SiaII but widely dispersed ST8SiaIV expression in all neocortical layers of young rats (Hildebrandt et al., 1998). In rats and mice, the PSA-positive cells in the cortex have been characterized as mature interneurons (Nacher et al., 2002b; Varea et al., 2005) (Nacher, unpublished results). As demonstrated for the prefrontal cortex, the PSA positive processes or punctae also belong to inhibitory interneurons (Varea et al., 2005).

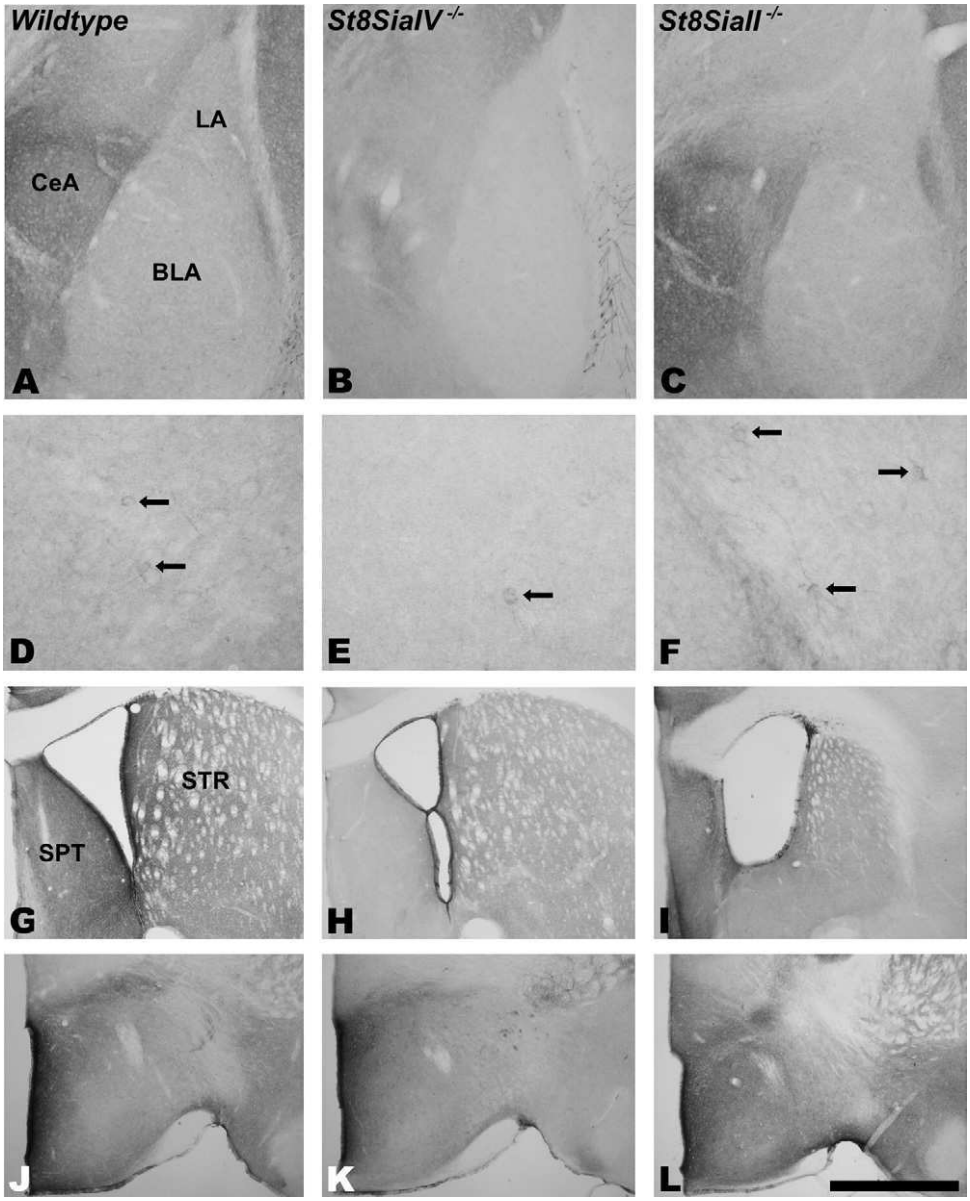

Fig. 6. PSA expression in cell somata and neuropil of different extracortical regions of wild type, St8SiaIV- and St8SiaII-deficient mice. (A–C) Amygdala. *St8siaIV*$^{-/-}$ mice display a severe reduction in the general intensity of PSA expression in the neuropil. However, some faint immunostaining can be detected in the central amygdala. (D–F) Basolateral amygdala. The number of PSA expressing cells (black arrows) and the neuropil intensity in this amygdaloid nucleus is reduced in the *St8siaIV*$^{-/-}$mice. However, some scarce small cells with faint PSA-NCAM expression can be observed in these animals. (G–I) Septum and striatum. The striatum of all the different animals studied shows a similar intensity of PSA-NCAM expression. However, a marked reduction in immunostaining can be seen in the septum of *St8siaIV*$^{-/-}$mice. (J–L) Hypothalamus. No major differences in PSA-NCAM expression can be observed in the neuropil of the hypothalamic regions observed. Scale bar: 40 μm. BLA, basolateral amygdaloid nucleus; CeA, central amygdaloid nucleus; LA, lateral amygdaloid nucleus; SPT, septum; STR, striatum.

The lack of PSA, therefore, indicates that ST8SiaIV is solely responsible for PSA synthesis in cortical interneurons during adulthood. The intriguing possibility that the disappearance of PSA expression in ST8SiaIV-deficient mice affects properties of cortical interneurons is currently investigated.

Consistent with these traits of PSA expression by neocortical interneurons, ST8SiaIV-deficient mice also lack PSA expressing cells with an interneuron-like appearance (i.e. multipolar cells lacking the characteristic soma morphology and dendritic arbor configuration of pyramidal cells) in the deep layers of the paleocortex. Moreover, PSA in the stratum lacunosum-moleculare of CA1 and most of the staining in the molecular layer of the dentate gyrus depends on ST8SiaIV. Only little is known on neuronal populations responsible for PSA expression in these two hippocampal regions. PSA expressing structures found in CA1 include axons of CA3 pyramidal cells (O'Connell et al., 1997), although the pyramidal cell somata were found to be PSA-negative (Bonfanti et al., 1992). Some of this

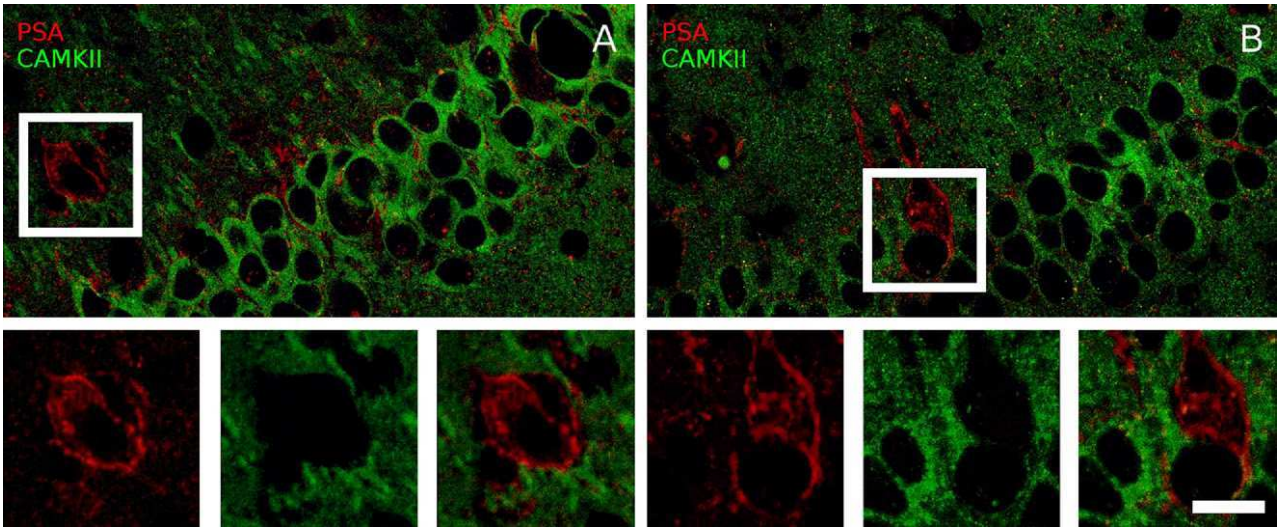

Fig. 7. PSA (red) and CAMKII (green) immunohistochemistry. Hippocampal CA1 stratum radiatum. (A) wild type. (B) St8SiaII-deficient mouse. Note that in both cases PSA expressing cells lack CAMKII immunoreactivity, which, by contrast, is specially intense in the pyramidal cell layer. All images in this figure are single confocal planes. Scale bar 20 μm for (A) and (B); 12.5 μm for insets. For interpretation of the references to color in this figure legend, the reader is referred to the Web version of this article.

PSA staining possibly originates from PSA expressing non-granule neurons, most of which have been classified as mature interneurons (Nacher et al., 2002b). Similarly, we also found a dramatic (although not complete) reduction of PSA-positive neuropil and in the number of PSA expressing cells in the amygdala of ST8SiaIV-deficient mice. In the wildtype, these cells have features of interneurons (Nacher, unpublished results), suggesting that also in this region ST8SiaIV is responsible for the polysialylation of mature interneurons. Similarly, we found that PSA expression of cells in the septum is uncompromised in both, ST8SiaIV- and in ST8SiaII-deficient mice. These cells, however, have previously been characterized as interneurons (Foley et al., 2003) indicating that both polysialyltransferases can incorporate PSA in interneurons outside of the cerebral cortex.

PSA expression in cortical interneurons is stable during aging (Varea et al., 2009), but is affected by pharmacological manipulations with dopaminergic or serotoninergic drugs (Varea et al., 2007a,b; Castillo-Gomez et al., 2008). The significance of PSA expression in mature interneurons is still unknown: This molecule may play a partial insulating role, similar to that described in the immature neurons in the paleocortex layer II (Gomez-Climent et al., 2008) and/or may facilitate plastic processes such as neurite, spine or synapse remodeling, as described in other systems (see; Sandi, 2004; Bonfanti, 2006; Gascon et al., 2007; Rutishauser, 2008 for review).

ST8SiaII is the major polysialyltransferase of immature neurons in the adult cerebral cortex

The present results demonstrate a predominant impact of ST8SiaII on PSA expression of specifically immature neuron populations in the adult cerebral cortex. On the one hand, ST8SiaII-but not ST8SiaIV-deficient animals have strongly reduced PSA expression in the neurogenic region of the hippocampal SGZ (as described before; Angata et al., 2004), as well as in the paleocortex layer II and certain amygdaloid nuclei, two other regions in the brain of young rodents in which immature cells have been described (Gomez-Climent et al., 2008; Shapiro et al., 2009). As noted before (Eckhardt et al., 2000; Angata et al., 2004), neither of the two polysialyltransferase-deficient single knockout strains displayed marked reductions of PSA staining of neuroblasts in the SVZ/RMS system. These data imply that in the neurogenic system of the anterior SVZ both polysialyltransferases are co-expressed and that under these conditions each enzyme can compensate, at least to a certain extent, for the loss of the other. Such a compensation is perfectly consistent with previous data obtained by analyses on the level of whole brain homogenates (Galuska et al., 2006). On the other hand, in almost all other forebrain areas of the 3 month old mice investigated in the current study, the loss of ST8SiaIV virtually eliminates PSA immunostaining, whereas ST8SiaII deficiency had no discernible effect.

During hippocampal neurogenesis granule cell precursors within the SGZ acquire PSA immunoreactivity at an early neuroblasts-like stage, before they migrate and differentiate into granule cells with transient PSA expression on their axonal and somato–dendritic compartments. By contrast, mature granule cells only retain PSA expression on their mossy fiber axons (Seki and Arai, 1993b, 1999; Schuster et al., 2001). As shown in the current study, expression of PSA on cell somata of granule cell precursors of the hippocampal SGZ in 3 month old mice depends mostly, but not exclusively, on the presence of ST8SiaII, while it was unaffected by the genetic ablation of ST8SiaIV. The residual PSA staining in the SGZ of ST8SiaII knockout mice was found on cells with only short processes suggesting a contribution of ST8SiaIV to polysialylation in some immature SGZ neurons. Complemen-

tary, PSA expression on mossy fibers was almost completely abolished in 3 months old *St8siaIV*$^{-/-}$ mice. Some of the remaining thin, isolated PSA-positive processes in the hilus and in the CA3 subfield arose from PSA expressing granule neurons in the SGZ. These profiles, therefore, seem to correspond to immature mossy fibers and, consequently, ST8SiaII may still contribute to PSA production during early stages of mossy fiber formation.

These findings are in good agreement with the first reports on ST8SiaII- and ST8SiaIV-deficient mice (Eckhardt et al., 2000; Angata et al., 2004) and in line with earlier in situ hybridization data showing ST8SiaII expression in the SGZ, where new granule cells are born, but ST8SiaIV in most mature granule cells (Hildebrandt et al., 1998). The differential loss of PSA in the dentate gyrus of the two polysialyltransferase knockout models, together with the expression patterns of the two enzymes, indicates that PSA is predominantly synthesized by ST8SiaII in newly generated and by ST8SiaIV in older granule cells. Thus, during hippocampus neurogenesis the general developmental profile of the two polysialyltransferases seems to be reproduced on the cellular level.

Despite the dramatic reduction of PSA expression, we found that the number of DCX-positive cells in the SGZ of ST8SiaII-deficient mice was unaffected, suggesting the uncompromised generation of granule cell precursors. This is consistent with unaltered rates of progenitor cell proliferation in the dentate gyrus reported for either ST8SiaII-deficency or in mice depleted of PSA due to ablation of NCAM (Angata et al., 2004; Aonurm-Helm et al., 2008). However, in *St8siaII*$^{-/-}$ mice we found an unusually high number of DCX-positive cells displaying abnormal lengths and trajectories of their dendritic trees, many of them ectopically located in the hilus, suggesting aberrant differentiation/migration of newly generated granule neurons. Significantly more immature DCX-positive cells were observed in the hippocampal SGZ of ST8SiaIV-deficient mice, as well as in piriform cortex layer II of *St8siaII*$^{-/-}$ and, more pronounced, *St8siaIV*$^{-/-}$ animals. Surprisingly, a concomitant increase of PSA-positive cells was also detected in the latter. One explanation for these increasing numbers could be that immature neurons accumulate in the absence ST8SiaIV, indicating that this enzyme is somehow necessary for the maturation of these cells and/or that its absence may prevent cell death. A defect in migration/maturation in the absence of ST8SiaIV may also explain the presence of some DCX expressing cells with multipolar morphology in piriform cortex layer III. Further experiments are needed to clarify the nature and fate of these cells.

Little is known on the nature and the fate of the PSA-positive cells of the paleocortex layer II. Although generated during prenatal development, these cells retain a phenotype of immature neurons in young-adult rodents (3 months-old) (Gomez-Climent et al., 2008). Since markers of immature neurons are almost absent from paleocortex layer II in middle aged (1 year old) rodents (Montaron et al., 1999; Varea et al., 2009), it seems likely that these cells are committed to differentiation or cell death. As revealed by the current study, PSA expression of these cells depends on the presence of ST8SiaII, but despite the dramatic reduction in PSA expression in paleocortex layer II of St8SiaII-deficient mice, the number of immature, DCX-positive neurons is preserved. Thus, PSA does not seem necessary for maintaining the immature phenotype of these cells. However, the marked increase of DCX-positive cells in layer II of the paleocortex of 3 months old ST8SiaIV-deficient mice indicates that expression of this molecule through ST8SiaIV affects the number of immature cells, either by influencing their migration, delaying their maturation or by preventing their death. In fact, the complete absence of PSA during development, by deletion of both polysialyltransferases, perturbs cell migration and results in increased numbers of apoptotic cells in the cerebral cortex (Angata et al., 2007). Finally, the presence of some PSA expressing cells in the amygdala of ST8SiaIV-deficient mice coincides with a low level of adult neurogenesis (Bernier et al., 2002; Shapiro et al., 2009). The few immature neurons in this region, therefore, may be polysialylated by ST8SiaII.

Taken together, the increase in the number of DCX-positive cells in the SGZ of ST8SiaIV-deficient mice and in the piriform cortex layer II of either ST8SiaIV- or, less pronounced, ST8SiaII-deficient animals, their altered morphology in the SGZ under *St8siaII*$^{-/-}$ conditions, as well as the increase of PSA-positive cells in the piriform cortex layer II points towards a prominent role of polysialylation in the development of these cell types. Thus, putative functions of these newly generated neurons in learning, memory or in the behavioral response to pharmacological treatments may be impaired under conditions of compromised polysialylation.

Acknowledgments—Deutsche Forschungsgemeinschaft DFGHi678/4-1 to H.H. Spanish Ministry of Science and Innovation (MICINN-FEDER) BFU2006-07313/BFI and BFU2009-12284/BFI, Generalitat Valenciana CS2009-AP-127 and ACOMP2009/271 to J.N.; Guirado R. has a FPI predoctoral fellowship from the Spanish Ministry of Education and Science (BES 2007-15757).

REFERENCES

Angata K, Huckaby V, Ranscht B, Terskikh A, Marth JD, Fukuda M (2007) Polysialic acid-directed migration and differentiation of neural precursors are essential for mouse brain development. Mol Cell Biol 27:6659–6668.

Angata K, Long JM, Bukalo O, Lee W, Dityatev A, Wynshaw-Boris A, Schachner M, Fukuda M, Marth JD (2004) Sialyltransferase ST8Sia-II assembles a subset of polysialic acid that directs hippocampal axonal targeting and promotes fear behavior. J Biol Chem 279:32603–32613.

Aonurm-Helm A, Jurgenson M, Zharkovsky T, Sonn K, Berezin V, Bock E, Zharkovsky A (2008) Depression-like behaviour in neural cell adhesion molecule (NCAM)-deficient mice and its reversal by an NCAM-derived peptide, FGL. Eur J Neurosci 28:1618–1628.

Bernier PJ, Bedard A, Vinet J, Levesque M, Parent A (2002) Newly generated neurons in the amygdala and adjoining cortex of adult primates. Proc Natl Acad Sci U S A 20:11464–11469.

Bonfanti L (2006) PSA-NCAM in mammalian structural plasticity and neurogenesis. Prog Neurobiol 80:129–164.

Bonfanti L, Olive S, Poulain DA, Theodosis DT (1992) Mapping of the distribution of polysialylated neural cell adhesion molecule throughout

the central nervous system of the adult rat: an immunohistochemical study. Neuroscience 49:419–436.

Brown JP, Couillard-Despres S, Cooper-Kuhn CM, Winkler J, Aigner L, Kuhn HG (2003) Transient expression of doublecortin during adult neurogenesis. J Comp Neurol 467:1–10.

Castillo-Gomez E, Gomez-Climent MA, Varea E, Guirado R, Blasco-Ibanez JM, Crespo C, Martinez-Guijarro FJ, Nacher J (2008) Dopamine acting through D2 receptors modulates the expression of PSA-NCAM, a molecule related to neuronal structural plasticity, in the medial prefrontal cortex of adult rats. Exp Neurol 214:97–114.

Cordero MI, Rodriguez JJ, Davies HA, Peddie CJ, Sandi C, Stewart MG (2005) Chronic restraint stress down-regulates amygdaloid expression of polysialylated neural cell adhesion molecule. Neuroscience 133:903–910.

Eckhardt M, Bukalo O, Chazal G, Wang L, Goridis C, Schachner M, Gerardy-Schahn R, Cremer H, Dityatev A (2000) Mice deficient in the polysialyltransferase ST8SiaIV/PST-1 allow discrimination of the roles of neural cell adhesion molecule protein and polysialic acid in neural development and synaptic plasticity. J Neurosci 20:5234–5244.

Foley AG, Ronn LC, Murphy KJ, Regan CM (2003) Distribution of polysialylated neural cell adhesion molecule in rat septal nuclei and septohippocampal pathway: transient increase of polysialylated interneurons in the subtriangular septal zone during memory consolidation. J Neurosci Res 74:807–817.

Galuska SP, Geyer R, Gerardy-Schahn R, Muhlenhoff M, Geyer H (2008) Enzyme-dependent variations in the polysialylation of the neural cell adhesion molecule (NCAM) in vivo. J Biol Chem 283:17–28.

Galuska SP, Oltmann-Norden I, Geyer H, Weinhold B, Kuchelmeister K, Hildebrandt H, Gerardy-Schahn R, Geyer R, Muhlenhoff M (2006) Polysialic acid profiles of mice expressing variant allelic combinations of the polysialyltransferases ST8SiaII and ST8SiaIV. J Biol Chem 281:31605–31615.

Gascon E, Vutskits L, Kiss JZ (2007) Polysialic acid-neural cell adhesion molecule in brain plasticity: from synapses to integration of new neurons. Brain Res Rev 56:101–118.

Gomez-Climent MA, Castillo-Gomez E, Varea E, Guirado R, Blasco-Ibanez JM, Crespo C, Martinez-Guijarro FJ, Nacher J (2008) A population of prenatally generated cells in the rat paleocortex maintains an immature neuronal phenotype into adulthood. Cereb Cortex 18:2229.

Hildebrandt H, Becker C, Murau M, Gerardy-Schahn R, Rahmann H (1998) Heterogeneous expression of the polysialyltransferases ST8Sia II and ST8Sia IV during postnatal rat brain development. J Neurochem 71:2339–2348.

Hildebrandt H, Muhlenhoff M, Oltmann-Norden I, Rockle I, Burkhardt H, Weinhold B, Gerardy-Schahn R (2009) Imbalance of neural cell adhesion molecule and polysialyltransferase alleles causes defective brain connectivity. Brain 132:2831–2838.

Hildebrandt H, Muhlenhoff M, Weinhold B, Gerardy-Schahn R (2007) Dissecting polysialic acid and NCAM functions in brain development. J Neurochem 103(Suppl 1):56–64.

Markram K, Gerardy-Schahn R, Sandi C (2007) Selective learning and memory impairments in mice deficient for polysialylated NCAM in adulthood. Neuroscience 144:788–796.

Montaron MF, Petry KG, Rodriguez JJ, Marinelli M, Aurousseau C, Rougon G, Le Moal M, Abrous DN (1999) Adrenalectomy increases neurogenesis but not PSA-NCAM expression in aged dentate gyrus. Eur J Neurosci 11:1479–1485.

Nacher J, Alonso-Llosa G, Rosell DR, McEwen BS (2002a) PSA-NCAM expression in the piriform cortex of the adult rat. Modulation by NMDA receptor antagonist administration. Brain Res 927: 111–121.

Nacher J, Blasco-Ibanez JM, McEwen BS (2002b) Non-granule PSA-NCAM immunoreactive neurons in the rat hippocampus. Brain Res 930:1–11.

Nacher J, Crespo C, McEwen BS (2001) Doublecortin expression in the adult rat telencephalon. Eur J Neurosci 14:629–644.

Nacher J, Lanuza E, McEwen BS (2002c) Distribution of PSA-NCAM expression in the amygdala of the adult rat. Neuroscience 113:479–484.

Nacher J, Varea E, Blasco-Ibanez JM, Castillo-Gomez E, Crespo C, Martinez-Guijarro FJ, McEwen BS (2005) Expression of the transcription factor Pax 6 in the adult rat dentate gyrus. J Neurosci Res 81:753–761.

O'Connell AW, Fox GB, Barry T, Murphy KJ, Fichera G, Foley AG, Kelly J, Regan CM (1997) Spatial learning activates neural cell adhesion molecule polysialylation in a corticohippocampal pathway within the medial temporal lobe. J Neurochem 68:2538–2546.

Oltmann-Norden I, Galuska SP, Hildebrandt H, Geyer R, Gerardy-Schahn R, Geyer H, Muhlenhoff M (2008) Impact of the polysialyltransferases ST8SiaII and ST8SiaIV on polysialic acid synthesis during postnatal mouse brain development. J Biol Chem 283: 1463–1471.

Ong E, Nakayama J, Angata K, Reyes L, Katsuyama T, Arai Y, Fukuda M (1998) Developmental regulation of polysialic acid synthesis in mouse directed by two polysialyltransferases, PST and STX. Glycobiology 8:415–424.

Rutishauser U (2008) Polysialic acid in the plasticity of the developing and adult vertebrate nervous system. Nat Rev Neurosci 9:26–35.

Sandi C (2004) Stress, cognitive impairment and cell adhesion molecules. Nat Rev Neurosci 5:917–930.

Schiff M, Weinhold B, Grothe C, Hildebrandt H (2009) NCAM and polysialyltransferase profiles match dopaminergic marker gene expression but polysialic acid is dispensable for development of the midbrain dopamine system. J Neurochem 110:1661–1673.

Schuster T, Krug M, Stalder M, Hackel N, Gerardy-Schahn R, Schachner M (2001) Immunoelectron microscopic localization of the neural recognition molecules L1, NCAM, and its isoform NCAM180, the NCAM-associated polysialic acid, beta1 integrin and the extracellular matrix molecule tenascin-R in synapses of the adult rat hippocampus. J Neurobiol 49:142–158.

Seki T (2002) Expression patterns of immature neuronal markers PSA-NCAM, CRMP-4 and NeuroD in the hippocampus of young adult and aged rodents. J Neurosci Res 70:327–334.

Seki T, Arai Y (1991) Expression of highly polysialylated NCAM in the neocortex and piriform cortex of the developing and the adult rat. Anat Embryol (Berl) 184:395–401.

Seki T, Arai Y (1993a) Distribution and possible roles of the highly polysialylated neural cell adhesion molecule (NCAM-H) in the developing and adult central nervous system. Neurosci Res 17: 265–290.

Seki T, Arai Y (1993b) Highly polysialylated neural cell adhesion molecule (NCAM-H) is expressed by newly generated granule cells in the dentate gyrus of the adult rat. J Neurosci 13:2351–2358.

Seki T, Arai Y (1999) Different polysialic acid-neural cell adhesion molecule expression patterns in distinct types of mossy fiber boutons in the adult hippocampus. J Comp Neurol 410:115–125.

Seki T, Rutishauser U (1998) Removal of polysialic acid-neural cell adhesion molecule induces aberrant mossy fiber innervation and ectopic synaptogenesis in the hippocampus. J Neurosci 18: 3757–3766.

Shapiro LA, Ng K, Zhou QY, Ribak CE (2009) Subventricular zone-derived, newly generated neurons populate several olfactory and limbic forebrain regions. Epilepsy Behav 14(Suppl 1):74–80.

Theodosis DT, Piet R, Poulain DA, Oliet SH (2004) Neuronal, glial and synaptic remodeling in the adult hypothalamus: functional consequences and role of cell surface and extracellular matrix adhesion molecules. Neurochem Int 45:491–501.

Varea E, Blasco-Ibanez JM, Gomez-Climent MA, Castillo-Gomez E, Crespo C, Martinez-Guijarro FJ, Nacher J (2007a) Chronic fluoxetine treatment increases the expression of PSA-NCAM in the medial prefrontal cortex. Neuropsychopharmacology 32:803–812.

Varea E, Castillo-Gomez E, Gomez-Climent MA, Blasco-Ibanez JM, Crespo C, Martinez-Guijarro FJ, Nacher J (2007b) Chronic antidepressant treatment induces contrasting patterns of synaptophysin and PSA-NCAM expression in different regions of the adult rat telencephalon. Eur Neuropsychopharmacol 17:546–557.

Varea E, Castillo-Gomez E, Gomez-Climent MA, Blasco-Ibanez JM, Crespo C, Martinez-Guijarro FJ, Nacher J (2007c) PSA-NCAM expression in the human prefrontal cortex. J Chem Neuroanat 33:202–209.

Varea E, Castillo-Gomez E, Gomez-Climent MA, Guirado R, Blasco-Ibañez JM, Crespo C, Martinez-Guijarro FJ, Nacher J (2009) Differential evolution of PSA-NCAM expression during aging of the rat telencephalon. Neurobiol Aging 30:11.

Varea E, Nacher J, Blasco-Ibanez JM, Gomez-Climent MA, Castillo-Gomez E, Crespo C, Martinez-Guijarro FJ (2005) PSA-NCAM expression in the rat medial prefrontal cortex. Neuroscience 136:435–443.

Weinhold B, Seidenfaden R, Rockle I, Muhlenhoff M, Schertzinger F, Conzelmann S, Marth JD, Gerardy-Schahn R, Hildebrandt H (2005) Genetic ablation of polysialic acid causes severe neurodevelopmental defects rescued by deletion of the neural cell adhesion molecule. J Biol Chem 280:42971–42977.

(Accepted 23 February 2010)
(Available online 3 March 2010)

Cerebral Cortex Advance Access published September 15, 2010

Cerebral Cortex
doi:10.1093/cercor/bhq177

The Polysialylated Form of the Neural Cell Adhesion Molecule (PSA-NCAM) Is Expressed in a Subpopulation of Mature Cortical Interneurons Characterized by Reduced Structural Features and Connectivity

María Ángeles Gómez-Climent[1], Ramón Guirado[1], Esther Castillo-Gómez[1], Emilio Varea[1], María Gutierrez-Mecinas[1,5], Javier Gilabert-Juan[1,2], Clara García-Mompó[1], Sandra Vidueira[1], David Sanchez-Mataredona[1], Samuel Hernández[1], José Miguel Blasco-Ibáñez[1], Carlos Crespo[1], Urs Rutishauser[3], Melitta Schachner[4] and Juan Nacher[1]

[1]Neurobiology Unit and Program in Basic and Applied Neurosciences, Department of Cell Biology, Universitat de València, 46100 Burjassot, Spain, [2]Centro de Investigación Biomédica en Red de Salud Mental, [3]Laboratory of Developmental Neuroscience, Cell Biology Program, Sloan-Kettering Institute, Memorial Sloan-Kettering Cancer Center, New York, NY 10065, USA, [4]Zentrum fuer Molekulare Neurobiologie, Universitaetskrankenhaus Eppendorf, D-20246 Hamburg, Germany and [5]Current address: Henry Wellcome Laboratories for Integrative Neuroscience and Endocrinology, University of Bristol, Bristol BS1 3NY, UK

Gómez-Climent and Guirado have contributed equally to this work

Address correspondence to Dr Juan Nacher, Neurobiology Unit, Department of Cell Biology, Universitat de València, Dr. Moliner, 50, 46100 Burjassot, Spain. Email: nacher@uv.es.

Principal neurons in the adult cerebral cortex undergo synaptic, dendritic, and spine remodeling in response to different stimuli, and several reports have demonstrated that the polysialylated form of the neural cell adhesion molecule (PSA-NCAM) participates in these plastic processes. However, there is only limited information on the expression of this molecule on interneurons and on its role in the structural plasticity of these cells. We have found that PSA-NCAM is expressed in mature interneurons widely distributed in all the extension of the cerebral cortex and have excluded the expression of this molecule in most principal cells. Although PSA-NCAM expression is generally considered a marker of immature neurons, birth-dating analyses reveal that these interneurons do not have an adult or perinatal origin and that they are generated during embryonic development. PSA-NCAM expressing interneurons show reduced density of perisomatic and peridendritic puncta expressing different synaptic markers and receive less perisomatic synapses, when compared with interneurons lacking this molecule. Moreover, they have reduced dendritic arborization and spine density. These data indicate that PSA-NCAM expression is important for the connectivity of interneurons in the adult cerebral cortex and that its regulation may play an important role in the structural plasticity of inhibitory networks.

Keywords: dendrite remodeling, dendritic arborization, interneuron subtypes, NCAM, neuronal structural plasticity, spine remodeling

Introduction

The neural cell adhesion molecule (NCAM), through the action of 2 polysialyltransferases, ST8SiaII and ST8SiaIV (Hildebrandt et al. 2008), is able to incorporate long chains of polysialic acid (PSA), which confers it antiadhesive properties. Consequently, PSA-NCAM expression facilitates structural remodeling and is involved in several neurodevelopmental events, such as neuronal migration, neurite outgrowth, or synaptogenesis (for review, see Bonfanti 2006; Gascon et al. 2007; Rutishauser 2008). Although NCAM is the major carrier of PSA in the central nervous system (CNS) (Hildebrandt et al. 2008), this sugar has also been detected on other proteins, such as neuropilin2 (Curreli et al. 2007), a sodium channel subunit (Zuber et al. 1992), SynCAM1 (Galuska et al. 2010), and the polysialyltransferases St8SiaII and St8SiaIV (Muhlenhoff et al. 1996; Close and Colley 1998).

PSA-NCAM is very abundant during CNS development, but it can also be found in several regions and cell populations during adulthood. Some of these cells are immature neurons, such as those found in the adult neurogenic regions (Seki and Arai 1993b; Rousselot et al. 1995; Bonfanti 2006) and the paleocortex layer II (Gomez-Climent et al. 2008). In addition, previous studies have indicated that PSA is also present in a subpopulation of mature interneurons in the hippocampus and the medial prefrontal cortex (mPFC) (Nacher, Blasco-Ibanez, and McEwen 2002; Varea et al. 2005; Varea, Castillo-Gomez, et al. 2007b). Moreover, pharmacological modulation of serotoninergic or dopaminergic neurotransmission results in parallel changes in the expression of PSA and molecules involved in γ-aminobutyric acidergic (GABAergic) neurotransmission in the mPFC of adult rats (Sairanen et al. 2007; Varea, Blasco-Ibanez, et al. 2007; Varea, Castillo-Gomez, et al. 2007b; Castillo-Gomez et al. 2008). Altogether, these results suggest that, at least in the mPFC, changes in PSA expression may be involved in the plasticity of inhibitory circuits. However, we still do not know whether similar interneurons express PSA in other cortical regions or whether this molecule is exclusively expressed by a subpopulation of interneurons and absent from most principal cells. Moreover, the functional significance of PSA expression in interneurons is still unresolved. The study of interneurons expressing PSA is also interesting because, although there is considerable information on the structural plasticity of cortical principal neurons, few reports have addressed this subject in inhibitory neurons (Lee et al. 2006, 2008).

The aims of this study are: 1) to offer a complete mapping of PSA expressing cells in the adult rodent cerebral cortex, 2) to determine the neurochemical phenotype of somata and neuropil elements expressing PSA in the adult cerebral cortex and to exclude its expression in principal cells, 3) to demonstrate that NCAM is the only carrier of PSA in adult cortical interneurons, using NCAM knockout mice, 4) to demonstrate that PSA expression in interneurons is not affected by genetic deletion of NCAM in principal cells, 5) to study the time of origin of PSA expressing interneurons and to exclude their postnatal generation, 6) to study the presence/density of different types of

synapses on PSA expressing interneurons and their ultrastructure and to compare them with those of interneurons lacking this molecule, and 7) by using transgenic mice expressing green fluorescent protein (GFP) under the promoter of GAD67, to analyze the dendritic arborization and spine density of PSA expressing interneurons, and to compare it with that of interneurons lacking PSA expression.

Materials and Methods

Animals and Treatments

Rats

Forty-one young adult male Sprague–Dawley (SD) rats (3 months old, 300 ± 15 g, Harlan Iberica) were separated into different groups. 1) Eight rats were used to study the neurochemical phenotype of PSA expressing cells and their perisomatic and peridendritic puncta, using immunohistochemistry and confocal microscopy. The phenotype of PSA expressing puncta in the neuropil was also analyzed in these animals. 2) Thirty rats were used to study whether PSA immunoreactive cells were generated during adulthood, using double PSA/5'BrdU immunohistochemistry. All the rats in this group received 4 intraperitoneal (i.p.) injections, 1 each 12 h, of 5′BrdU (Sigma; 50 mg/kg, in sterile saline) when they were 3 months old and were sacrificed 2, 4, 7, 14, 21, or 30 days after the last injection (n = 5 per group). 3) Three SD rats were used for PSA preembedding immunohistochemistry for electron microscopy.

Twelve perinatal SD male rats were used to study whether PSA immunoreactive cells were generated during perinatal development, using double PSA/5′BrdU immunohistochemistry. The rats in this group underwent the same 5′BrdU injection protocol described above at postnatal days P0, P10, and P20 (n = 4 per group) and were sacrificed when they were 3 months old.

Eight pregnant SD rats (Harlan Iberica) received 2 i.p. injections of 5′BrdU (50 mg/kg), 8 h apart, on the following days after coupling: E11.5, E13.5, E15.5, and E17.5 (n = 2 per group) in order to identify whether PSA expressing cells were generated during embryogenesis. The first 24 h after coupling were designated as embryonic day 0 (E0). Four males (3 months old, 306 ± 32 g) were selected from each offspring and processed for double PSA/5′BrdU immunohistochemistry.

Mice

Twelve young adult male GIN (GFP-expressing inhibitory neurons, Tg(GadGFP)45704Swn) mice (3 months old, 27.5 ± 4 g, purchased from Jackson laboratories and bred in our animal facility) were separated into different groups. 1) Six mice were used to study the neurochemical phenotype of GFP/PSA-expressing interneurons using confocal microscopy and immunohistochemistry for several markers. 2) Six mice were used for the analysis of dendritic arborization and spine density of GFP-expressing interneurons with or without PSA expression.

Three B6.Cg-Tg(Thy1-YFPH)2Jrs/J young adult male mice (3 months old, 26.8 ± 5 g, purchased from Jackson laboratories and bred in our animal facility), in which subsets of pyramidal neurons are "Golgi-like" labeled (Gogolla et al. 2009), were used to exclude the expression of PSA in pyramidal neurons of the cerebral cortex.

Five NCAM (−/−) mice and 5 wild-type littermates on a C57BL/6 background (males, 3 months old) (Cremer et al. 1994) were used to study whether PSA expression in interneurons was associated to NCAM or to other putative polysialylated proteins. These animals were processed for double PSA/GAD67 immunofluorescence as described below.

Four NCAMff+ (CaMKII) and 4 wild-type littermates (NCAMff–) (males, 3 months old) were used to study whether PSA expression was present in principal neurons. These mice were generated by a Cre-loxP recombination system to generate a mutant, in which the NCAM gene is ablated under the control of the CaMKII promoter (Bukalo et al. 2004). These animals were processed for double PSA/GAD67 immunofluorescence as described below.

Histological Procedures

Rats and mice destined for confocal microscopy studies were perfused transcardially under deep chloral hydrate anesthesia, with saline and then 4% paraformaldehyde in sodium phosphate buffer 0.1 M, pH 7.4 (PB). Rat brains destined for fluorescence immunohistochemistry were cut with a vibratome (Leica VT 1000E, Leica), and 50-μm thick coronal sections were collected and kept in cold PB (4 °C) before processing. In the case of GIN mice, the brains were cut into 150-μm thick sections with a vibratome for the study of dendritic arborization and dendritic spine density. Brains for conventional immunohistochemistry were cryoprotected with 30% sucrose in PB, coronal sections (50 μm) were obtained with a sliding freezing microtome (Leica SM2000R) and stored at –20 °C in 30% glycerol, 30% ethylene glycol in PB until used.

The rats processed for electron microscopy were perfused transcardially under deep chloral hydrate anesthesia, first with saline for 1 min, followed by 450-mL solution of paraformaldehyde 2% in a lysine-phosphate buffer, pH 7.4 (see Supplementary experimental procedures). Brains were then extracted and sliced with a vibratome at 50 μm as described above.

All animal experimentation was conducted in accordance with the European Communities Council Directive of November 24th 1986 (86/609/EEC) and was approved by the Committee on Bioethics of the Universitat de València. Every effort was made to minimize the number of animals used and their suffering.

Immunohistochemistry for Conventional Light Microscopy, Fluorescence Microscopy, and 5′ BrdU Detection

Tissue was processed "free-floating" for immunohistochemistry as described (Nacher et al. 2005; Varea et al. 2005). Detailed information on the methodology and the specificity of the anti-PSA antibody can be found in the Supplementary experimental procedures section. This antibody recognizes exclusively the PSA (Rougon et al. 1986), but since in the adult CNS most, if not all, PSA expression is associated to NCAM, it is frequently denominated anti-PSA-NCAM (Rutishauser 2008).

In order to characterize neurochemically the somata and neuropil elements expressing PSA as well as the immunoreactive puncta apposed to the PSA-expressing somata and dendrites, we have performed double or triple immunohistochemistry using primary antibodies against PSA and against different markers of immature neurons, mature neurons, interneurons, astrocytes, oligodendrocytes, microglia, proteins related to neuronal activity, and synaptic contacts (see Supplementary Table 1). For detailed information on PSA/5′BrdU immunohistochemistry, see Supplementary experimental procedures section.

Observation and Quantification of Double-Labeled PSA-Expressing Somata

All sections processed for fluorescence immunohistochemistry were mounted on slides and coverslipped using DakoCytomation fluorescent mounting medium (Dako North America, Inc.). Then, the sections were observed under a confocal microscope (Leica TCS SPE) using a ×63 oil objective. *Z*-series of optical sections (1-μm apart) were obtained using the sequential scanning mode. These stacks were processed with LSM 5 image software. One in 10 series of telencephalic sections from each animal was double-labeled as described. Fifty randomly selected immunoreactive cells were analyzed in each case to determine the coexpression of PSA and the markers described above. This study was performed in deep layers of paleocortex (piriform cortex layer III and lateral entorhinal cortex layers III to VI), in the nongranule cells of hippocampus and in the mPFC, in order to complete previous studies (Nacher, Blasco-Ibanez, and McEwen 2002; Varea et al. 2005). A similar methodology was applied when analyzing PSA expression in pyramidal neurons of Thy1-YFP mice. Seventy pyramidal neurons (selected by morphological criteria) per animal were analyzed in all the extension of the neocortex and paleocortex.

Quantification of PSA-Expressing Somata and Neuropil Immunoreactivity in the Hippocampus of NCAMff+ and NCAMff- Transgenic Mice

The number of PSA-expressing neurons in the hippocampal CA1 region was estimated using a modified version of the fractionator method (West 1993), as described before (Nacher, Alonso-Llosa, et al. 2002). In order to determine PSA immunoreactivity intensity, tissue was analyzed with confocal microscopy in order to obtain optical densities of the regions of interest. A detailed description of the stereological and densitometric procedures can be found in the Supplementary experimental procedures section. Means were determined for NCAMff+ and NCAMff– mice, and the data were subjected to statistical analysis using the unpaired Student's *t*-test.

Analysis of Perisomatic and Peridendritic Puncta on PSA-Expressing Interneurons

All sections processed for fluorescence immunohistochemistry were processed as described above and observed under a confocal microscope. *Z*-series of optical sections (0.5-μm apart) were obtained using sequential scanning mode. Twenty randomly selected PSA-expressing cells, from deep layers of paleocortex and nongranule cells of hippocampus in each case, were analyzed using different presynaptic and postsynaptic markers (Table 1). The profile of these cells was drawn and only puncta contacting this profile were analyzed. The colocalization of PSA and synaptic markers was analyzed in 4 consecutive confocal planes of each selected neuron, in which the penetration of both antibodies was optimal.

In order to compare the number of perisomatic and peridendritic puncta between PSA-expressing interneurons and those lacking PSA expression, we analyzed a randomly selected sample of glutamic acid decarboxylase-67 (GAD67)-expressing cells of the CA3 region in the ventral hippocampus in 4 different rats (10 GAD67+/PSA+ and 10 GAD67+/PSA–). The profiles of the somata and the proximal portion of a dendrite were drawn in 4 consecutive confocal planes of each selected neuron, in which the penetration of both antibodies was optimal. The number of synaptophysin (SYN)-expressing puncta per micron of soma or dendrite profile was counted, and means were obtained and compared using unpaired Student's *t*-test analysis.

Table 1

Phenotypic characterization of PSA-expressing cells in the rat Paleocortex deep layers, mPFC, and in hippocampal nongranule neurons

Markers	Paleocortex deep layer	Hippocampal nongranule cells	Prefrontal cortex
ARC	0	52 ± 1	5 ± 1
c-FOS	10 ± 4	2 ± 0.5	6 ± 0.5
CAMKII	0	0	0
CB	30 ± 8	10 ± 2	65 ± 5
CCK	17 ± 5	54 ± 10	16 ± 0
CR	0	33 ± 7	3 ± 1
GAD67	77.3 ± 6.9	84 ± 1	59 ± 7
GFAP	0	0	0
GR	47 ± 1	8 ± 0.5	90 ± 1.5
NeuN	83.33 ± 4	100	100
NPY	23.5 ± 3.5	9 ± 4	18 ± 2
NR1	97 ± 1	91 ± 1	91 ± 1
OX-42	0	0	0
p-CREB	20 ± 2	34 ± 6	48 ± 2
PV	20 ± 5	6 ± 2	1 ± 1
Rip	0	0	0
SST	53.3 ± 7.6	8 ± 0.5	62 ± 2
VIP	2 ± 2	0	2 ± 2
5′BrdU—E 11.5	10 ± 2	9 ±1.4	0 ± 0
5′BrdU—E 13.5	25 ± 1	18 ± 1	2 ± 2
5′BrdU—E 15.5	34 ± 5	39 ± 11	25 ± 3.5
5′BrdU—E 17.5	12.25 ± 4.34	5.44 ± 1.28	15.76 ± 4.83

Percentages of GAD67 expressing cells co-expressing PSA in the rat cerebral cortex

Markers	Paleocortex	Hippocampus	Prefrontal cortex
PSA	10.5 ± 1.5	9 ± 2	8 ± 2

Note: Numbers indicate the percentage (±standard error of the mean) of PSA-expressing cells that coexpress the different cellular markers. GFAP, glial fibrillary acidic protein.

Analysis of PSA-Expressing Puncta in the Neuropil

All sections were processed and observed as described above. *Z*-series of optical sections (0.5-μm apart) were obtained using sequential scanning mode. One hundred PSA immunoreactive puncta were analyzed in each region and animal (n = 4) to determine the coexpression of PSA and different markers of excitatory and inhibitory elements and general synaptic markers (Table 1). This study was performed in deep layers of entorhinal and prelimbic cortices.

Avidin–Biotin–Immunoperoxidase and Immunogold-Silver Detection for Electron Microscopy

The sections destined to electron microscopy were cryoprotected for 30 min by immersion in 25% sucrose and 10% glycerol in 0.01 M PB and then underwent freeze thawing 3 times with liquid nitrogen to enhance antibody penetration. Detailed information on the methodology used for preembedding avidin–biotin–immunoperoxidase and preembedding immunogold-silver detection for electron microscopy, as well as on the inclusion and ultramicrotomy, can be found in the Supplementary experimental procedures section.

Analysis of Synaptic Density in the Perisomatic Region of PSA Versus Non–PSA-Expressing Interneurons. Ultrastructural Analysis of PSA Expression in Pyramidal Neuron Somata

The density of synaptic contacts on the plasma membrane was studied analyzing profiles of interneuron somata from selected regions of the ventral hippocampus and the deep layers of mPFC, where PSA interneurons were specially abundant, both from DAB- and gold-stained material. The interneurons were identified by their profound invagination of the nucleus and an electron-dense cytoplasm with high density of mitochondria, endoplasmic reticulum, and Golgi apparatus. Nine interneurons expressing PSA in the plasma membrane and 9 lacking expression of this molecule were analyzed in each region.

Thirty profiles of pyramidal neuron somata of the mPFC cortex were also studied under the electron microscope in order to analyze PSA expression in their perisomatic region.

Analysis of Dendritic Arborization and Spine Density in GAD-GFP and PSA/GAD-GFP Expressing Interneurons

The study of dendritic arborization, using Sholl analysis (Sholl 1953), and the study of spine density were performed in GFP-expressing cells located in the CA3 region of the dorsal and ventral hippocampus. Detailed information on these methodologies can be found in the Supplementary experimental procedures section.

Results

PSA-Expressing Cells with Typical Interneuron Morphology Are Widely Distributed in the Adult Rodent Telencephalon

The distribution of PSA-expressing cells was similar in the rat and mouse telencephalon (Fig. 1). PSA-expressing cells, mostly multipolar and resembling typical interneurons, were found widely dispersed in every region and layer of the neocortex, although they were more abundant in deep layers. These cells also populated the deep layers of paleocortex (piriform cortex layer III and entorhinal cortex layers III to VI) but were extremely rare in layers II or I. In layer II, most of the cells expressing PSA were tangled or semilunar-pyramidal transitional neurons (Gomez-Climent et al. 2008). The distribution of PSA-expressing nongranule neurons in the hippocampus was similar to that described previously in the rat (Nacher, Blasco-Ibanez, and McEwen 2002).

PSA expression was detected in the neuropil of neocortical and paleocortical regions and was generally more intense in deep layers, as described before (Nacher, Alonso-Llosa, et al.

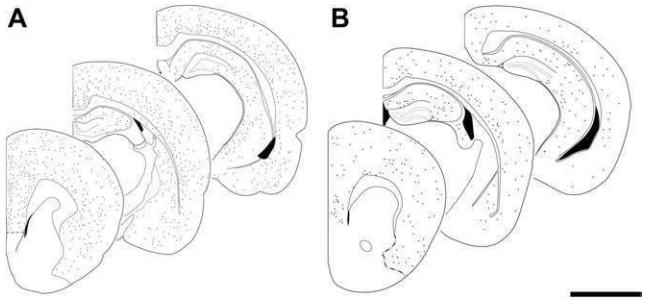

Figure 1. Distribution of PSA-expressing cells in the cerebral cortex of adult rats (*A*) and mice (*B*). Camera lucida drawings representing of 3 representative 50-μm coronal sections covering the rostral to caudal extent of the rodent cerebral cortex. The somata of PSA-immunoreactive cells with the characteristic morphology of interneurons have been represented as small dots. PSA-immunoreactive cells in the hippocampal subgranular zone and the paleocortex layer II have been omitted from the drawings. Scale bar: 3.4 mm for *A* and 2 mm for *B*. The profiles of the representative sections have been modified from those in Paxinos and Watson (1986) and Paxinos and Franklin (1997).

2002; Varea et al. 2005; Varea, Castillo-Gomez, et al. 2007). Hippocampal PSA expression was in consonance with previous reports (Seki and Arai 1993). In some cases, particularly in neocortical layers III and V, some PSA-expressing puncta were found delineating the profiles of the soma and the juxtasomatic portion of the principal apical dendrite of pyramidal neurons (Supplementary Fig. 1).

Cell Somata and Neuropil Elements–Expressing PSA in the Adult Cerebral Cortex Correspond to Mature Interneurons

PSA-NCAM–Expressing Cells Are Not Glial Cells

Double immunohistochemistry using an anti-PSA antibody in combination with anti-glial fibrillary acidic protein, anti-rip, or anti-OX42 antibodies revealed that none of the PSA-expressing cells in all the regions studied could be classified as an astrocyte, an oligodendrocyte or a microglial cell (Supplementary Fig. 2).

PSA Expression Is Detectable in a Subpopulation of Mature Interneurons and It Is Absent from Principal Neurons

All PSA-expressing cells in the hippocampus (excluding those in the subgranular zone) and the mPFC expressed NeuN, a marker of mature neurons (Mullen et al. 1992) (Fig. 2*A*,*B* and Table 1). The situation was similar in the deep layers of the paleocortex, although in this region some scarce PSA-expressing cells lacked this marker of mature neurons, as previously described (Nacher, Alonso-Llosa, et al. 2002).

None of the PSA-expressing cells in these regions expressed the marker of principal neurons Ca(2+)/CaM-dependent protein kinase II (CAMKII, Fig. 2*C* and Table 1). In consonance with these results, the analysis of pyramidal neurons in Thy1-YFP mice revealed that none of these cells expressed PSA, neither in its soma nor in their proximal dendritic tree (Supplementary Fig. 3). By contrast, many PSA-expressing cells coexpressed GAD67, a marker of interneurons (Fig. 2*D* and Table 1). These cells also expressed different calcium-binding proteins and neuropeptides, although the percentages of coexpression varied between the different molecules studied and the cortical regions analyzed (Fig. 2*E*–*F* and Table 1).

Since the PSA-expressing nongranule cells of the hippocampus were also studied in adult GIN mice (see "PSA-NCAM-Expressing Interneurons Have Reduced Dendritic Arborization and Spine Density Compared With Interneurons Lacking PSA-NCAM" section below), their phenotype was also analyzed and found to be similar to that described in rats (Supplementary Table 2 and Fig. 4): Most PSA-expressing cells coexpressed NeuN and many of them expressed GAD67, calcium-binding proteins and neuropeptides.

In order to estimate the proportion of the general population of interneurons that coexpressed PSA in rats and mice, we also studied the percentage of GAD67-expressing interneurons coexpressing PSA. All percentages observed in the different rat cortical regions range between 8% and 10.5% (Table 1), although a higher percentage was found in the hippocampus of GIN mice (34 ± 1.41%).

Ultrastructural analysis of cortical pyramidal cells in pre-embedding PSA immunostained sections revealed that, contrary to what was observed in interneurons (see density of synaptic contacts chapter below), none of these cells expressed PSA in the perisomatic region of its plasma membrane.

PSA-Expressing Interneurons Express Low Levels of Cell Activity Markers but High Levels of NMDA and Glucocorticoid Receptors

In order to know whether the expression of PSA interferes with the activity of interneurons, we studied the expression of the most commonly used cell activity markers in the CNS, c-Fos, and Arc. Only very low percentages of the PSA-expressing interneurons studied coexpressed c-Fos (Table 1). The percentages of Arc coexpression were also low, except in the case of hippocampal nongranule cells (Table 1 and Supplementary Fig. 5*A*). By contrast, most PSA-expressing cells in all the regions studied coexpressed the NR1 NMDA receptor subunit (Table 1). The expression of glucocorticoid receptors (GRs) in PSA-expressing cells was variable among the different areas studied (Table 1): Most of these cells coexpressed GR in the mPFC, about half of them coexpressed this receptor in the paleocortex, but only very few hippocampal nongranule cells coexpressed PSA and GR (Table 1 and Supplementary Fig. 5*B*).

PSA-Expressing Elements in the Cortical Neuropil Correspond to Inhibitory Structures

None of the PSA-expressing puncta in the neuropil of deep layers of entorhinal and prelimbic cortices expressed the vesicular glutamate transporter 1 (VGLUT1, Fig. 3*A*), a molecule responsible for the active transport of L-glutamate into synaptic vesicles, which is generally used as a marker of excitatory synapses in the telencephalon.

By contrast, we found that, in all the regions studied, some PSA-expressing puncta coexpressed the vesicular GABA transporter (VGAT, Fig. 3*B* and Table 2), which is associated with synaptic vesicles in GABAergic synapses and is crucial for inhibitory function (McIntire et al. 1997). GAD67 was also expressed, with similar percentages in some PSA-expressing puncta (Fig. 3*C* and Table 2), except in the neuropil of the prelimbic cortex, where a higher degree of colocalization was observed. In agreement with the VGAT and GAD67 coexpression, we also found that a similar percentage of PSA-expressing puncta in every region studied was found closely apposed to puncta-expressing gephyrin (Fig. 3*D* and Table 2), a protein involved in the clustering of glycine and GABA(A) receptors, which is detectable in the postsynaptic density of inhibitory synapses (Fritschy et al. 2008). A small percentage of

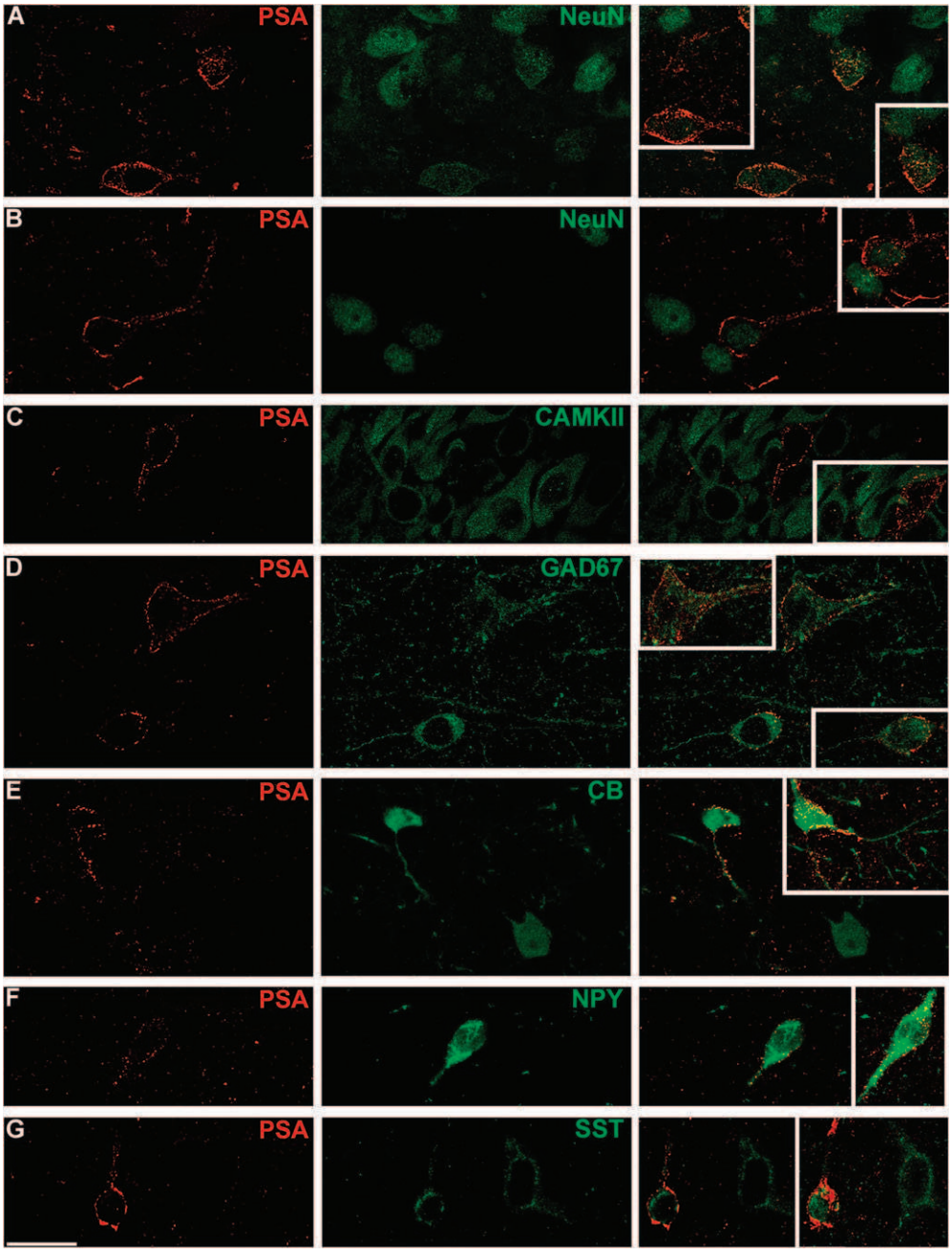

Figure 2. Confocal microscopic analysis of the phenotype of PSA-expressing cells in selected adult rat cortical regions. (*A* and *B*) NeuN coexpression. (*A*) Hippocampal nongranule cells. (*B*) Deep layers of entorhinal cortex. (*C*) Hippocampal nongranule cell lacking CAMKII expression. (*D*) Hippocampal nongranule cells coexpressing GAD67. (*E*) Cells coexpressing CB in deep layers of entorhinal cortex. (*F*) Cell coexpressing NPY in entorhinal cortex layer III. (*G*) Cell coexpressing SST in piriform cortex layer III. Scale bar: 25 μm. Insets are 2D projections of 4 (*A*), 5 (*B*), 9 (*C*), 6 (*D*), 13 (*E*), 10 (*F*), or 15 (*G*) consecutive confocal planes located 1-μm apart. NeuN, neuronal nuclear antigen; CAMKII, Ca^2+calmodulin dependent protein kinase II; GAD67, glutamate decarboxylase, isoform 67; CB, calbindin-D28K; NPY, neuropeptide Y; SST, somatostatin.

PSA-expressing puncta also coexpressed SYN, a synaptic vesicle membrane protein (Greengard et al. 1993), in the neuropil of all the areas analyzed (Fig. 3*E* and Table 2).

PSA-Expressing Interneurons Are Generated during Embryonic Development

Embryonic Neurogenesis

The analysis of the hippocampus, paleocortex, and mPFC of adult rats, which received 5′BrdU at different embryonic stages (E11.5, E13.5, E15.5, and E17.5), revealed that the highest proportion of PSA-expressing cells displaying 5′BrdU-labeled nuclei was found in those injected at E15.5 (Supplementary Fig. 5*C*), although there were small differences between the 3 regions analyzed (for details, see Table 1).

Early Postnatal and Adult Neurogenesis

In all the groups, some scarce 5′BrdU-labeled nuclei were found in all the regions studied (many of them appeared in pairs), we never observed any of these nuclei located inside a PSA-expressing soma. By contrast, several PSA-immunoreactive cells displaying a 5′BrdU-labeled nucleus could be observed in areas with known

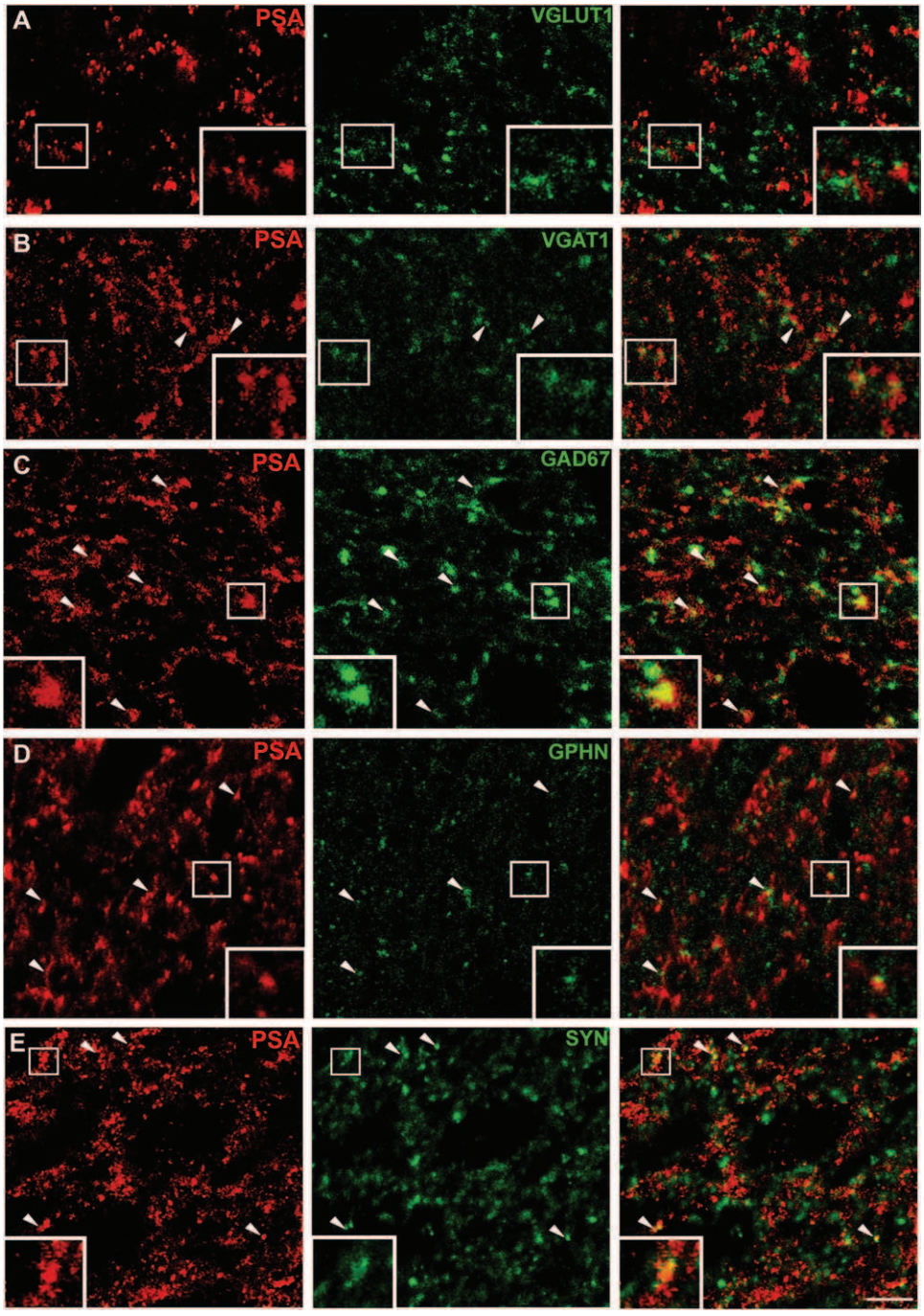

Figure 3. Confocal microscopic analysis of the phenotype of PSA-expressing puncta in the neuropil of the adult rat cerebral cortex. (*A*) VGLUT1 expression in the neuropil of deep layers of prelimbic cortex. A complete lack of colocalization is observed, although some scarce puncta expressing PSA can be seen close to one expressing VGLUT1 (please see enlarged view in inset). (*B*) PSA- and VGAT-expressing puncta in the neuropil of the prelimbic cortex (arrowheads and enlarged view in inset). (*C*) Coexpression of PSA and GAD67 in the neuropil of the entorhinal cortex. Note the abundance of puncta coexpressing both markers. It is also very frequent to see GAD67-expressing puncta surrounded by PSA immunoreactivity (please see enlarged view in inset). (*D*) PSA- and gephyrin-expressing puncta in the piriform cortex layer III neuropil. Arrowheads indicate double-labeled puncta, and the inset shows a pair of closely apposed gephyrin/PSA-expressing structures. (*E*) PSA- and SYN-expressing puncta in the neuropil of the deep layers of prelimbic cortex. Note the abundance of puncta coexpressing both molecules (arrowheads and enlarged view in inset). All the images in this figure are taken from unique confocal planes. Scale bar: 5 μm. Squared areas are enlarged twice in the insets. GAD67, glutamate decarboxylase, isoform 67.

adult neurogenic activity (subventricular zone, rostral migratory stream, olfactory bulb, and subgranular zone). This expression pattern was observed in 1) the animals injected with 5′BrdU in postnatal days P0, P10, and P20 and sacrificed when 3 months old and 2) in the 3-month-old rats injected with 5′BrdU and sacrificed 2, 4, 7, 14, 21, or 30 days later.

NCAM Is the Only Polysialylated Protein in Interneurons

Although NCAM is the major carrier of PSA in the vertebrate CNS (Hildebrandt et al. 2008), different reports have described the presence of this complex sugar in some other proteins (for details, see Introduction). Since the antibody used in this study recognizes only PSA but not the protein to which it is attached,

Table 2
Percentages of PSA-expressing puncta coexpressing different neurochemical and synaptic markers in the neuropil of the rat cerebral cortex

	Paleocortex	Prelimbic cortex
VGLUT1	0	0
VGAT	17 ± 1	19 ± 1
GAD67	18 ± 0.5	39 ± 12
Gephyrin	10 ± 5	15 ± 1.5
SYN	10 ± 1.5	13 ± 0.5

Table 3
Number of perisomatic and peridendritic puncta per micron on PSA-NCAM-expressing cells

	Entorhinal cortex (soma)	Entorhinal cortex (dendrites)	Nongranule cells (soma)	Nongranule cells (dendrites)
VGLUT1	0.11 ± 0.01	0.15 ± 0.02	0.07 ± 0.01	0.06 ± 0.01
GAD67	0.08 ± 0.02	0.18 ± 0.03	0.20 ± 0.03	0.28 ± 0.02
SYN	0.17 ± 0.03	0.33 ± 0.03	0.19 ± 0.03	0.24 ± 0.1

we analyzed inhibitory elements in NCAM-deficient mice using PSA immunohistochemistry. Our study revealed the absence of PSA expression in cortical somata or neuropil elements expressing GAD67 (Fig. 4*A*,*B*), indicating that in inhibitory elements, PSA was exclusively associated to NCAM. Consequently, from this point, the antigen recognized by our antibody is denominated PSA-NCAM.

The Expression of PSA-NCAM in Interneurons Is Not Affected by Genetic Deletion of NCAM in Principal Cells

The analysis of PSA-NCAM expression in NCAMff+ mice (in which the NCAM gene is ablated under the control of the CaMKII promoter and thus absent from principal neurons) has revealed very few differences when comparing these animals with their wild-type littermates. NCAMff+ mice lacked PSA-NCAM expression in their hippocampal mossy fibers but presented several labeled cells in the SGZ of the dentate gyrus, as described (Bukalo et al. 2004). Typical PSA-NCAM–expressing interneurons were found in all the regions studied, with similar morphology and distribution to those described in GIN mice, many of which coexpressed GAD67 (Fig. 4*C*,*D*). We estimated the number of PSA-NCAM–expressing cells in the CA1 region of the entire hippocampus, and there were no significant differences between NCAMff– (1892 ± 224.4) and NCAMff+ mice (2004 ± 70.8) (Unpaired student's *t*-test, $P = 0.86$). However, densitometric analysis revealed that NCAMff+ mice showed a small, but significant, reduction in PSA-NCAM expression in the neuropil of CA1 lacunosum moleculare (wild type: 83.556 ± 7.601, NCAMff+: 28.667 ± 3.908; $P = 0.046$, Fig. 4*E*,*F*). This reduction was not detectable in deep layers of the infralimbic cortex (wild type: 24.443 ± 6.738, NCAMff+: 36.113 ± 10.794; $P = 0.932$, Fig. 4*G*,*H*).

PSA-NCAM–Expressing Interneurons Have Lower Density of Perisomatic and Peridendritic Puncta than Interneurons Lacking PSA-NCAM

The analysis of perisomatic and peridendritic puncta on PSA-NCAM–expressing interneurons was performed in deep layers of the paleocortex and in the ventral hippocampus (Tables 3 and 4). These cells displayed perisomatic and peridendritic puncta expressing different markers of presynaptic excitatory

Table 4
Comparison of the number of perisomatic and peridendritic SYN puncta/micron between GAD67-expressing cells and GAD67/PSA-NCAM coexpressing cells

	Nongranule cells (perisomatic puncta)	Nongranule cells (peridendritic puncta)
GAD67+/PSA-NCAM–	0.39 ± 0.03	0.66 ± 0.08
GAD67+/PSA-NCAM+	0.19 ± 0.03	0.24 ± 0.04

(VGLUT1, Fig. 5*A*) and inhibitory (VGAT and GAD67, Fig. 5*B*,*C*) elements as well as the general synaptic marker SYN (Fig. 6*A*).

The differences in the number of SYN-expressing puncta per micron of soma or dendrite profile between interneurons expressing PSA-NCAM with those lacking this molecule were studied in the ventral hippocampus (Table 4, Fig. 6). In this region, the number of puncta per micron was significantly lower in PSA-NCAM–expressing interneurons, both in the perisomatic and in the peridendritic regions (unpaired Student's *t*-test, $P = 0.0005$ and $P = 0.001$, respectively).

PSA-NCAM–Expressing Interneurons Have Lower Density of Perisomatic Synapses than Interneurons Lacking PSA-NCAM

The ultrastructure of PSA-NCAM–expressing nongranule neurons in the ventral region of the hippocampus and of interneurons in deep layers of the mPFC was studied with transmission electron microscopy (Fig. 7). All the cells studied showed typical interneuron features, such as a profound invagination of the nucleus, reduced soma size when compared with pyramidal neurons, and an electron-dense cytoplasm with high density of mitochondria, endoplasmic reticulum, and Golgi apparatus (Schwartzkroin and Kunkel 1985; Babb et al. 1988). Excitatory and inhibitory synaptic contacts were observed in the perisomatic region of these interneurons. PSA-NCAM expression was found restricted to the plasma membrane and located exclusively at the extracellular surface (Fig. 7*A*,*B*). Although immunolabeling was present in most of the surface of the somata studied, it was never found on the surface contacting a presynaptic membrane. By contrast, pyramidal neuron somata in the hippocampus and mPFC cortex never showed PSA-NCAM expression in their plasma membrane.

Since the qualitative estimation of the number of perisomatic synaptic contacts per micron of membrane in these hippocampal PSA-NCAM interneurons revealed differences with those lacking PSA-NCAM expression in their vicinity, a detailed comparison of this number was made. The number of perisomatic synaptic contacts normalized to the cell perimeters sampled in PSA-NCAM–expressing interneurons was significantly smaller than in those lacking expression of this molecule (Fig. 7*C*).

PSA-NCAM–Expressing Interneurons Have Reduced Dendritic Arborization and Spine Density Compared With Interneurons Lacking PSA-NCAM

In the ventral hippocampus, Sholl analysis revealed reduced dendritic arborization in GFP+/PSA-NCAM+–expressing interneurons when compared with GFP+/PSA-NCAM– cells (Fig. 8*A*,*B*). These differences were significant in the 2–6 segments (20 μm) of distance from the soma, reaching a maximum difference in the fourth segment (Fig. 8*C*). The number of bifurcations was also significantly smaller in PSA-NCAM–expressing interneurons (Fig. 8*D*).

The analysis of dendritic spine density also showed significant differences in the dendrites of the PSA-NCAM–expressing

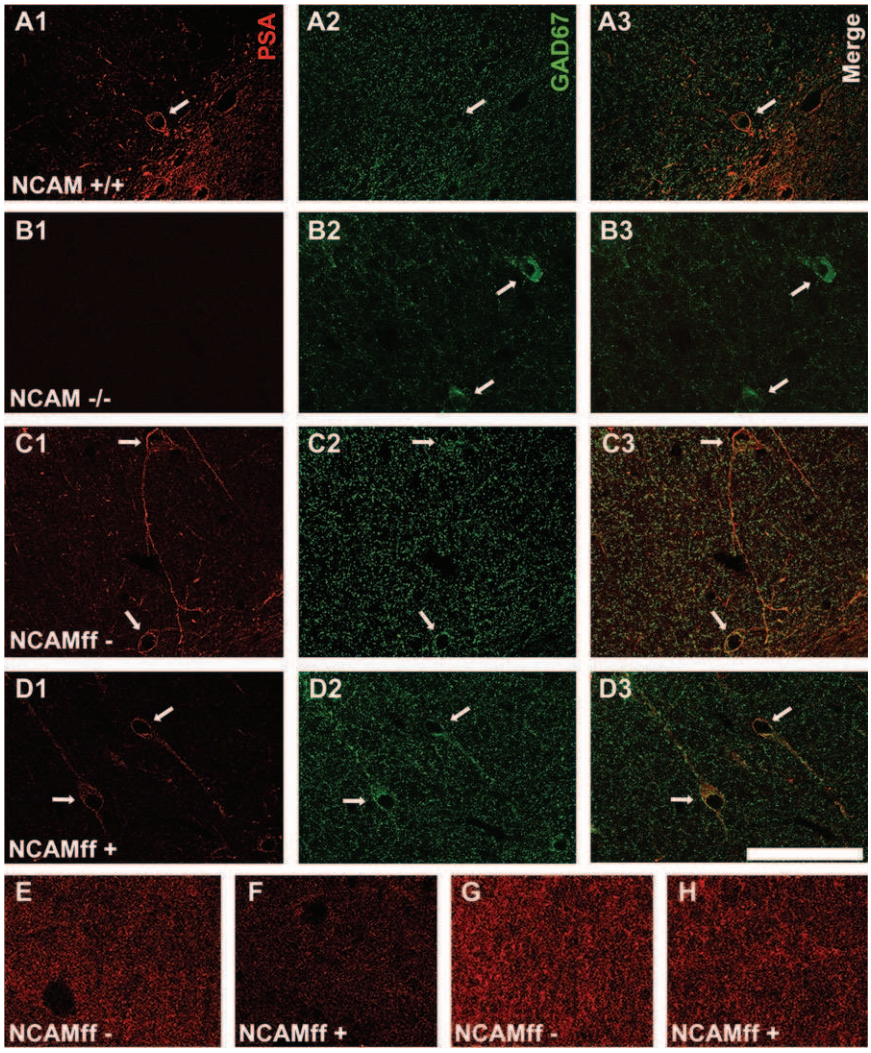

Figure 4. Confocal microscopic analysis of PSA expression in inhibitory elements (expressing GAD67) in NCAM-deficient mice and NCAMff mice. GAD67- and PSA-expressing interneuronal somata are indicated by arrows. (*A–F*) CA1 hippocampal stratum radiatum and (*G* and *H*) prelimbic cortex. (*A*) $NCAM^{+/+}$ mice display PSA and GAD67 immunoreactivity in neuronal somata and neuropil. (*B*) In $NCAM^{-/-}$ mice, although GAD67 expression is still present, PSA-NCAM labeling is completely absent. (*C*) NCAMff− mice show normal PSA-NCAM and GAD67 expression. (*D*) This expression pattern is preserved in NCAMff+ mice. (*E* and *F*) PSA-NCAM expression in the CA1 stratum lacunosum moleculare. Observe that immunoreactivity is considerably reduced in NCAMff+ mice. (*G* and *H*) PSA-NCAM expression in prelimbic cortex layer IV. No differences in immunoreactivity intensity can be observed between NCAMff− and NCAMff+ mice. All images are single confocal sections. Scale bar: 75 μm for *A–D* and 25 μm for *E–H*.

interneurons (Fig. 8*E,F*). The dendrites of interneurons expressing GFP were divided into 3 segments of 60 μm. We found a significant reduction in the dendritic spine density of PSA-NCAM–expressing interneurons in the 2 distal segments (Fig. 8*G*). This reduction was also significant when taking into account the whole length of the dendrite fragment studied (Fig. 8*H*).

Discussion

PSA-NCAM–Expressing Cells Are Mature Interneurons Widely Distributed in the Adult Rodent Cerebral Cortex

The present results describe a widespread distribution of mature PSA-expressing neurons in the adult rodent cerebral cortex. They expand previous findings describing the existence of PSA-expressing cells in the hippocampus outside the subgranular zone (Nacher, Blasco-Ibanez, and McEwen 2002) and in the mPFC (Varea, Castillo-Gomez, et al. 2007). Other authors previously also acknowledged briefly the existence of these cells in the hippocampus (Bonfanti et al. 1992) and in the ventral cingulate cortex of rodents (Seki and Arai 1991) and the neocortex, hippocampal formation, and entorhinal cortex of humans (Mikkonen et al. 1999; Arellano et al. 2002; Varea, Castillo-Gomez, et al. 2007). However, a detailed analysis of the distribution of these cells and their phenotype has only been performed in the hippocampus and mPFC of rodents.

Although NCAM is not the exclusive carrier of PSA (Zuber et al. 1992; Close and Colley 1998; Curreli et al. 2007; Galuska et al. 2010), the present results strongly suggest that NCAM is its only carrier in cortical interneurons. Consequently, following the terminology used in our previous reports and in that of other laboratories, in this discussion and the appropriate parts of the Results section, we refer to this molecule as PSA-NCAM.

Due to its intense expression in immature neurons, PSA-NCAM has been erroneously considered in many studies an exclusive developmental marker. However, previous works have clearly demonstrated its presence in mature neurons and its involvement in their structural plasticity (for review, see

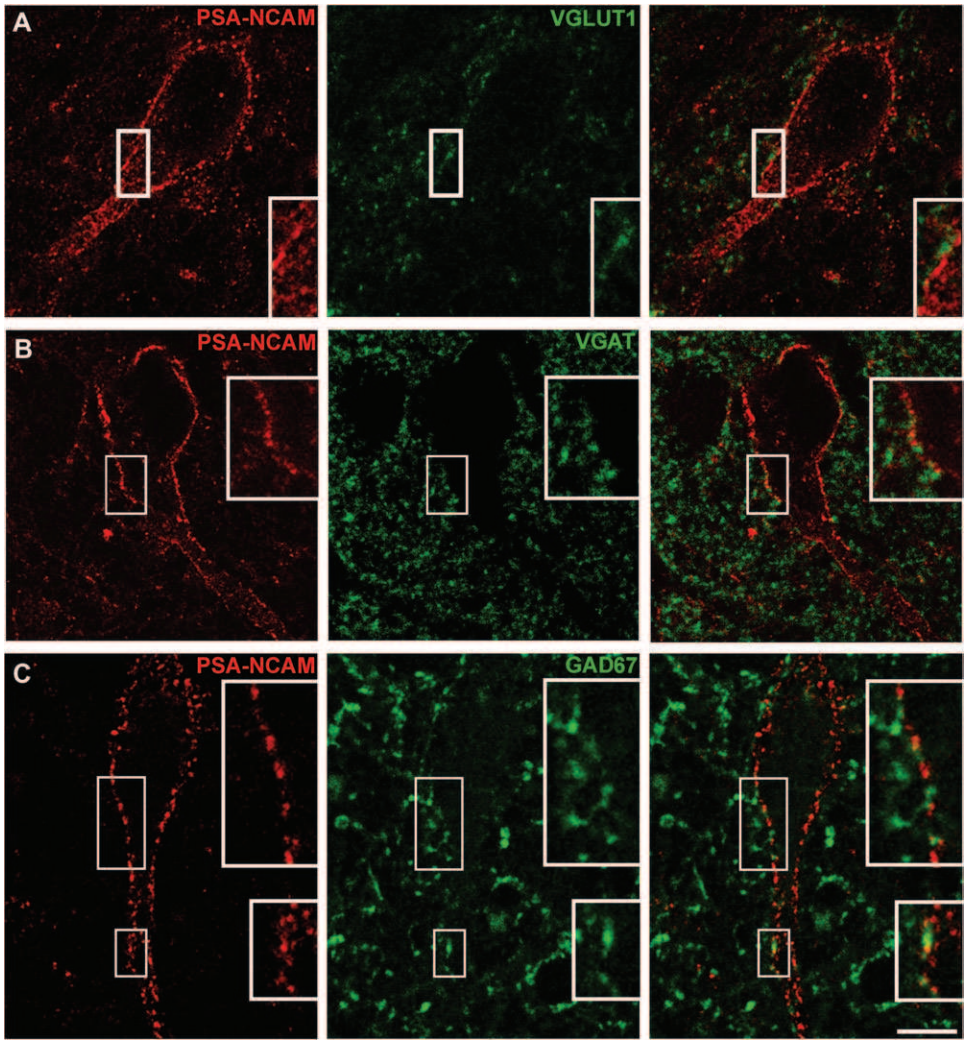

Figure 5. Confocal microscopic analysis of perisomatic and peridendritic puncta on PSA-NCAM–expressing interneurons of adult rats. Ventral hippocampus. (*A*) VGLUT1-expressing puncta on PSA-NCAM–expressing cells. (*B* and *C*) VGAT (*B*) and GAD67 (*C*) expressing puncta on PSA-NCAM–expressing cells. Note the abundance of perisomatic and peridendritic puncta on the cell surface (insets). All the images in this figure are taken from single confocal planes. Scale bar: 5 μm. (Insets in the figures are ×2 enlargements.) GAD67, glutamate decarboxylase, isoform 67.

Bonfanti 2006; Gascon et al. 2007; Rutishauser 2008). The present work also argues against this incorrect view and clearly indicates that most PSA-NCAM–expressing cells outside adult neurogenic regions and paleocortex layer II are mature neurons, most of which have been generated during embryonic development.

Different lines of evidence indicate that mature cortical neurons expressing PSA-NCAM constitute a subpopulation of interneurons: 1) the expression of the enzyme responsible for GABA synthesis (revealed by GAD67 immunohistochemistry and by the analysis of transgenic mice expressing GFP under the GAD67 promoter), 2) the ultrastructural characteristics, and 3) the expression of different neuropeptides and calcium-binding proteins considered exclusive markers of mature interneurons.

The fact that many PSA-NCAM–expressing cells do not appear to colocalize with inhibitory markers can be explained because none of these markers is present in all interneurons. Even the expression of GABA or their synthesizing enzymes is not found in all interneuronal somata; some interneurons, depending on their activity or the distance to their axonal terminals, may have low levels of these molecules in their somata (Freund and Buzsaki 1996). The differences observed in the percentages of PSA-NCAM/GAD67–expressing hippocampal nongranule neurons between rats and mice may be due to species differences in the expression of the enzyme or in its antigenicity since the methodology used and the region studied were the same in both species.

PSA-NCAM–expressing elements in the cortical neuropil also appear to belong to inhibitory neurons because they express markers associated with interneuronal neurites or synapses. Most of these elements must correspond to neurites of local interneurons, although, since PSA-NCAM is expressed in interneurons of extracortical regions, such as the amygdala (Nacher J and Gomez-Climent MA, unpublished data) or the septum (Foley et al. 2003), some of them may correspond to projections from extracortical origin.

Moreover, our data demonstrate that PSA-NCAM expression is clearly absent from mature principal neuron somata in the adult cerebral cortex, using electron microscopy, CAMKII

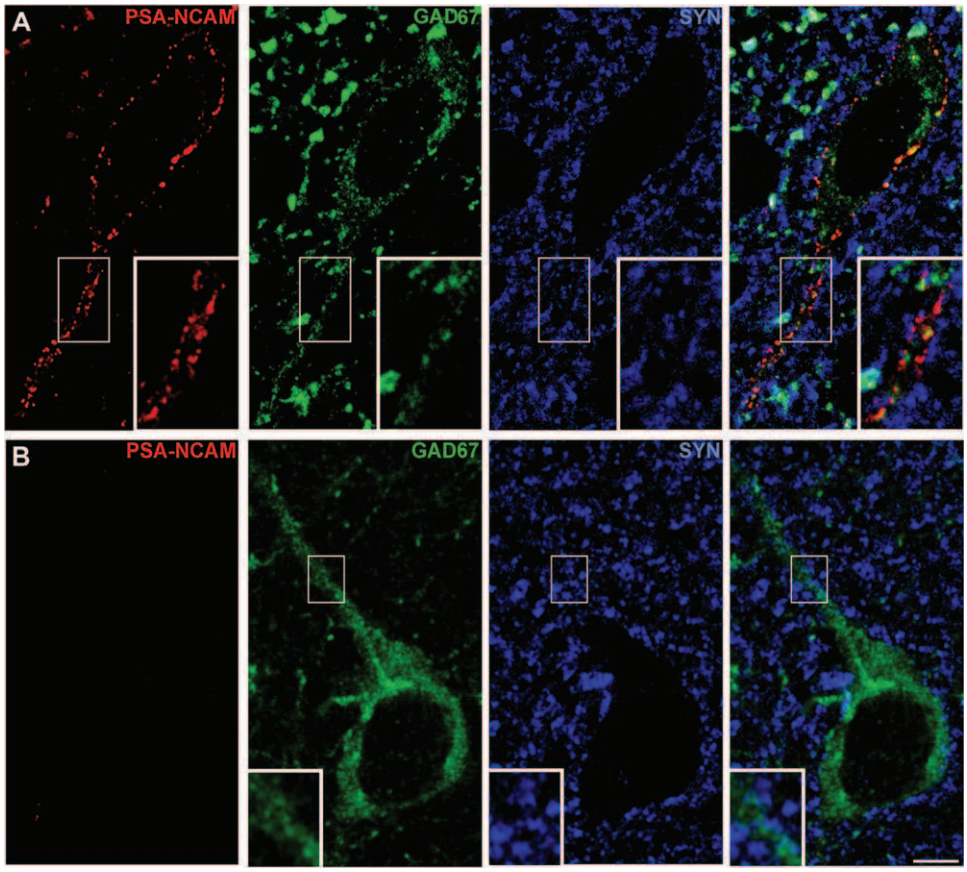

Figure 6. Confocal microscopic analysis of perisomatic and peridendritic puncta on PSA-NCAM–expressing versus non-PSA-NCAM–expressing interneurons of adult rats. Ventral hippocampus. (*A*) SYN-expressing puncta on a cell coexpressing PSA-NCAM and GAD67. (*B*) SYN-expressing puncta on a GAD67-expressing cell lacking PSA-NCAM expression. All the images in this figure are taken from single confocal planes. Scale bar: 5 μm. (Insets in the figures are ×2 enlargements.) GAD67, glutamate decarboxylase, isoform 67.

immunohistochemistry, and transgenic mice, in which pyramidal neurons can be unequivocally identified by YFP expression. The absence of PSA-NCAM expression in principal neurons of the neocortex is also supported by our analysis of NCAMff+ transgenic mice, in which NCAM is absent from excitatory neurons. However, certain mature excitatory neuronal populations in the hippocampus of wild-type rodents express PSA-NCAM only in their axons or their terminal boutons: the axons (mossy fibers) of most mature granule cells in the hilus and CA3 stratum lucidum (Seki and Arai 1999) and the terminal boutons of axons of CA3 pyramidal neurons (Schaffer collaterals), some of which terminate in the CA1 stratum lacunosum moleculare (Muller et al. 1996; Schuster et al. 2001). This may explain the lack of PSA-NCAM expression in the mossy fibers of NCAMff+ mice (Bukalo et al. 2004), and its reduction in the stratum lacunosum moleculare (present results). However, in NCAMff+ mice, not only PSA but also NCAM are ablated and, consequently, the effects observed may be NCAM dependent.

Cortical interneurons can be classified on basis of their neurochemical properties by the expression of different calcium-binding proteins and neuropeptides (for review, see Freund and Buzsaki 1996; Markram et al. 2004; Ascoli et al. 2008). The present results indicate that cortical PSA-NCAM–expressing interneurons do not belong to any of the previously described categories. Moreover, there are substantial differences in the coexpresssion of PSA-NCAM and different calcium-binding proteins/neuropeptides between different cortical regions, especially in the hippocampus. In the paleocortex and neocortex, many of the PSA-NCAM–expressing cells express calbindin and somatostatin, while few of them express parvalbumin, calretinin, neuropeptide Y, or vasointestinal peptide. By contrast, in the hippocampus, many PSA-NCAM–expressing nongranule neurons express calretinin. It is also conceivable that some interneurons do not express PSA-NCAM in their somata but only in their terminal fields.

Possible Dynamics of PSA-NCAM Expression in Interneurons

In contrast to PSA-NCAM expression in the hippocampal subgranular zone or the paleocortex layer II, which is strongly downregulated during aging (Seki and Arai 1995; Abrous et al. 1997; Varea et al. 2009), PSA-NCAM expression in cortical interneurons is stable over lifetime (both in the number of PSA-NCAM–expressing cells and in the intensity of PSA-NCAM–expressing neuropil) (Varea et al. 2009). However, we do not know whether PSA-NCAM is expressed always in the same subgroup of interneurons or whether different groups of interneurons can switch on and off this expression depending on synaptic activity. It is also possible that all, or a subset, of PSA-NCAM–expressing interneurons retain this expression constitutively since their generation during embryonic development. In any case, our laboratory has demonstrated that different pharmacological manipulations can increase or decrease the number of PSA-NCAM–expressing neurons in the

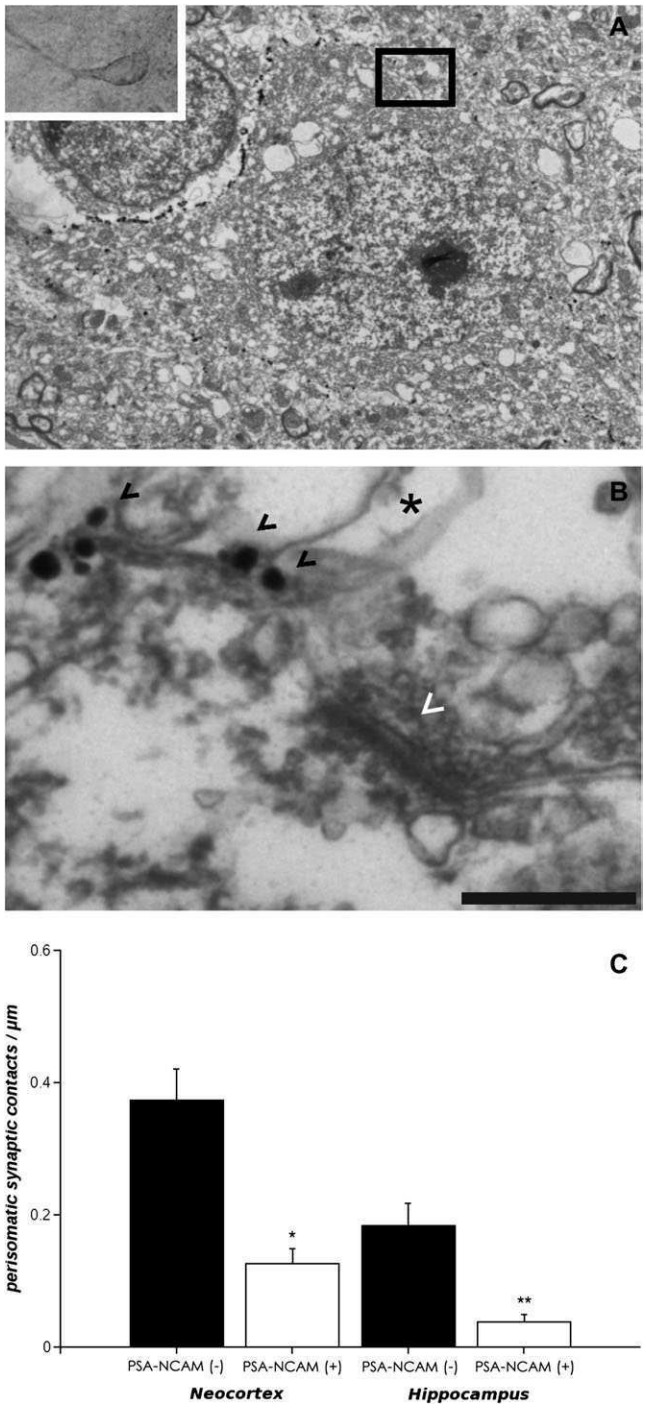

Figure 7. (*A* and *B*) Electron micrographs of gold-immunolabeled PSA-NCAM–expressing cells in the ventral hippocampus of adult rats. (*A*) Panoramic view of a PSA-NCAM–expressing interneuron soma. Black arrowheads point to antigen location on the surface of the plasma membrane The small inset, in the right top of the figure, show an optical micrograph of the PSA-NCAM–expressing neuron in the resin-embedded sections from where ultrathins were obtained. (*B*) Detailed view of the squared area in *A*, showing an asymmetric synaptic contact (white arrowhead) on the surface of the cell somata. Note that gold particles (black arrowheads) are found in the surroundings of the synapse but not inside it. (*C*) Histogram showing the differences in the number of perisomatic synapses per micron between interneurons lacking PSA-NCAM expression and those expressing this molecule. Asterisks indicate statistically significant differences ($^*P < 0.05$, $^{**}P < 0.01$), and values represent means ± standard error of the mean. Scale bar = 5 µm for *A*, 0.5 µm for *B*.

adult cerebral cortex (Varea, Blasco-Ibanez, et al. 2007; Varea, Castillo-Gomez, et al. 2007; Castillo-Gomez et al. 2008), indicating that, at least to some extent, inhibitory neurons can stop expressing, express de novo, or reexpress PSA-NCAM. Although there are reports on postnatal generation of interneurons in the neocortex (Cameron and Dayer 2008; Ohira et al. 2010), our 5′BrdU studies do not support the possibility that PSA-NCAM–expressing interneurons belong to this subpopulation of recently generated neurons.

Functional Significance of PSA-NCAM Expression in Interneurons

The most important issue in our study is the question relating to the physiological consequences for an interneuron to express PSA-NCAM on its plasma membrane. Two nonexcluding hypotheses can be formulated. First, the presence of PSA-NCAM reduces cell-to-cell and cell-to-extracellular matrix adhesion, thus allowing interneurons to remodel the structure of their neurites, spines, and/or synapses. Thus, the morphology of PSA-NCAM–expressing interneurons may be just an instantaneous "picture" of a dynamic remodeling process. Whether PSA-NCAM expression is necessary for arbor rearrangements observed in cortical interneurons in vivo (Lee et al. 2006) remains to be explored. Logically, the next step would be to study the effects of PSA depletion on interneuronal structure and preliminary experiments in our laboratory indicate that these effects are indeed intense.

The second hypothesis would imply that PSA-NCAM expression plays an insulatory role, restricting the possibility of establishing synaptic contacts in the plasma membrane regions where it is present. In fact, under the electron microscope, we never have found a synapse in a portion of surface displaying PSA-NCAM expression, and previous reports have suggested that reduced NCAM function (for instance by the addition of PSA) may lead to a decreased stability of synaptic contacts (De Paola et al. 2003). We cannot exclude, however, that the absence of PSA-NCAM in some of these synapses may be due to problems with antibody penetration or immunodetection protocols in the material destined to electron microscopic studies. Additionally, it has to be noted that the detection of perisomatic puncta using immunohistochemistry and confocal microscopy suggests, but does not demonstrate, the presence of synapses. Only transmission electron microscopy can clearly show these structures. The spatial resolution provided by conventional confocal microscopy may be insufficient to discriminate the location of the molecules in the synapse or to clearly distinguish the puncta that make synapses with PSA-NCAM–expressing neurons from closely located ones that may not have synaptic contacts.

We have recently described that immature PSA-NCAM–expressing neurons in the adult paleocortex layer II are completely isolated from synaptic input, probably due to the presence of PSA-NCAM and glial processes in most of their surface (Gomez-Climent et al. 2008). By contrast, this insulation is incomplete in PSA-NCAM–expressing interneurons, since we have found that some excitatory and inhibitory puncta are found close to their perisomatic and peridendritic surface, and both excitatory and inhibitory synapses contact at least the perisomatic region of these interneurons. Consequently, PSA-NCAM–expressing interneurons are integrated in the cortical circuits but, since they receive less input, they may

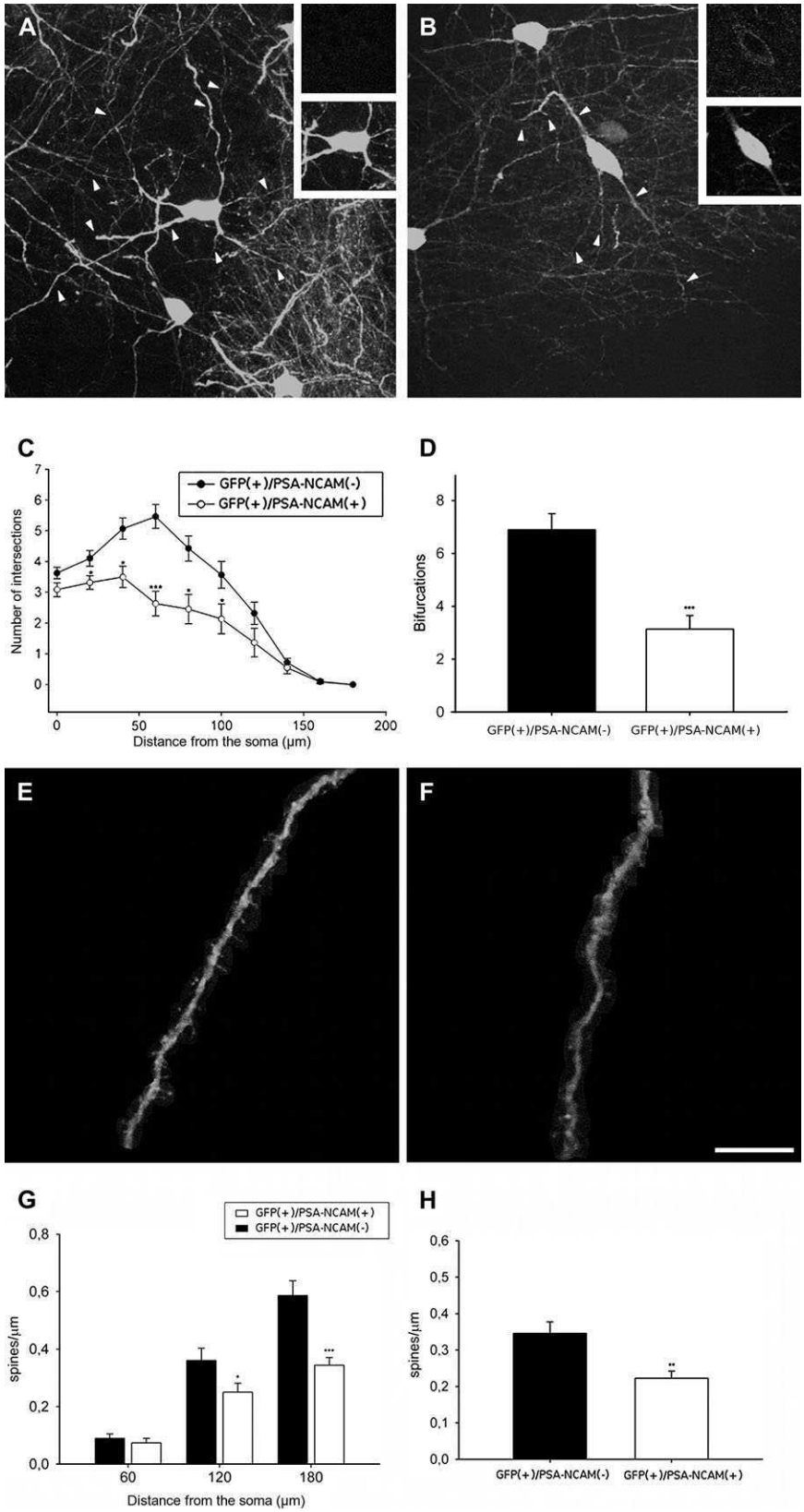

Figure 8. Dendritic arborization and spine density in GFP+/PSA-NCAM− versus GFP+/PSA-NCAM+ expressing interneurons in the ventral hippocampus of GIN mice. (*A* and *B*) 3D reconstructions of GFP-expressing interneurons lacking PSA-NCAM expression (*A*) and coexpressing PSA-NCAM (*B*). Insets are views of the somata displayed in *A* and *B* showing coexpression of PSA-NCAM (up) and GFP (bottom). (*C* and *D*) Sholl analysis of GFP-expressing interneurons, showing intersection number per 20-μm dendritic radial unit distance from the soma (*C*) and bifurcation number (*D*). White circles (*C*) and bars (*D*) indicate interneurons lacking PSA-NCAM expression and black circles and bars correspond to PSA-NCAM–expressing interneurons. (*E* and *F*) Compositions, using fragments of different confocal planes, of spinous dendrites of GFP-expressing cells in interneurons expressing PSA-NCAM (*E*) and in interneurons lacking this molecule (*F*). (*G* and *H*) Histograms of the differences in dendritic spine density in segments at different distances from the soma (*G*) and the total density of dendritic spines (*H*). Scale bar = 10 μm (*E* and *F*) and 50 μm (*A* and *B*). Asterisks indicate statistically significant differences (*$P < 0.05$, **$P < 0.01$, ***$P < 0.001$). Values represent means ± standard error of the mean.

have reduced activity, possibly resulting in reduced dendritic arborization, decreased spine density, and low expression of cell activity markers. Electrophysiology experiments need to be performed to verify this hypothesis. However, new techniques for identifying PSA-NCAM–expressing cells, which do not affect PSA function/structure, should be developed before conducting these experiments. It is tempting to think that PSA-NCAM–expressing interneurons may constitute a reservoir, which, after downregulating PSA-NCAM expression, may receive more synaptic contacts and thus become more integrated in the circuitry. Conversely, PSA-NCAM upregulation in interneurons may lead to the opposite effect.

It has to be noted that, in contrast with our results, a previous report described that PSA-NCAM–expressing neurons receive more synapses than those lacking NCAM (and consequently PSA) (Dityatev et al. 2000), suggesting that the presence of PSA-NCAM may promote synapse formation. However, these were cultured neurons from very young animals. It is possible that in the environment of the control adult cerebral cortex, in which plasticity is reduced, the presence of PSA-NCAM in interneurons may mainly have an insulating role.

The presence of PSA-NCAM on interneurons may also interfere with NCAM-signaling pathways in these cells or their synaptic input: Different reports have demonstrated that polysialylation of NCAM decreases homophilic binding and may influence the interactions with heterophilic-binding partners, such as growth factor receptors (for review, see Gascon et al. 2007) or, as it has been recently described, glutamate receptors (Kochlamazashvili et al. 2010).

In conclusion, expression of PSA-NCAM on interneurons may have important implications on the structure and physiology of cortical inhibitory circuits. This expression may also be relevant for the understanding of the etiology of certain psychiatric disorders, in which alteration of inhibitory networks has been described. Recent work in our laboratory has demonstrated PSA-NCAM expression in the neocortex is regulated by dopamine (Castillo-Gomez et al. 2008) and serotonin (Varea, Blasco-Ibanez, et al. 2007; Varea, Castillo-Gomez, et al. 2007), which are profoundly implicated in the etiology and pharmacological treatment of schizophrenia and major depression. Moreover, this expression is also regulated in animal models of depression, (Pham et al. 2003; Cordero et al. 2005), and in the hippocampus of schizophrenic patients (Barbeau et al. 1995).

Funding

Spanish Ministry of Science and Innovation (MICINN-FEDER) BFU2007-64130/BFI and BFU2009-12284/BFI; Generalitat Valenciana CS2009-AP-127 and ACOMP2009/271; Foundation Jerome Lejeune; Stanley Medical research Institute. E.C.-G. and M.A.G.-C. have FPU predoctoral fellowships from the Spanish Ministry of Education and Science (AP2006-01953 and AP2005-4672). R.G. has an FPI predoctoral fellowship from the Spanish Ministry of Education and Science (BES 2007-15757).

Supplementary Material

Supplementary material can be found at: http://www.cercor.oxfordjournals.org/

Notes

Conflict of Interest: None declared.

References

Abrous DN, Montaron MF, Petry KG, Rougon G, Darnaudery M, Le Moal M, Mayo W. 1997. Decrease in highly polysialylated neuronal cell adhesion molecules and in spatial learning during ageing are not correlated. Brain Res. 744:285–292.

Arellano JI, DeFelipe J, Munoz A. 2002. PSA-NCAM immunoreactivity in chandelier cell axon terminals of the human temporal cortex. Cereb Cortex. 12:617–624.

Ascoli GA, Alonso-Nanclares L, Anderson SA, Barrionuevo G, Benavides-Piccione R, Burkhalter A, Buzsaki G, Cauli B, Defelipe J, Fairen A, et al. 2008. Petilla terminology: nomenclature of features of GABAergic interneurons of the cerebral cortex. Nat Rev Neurosci. 9:557–568.

Babb TL, Pretorius JK, Kupfer WR, Brown WJ. 1988. Distribution of glutamate-decarboxylase-immunoreactive neurons and synapses in the rat and monkey hippocampus: light and electron microscopy. J Comp Neurol. 278:121–138.

Barbeau D, Liang JJ, Robitalille Y, Quirion R, Srivastava LK. 1995. Decreased expression of the embryonic form of the neural cell adhesion molecule in schizophrenic brains. Proc Natl Acad Sci U S A. 92:2785–2789.

Bonfanti L. 2006. PSA-NCAM in mammalian structural plasticity and neurogenesis. Prog Neurobiol. 80:129–164.

Bonfanti L, Olive S, Poulain DA, Theodosis DT. 1992. Mapping of the distribution of polysialylated neural cell adhesion molecule throughout the central nervous system of the adult rat: an immunohistochemical study. Neuroscience. 49:419–436.

Bukalo O, Fentrop N, Lee AY, Salmen B, Law JW, Wotjak CT, Schweizer M, Dityatev A, Schachner M. 2004. Conditional ablation of the neural cell adhesion molecule reduces precision of spatial learning, long-term potentiation, and depression in the CA1 subfield of mouse hippocampus. J Neurosci. 24:1565–1577.

Cameron HA, Dayer AG. 2008. New interneurons in the adult neocortex: small, sparse, but significant? Biol Psychiatry. 63: 650–655.

Castillo-Gomez E, Gomez-Climent MA, Varea E, Guirado R, Blasco-Ibanez JM, Crespo C, Martinez-Guijarro FJ, Nacher J. 2008. Dopamine acting through D2 receptors modulates the expression of PSA-NCAM, a molecule related to neuronal structural plasticity, in the medial prefrontal cortex of adult rats. Exp Neurol. 214(1):97–111.

Close BE, Colley KJ. 1998. In vivo autopolysialylation and localization of the polysialyltransferases PST and STX. J Biol Chem. 273: 34586–34593.

Cordero MI, Rodriguez JJ, Davies HA, Peddie CJ, Sandi C, Stewart MG. 2005. Chronic restraint stress down-regulates amygdaloid expression of polysialylated neural cell adhesion molecule. Neuroscience. 133:903–910.

Cremer H, Lange R, Christoph A, Plomann M, Vopper G, Roes J, Brown R, Baldwin S, Kraemer P, Scheff S. 1994. Inactivation of the N-CAM gene in mice results in size reduction of the olfactory bulb and deficits in spatial learning. Nature. 367:455–459.

Curreli S, Arany Z, Gerardy-Schahn R, Mann D, Stamatos NM. 2007. Polysialylated neuropilin-2 is expressed on the surface of human dendritic cells and modulates dendritic cell-T lymphocyte interactions. J Biol Chem. 282:30346–30356.

De Paola V, Arber S, Caroni P. 2003. AMPA receptors regulate dynamic equilibrium of presynaptic terminals in mature hippocampal networks. Nat Neurosci. 6:491–500.

Dityatev A, Dityateva G, Schachner M. 2000. Synaptic strength as a function of post- versus presynaptic expression of the neural cell adhesion molecule NCAM. Neuron. 26:207–217.

Foley AG, Ronn LC, Murphy KJ, Regan CM. 2003. Distribution of polysialylated neural cell adhesion molecule in rat septal nuclei and septohippocampal pathway: transient increase of polysialylated interneurons in the subtriangular septal zone during memory consolidation. J Neurosci Res. 74:807–817.

Freund TF, Buzsaki G. 1996. Interneurons of the hippocampus. Hippocampus. 6:1–470.
Fritschy JM, Harvey RJ, Schwarz G. 2008. Gephyrin: where do we stand, where do we go? Trends Neurosci. 31:257–264.
Galuska SP, Rollenhagen M, Kaup M, Eggers K, Oltmann-Norden I, Schiff M, Hartmann M, Weinhold B, Hildebrandt H, Geyer R, et al. 2010. Synaptic cell adhesion molecule SynCAM 1 is a target for polysialylation in postnatal mouse brain. Proc Natl Acad Sci U S A. 107:10250–10255.
Gascon E, Vutskits L, Kiss JZ. 2007. Polysialic acid-neural cell adhesion molecule in brain plasticity: from synapses to integration of new neurons. Brain Res Rev. 56:101–118.
Gogolla N, Galimberti I, Deguchi Y, Caroni P. 2009. Wnt signaling mediates experience-related regulation of synapse numbers and mossy fiber connectivities in the adult hippocampus. Neuron. 62:510–525.
Gomez-Climent MA, Castillo-Gomez E, Varea E, Guirado R, Blasco-Ibanez JM, Crespo C, Martinez-Guijarro FJ, Nacher J. 2008. A population of prenatally generated cells in the rat paleocortex maintains an immature neuronal phenotype into adulthood. Cereb Cortex. 18:2229.
Greengard P, Valtorta F, Czernik AJ, Benfenati F. 1993. Synaptic vesicle phosphoproteins and regulation of synaptic function. Science. 259:780–785.
Hildebrandt H, Muhlenhoff M, Gerardy-Schahn R. 2008. Polysialylation of NCAM. Neurochem Res. doi:10.1007/s11064-008-9724-7.
Kochlamazashvili G, Senkov O, Grebenyuk S, Robinson C, Xiao MF, Stummeyer K, Gerardy-Schahn R, Engel AK, Feig L, Semyanov A, et al. 2010. Neural cell adhesion molecule-associated polysialic acid regulates synaptic plasticity and learning by restraining the signaling through GluN2B-containing NMDA receptors. J Neurosci. 30:4171–4183.
Lee WC, Chen JL, Huang H, Leslie JH, Amitai Y, So PT, Nedivi E. 2008. A dynamic zone defines interneuron remodeling in the adult cortex. Proc Natl Acad Sci U S A. 105:6.
Lee WC, Huang H, Feng G, Sanes JR, Brown EN, So PT, Nedivi E. 2006. Dynamic remodeling of dendritic arbors in GABAergic interneurons of adult visual cortex. PLoS Biol. 4:e29.
Markram H, Toledo-Rodriguez M, Wang Y, Gupta A, Silberberg G, Wu C. 2004. Interneurons of the neocortical inhibitory system. Nat Rev Neurosci. 5:793–807.
McIntire SL, Reimer RJ, Schuske K, Edwards RH, Jorgensen EM. 1997. Identification and characterization of the vesicular GABA transporter. Nature. 389:870–876.
Mikkonen M, Soininen H, Tapiola T, Alafuzoff I, Miettinen R. 1999. Hippocampal plasticity in Alzheimer's disease: changes in highly polysialylated NCAM immunoreactivity in the hippocampal formation. Eur J Neurosci. 11:1754–1764.
Muhlenhoff M, Eckhardt M, Bethe A, Frosch M, Gerardy-Schahn R. 1996. Autocatalytic polysialylation of polysialyltransferase-1. EMBO J. 15:6943–6950.
Mullen RJ, Buck CR, Smith AM. 1992. NeuN, a neuronal specific nuclear protein in vertebrates. Development. 116:201–211.
Muller D, Wang C, Skibo G, Toni N, Cremer H, Calaora V, Rougon G, Kiss JZ. 1996. PSA-NCAM is required for activity-induced synaptic plasticity. Neuron. 17:413–422.
Nacher J, Alonso-Llosa G, Rosell DR, McEwen BS. 2002. PSA-NCAM expression in the piriform cortex of the adult rat. Modulation by NMDA receptor antagonist administration. Brain Res. 927:111–121.
Nacher J, Blasco-Ibanez JM, McEwen BS. 2002. Non-granule PSA-NCAM immunoreactive neurons in the rat hippocampus. Brain Res. 930:1–11.
Nacher J, Varea E, Blasco-Ibanez JM, Castillo-Gomez E, Crespo C, Martinez-Guijarro FJ, McEwen BS. 2005. Expression of the transcription factor Pax 6 in the adult rat dentate gyrus. J Neurosci Res. 81:753–761.
Ohira K, Furuta T, Hioki H, Nakamura KC, Kuramoto E, Tanaka Y, Funatsu N, Shimizu K, Oishi T, Hayashi M, et al. 2010. Ischemia-induced neurogenesis of neocortical layer 1 progenitor cells. Nat Neurosci. 13:173–179.
Paxinos G, Franklin KBJ. 1997. The mouse brain in stereotaxic coordinates. London: Academic Press.
Paxinos G, Watson C. 1986. The rat brain in stereotaxic coordinates. London: Academic Press.
Pham K, Nacher J, Hof PR, McEwen BS. 2003. Repeated restraint stress suppresses neurogenesis and induces biphasic PSA-NCAM expression in the adult rat dentate gyrus. Eur J Neurosci. 17:879–886.
Rougon G, Dubois C, Buckley N, Magnani JL, Zollinger W. 1986. A monoclonal antibody against meningococcus group B polysaccharides distinguishes embryonic from adult N-CAM. J Cell Biol. 103:2429–2437.
Rousselot P, Lois C, Alvarez-Buylla A. 1995. Embryonic (PSA) N-CAM reveals chains of migrating neuroblasts between the lateral ventricle and the olfactory bulb of adult mice. J Comp Neurol. 351:51–61.
Rutishauser U. 2008. Polysialic acid in the plasticity of the developing and adult vertebrate nervous system. Nat Rev Neurosci. 9:26–35.
Sairanen M, O'Leary OF, Knuuttila JE, Castren E. 2007. Chronic antidepressant treatment selectively increases expression of plasticity-related proteins in the hippocampus and medial prefrontal cortex of the rat. Neuroscience. 144:368–374.
Schuster T, Krug M, Stalder M, Hackel N, Gerardy-Schahn R, Schachner M. 2001. Immunoelectron microscopic localization of the neural recognition molecules L1, NCAM, and its isoform NCAM180, the NCAM-associated polysialic acid, beta1 integrin and the extracellular matrix molecule tenascin-R in synapses of the adult rat hippocampus. J Neurobiol. 49:142–158.
Schwartzkroin PA, Kunkel DD. 1985. Morphology of identified interneurons in the CA1 regions of guinea pig hippocampus. J Comp Neurol. 232:205–218.
Seki T, Arai Y. 1991. Expression of highly polysialylated NCAM in the neocortex and piriform cortex of the developing and the adult rat. Anat Embryol (Berl). 184:395–401.
Seki T, Arai Y. 1993a. Distribution and possible roles of the highly polysialylated neural cell adhesion molecule (NCAM-H) in the developing and adult central nervous system. Neurosci Res. 17:265–290.
Seki T, Arai Y. 1993b. Highly polysialylated neural cell adhesion molecule (NCAM-H) is expressed by newly generated granule cells in the dentate gyrus of the adult rat. J Neurosci. 13:2351–2358.
Seki T, Arai Y. 1995. Age-related production of new granule cells in the adult dentate gyrus. Neuroreport. 6:2479–2482.
Seki T, Arai Y. 1999. Different polysialic acid-neural cell adhesion molecule expression patterns in distinct types of mossy fiber boutons in the adult hippocampus. J Comp Neurol. 410:115–125.
Sholl DA. 1953. Dendritic organization in the neurons of the visual and motor cortices of the cat. J Anat. 87:387–406.
Varea E, Blasco-Ibanez JM, Gomez-Climent MA, Castillo-Gomez E, Crespo C, Martinez-Guijarro FJ, Nacher J. 2007. Chronic fluoxetine treatment increases the expression of PSA-NCAM in the medial prefrontal cortex. Neuropsychopharmacology. 32:803–812.
Varea E, Castillo-Gomez E, Gomez-Climent MA, Blasco-Ibanez JM, Crespo C, Martinez-Guijarro FJ, Nacher J. 2007a. Chronic antidepressant treatment induces contrasting patterns of synaptophysin and PSA-NCAM expression in different regions of the adult rat telencephalon. Eur Neuropsychopharmacol. 17:546–557.
Varea E, Castillo-Gomez E, Gomez-Climent MA, Blasco-Ibanez JM, Crespo C, Martinez-Guijarro FJ, Nacher J. 2007b. PSA-NCAM expression in the human prefrontal cortex. J Chem Neuroanat. 33:202–209.
Varea E, Castillo-Gomez E, Gomez-Climent MA, Guirado R, Blasco-Ibañez JM, Crespo C, Martinez-Guijarro FJ, Nacher J. 2009. Differential evolution of PSA-NCAM expression during aging of the rat telencephalon. Neurobiol Aging. 30:11.
Varea E, Nacher J, Blasco-Ibanez JM, Gomez-Climent MA, Castillo-Gomez E, Crespo C, Martinez-Guijarro FJ. 2005. PSA-NCAM expression in the rat medial prefrontal cortex. Neuroscience. 136:435–443.
West MJ. 1993. New stereological methods for counting neurons. Neurobiol Aging. 14:275–285.
Zuber C, Lackie PM, Catterall WA, Roth J. 1992. Polysialic acid is associated with sodium channels and the neural cell adhesion molecule N-CAM in adult rat brain. J Biol Chem. 267:9965–9971.

BMC Neuroscience

RESEARCH ARTICLE Open Access

Chronic fluoxetine treatment in middle-aged rats induces changes in the expression of plasticity-related molecules and in neurogenesis

Ramon Guirado[1,2], David Sanchez-Matarredona[1], Emilo Varea[1,2], Carlos Crespo[1,2], José Miguel Blasco-Ibáñez[1,2] and Juan Nacher[1,2*]

Abstract

Background: Antidepressants promote neuronal structural plasticity in young-adult rodents, but little is known of their effects on older animals. The polysialylated form of the neural cell adhesion molecule (PSA-NCAM) may mediate these structural changes through its anti-adhesive properties. PSA-NCAM is expressed in immature neurons and in a subpopulation of mature interneurons and its expression is modulated by antidepressants in the telencephalon of young-adult rodents.

Results: We have analyzed the effects of 14 days of fluoxetine treatment on the density of puncta expressing PSA-NCAM and different presynaptic markers in the medial prefrontal cortex, hippocampus and amygdala of middle-aged (8 months old) rats. The density of puncta expressing PSA-NCAM increased in the dorsal cingulate cortex, as well as in different hippocampal and amygdaloid regions. In these later regions there were also increases in the density of puncta expressing glutamic acid decarboxylase 65/67 (GAD6), synaptophysin (SYN), PSA-NCAM/SYN and PSA-NCAM/GAD6, but a decrease of those expressing vesicular glutamate transporter 1 (VGluT1). Since there is controversy on the effects of antidepressants on neurogenesis during aging, we analyzed the number of proliferating cells expressing Ki67 and that of immature neurons expressing doublecortin or PSA-NCAM. No significant changes were found in the subgranular zone, but the number of proliferating cells decreased in the subventricular zone.

Conclusions: These results indicate that the effects of fluoxetine in middle-aged rats are different to those previously described in young-adult animals, being more restricted in the mPFC and even following an opposite direction in the amygdala or the subventricular zone.

Background

Recent hypotheses support the idea that abnormalities in neuronal structural plasticity may underlie the etiopathogenesis of major depression [1,2]. Accordingly, it has been shown that patients and animal models of this disorder show changes in the volume of certain cerebral regions, such as the hippocampus, the medial prefrontal cortex or the amygdala, which are related to the reorganization of neuronal structure and may affect their connectivity [3,4]. However, these structural changes are not limited to neuronal remodeling, they may also affect the production of new neurons, specially in the adult hippocampus [5-8]. Interestingly, antidepressant treatment is able to revert or block this plasticity in experimental animals and humans [9-13]. In fact, different lines of evidence indicate that both neuronal remodeling [14-17] and adult neurogenesis [12,18] may play an important role in the way of action of antidepressant drugs.

The regulation of the expression of cell adhesion molecules is critical for the neuronal structural remodeling induced by aversive experiences or by antidepressant treatments [19]. Previous results from our laboratory have shown that chronic treatment with the serotonin (5HT) reuptake inhibitor fluoxetine, a commonly used antidepressant, influences the expression of the

* Correspondence: nacher@uv.es
[1]Neurobiology Unit and Program in Basic and Applied Neurosciences, Cell Biology Dpt., Universitat de València, Spain
Full list of author information is available at the end of the article

polysialylated form of the neural cell adhesion molecule (PSA-NCAM) in different regions of the CNS of young-adult animals [20,21]. Similar results have been obtained with another antidepressant, imipramine [17]. PSA-NCAM, due to its anti-adhesive properties, creates a steric impediment for cell adhesion and, consequently, promotes structural plasticity [22]. In fact, the changes in PSA-NCAM expression induced by chronic fluoxetine treatment are accompanied by parallel changes in the expression of the synaptic protein synaptophysin (SYN), suggesting the occurrence of synaptic remodeling [21]. PSA-NCAM expression is abundant during development and, although it decreases markedly during adulthood, it is still detectable in many cerebral regions, such as the medial prefrontal cortex (mPFC) [23,24], amygdala [25] and hippocampus [26], which are known to be involved in major depression. In these regions, PSA-NCAM is expressed in immature neu-rons, such as those in the hippocampal subgranular zone (SGZ) [27] and the subventricular zone (SVZ) [28], but it is also expressed in a subpopulation of mature interneurons [29,24], which have reduced syn-aptic input and morphological features compared with other interneurons lacking PSA-NCAM [30]. Pre-vious work in our laboratory demonstrated that 5HT, acting via 5HT3 receptors is able to regulate PSA-NCAM expression in the mPFC of adult rats [20].

The effects of antidepressants on neuronal plasticity are not restricted to structural remodeling of neurons and their connections, they may also influence the generation and incorporation of new neurons in the adult CNS. Chronic antidepressant treatments increase neurogenesis in the SGZ of the dentate gyrus and the SVZ of young-adult rodents [31,32], and this increase appears to be required at least for part of the behavioral improvement observed in the treated animals [18]. However, other studies are in disagreement with these findings and have found that antidepressants do not produce an increase in neurogenesis in the SGZ [33,34].

Despite all these interesting findings regarding the effects of antidepressants on neuronal plasticity, it has to be noted that most of the experiments have been performed using young-adult rodents, usually 2-3 months old. Consequently, there is controversy on whether antidepressants, and specifically 5HT reuptake inhibitors, exhibit the same efficacy within different age groups. This is particularly interesting because aging influences both neurogenesis [35] and PSA-NCAM expression [36]. Studies on the effects of antidepressant treatment using older animals are still scarce: Only a few works have studied neurogenesis in the SGZ [32,37], but not in the SVZ and, to our knowledge, none has studied other types of neuronal structural plasticity.

We have analyzed the effects of 14 days of chronic fluoxetine treatment on middle-aged (8 month old) rat brains, studying the expression of PSA-NCAM and that of different presynaptic proteins in regions known to be specially affected in patients and in animal models of major depression, as well as by antidepressant treatment, such as the mPFC, the amygdala, and the hippocampus [38-42]. We have studied the expression of SYN a general synaptic marker, glutamic acid decarboxylase 65/67 (GAD6), a marker for inhibitory synapses and the vesicular glutamate transporter 1 (VGluT1), a marker of excitatory synapses. To study the effects of fluoxetine on adult neurogenesis, we have analyzed the numbers of im-mature cells, using immunohistochemistry for doublecortin (DCX) and PSA-NCAM, and those of proliferating cells with Ki67 in the two neurogenic niches of the adult brain: the SGZ and the SVZ.

Methods

Animal treatments

Fourteen adult male Wistar rats (8 months old) were used in this experiment. All the rats were maintained in standard conditions of light (12 hour cycles) and temperature, with no limit in the access to food or water. All animal experimentation was conducted in accordance with the Directive 2010/63/EU of the European Parliament and of the Council of 22 September 2010 on the protection of animals used for scientific purposes and was approved by the Committee on Bioethics of the Universitat de València. Every effort was made to minimize the number of animals used and their suffering. Rats were chronically injected intraperitoneally either with the antidepressant fluoxetine (n = 7, 10 mg/kg), or with saline solution (n = 7), during 14 days (once daily at 10.00 am). Previous studies have shown that this dose produces behavioral changes and increases in the expression of plasticity-related molecules [21,58]. The day after these treatments, rats were perfused transcardially under deep chloral hydrate anesthesia (chloral hydrate 4%, 1 ml/100 gr), first with saline and then with 4% paraformaldehyde in so-dium phosphate buffer (PB 0.1 M, pH 7.4). After perfusion, the brains were extracted and cryoprotected with 30% sucrose in PB. Brains were cut into 50 μm thick sections with a freezing sliding microtome, collected in 10 subseries and stored at - 20°C in 30% glycerol, 30% ethylene glycol in PB 0.1 M until used.

Immunohistochemistry

Tissue was processed free-floating as follows: Briefly, sections were incubated for 1 min in an antigen unmasking solution (0.01 M citrate buffer, pH 6) at 100° C. After cooling down the sections to room temperature, the endogenous peroxidase was blocked with 10 min incubation in a solution of 3% H_2O_2 in phosphate buffered saline (PBS). Afterwards, slices were incubated

in 10% normal donkey serum (NDS) (Abcys SA), 0.2% Triton-X100 (Sigma) in PBS with for 1 hour; then, they were incubated overnight at room temperature with goat polyclonal anti-doublecortin (DCX) (C-18; 1:250; Santa Cruz Biotechnology, Inc.), mouse monoclonal anti-PSA-NCAM IgM (1:1400; Abcys SA) or mouse monoclonal anti-Ki67 IgG (1:2000; Novocastra). After washing, sections were incubated for 30 min with biotinylated donkey anti-goat IgG, donkey anti-mouse IgM or donkey anti-mouse IgG (1:200; Jackson Immunoresearch) antibodies, followed by an avidin-biotin-peroxidase complex (ABC, Vector Laboratories) for 30 min in PBS. Color development was achieved by incubating with 0,5% 3,3' diaminobenzidine tetrahydrochloride (DAB, Sigma) and H2O2 for 4 min. All the sections passed through all procedures simultaneously to minimize any difference from immunohistochemical staining itself.

For double fluorescence immunohistochemistry, slices were incubated overnight with rabbit polyclonal anti-synaptophysin (SYN) IgG (1:1000; Chemicon Int. Inc.) and mouse monoclonal anti-PSA-NCAM IgM (1:1400; Abcys SA). Then, were incubated for 1 hour with donkey anti-rabbit IgG Dylight 488 and donkey anti-mouse IgM Dylight 555 (1:200; Jackson Immunoresearch).

For triple immunohistochemistry, the procedure was similar but using a combination of anti-PSA-NCAM, anti-glutamic acid decarboxylase 65/67 (GAD6; 1:500; Developmental Studies Hybridoma Bank) and anti-vesicular glutamate transporter (VGluT1; 1:2000; Chemicon Int. Inc.) antibodies. In this case the following secondary antibodies were used: anti-mouse IgM Dylight 555, anti-mouse IgG subtype 1 specific Dylight 488 and anti-guinea pig IgG Dylight 647 respectively.

Quantitative analysis

All the slides containing sections destined to quantitative analysis were coded and their code was not broken until the analyses were finished.

The volume of the mPFC, the hippocampus and the lateral and basolateral region of the amygdala was estimated using Volumest, an ImageJ plugin for volume estimation using an stereological method. For this analysis we used the tissue processed with PSA-NCAM immunohistochemistry and developed with DAB was used.

The images used for the analysis of neuropil puncta were obtained with a confocal microscope (Leica TCS SPE) and parallel subseries of Nissl stained sections were used as guides to help locate the regions of interest. We analyzed layer V of two different regions of the medial prefrontal cortex (mPFC): the prelimbic cortex (PrL) in **a single** section corresponding to Bregma +2.20 mm and **another one of** the dorsal cingulate cortex (Cg2) (Bregma +1 mm). In the amygdala, five nuclei were analyzed **in one section** (Bregma -3.30 mm): basomedial, lateral, medial, central and basolateral. Different regions and strata of the hippocampus were also analyzed in **another** section (Bregma -4.30 mm): the molecular layer of the dentate gyrus, the strata lacunosum-moleculare, radiatum and oriens of CA1 and the stratum lucidum of CA3. Confocal z-stacks covering the whole depth of the sections were taken with 1 μm step size and only subsets of confocal planes with the optimal penetration level for each antibody were selected. On these planes, small regions of the neuropil (505 μm^2) were selected for analysis, in order to avoid blood vessels and cell somata.

Images were processed using ImageJ software as follows: the background was substracted with rolling value of 50, converted to 8-bit deep images and binarized using a determined threshold value. This value depended on the marker and the area analyzed and was kept the same for all images with the same marker and area. Then, the images were processed with a blur filter to reduce noise and separate closely apposed puncta. Finally, the number of the resulting dots per region was counted, as well as the colocalization between PSA-NCAM and the different pre-synaptic markers (Additional File 1, Figure S1). **In addition, we also analyzed the size of the dots and the total surface covered by the puncta after binarization**. Means were determined for each animal group and the data were subjected to two-way ANOVAs with repeated measures followed by Bonferroni *post hoc* test.

The density of DCX, PSA-NCAM and Ki67 expressing cells in the SGZ of the dentate gyrus was estimated as described before [25]. Briefly, sections were selected by a 1:10 fractionator sampling covering the whole rostral to caudal extension of the dentate gyrus and on each section all labeled cells within the region of interest were counted. Cell somata were identified and counted with a 40 × objective using an Olympus CX41 microscope. The volume of the different areas analyzed was determined for each animal using the Cavalieri's method. Student's t-test was performed for statistical analysis.

In the SVZ, a single section between Bregma +0.48 and +0.7 mm, was analyzed for DCX, PSA-NCAM and Ki67 immunohistochemistry. The number of immunoreactive cells was estimated following a modification of the method described by Hansson *et al*. [43]. Ki67 expressing nuclei were counted using automatic counting software as described above for immunoreactive puncta, analyzing an area of 100 μm^2 and then expressed as the number of immunoreactive positive cells per mm^2. Densities of DCX and PSA-NCAM expressing cells were too high for a correct individual

cell count. Therefore, we performed densitometry of small areas within the SVZ, using a 40 × magnification, as described before [20].

Results

Weight of the animals and volume of the different structures analyzed

In concordance with previous studies [44,45], chronic fluoxetine treatment produced a significant diminution of weight gain ($p < 0.001$) after 14 days, when comparing the relation final weight/initial weight between the treated animals (0.877 ± 0.017) and the controls (1.017 ± 0.009) (Figure 1).

We also analyzed the effects of chronic fluoxetine treatment on the volume of the different cerebral structures studied. We did not observe changes in the volume of the mPFC or the amygdala, but we found an increase in the volume of the hippocampus of the animals treated with fluoxetine ($p = 0.001$, Figure 1).

Expression of plasticity-related Molecules

Medial prefrontal cortex

The expression pattern of PSA-NCAM in the mPFC was similar to that described previously [23]: All regions within the mPFC showed a moderate intensity of staining in layer I, nearly lack of staining in layer II, weak staining in layer III and intense staining in layers V-VI (Figure 2).

In this cortical region, there was an increase in the density of PSA-NCAM expressing puncta in the fluoxetine treated animals in the dorsal cingulate cortex (Cg2) ($p = 0.043$), but not in the prelimbic cortex (PrL) (Figure 3 and Additional File 2, Table S1). No differences were found in the density of puncta expressing synaptophysin (SYN), glutamic acid decarboxylase 65/67 (GAD6), or vesicular glutamate transporter 1 (VGluT1) in any of the regions studied (Figure 3 and Additional File 2, Table S1)). We did not find changes in the density of puncta colocalizing PSA-NCAM/SYN, PSA-NCAM/GAD6 or PSA-NCAM/VGluT1 neither in the PrL nor in the Cg2 (Figure 2 and Additional File 2, Table S1).

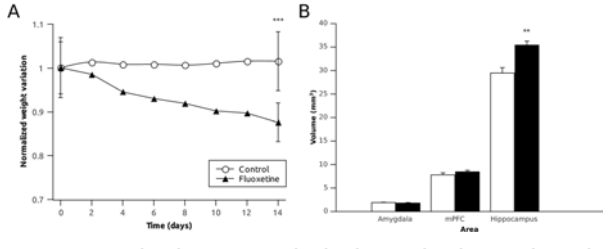

Figure 1 Graphs showing (A) the body weight change through the experiment for the control and fluoxetine group and (B) the effect of the chronic fluoxetine treatment on the volume of the different structures studied. Statistically significant (* $P < 0.05$, ** $P < 0.01$, *** $P < 0.001$) Student t-test.

We did not find changes neither in the dot size nor in the surface covered by puncta in any of the regions and the markers analyzed (Additional File 3, Figure S2).

Amygdala

As described previously [24], low levels of PSA-NCAM expression were found in the neuropil of the lateral and basolateral amygdaloid nuclei. By contrast, PSA-NCAM expression was denser and more intense in the central, medial and basomedial nuclei (Figure 2).

In the fluoxetine treated group we found significant increases in the density of PSA-NCAM expressing puncta in the central amygdaloid nucleus ($p = 0.001$), of SYN expressing puncta in the lateral ($p = 0.049$) and basolateral amygdaloid nuclei ($p = 0.047$) and of GAD6 expressing puncta in the basolateral nucleus ($p = 0.005$) (Figure 4 and Additional File 2, Table S1). On the contrary, we found a significant decrease in the number of VGluT1 expressing puncta in the basolateral amygdaloid nucleus ($p = 0.04$) (Figure 4 and Additional File 2, Table S1). We also found an increase in PSA-NCAM/SYN ($p = 0.007$) and PSA-NCAM/GAD6 ($p = 0.041$) expressing puncta in the central amygdala. No changes in the density of these double-labeled puncta were observed in any of the other amygdaloid nuclei studied (Figure 4 and Additional File 2, Table S1).

We also found changes similar to those described for puncta density when analyzing the dot size and the surface covered by these puncta. In the central amygdaloid nucleus we observed an increase both in the dot size and the surface covered by PSA-NCAM expressing puncta ($p = 0.027$ and 0.011). In the lateral nucleus we only observed an increase in the dot size of puncta expressing SYN ($p = 0.038$). By contrast, in the basolateral nucleus we found an increase in the dot size and surface covered by puncta expressing GAD6 ($p = 0.011$ and 0.018) and a decrease in both, the dot size and the surface covered by puncta expressing VGluT1 ($p = 0.005$ and 0.007) (Additional File 4, Figure S3).

Hippocampus

PSA-NCAM expression in the hippocampus was similar to that described previously [26]: briefly, the most intense expression of PSA-NCAM was located in the somata and apical dendrites of granule cells in the SGZ of the dentate gyrus, as well as in the neuropil of the hilus and the mossy fibers. A weaker and more diffuse expression of PSA-NCAM could be found in the neuropil of other regions of the hippocampus, such as the molecular layer of the dentate gyrus and the strata lacunosum-moleculare, radiatum and oriens of CA1 and CA3 (Figure 2), where PSA-NCAM expressing cell somata could also be found [29].

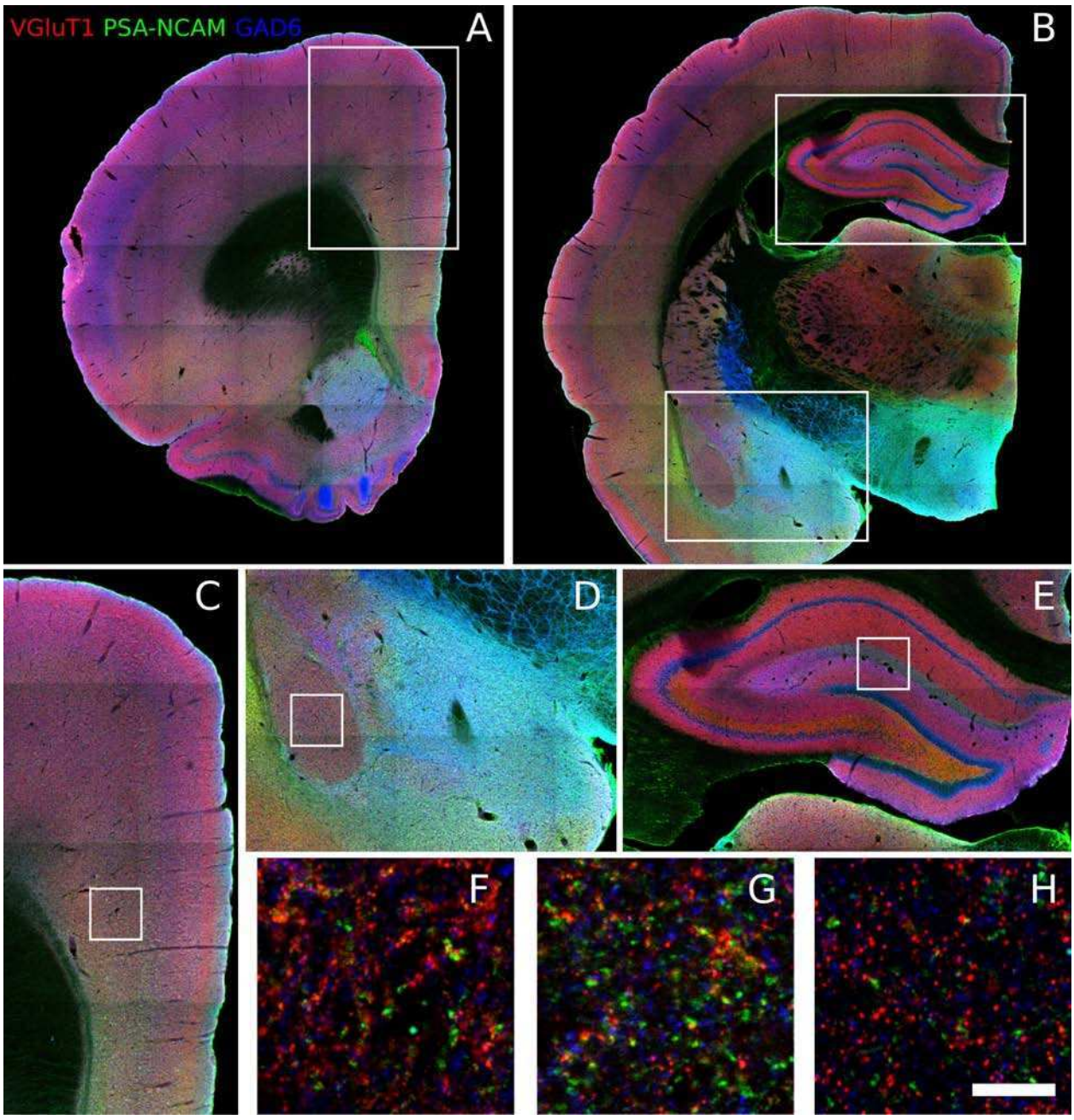

Figure 2 Confocal images showing the expression of PSA-NCAM, VGluT1 and GAD6 in the different regions of the hippocampus (B, E and H), the amygdala (B, D and G) and the mPFC (A, C and F). Scale bar = 200 μm in A and B, 100 μm in C, D and E and 1 μm in F, G and H.

After chronic fluoxetine treatment, we found significant increases in the density of PSA-NCAM expressing puncta in the molecular layer ($p = 0.045$), stratum lucidum ($p = 0.032$) and stratum lacunosum-moleculare ($p < 0.001$) (Figure 5 and Additional File 2, Table S1). Similar increases were found in the density of SYN expressing puncta in the strata lucidum ($p = 0.012$) and lacunosum-moleculare ($p = 0.038$). We also found a significant increase ($p = 0.018$) in the density of GAD6 expressing puncta in the stratum lacunosum-moleculare. By contrast, we found a decrease in the density of VGluT1 expressing puncta in the strata lacunosum-moleculare ($p = 0.021$) and radiatum ($p = 0.030$) of CA1 (Figure 5 and Additional File 2, Table S1). When studying the density of puncta co-expressing PSA-NCAM and each of the other markers, we observed an increase

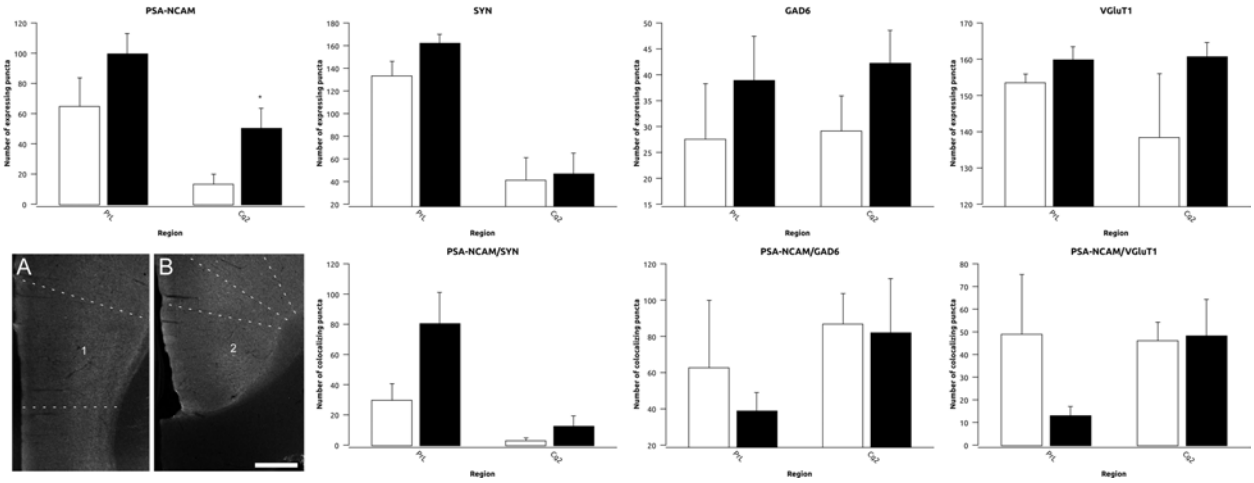

Figure 3 Graphs representing the expression of puncta for the different markers and its colocalization in the prelimbic and cingulate cortex of the medial prefrontal cortex. White bars represent control animals and black bars represent fluoxetine treated animals respectively. A and B are focal planes showing the expression of PSA-NCAM in (1) the prelimbic and (2) the cingulate cortex. Scale bar: 200 μm.

in the density of puncta co-expressing PSA-NCAM/SYN (p = 0.008) in the stratum lacunosum-moleculare, but no change was observed in those co-expressing PSA-NCAM/GAD or PSA-NCAM/VGluT1 (Figure 5 and Additional File 2, Table S1).

Finally, when analyzing the dot size and the surface covered by immunoreactive puncta, we also observed changes in most of the regions that showed differences in the density of puncta in these structures. In the stratum lacunosum-moleculare we observed an increase in the dot size and the surface covered by puncta expressing PSA-NCAM (p = 0.011 and < 0.001) and GAD6 (p = 0.047 and 0.021), while there was only an increase in dot size in those expressing SYN (p = 0.044) and a decrease in both dot size and surface covered by those expressing VGluT1 (p = 0.035 and 0.017). We also find a decrease in both the dot size and the surface covered by puncta expressing VGluT1 in the stratum radiatum (p = 0.015 and 0.007) (Additional File 5, Figure S4).

Adult neurogenesis

No change in the density of cells expressing DCX or PSA-NCAM was observed in the subgranular zone (SGZ) of the dentate gyrus after chronic fluoxetine treatment (Figure 6). However, when analyzing the number of Ki67 expressing nuclei there was a trend

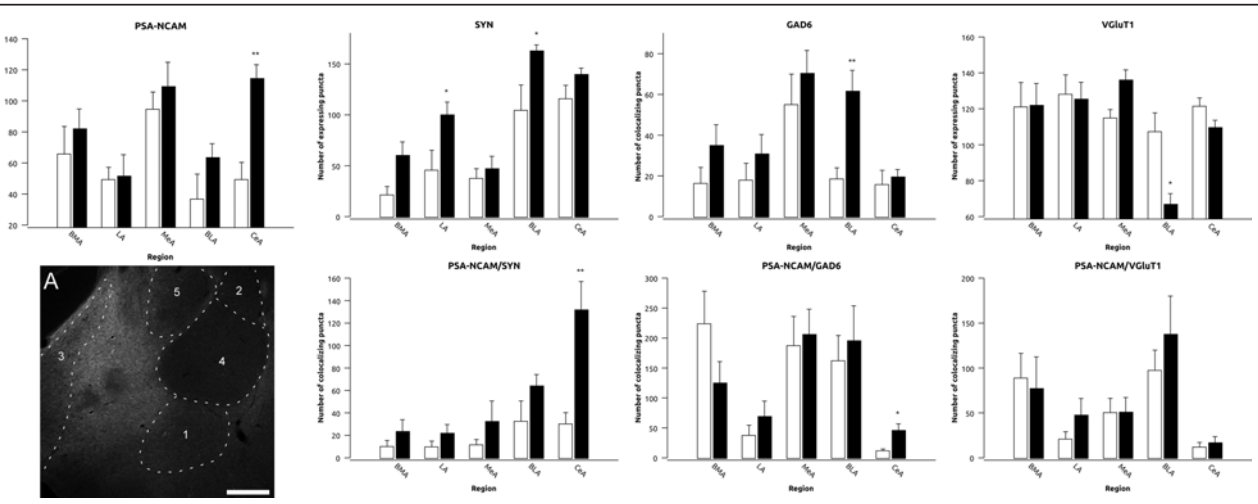

Figure 4 Graphs representing the expression of puncta for the different markers and its colocalization in different areas of the amygdala. White bars represent control animals and black bars represent fluoxetine treated animals respectively. A is a focal plane showing the expression of PSA-NCAM in the (1) basomedial (2) lateral, (3) medial, (4) basolateral and (5) central nuclei of the amygdala. Scale bar: 200 μm.

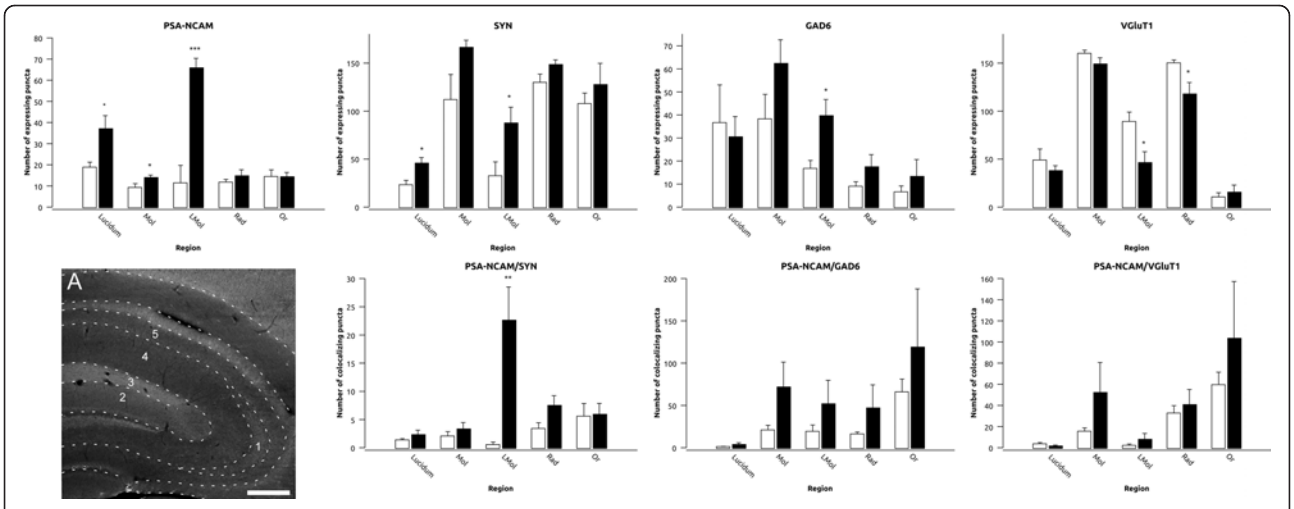

Figure 5 Graphs representing the expression of puncta for the different markers and its colocalization in different areas of the hippocampus. White bars represent control animals and black bars represent fluoxetine treated animals respectively. A is a focal plane showing the expression of PSA-NCAM in the strata (1) Lucidum, (2) Molecular, (3) Lacunosum Moleculare, (4) Radiatum and (5) Oriens of the hippocampus. Scale bar: 200 μm.

towards a decrease in the treated group ($p = 0.061$) (Figure 6). In the subventricular zone (SVZ) we also failed to find changes in the expression of DCX or PSA-NCAM, but we observed a dramatic significant decrease in the number of Ki67 immunoreactive nuclei in the treated group ($p < 0.001$) (Figure 6).

Discussion

Our results indicate that in middle-aged rats chronic fluoxetine treatment induces changes in the expression of molecules related to neuronal structural plasticity. These changes occur in the same direction of those observed previously in young-adult animals in the hippocampus and the mPFC, although to a reduced extent in this later region. However, they follow the opposite direction in the amygdala. We have also observed that, in contrast with what has been observed in young-adult rats, there is a negative impact of fluoxetine **on cell proliferation** in the SVZ and apparently a lack of effect in the SGZ.

PSA-NCAM expression as an indicator of neuronal structural plasticity

Previous experiments have demonstrated that PSA-NCAM expression is sensible to fluoxetine treatment, acting through 5HT3 receptors [20]. However, since other 5HT receptors are known to mediate the effects of fluoxetine, they may also influence PSA-NCAM expression [46-51]. Many PSA-NCAM expressing structures in the cerebral cortex [24,29,30] and the amygdala [52] of rodents belong to mature interneurons. Consequently, changes in PSA-NCAM expression should primarily affect the structure of these inhibitory. In this line, we have recently reported that PSA-NCAM expressing cortical interneurons have reduced synaptic input and decreased dendritic arborization and spine density when compared with neighboring interneurons lacking PSA-NCAM [30]. In fact, a previous report from our laboratory using a dopamine D2 receptor antagonist, which increases PSA-NCAM expression in the mPFC, also resulted in a parallel upregulation of GAD67 expression [53]. It is possible then, that the changes in PSA-NCAM expression observed in the present study affect the connectivity of certain interneurons, regulating the surface of preexisting plasma membrane available for the establishment of synaptic contacts. Another non-excluding possibility may be that, given its anti-adhesive properties, changes in PSA-NCAM expression may regulate the ability of certain interneurons to remodel the structure of their neurites, and consequently their connections, in response to fluoxetine treatment.

Comparison of the effects of chronic fluoxetine treatment on the expression of PSA-NCAM and presynaptic markers between middle-aged and young-adult animals

The present results in the mPFC, showing only an increase in the density of PSA-NCAM expressing puncta in the dorsal cingulate cortex, are more restricted than those found previously in young-adult rats, which showed increases in every region and layer of the mPFC [20]. The lack of changes in the density of puncta expressing presynaptic markers is also in contrast with previous reports using young-adult rats, which showed increases in SYN expression in deep layers of the prelimbic and infralimbic cortices [21] and of VGluT-1 mRNA expression in the cingulate cortex [54].

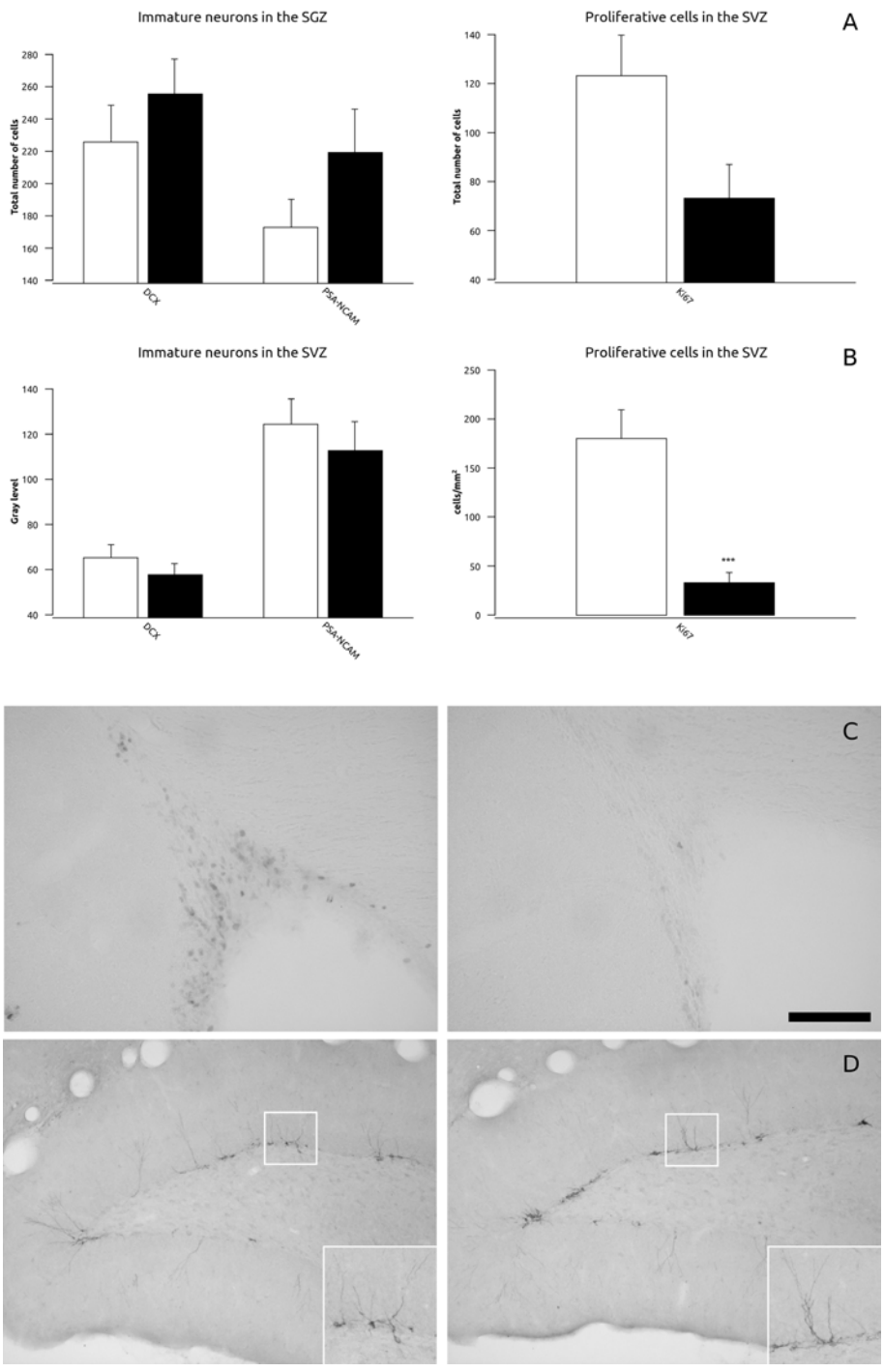

Figure 6 Graphs representing (A) the total number of cells expressing immature and proliferative markers in the subgranular zone (SGZ) of the hippocampus and (B) the gray level of doublecortin (DCX) and PSA-NCAM and the density of Ki67 in the subventricular zone (SVZ). White bars represent control animals and black bars represent fluoxetine treated animals respectively. (C) Micrographs showing the expression of Ki67 in the SVZ and (D) DCX in the SGZ. Scale bar: 100 μm (C and D) and 50 μm (insets in D).

In the hippocampus, previous studies with young-adult rats found a similar increase in PSA-NCAM expression in the stratum lucidum, but not in the rest of hippocampal strata studied [21]. Since in young-adult rats antidepressants promote an increase in the density of PSA-NCAM expressing cells in the SGZ [17], fluoxetine may be affecting PSA-NCAM expression in the stratum lucidum by increasing the production or

accelerating the maturation of immature granule cells, some of which may have already sent PSA-NCAM expressing mossy fibers to this layer [55]. However, our results clearly indicate that the number of these cells is not affected by fluoxetine in middle-aged rats, suggesting that changes in PSA-NCAM expressing puncta are not linked to adult neurogenesis. In connection to this, a recent report has shown that chronic fluoxetine treatment may produce a dematuration of granule cells [56]. Since many mossy fibers in the stratum lucidum are polysialylated by St8SiaII, the enzyme responsible for the polysialylation of immature neurons in the adult cerebral cortex [57], this putative dematuration induced by fluoxetine may explain the increase in PSA-NCAM expression that we observe in this stratum. In consonance with this hypothesis and with previous studies in young-adult rats [21,58], we have failed to find any significant difference in the density of SYN expressing puncta in the stratum lucidum, which may indicate that the changes in PSA-NCAM are not related to the genesis of new functional synaptic contacts. By contrast, the increase of PSA-NCAM expressing puncta in the stratum lacunosum-moleculare of middle-aged rats is accompanied by an increase in the density of SYN expressing puncta and of puncta co-expressing PSA-NCAM/SYN, suggesting that these structures correspond to synapses. Interestingly, in the stratum lacunosum-moleculare of middle-aged animals we also found an increase in the density of GAD6 expressing puncta, and a decrease in the density of those expressing VGluT1, which may indicate that the upregulation of PSA-NCAM expression may be linked to changes in inhibitory circuits, probably involving the formation of inhibitory synapses.

Chronic fluoxetine treatment in young-adult rats decreases PSA-NCAM and SYN expression in most amygdaloid nuclei [21] and decreases the number of PSA-NCAM expressing neurons in this limbic region [59]. By contrast, in middle-aged rats we not only have failed to observe decreases in the density of puncta expressing PSA-NCAM or SYN, but have observed significant increases in the density of PSA-NCAM expressing puncta in the central nucleus and of those expressing SYN in the lateral and basolateral nuclei. There is, in fact, a general tendency for an increase in the density of puncta expressing PSA-NCAM, SYN and GAD6 in all the amygdaloid nuclei studied. Moreover, despite the fact that no significant changes in puncta expressing exclusively GAD6 or SYN were observed in the central amygdala, the density of puncta coexpressing PSA-NCAM and each of these two markers also increases significantly, suggesting that changes in PSA-NCAM expression may be associated to the generation or remodeling of inhibitory synapses in this region. In the basolateral amygdala, chronic fluoxetine treatment may also influence positively synaptic plasticity of inhibitory circuits, as indicated by increased densities of GAD6 and SYN expressing puncta, while the density of those expressing VGluT1 is decreased.

It is possible that substantial differences in 5HT content and in the expression of its receptors, transporters, etc... exist in middle-aged animals. The levels of 5HT are generally reduced in the brain of aged rats [60] and, although there are no studies in middle-aged animals, it is possible that they are already reduced at this age. There is also evidence indicating that the expression 5HT1A receptor, which has an important role in the antidepressant effects of 5HT reuptake inhibitors [61,62], is lower in young-adult than in adolescent rats [59]. Additionally, other factors such as changes in inhibitory neurotransmission may also influence the effects of fluoxetine in middle-aged animals, particularly in the amygdala, where decreases in GABA concentration and hyperactivity have been described during aging [63,64].

Effects of fluoxetine treatment on neurogenesis

The present results on adult hippocampal neurogenesis are in agreement with previous studies showing that neither proliferation nor neuronal survival/differentiation is affected by chronic antidepressant treatment in middle-aged rodents [32,37]. This lack of response of the SGZ in middle-aged animals must be due to changes that alter the molecular pathways by which 5HT stimulates neurogenesis. There is an age-dependent reduction in the levels of 5HT [60] and some of its receptors [65] in the hippocampus. Since glucocorticoids are important modulators of adult hippocampal neurogenesis and these steroids are particularly elevated during aging [66], they may also influence the neurogenic response to antidepressants in middle-aged animals. In fact, glucocorticoids decrease 5HT transporter expression [67] and the neurogenic action of fluoxetine is blocked by a flattened corticosterone rhythm induced by artificially enhanced glucocorticoid levels [68]. Additionally, a previous study has clearly shown that intraperitoneal injections *per se* have effects on the structure of neurons, at least in the mPFC [69]. This effects are similar to those observed after chronic stress [41]and it is very likely that this procedure also affects some of the plasticity parameters measured in our study, including neurogenesis, which is importantly influenced by chronic stress [8].

Other molecules known to modulate adult neurogenesis, including neurotransmitters, such as glutamate acting on NMDA receptors [70] and GABA [71], or trophic factors, such as BDNF [72], can be influenced by antidepressants, including fluoxetine [73-76]. Consequently, age-dependent changes in their expression or in the molecular pathways in which these molecules are

involved may also lead to changes in the pro-neurogenic effects of antidepressants.

In contrast with previous studies using fluoxetine [31] and 5HT receptor agonists [77] in young-adult rodents, which found increases in the number of proliferating cells in the SVZ, we have found the opposite effect. On the other hand, our results are in agreement with a recent report describing that in young-adult mice 3 weeks of fluoxetine treatment do not affect cell proliferation in the SVZ, but that the extension of this treatment to 6 weeks produces a significant deficit in the number of dividing cells in this region [78]. These results indicate that the SVZ of middle-aged rodents is more sensible to fluoxetine treatment, since a significant decrease in cell proliferation can be achieved with a shorter treatment. It is possible that the lack of differences in the number of neuroblasts in the SVZ may be due to a homeostatic parallel change in the number of apoptotic cells in this region, as suggested previously [79]. Alternatively, fluoxetine could impair neuronal migration, which may cause accumulation of neuroblasts in the SVZ.

Implication of the present results on antidepressant therapy

In light of the neuroplastic hypothesis of depression [1], our results indicate that antidepressant treatment in middle-aged individuals also has an important impact on neuronal structure and connectivity. Consequently, it may have relevant consequences on the therapeutics of major depression. In the present results, we have shown that chronic fluoxetine treatment increases the volume of the hippocampus and the expression of molecules related to structural plasticity and inhibitory neurotransmission. These phenomena may counteract the decreases in hippocampal volume and balance the increases in excitatory neurotransmission observed in depressed patients and in animal models of this disorder [8]. Similar, although lighter, effects have been observed in the amygdala. In this region, the increases in the expression of molecules related to structural plasticity and inhibitory neurotransmission may compensate the structural changes observed in inhibitory and excitatory neurons, which accompany the increased excitation observed in this limbic region in animal models of depression [80]. The effects of fluoxetine in the mPFC of middle-aged rats are more discrete, but it is reasonable to think that the increase in PSA-NCAM expression may facilitate compensatory structural changes to overcome the structural atrophy of pyramidal neurons observed in animal models of depression [42].

By contrast, our results on the effects of fluoxetine on adult neurogenesis do not seem to give support to the idea that this type of plasticity is important for the treatment of depression, at least in middle-aged rodents. It has to be noted, however, that our experiment has been performed in control animals and that the effects of fluoxetine on molecules related to neuronal structural plasticity or in neurogenesis may be more intense or follow a different direction when applied to animal models of this psychiatric disorder.

Conclusions

Our results indicating substantial differences in the plastic response of the CNS to fluoxetine in middle-aged animals may be relevant when considering what are the cellular bases of the behavioral changes associated to antidepressant action.

As it happens with rodents, middle-aged humans may also show reduced plasticity in response to antidepressant and, what is more important, this plasticity may follow a different direction in certain brain regions, such as the SVZ or the amygdala. These results indicate that the response to antidepressant treatment is more complex than previously thought and that the age of the subjects receiving these drugs is an important factor to consider and a subject for more intensive research.

Additional material

Additional file 1: Quantification of PSA-NCAM and SYN expressing puncta in the hippocampus. Confocal image showing the expression of PSA-NCAM and SYN in the hippocampus. Focal planes showing the original image and the processed image for the puncta analysis for (B1 and B2) PSA-NCAM, (C1 and C2) SYN and (D1 and D2) the composite image. Scale bar: 320 μm in A and 5 μm in the rest.

Additional file 2: Statistical values of puncta expressing different markers. Statistical information of the expression of the different markers and its colocalization in the diferent regions of the mPFC, the hippocampus and the amygdala.

Additional file 3: Graphs for the dot size and surface covered by puncta expressing different markers in the Mpfc. Graphs representing the dot size and surface covered by puncta expressing different markers in the prelimbic and cingulate cortex of the medial prefrontal cortex. White bars represent control animals and black bars represent fluoxetine treated animals respectively.

Additional file 4: Graphs for the dot size and surface covered by puncta expressing different markers in the amygdala. Graphs representing the dot size and surface covered by puncta expressing different markers in different areas of the amygdala. White bars represent control animals and black bars represent fluoxetine treated animals respectively.

Additional file 5: Graphs for the dot size and surface covered by puncta expressing different markers in the hippocampus. Graphs representing the dot size and surface covered by puncta expressing different markers in different areas of the hippocampus. White bars represent control animals and black bars represent fluoxetine treated animals respectively.

Acknowledgements and funding

Spanish Ministry of Science and Innovation (MICINN-FEDER) BFU2009-12284/BFI, MICINN-PIM2010ERN-00577/NEUCONNECT in the frame of ERA-NET NEURON" and the Stanley Medical Research Institute to JN. Ramón Guirado

has a FPI predoctoral fellowship from the Spanish Ministry of Education and Science (BES 2007-15757).

Author details
[1]Neurobiology Unit and Program in Basic and Applied Neurosciences, Cell Biology Dpt., Universitat de València, Spain. [2]INCLIVA: Fundación Hospital Clínico Universitario de Valencia, València, Spain.

Authors' contributions
RG carried out the animal experimentation, the histology, the image acquisition and processing, the statistics and drafted the manuscript. DSM participated in the image acquisition and processing. EV, CC and JMBI have revised critically the content of the manuscript. JN conceived and designed the experimental work, helped to draft the manuscript and wrote its final version. All authors read and approved the final manuscript.

Competing interests
The authors declare that they have no competing interests.

Received: 26 September 2011 Accepted: 5 January 2012
Published: 5 January 2012

References

1. Castrén E: **Is mood chemistry?** *Nature Reviews Neuroscience* 2005, **6**:241-6.
2. Mattson MP, Maudsley S, Martin B: **BDNF and 5-HT: a dynamic duo in age-related neuronal plasticity and neurodegenerative disorders.** *Trends in Neurosciences* 2004, **27**:589-94.
3. Phillips ML, Drevets WC, Rauch SL, Lane R: **Neurobiology of emotion perception II: Implications for major psychiatric disorders.** *Biological Psychiatry* 2003, **54**:515-28.
4. Tata DA, Anderson BJ: **The effects of chronic glucocorticoid exposure on dendritic length, synapse numbers and glial volume in animal models: implications for hippocampal volume reductions in depression.** *Physiology & Behavior* 2010, **99**:186-93.
5. Duman RS, Malberg J, Nakagawa S, D'Sa C: **Neuronal plasticity and survival in mood disorders.** *Biological Psychiatry* 2000, **48**:732-9.
6. Jacobs BL, van Praag H, Gage FH: **Adult brain neurogenesis and psychiatry: a novel theory of depression.** *Molecular Psychiatry* 2000, **5**:262-9.
7. Kempermann G, Kronenberg G: **Depressed new neurons–adult hippocampal neurogenesis and a cellular plasticity hypothesis of major depression.** *Biological Psychiatry* 2003, **54**:499-503.
8. McEwen BS: **Effects of adverse experiences for brain structure and function.** *Biological Psychiatry* 2000, **48**:721-31.
9. Boldrini M, Underwood MD, Hen R, Rosoklija GB, Dwork AJ, John Mann J, Arango V: **Antidepressants increase neural progenitor cells in the human hippocampus.** *Neuropsycho-pharmacology* 2009, **34**:2376-89.
10. Henn FA, Vollmayr B: **Neurogenesis and depression: etiology or epiphenomenon?** *Biological Psychiatry* 2004, **56**:146-50.
11. Magariños AM, Deslandes A, McEwen BS: **Effects of antidepressants and benzodiazepine treatments on the dendritic structure of CA3 pyramidal neurons after chronic stress.** *European Journal of Pharmacology* 1999, **371**:113-22.
12. Malberg JE, Eisch AJ, Nestler EJ, Duman RS: **Chronic antidepressant treatment increases neurogenesis in adult rat hippocampus.** *Journal of Neuroscience* 2000, **20**:9104-10.
13. Vermetten E, Vythilingam M, Southwick SM, Charney DS, Bremner JD: **Long-term treatment with paroxetine increases verbal declarative memory and hippocampal volume in posttraumatic stress disorder.** *Biological Psychiatry* 2003, **54**:693-702.
14. Ampuero E, Rubio FJ, Falcon R, Sandoval M, Diaz-Veliz G, Gonzalez RE, Earle N, Dagnino-Subiabre A, Aboitiz F, Orrego F, Wyneken U: **Chronic fluoxetine treatment induces structural plasticity and selective changes in glutamate receptor subunits in the rat cerebral cortex.** *Neuroscience* 2010, **169**:98-108.
15. Guirado R, Varea E, Castillo-Gómez E, Gómez-Climent MA, Rovira-Esteban L, Blasco-Ibáñez JM, Crespo C, Martínez-Guijarro FJ, Nàcher J: **Effects of chronic fluoxetine treatment on the rat somatosensory cortex: activation and induction of neuronal structural plasticity.** *Neuroscience Letters* 2009, **457**:12-5.
16. Hajszan T, MacLusky NJ, Leranth C: **Short-term treatment with the antidepressant fluoxetine triggers pyramidal dendritic spine synapse formation in rat hippocampus.** *European Journal of Neuroscience* 2005, **21**:1299-303.
17. Sairanen M, O'Leary OF, Knuuttila JE, Castrén E: **Chronic antidepressant treatment selectively increases expression of plasticity-related proteins in the hippocampus and medial prefrontal cortex of the rat.** *Neuroscience* 2007, **144**:368-74.
18. Santarelli L, Saxe M, Gross C, Surget A, Battaglia F, Dulawa S, Weisstaub N, Lee J, Duman R, Arancio O, Belzung C, Hen R: **Requirement of hippocampal neurogenesis for the behavioral effects of antidepressants.** *Science* 2003, **301**:805-9.
19. Sandi C: **Stress, cognitive impairment and cell adhesion molecules.** *Nature Reviews Neuroscience* 2004, **5**:917-930.
20. Varea E, Blasco-Ibáñez JM, Gómez-Climent MA, Castillo-Gómez E, Crespo C, Martínez-Guijarro FJ, Nácher J: **Chronic fluoxetine treatment increases the expression of PSA-NCAM in the medial prefrontal cortex.** *Neuropsychopharmacology* 2007, **32**:803-12.
21. Varea E, Castillo-Gómez E, Gómez-Climent MA, Blasco-Ibáñez JM, Crespo C, Martínez-Guijarro FJ, Nàcher J: **Chronic antidepressant treatment induces contrasting patterns of synaptophysin and PSA-NCAM expression in different regions of the adult rat telencephalon.** *European Neuropsychopharmacology* 2007, **17**:546-57.
22. Rutishauser U: **Polysialic acid in the plasticity of the developing and adult vertebrate nervous system. Nature Reviews.** *Neuroscience* 2008, **9**:26-35.
23. Varea E, Castillo-Gómez E, Gómez-Climent MA, Blasco-Ibáñez JM, Crespo C, Martínez-Guijarro FJ, Nàcher J: **PSA-NCAM expression in the human prefrontal cortex.** *Journal of Chemical Neuroanatomy* 2007, **33**:202-9.
24. Varea E, Nácher J, Blasco-Ibáñez JM, Gómez-Climent MA, Castillo-Gómez E, Crespo C, Martínez-Guijarro FJ: **PSA-NCAM expression in the rat medial prefrontal cortex.** *Neuroscience* 2005, **136**:435-43.
25. Nacher J, Lanuza E, McEwen BS: **Distribution of PSA-NCAM expression in the amygdala of the adult rat.** *Neuroscience* 2002, **113**:479-84.
26. Seki T, Arai Y: **Distribution and possible roles of the highly polysialylated neural cell adhesion molecule (NCAM-H) in the developing and adult central nervous system.** *Neuroscience Research* 1993, **17**:265-90.
27. Seki T, Arai Y: **The persistent expression of a highly polysialylated NCAM in the dentate gyrus of the adult rat.** *Neuroscience Research* 1991, **12**:503-13.
28. Rousselot P, Lois C, Alvarez-Buylla A: **Embryonic (PSA) N-CAM reveals chains of migrating neuroblasts between the lateral ventricle and the olfactory bulb of adult mice.** *Journal of Comparative Neurology* 1995, **351**:51-61.
29. Nacher J, Blasco-Ibáñez JM, McEwen BS: **Non-granule PSA-NCAM immunoreactive neurons in the rat hippocampus.** *Brain Research* 2002, **930**:1-11.
30. Gómez-Climent MÁ, Guirado R, Castillo-Gómez E, Varea E, Gutierrez-Mecinas M, Gilabert-Juan J, García-Mompó C, Vidueira S, Sanchez-Mataredona D, Hernández S, Blasco-Ibáñez JM, Crespo C, Rutishauser U, Schachner M, Nacher J: **The Polysialylated Form of the Neural Cell Adhesion Molecule (PSA-NCAM) Is Expressed in a Subpopulation of Mature Cortical Interneurons Characterized by Reduced Structural Features and Connectivity.** *Cerebral Cortex* 2010, **21**:1028-41.
31. Nasrallah HA, Hopkins T, Pixley SK: **Differential effects of antipsychotic and antidepressant drugs on neurogenic regions in rats.** *Brain Research* 2010, **1354**:23-9.
32. Couillard-Despres S, Wuertinger C, Kandasamy M, Caioni M, Stadler K, Aigner R, Bogdahn U, Aigner L: **Ageing abolishes the effects of fluoxetine on neurogenesis.** *Molecular Psychiatry* 2009, **14**:856-64.
33. Marlatt MW, Lucassen PJ, van Praag H: **Comparison of neurogenic effects of fluoxetine, duloxetine and running in mice.** *Brain Research* 2010, **1341**:93-9.
34. Navailles S, Hof PR, Schmauss C: **Antidepressant drug-induced stimulation of mouse hippocampal neurogenesis is age-dependent and altered by early life stress.** *Journal of Comparative Neurology* 2008, **509**:372-81.
35. Kuhn HG, Dickinson-Anson H, Gage FH: **Neurogenesis in the dentate gyrus of the adult rat ceases during aging.** *European Journal of Neuroscience* 1995, **8(Suppl)**:89.
36. Varea E, Castillo-Gómez E, Gómez-Climent MA, Guirado R, Blasco-Ibáñez JM, Crespo C, Martínez-Guijarro FJ, Nácher J: **Differential evolution of PSA-**

NCAM expression during aging of the rat telencephalon. *Neurobiology of Aging* 2009, **30**:808-18.
37. Cowen DS, Takase LF, Fornal CA, Jacobs BL: **Age-dependent decline in hippocampal neurogenesis is not altered by chronic treatment with fluoxetine.** *Brain Research* 2008, **1228**:14-9.
38. Magariños AM, McEwen BS: **Stress-induced atrophy of apical dendrites of hippocampal CA3c neurons: involvement of glucocorticoid secretion and excitatory amino acid receptors.** *Neuroscience* 1995, **69**:89-98.
39. Marcuzzo S, Dall'oglio A, Ribeiro MFM, Achaval M, Rasia-Filho AA: **Dendritic spines in the posterodorsal medial amygdala after restraint stress and ageing in rats.** *Neuroscience Letters* 2007, **424**:16-21.
40. Mitra R, Jadhav S, McEwen BS, Vyas A, Chattarji S: **Stress duration modulates the spatiotemporal patterns of spine formation in the basolateral amygdala.** *Proceedings of the National Academy of Sciences of the United States of America* 2005, **102**:9371-6.
41. Radley JJ, Sisti HM, Hao J, Rocher AB, McCall T, Hof PR, McEwen BS, Morrison JH: **Chronic behavioral stress induces apical dendritic reorganization in pyramidal neurons of the medial prefrontal cortex.** *Neuroscience* 2004, **125**:1-6.
42. Radley JJ, Rocher AB, Miller M, Janssen WGM, Liston C, Hof PR, McEwen BS, Morrison JH: **Repeated stress induces dendritic spine loss in the rat medial prefrontal cortex.** *Cerebral Cortex* 2006, **16**:313-20.
43. Hansson AC, Nixon K, Rimondini R, Damadzic R, Sommer WH, Eskay R, Crews FT, Heilig M: **Long-term suppression of forebrain neurogenesis and loss of neuronal progenitor cells following prolonged alcohol dependence in rats.** *International Journal of Neuropsychopharmacology* 2010, **13**:583-93.
44. McNamara RK, Able JA, Rider T, Tso P, Jandacek R: **Effect of chronic fluoxetine treatment on male and female rat erythrocyte and prefrontal cortex fatty acid composition.** *Progress in Neuro-psychopharmacology & Biological Psychiatry* 2010, **34**:1317-21.
45. Thompson MR, Li KM, Clemens KJ, Gurtman CG, Hunt GE, Cornish JL, McGregor IS: **Chronic fluoxetine treatment partly attenuates the long-term anxiety and depressive symptoms induced by MDMA ('Ecstasy') in rats.** *Neuropsychopharmacology* 2004, **29**:694-704.
46. Hewlett WA, Trivedi BL, Zhang Z-J, de Paulis T, Schmidt DE, Lovinger DM, Ansari MS, Ebert MH: **Characterization of (S)-Des-4-amino-3-[125I] iodozacopride ([125I]DAIZAC), a Selective High-Affinity Radioligand for 5-Hydroxytryptamine3 Receptors.** *Journal of Pharmacology and Experimental Therapies* 1999, **288**:221-231.
47. Li Q, Wichems CH, Ma L, Van de Kar LD, Garcia F, Murphy DL: **Brain region-specific alterations of 5-HT 2A and 5-HT 2C receptors in serotonin transporter knockout mice.** *Journal of Neurochemistry* 2003, **84**:1256-1265.
48. McDonald AJ, Mascagni F: **Neuronal localization of 5-HT type 2A receptor immunoreactivity in the rat basolateral amygdala.** *Neuroscience* 2007, **146**:306-20.
49. Morales M, Battenberg E, Bloom FE: **Distribution of neurons expressing immunoreactivity for the 5HT3 receptor subtype in the rat brain and spinal cord.** *Journal of Comparative Neurology* 1998, **402**:385-401.
50. Puig MV, Santana N, Celada P, Mengod G, Artigas F: **In vivo excitation of GABA interneurons in the medial prefrontal cortex through 5-HT3 receptors.** *Cerebral Cortex* 2004, **14**:1365-75.
51. Weber ET, Andrade R: **Htr2a Gene and 5-HT(2A) Receptor Expression in the Cerebral Cortex Studied Using Genetically Modified Mice.** *Frontiers in Neuroscience* 2010, 4.
52. Gilabert-Juan J, Castillo-Gomez E, Pérez-Rando M, Moltó MD, Nacher J: **Chronic stress induces changes in the structure of interneurons and in the expression of molecules related to neuronal structural plasticity and inhibitory neurotransmission in the amygdala of adult mice.** *Experimental Neurology* 2011, **232**:33-40.
53. Castillo-Gómez E, Gómez-Climent MA, Varea E, Guirado R, Blasco-Ibáñez JM, Crespo C, Martínez-Guijarro FJ, Nácher J: **Dopamine acting through D2 receptors modulates the expression of PSA-NCAM, a molecule related to neuronal structural plasticity, in the medial prefrontal cortex of adult rats.** *Experimental neurology* 2008, **214**:97-111.
54. Tordera RM, Pei Q, Sharp T: **Evidence for increased expression of the vesicular glutamate transporter, VGLUT1, by a course of antidepressant treatment.** *Journal of Neurochemistry* 2005, **94**:875-83.
55. Seki T, Arai Y: **Different polysialic acid-neural cell adhesion molecule expression patterns in distinct types of mossy fiber boutons in the adult hippocampus.** *Journal of Comparative Neurology* 1999, **410**:115-25.
56. Kobayashi K, Ikeda Y, Sakai A, Yamasaki N, Haneda E, Miyakawa T, Suzuki H: **Reversal of hippocampal neuronal maturation by serotonergic antidepressants.** *Proceedings of the National Academy of Sciences of the United States of America* 2010, **107**:8434-9.
57. Nacher J, Guirado R, Varea E, Alonso-Llosa G, Röckle I, Hildebrandt H: **Divergent impact of the polysialyltransferases ST8SiaII and ST8SiaIV on polysialic acid expression in immature neurons and interneurons of the adult cerebral cortex.** *Neuroscience* 2010, **167**:825-37.
58. Reinés A, Cereseto M, Ferrero A, Sifonios L, Podestá MF, Wikinski S: **Maintenance treatment with fluoxetine is necessary to sustain normal levels of synaptic markers in an experimental model of depression: correlation with behavioral response.** *Neuropsychopharmacology* 2008, **33**:1896-908.
59. Homberg JR, Olivier JDA, Blom T, Arentsen T, van Brunschot C, Schipper P, Korte-Bouws G, van Luijtelaar G, Reneman L: **Fluoxetine exerts age-dependent effects on behavior and amygdala neuroplasticity in the rat.** *PloS one* 2011, **6**:e16646.
60. Arivazhagan P, Panneerselvam C: **Neurochemical changes related to ageing in the rat brain and the effect of DL-α-lipoic acid.** *Experimental Gerontology* 2002, **37**:1489-1494.
61. Blier P: **Altered function of the serotonin 1A autoreceptor and the antidepressant response.** *Neuron* 2010, **65**:1-2.
62. Hensler JG: **Differential regulation of 5-HT1A receptor-G protein interactions in brain following chronic antidepressant administration.** *Neuropsychopharmacology* 2002, **26**:565-73.
63. Lolova I, Davidoff M: **Changes in GABA-immunoreactivity and GABA-transaminase activity in rat amygdaloid complex in aging.** *Journal für Hirnforschung* 1991, **32**:231-8.
64. Nakanishi H: **Hyperexcitability of amygdala neurons of Senescence-Accelerated Mouse revealed by electrical and optical recordings in an in vitro slice preparation.** *Brain Research* 1998, **812**:142-149.
65. Marcusson J, Morgan D, Winblad B, Finch C: **Serotonin-2 binding sites in human frontal cortex and hippocampus. Selective loss of S-2A sites with age.** *Brain Research* 1984, **311**:51-56.
66. Mcewen BS, Magarinos AM, Reagan LP: **Structural plasticity and tianeptine: cellular and molecular targets.** *Psychiatry: Interpersonal and Biological Processes* 2002, 5-9.
67. Slotkin TA, McCook EC, Ritchie JC, Carroll BJ, Seidler FJ: **Serotonin transporter expression in rat brain regions and blood platelets: aging and glucocorticoid effects.** *Biological Psychiatry* 1997, **41**:172-83.
68. Huang G-J, Herbert J: **Stimulation of neurogenesis in the hippocampus of the adult rat by fluoxetine requires rhythmic change in corticosterone.** *Biological Psychiatry* 2006, **59**:619-24.
69. Seib LM, Wellman CL: **Daily injections alter spine density in rat medial prefrontal cortex.** *Neuroscience Letters* 2003, **337**:29-32.
70. Nacher J, McEwen BS: **The role of N-methyl-D-asparate receptors in neurogenesis.** *Hippocampus* 2006, **16**:267-70.
71. Markwardt S, Overstreet-Wadiche L: **GABAergic signalling to adult-generated neurons.** *Journal of Physiology* 2008, **586**:3745-9.
72. Marlatt MW, Philippens I, Manders E, Czeh B, Joels M, Krugers H, Lucassen PJ: **Distinct structural plasticity in the hippocampus and amygdala of the middle-aged common marmoset (Callithrix jacchus).** *Experimental neurology* 2011, **230**:291-301.
73. Castrén E, Rantamäki T: **The role of BDNF and its receptors in depression and antidepressant drug action: Reactivation of developmental plasticity.** *Developmental Neurobiology* 2010, **70**:289-97.
74. Wu X, Castrén E: **Co-treatment with diazepam prevents the effects of fluoxetine on the proliferation and survival of hippocampal dentate granule cells.** *Biological Psychiatry* 2009, **66**:5-8.
75. Li Y-F, Zhang Y-Z, Liu Y-Q, Wang H-L, Cao J-B, Guan T-T, Luo Z-P: **Inhibition of N-methyl-D-aspartate receptor function appears to be one of the common actions for antidepressants.** *Journal of Psychopharmacology* 2006, **20**:629-35.
76. Saarelainen T, Hendolin P, Lucas G, Koponen E, Sairanen M, MacDonald E, Agerman K, Haapasalo A, Nawa H, Aloyz R, Ernfors P, Castren E: **Activation of the TrkB Neurotrophin Receptor Is Induced by Antidepressant Drugs and Is Required for Antidepressant-Induced Behavioral Effects.** *Journal of Neuroscience* 2003, **23**:349-357.
77. Banasr M, Hery M, Printemps R, Daszuta A: **Serotonin-induced increases in adult cell proliferation and neurogenesis are mediated through different**

and common 5-HT receptor subtypes in the dentate gyrus and the subventricular zone. *Neuropsychopharmacology* 2004, **29**:450-60.
78. Ohira K, Miyakawa T: **Chronic treatment with fluoxetine for more than 6 weeks decreases neurogenesis in the subventricular zone of adult mice.** *Molecular Brain* 2011, **4**:10.
79. Sairanen M, Lucas G, Ernfors P, Castrén M, Castrén E: **Brain-derived neurotrophic factor and antidepressant drugs have different but coordinated effects on neuronal turnover, proliferation, and survival in the adult dentate gyrus.** *Journal of Neuroscience* 2005, **25**:1089-94.
80. Roozendaal B, McEwen BS, Chattarji S: **Stress, memory and the amygdala.** *Nature Reviews Neuroscience* 2009, **10**:423-33.

doi:10.1186/1471-2202-13-5
Cite this article as: Guirado *et al.*: Chronic fluoxetine treatment in middle-aged rats induces changes in the expression of plasticity-related molecules and in neurogenesis. *BMC Neuroscience* 2012 **13**:5.